

PHOTOGRAPH THIS SHEET

AD-A954 884

DTIC ACCESSION NUMBER

LEVEL

INVENTORY

WAL 710/892-10

DOCUMENT IDENTIFICATION

31 OCT 1949

This document has been approved for public release and sale; its distribution is unlimited.

DISTRIBUTION STATEMENT

ACCESSION FOR

NTIS GRA&I

DTIC TAB

UNANNOUNCED

JUSTIFICATION *per ltr*

BY

DISTRIBUTION /

AVAILABILITY CODES

DIST

AVAIL AND/OR SPECIAL

A-1

DISTRIBUTION STAMP

UNANNOUNCED



DTIC
ELECTED
AUG 06 1985
S E D

DATE ACCESSIONED

DATE RETURNED

85 8 2 077

DATE RECEIVED IN DTIC

REGISTERED OR CERTIFIED NO.

PHOTOGRAPH THIS SHEET AND RETURN TO DTIC-DDAC

midwest rese

AD-A954 884

K A Z S A S C I T Y 3 M I S U R T

CONFIDENTIAL
Approved for Release by NSA
in accordance with E.O. 13526
380-5, 381 & 382
Data
M. S. Forms
Sec 1.4
LABORATORY
INDEXED
CONFIDENTIAL



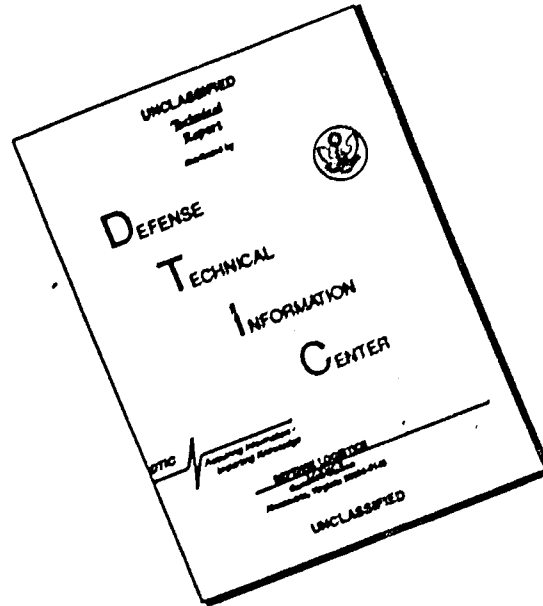
CONFIDENTIAL
CONFIDENTIAL
CONFIDENTIAL

Return to 46 17
See A ORDBE 400 33/5121
25-51-1539

01-868/014

11-18-10

DISCLAIMER NOTICE



THIS DOCUMENT IS BEST QUALITY AVAILABLE. THE COPY FURNISHED TO DTIC CONTAINED A SIGNIFICANT NUMBER OF PAGES WHICH DO NOT REPRODUCE LEGIBLY.

CONFIDENTIAL

RESTRICTED AUTHORIZED

RESTRICTED

DISTRIBUTION

<u>Copy No.</u>	<u>To Whom</u>	<u>Organization</u>
1-2-3-4	Lt. Colonel J. D. Childs	St. Louis Ordnance District
5-6	Mr. J. F. Sullivan	Watertown Arsenal
7-8	Colonel R. R. Studler	Office, Chief of Ordnance Washington, D. C.
9-10-11 12	Mr. A. C. Bonkemeyer	Office, Chief of Ordnance Washington, D. C.
13	Dr. George E. Ziegler	Midwest Research Institute
14	Mr. Martin Goland	Midwest Research Institute
15	Engineering Mechanics Division File	Midwest Research Institute
16	Library	Midwest Research Institute

CONFIDENTIAL RESTRICTED AUTHORIZED

M I D W E S T R E S E A R C H I N S T I T U T E

RESTRICTED

~~CONFIDENTIAL~~
~~RESTRICTED~~
~~UNAUTHORIZED~~

RESTRICTED

CONTENTS

	<u>Page</u>
Summary	10-1
I. Introduction	10-2
II. Description of Equipment	10-2
III. Description and Application of Evaluation Method	10-4
IV. Discussion	10-6
A. Performance Curves and "d" Relations.	10-6
B. Comparative Curves for Various Materials	10-7
C. Incidence Angle.	10-8
D. Nose Shape	10-10
E. Fabric	10-11
F. Multiple Laminations of Metal.	10-11
G. Metal and Fabric	10-13
V. Conclusions.	10-14
Appendix A	10-18
Index to Curves.	10-19, 10-20
Performance Curves; Figures 1 through 167	
Appendix B	10-21
Schematic Diagram of Pulse Amplifier	

~~CONFIDENTIAL~~
~~RESTRICTED~~
~~UNAUTHORIZED~~

CONFIDENTIAL

RESTRICTED

MODIFIED UNCLASSIFIED AUTHORIZED

SUMMARY

Under the present contract, the basic method for predicting the performance of light personnel armor previously developed under Contract No. W23-072-ORD-2123 has been extended to include other variables which enter the problem of armor design. The major portion of the work under the previous contract was limited to the study of flat-nosed fragments fired perpendicularly at plates using comparatively low striking velocities. This study has been extended to include the effects of various fragment nose shapes, angles of incidence, higher velocities and smaller fragments.

It was found that the previously developed formula for predicting light armor performance remains valid over the extended range of conditions for most of the materials studied. It is shown that the original formula can be modified to enable a designer to account for the effect of angle of incidence for metallic materials. Except in the case of fibrous materials, the effect of nose shape was found to be comparatively small for the range of shapes studied; hence, no shape factor was included in the formula.

CONFIDENTIAL

MODIFIED UNCLASSIFIED AUTHORIZED

CONFIDENTIAL

RESTRICTED

INTRODUCTION

During the course of the preceding contract, the Midwest Research Institute developed a method for the evaluation of the resistance of certain materials to penetration by fragments having various masses and striking velocities. The final report for that contract presented data taken with cylindrical, flat-nosed fragments of 1/2-inch diameter which were projected perpendicularly against the armor materials.

One objective of the work under the present contract has been to explore an extended range of conditions to determine what limitations might be presented by this method of evaluation. Accordingly, studies have been made of the effects of: 1) various angles of incidence of the approaching fragment; 2) different fragment nose shapes; 3) different fragment perimeters; and 4) higher striking velocities.

It is a purpose of this report to present data which will extend the scope of the previously developed semi-empirical assessment method and to indicate the comparative reactions of different materials to various conditions of penetration.

II. DESCRIPTION OF EQUIPMENT

The equipment used for obtaining the data of this report is, with a few exceptions, the same as that used in the previous contract. For a complete description, including photographs and wiring diagrams, reference should be made to the final report of Contract No. W-774-ORD-2123.

CONFIDENTIAL

RESTRICTED

MODIFIED - UNCLASSIFIED - AUTHORIZED

Equipment changes include a new laboratory location, a new design of pick-up for the measurement of residual velocity, and special Tempo Tool barrels for higher striking velocities.

The laboratory location has greatly improved working conditions for both personnel and instruments. All the original safety features remain the same.

The new design of residual velocity pick-up provides a higher signal-to-noise ratio to enable velocity measurements of small fragments to be made at the wide divergence angles resulting from oblique impact. The signal-to-noise ratio was improved by providing a transverse magnetic field for the screens as contrasted to the axial field formerly used. The new arrangement minimizes screen coupling. Pole pieces having a width of 3 1/2 inches in the plane of the screen are provided. They are separated by an air gap of 3 inches, thus providing a sufficiently large screen area to accommodate the divergence angles resulting from most of the oblique impact conditions.

The pulses derived from the residual velocity magnetic screens are admitted to two amplifiers (see Appendix B) whose outputs are connected to the start and stop inputs, respectively, of the counter chronograph. These amplifiers are identical and are fairly simple in their design. The requirements are for high gain and relatively narrow band width. The tube line-up consists of a 6AU6 pentode input, followed by a 12AU7 twin triode cascade amplifier which feeds into the grid of a 2D21 thyratron. The output pulse from the thyratron cathode is used to operate the chronograph.

ALL INFORMATION CONTAINED HEREIN IS UNCLASSIFIED

CONFIDENTIAL

RESTRICTED

~~CONFIDENTIAL~~
~~MODIFIED HANDLING AUTHORIZED~~

RESTRICTED

DESCRIPTION AND APPLICATION OF EVALUATION METHOD

A thorough description of the semi-empirical assessment method for the performance of armor materials is to be found in the final report of Contract No. W23-072-ORD-2123. Briefly, it consists of the following relationship for metals:

$$d = \frac{M_0}{M} \times \frac{P}{P_0} \times \frac{h}{h_0}$$

where M = mass of striking fragment

P = perimeter of fragment

h = thickness of plate

$M_0 = 10 \times 10^{-4}$ slugs

$P_0 = 1.0$ inches

$h_0 = 0.1$ inches

and for fabric:

$$d_F = \frac{M_0}{M} \times \frac{P}{P_0} \times \frac{n}{n_0}$$

where M = mass of striking fragment

P = perimeter of fragment

n = number of layers of fabric

$M_0 = 10 \times 10^{-4}$ slugs

$P_0 = 1.0$ inches

$n_0 = 10$ layers

It should be noted that the "d" relationship for fabric has been somewhat revised to account for the variation of fragment perimeter.

~~CONFIDENTIAL~~
~~MODIFIED HANDLING AUTHORIZED~~

M I D W E S T R E S E A R C H I N S T I T U T E

~~CONFIDENTIAL~~
~~RESTRICTED~~

RESTRICTED

When using the evaluation method to determine the relative performance of various materials, one should avoid drawing general conclusions covering a wide range of "a" values. The "a" curves for various materials are sufficiently different in shape to indicate that the relative merits of the materials may even become reversed when the plate thickness, fragment perimeter or mass is changed sufficiently. Consequently, when making comparisons between materials under a given set of conditions, the recommended procedure is to determine the appropriate value of a for each material from the values of plate thickness, fragment perimeter, and mass. (When considering oblique impact, the values of plate thickness and fragment perimeter should be modified as outlined in Section IV-C.) Then a curve having the required value of a can be chosen from the family of "a" curves given in this report for the material in question. In cases of non-integral values of a , the desired curves can be constructed by interpolation. If the material is one the resistance of which is markedly affected by nose shape, this effect can be estimated by reference to a curve of data taken under similar conditions. Then the "a" curve, after being adjusted for nose shape, should predict the performance of the material under the stated conditions with a reasonable degree of accuracy.

~~CONFIDENTIAL~~ ~~RESTRICTED~~
RESEARCH INSTITUTE
10-5
RESTRICTED

IV. DISCUSSION

A. Performance Curves and "α" Relations

Figures 62 through 167 in Appendix A represent all the data obtained during the term of this contract. Experimental points are indicated by plus marks and their average loci by solid lines. The dashed curves are values of α corresponding to the experimental data in each case. The values of α are taken from the families of "α" curves shown in Figures 1 through 4.

These families of "α" curves have been derived as suggested in the previous contract with the exception that they are based on data taken from the middle of the range of "α" values covered in the present investigation. This modification provides better agreement for data having high α values without detrimental effect on those of low α values.

Hadfield Steel has not conformed in general with the "α" method of evaluation. Further investigation may reveal some such relationship within specified limits. Figures 60 and 61 suggest this possibility wherein the limiting condition would be constant fragment perimeter. At the present time, no comparison can be made between the relative performance of different thicknesses of Hadfield Steel. The reason is that the two thicknesses investigated, i.e., .036-inch and .048-inch, were supplied in different degrees of hardness. The average hardness of the .036-inch sheet, as measured on the Rockwell B scale was 52 and that of the .048-inch sheet was 59.

B. Comparative Curves for Various Materials

Figure 5 compares 2S0, 24ST, and 75ST aluminum alloys with nylon duck having a weight per ply of 13 ounces per square yard. The curves are taken from their respective "a" families and have values of α which give approximately equal weight per unit area.

The curves of Figure 6, which are taken directly from experimental data, are included for purposes of comparison with Figure 5. For additional comparison, the experimental curve of .048-inch Hadfield Steel has been included. Figures 6 through 9 each contain curves for different armor materials when subjected to the same conditions of impact. Because of the variables involved, these curves were taken directly from experimental data. They furnish some measurement of the relative merits of the different materials under specific conditions. It will be noted from Figures 6 and 7 that the behaviors of the metallic materials do not differ greatly one from another under some of the conditions shown. It is difficult to draw accurate conclusions regarding the relative critical velocities of the metallic materials in cases where these velocities were nearly equal to each other. The reason for this is that critical velocity varies considerably from one test to another, using specimens of a given material. By mutual agreement with the sponsor, it was decided that the extensive effort required to get accurate determination of critical velocities was not warranted in this investigation.

Figure 6 indicates that nylon duck has a comparatively high critical velocity when exposed to normal impact by flat-nosed fragments. However, this critical velocity was greatly reduced by oblique impact of flat-nosed fragments and still further reduced by conical-nosed fragments. These trends are observed in Figures 11, 12, 31 and 32.

Figures 8 and 9 indicate that the performance of 2S0 aluminum alloy is appreciably inferior to that of 24ST under 45° impact by either flat- or conical-nosed fragments. Figures 6 and 7 indicate that 2S0 has approximately the same performance as that of 24ST under normal impact by either flat- or conical-nosed fragments. These comparisons may apply only for an " α " value of approximately 2.3. When the value of α is increased to 7.0, Figures 100 and 133 show by comparison that the performance of 2S0 is greatly inferior to that of 24ST under normal impact by flat-nosed fragments.

C. Incidence Angle

Angle of incidence as defined in this report is the angle formed between the path of an approaching fragment and the perpendicular to the plane of the armor material.

Figures 10 through 39 illustrate the effects on fragments of certain nose shapes produced by varying the incidence angle of the armor materials. The nose shapes studied were flat, horizontal, and conical (90° apex angle).

To predict the approximate effect of varying the angle of incidence for metals, allowance must be made for the effective change in plate thickness and perimeter of the cap punched out during impact. The new values of thickness and perimeter thus obtained can then be substituted in the " α " equation and a suitable value obtained for α .

In the case of aluminum, it is observed that the mode of failure remains that of a simple shear over the entire elliptical perimeter. The new perimeter, therefore, is that of the ellipse produced by the oblique angle of penetration. The new effective plate thickness is measured through the hole in a direction parallel to the approach of the bullet. This may be determined by multiplying the actual plate thickness "h" by the secant of the angle of incidence.

In the case of Hadfield Steel, it is noted that the manner of failure is somewhat different. Under normal impact, the fragment produces a uniform type of failure around the entire perimeter of the cap punched out of the plate. At incidence angles of 15° and more, the nature of failure is uniform around part of the perimeter while the balance fails in a combined tearing and bending action.

In the studies to date, this latter action occurs over approximately one-fourth or one-fifth of the elliptical perimeter. The apparent case of this type of failure is occasionally indicated when the portion of the cap initially punched out of the plate swings around, as if on a hinge, with sufficient velocity to dent the reverse side of the plate. If it may

be assumed the energy absorbed in the latter portion of the failure is small compared to that absorbed by the initial and uniform type failure, then a factor is apparent which may be used to modify the elliptical perimeter. Thus far, it appears to be $3/4$ to $4/5$.

The modified plate thickness is obtained as in the case of aluminum by multiplying the actual plate thickness by the secant of the angle of incidence.

For aluminum, the modified α values have been computed and their corresponding curves appear as dashed lines on each related graph. In the case of Hadfield Steel, this has not been done because of the limitations for " α " evaluation discussed in Section IV-A of this report.

D. Nose Shape

Figures 40 through 59 compare for a given material the respective performances of fragments having different nose shapes, viz., flat, hemispherical, and conical. Comparisons are given at incidence angles of 0° and 45° .

It does not appear feasible to attempt to draw detailed conclusions regarding the relative effects of the various nose shapes because of the inconsistent behavior noted in Figures 43 through 50. It is believed that these inconsistencies are due to two factors: (1) the variation in performance of different specimens of a given material under supposedly identical impact conditions; and, (2) the errors involved in measuring both striking and residual velocities. The velocity-measuring errors are due primarily

to the short base lines used. In the case of striking velocity, a short base line is necessitated by the need for guiding the fragment up to the plate. In the case of residual velocity measurement, the short base line is necessitated by the wide angles of divergence encountered under oblique impact conditions.

Curves which are believed to represent the approximate extremes of combined errors and material variations are shown in Figures 47 and 49.

E. Fabric

Curves 10, 11, 12, 31 and 32 show that the performance of nylon duck is not appreciably affected by varying the incidence angle. However, when a large number of plies is used, certain nose shapes have a pronounced effect. Figures 41 and 42 show that when there is a large number of plies the conical nose fragment penetrates much more readily than the flat nose fragment; however, when a small number of plies is used, the difference in nose shape has a negligible effect, as illustrated in Figure 40.

F. Multiple Laminations of Metal

The investigation of the performance of multiple laminations of metal was limited to the study of four contiguous layers of .032-inch 24ST-3 aluminum alloy. The results of the study indicate that, for the conditions tested, the performance of the laminated material is slightly inferior to that of an equivalent thickness of solid material. A comparison of the two can be obtained by referring to Figures 157 and 137.

The dashed curve on Figure 167 was determined by applying the evaluation method successively to four separate plies. The method was to take a given striking velocity and, using a value of α equal to 1.18 (obtained by interpolation from the "a" curves given in Figure 3), determine the residual velocity of the fragment as it leaves the first ply. This residual velocity was then considered to be the striking velocity for the second ply. By using the same value of α again, the residual velocity of the second ply was determined. This procedure was repeated for the third and fourth plies. The entire procedure was then repeated for other values of initial striking velocity. The curve was then constructed by plotting residual velocity versus striking velocity. It will be noted that the evaluation method applied above to multiple laminations is the same as that described in the final report of Contract No. W23-072-ORD-2123, with the exception that the mass of the penetrating fragment was considered to be constant throughout.

In the previous contract, the mass of the fragment when striking each successive layer was considered to be increased by the mass of the cap torn from the preceding layer. This was based on the assumption that the cap was broken away from the surrounding material before the full extent of permanent deformation had been reached. The study of time of impact made with the six-channel oscillograph, together with observations of partial penetration of laminated plates, indicates that all or a large portion of the permanent deformation occurs before the fracture is complete.

This indicates that, in the case of laminated constructions consisting of contiguous layers of stiff materials, the force of penetration begins to be transmitted to successive layers before the failure of the first layer is complete. Thus, it would seem logical to consider the mass of the penetrating fragment as being constant throughout the penetration process.

Upon reviewing the data of the previous contract, it was found that closer agreement between experimental curves and those predicted by the evaluation method could be obtained when the mass of the penetrating fragment was considered constant.

G. Metal and Fabric

Figures 164 through 166 indicate that the "Q" relation can be used to predict the performance of composite materials with a fair degree of accuracy. For these figures, the "Q" curves were constructed in a manner similar to that described in Section F. In this case, it is probable that the mass of the penetrating fragment should be considered to be increased by the mass of the aluminum cap before it contacts the succeeding layers of nylon for the reason that fracture of the aluminum is probably completed before the succeeding layers of nylon are fully loaded. However, it was felt that the position of the "Q" curve would not be appreciably affected by the small mass of the .064-inch cap and, for the sake of simplicity, the fragment mass was considered constant.

2. Of the various conditions studied, those which are critical for nylon duck are normal impact by conical-nosed fragments and 45° impact by flat-nosed fragments.

3. The critical condition for Hadfield Steel is oblique impact at approximately 15°.

4. Solid aluminum apparently has a slightly greater penetration resistance than an equivalent thickness of laminated aluminum under normal impact by 1/4-inch diameter, flat-nosed fragments.

5. Aluminum alloys and nylon duck conform to the "a" relation, at least for the range of conditions studied.

This relation permits one to construct a family of curves for a given material from one basic curve determined experimentally. This family of curves can then be used to predict the performance of various thicknesses or numbers of layers of a given material for normal impact by flat-nosed, cylindrical fragments of different masses and diameters over a range of striking velocities. Hadfield Steel does not appear to conform to this relation.

6. For conditions of oblique impact by flat-nosed fragments, the performance of aluminum alloys can be predicted with reasonable accuracy from a family of

"Q" curves by modifying the values of plate thickness and fragment perimeters to correspond to the angle in question.

7. For most of the conditions studied, the penetration resistance of aluminum alloys and Hadfield Steel is not affected by fragments of various nose shapes in a sufficiently consistent manner to permit the formulation of a rule to predict the performance accurately.

8. Comparing the tested materials on the basis of equal weight per unit area, only one of these materials, viz., 250 aluminum alloy, has shown consistently inferior performance over most of the range of test conditions. Nylon duck shows a remarkably superior critical velocity under impact by flat-nosed fragments. The other materials, viz., Hadfield Steel, 24ST, and 75ST aluminum alloys, are roughly equal in over-all performance.

9. It may be possible to utilize the advantages of some materials under certain conditions provided that some special types of armor construction or other means can be found to avoid exposing the material in question to other conditions for which it is not well suited.

Examples of these situations follow:

a. The characteristic of nylon, whereby this material exhibits a high critical velocity under normal impact by flat-nosed fragments, indicates that it may possibly be used as the interior material in composite armor, provided that a form of construction can be found which will circumvent the disadvantage of excessive detrusion under impact. However, the advantage of high critical velocity would not be realized under impact by conical-nosed fragments unless the cap from the outside material (presumably metal) is sufficiently flat to make the cap and fragment act as a flat-nosed fragment when the cap contacts the nylon.

b. The reduced resistance of Hadfield Steel under 15° and 30° impact may conceivably be improved if it can be backed up with a material which will force the steel to fail uniformly around the entire perimeter of the cap. However, it is probable that a suitable material, that is, one having adequate stiffness for this purpose, would be too heavy to use in conjunction with Hadfield Steel.

RESTRICTED

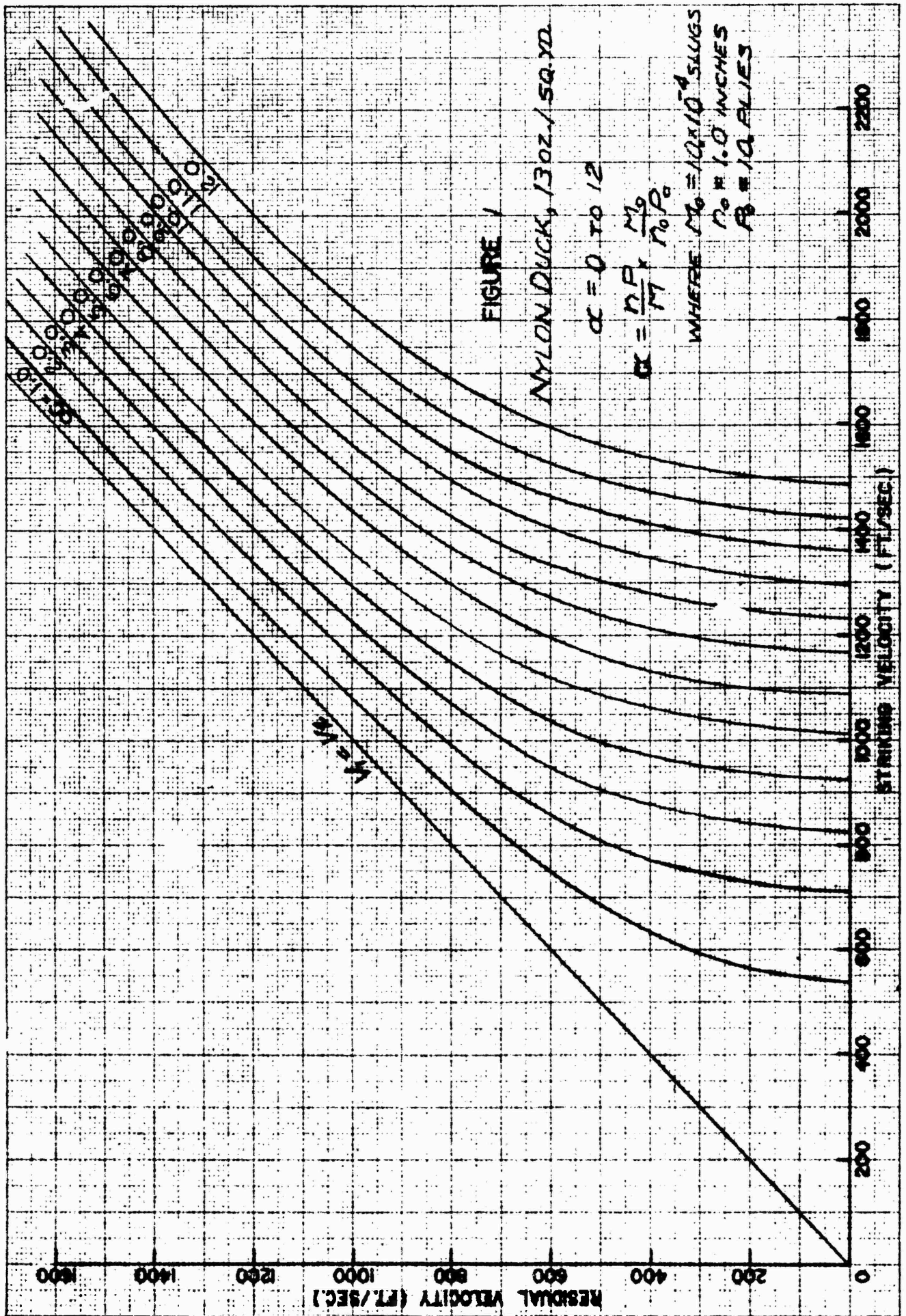
APPENDIX A

INDEX TO CURVES

	<u>Figure</u>
I. "Q" Families	
A. Nylon Duck, 13 oz. per sq. yd.	1
B. 250 Aluminum.	2
C. 24ST Aluminum	3
D. 75ST Aluminum	4
II. Comparisons of Performance Given by Materials	
Investigated.	5-9
III. Effects on Performance of Materials Caused by Varying the Incidence Angle	
A. For Flat-Nosed Fragments.	10-25
B. For Hemispherical-Nosed Fragments	26-30
C. For 90° Conical-Nosed Fragments	31-39
IV. Effects on Performance of Materials Caused by Varying the Fragment Nose Shape	
A. At 0° Incidence Angle	40-50
B. At 45° Incidence Angle.	51-59
V. Comparative Behavior of Hadfield Steel.	60-61

INDEX TO CURVES (Concluded)

	<u>Figure</u>
VI. Basic Data	
A. Nylon Duck, 13 oz. per sq. yd.	62-76
("α" curves superimposed for data of flat-nosed fragments at 0° incidence angle)	
B. Hadfield Steel.	77-91
C. 2S0 Aluminum.	92-100
("α" curves superimposed for data of flat-nosed fragments at 0° and 45° incidence angles)	
D. 24ST Aluminum	101-150
("α" curves superimposed for data of flat-nosed fragments at 0° and 45° incidence angles)	
E. 75ST Aluminum	151-163
("α" curves superimposed for data of flat-nosed fragments at 0° and 45° incidence angles)	
F. Laminated Constructions	164-167
("α" curves superimposed for data of flat-nosed fragments at 0° incidence angle)	



RESTRICTED

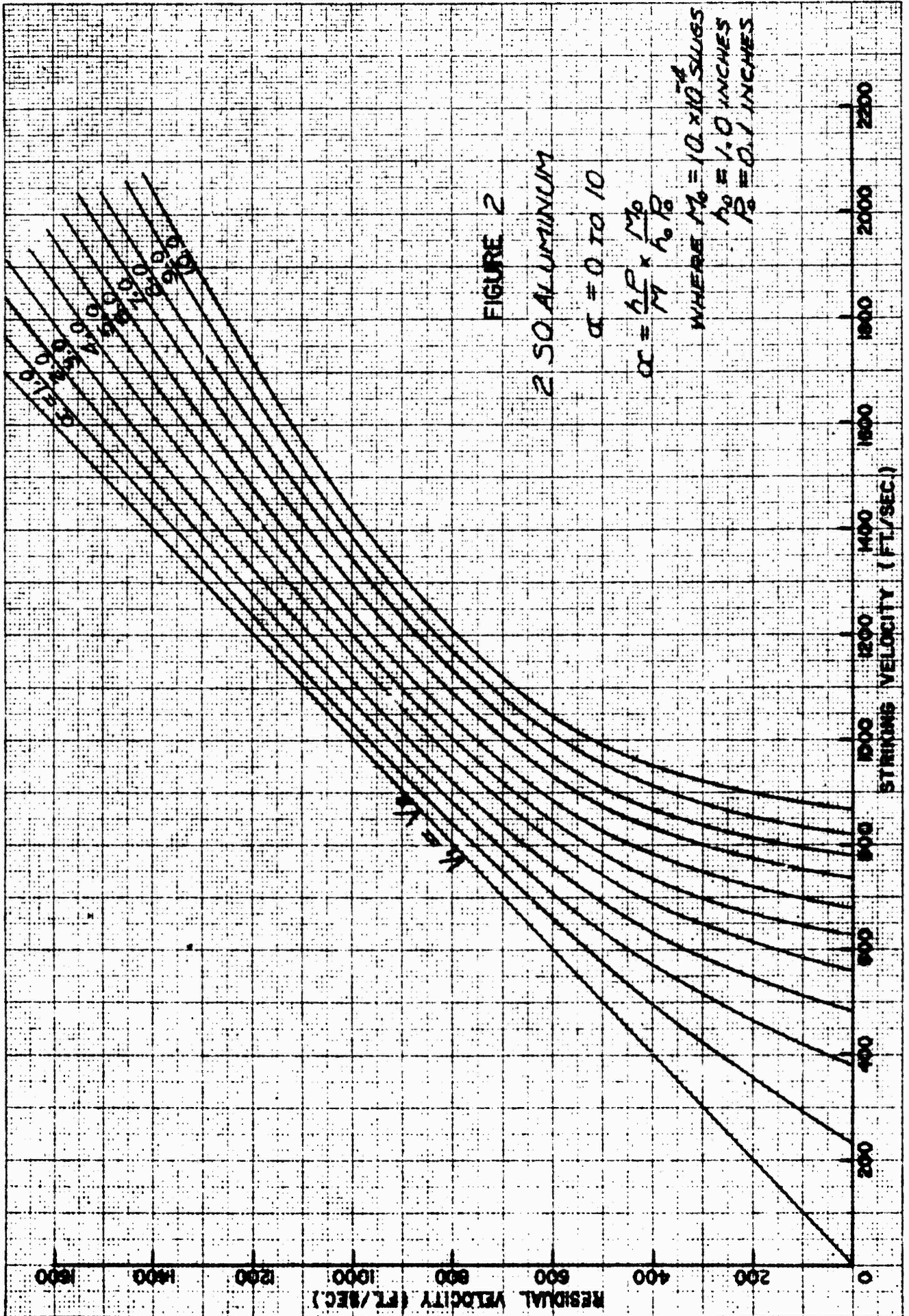


FIGURE 2

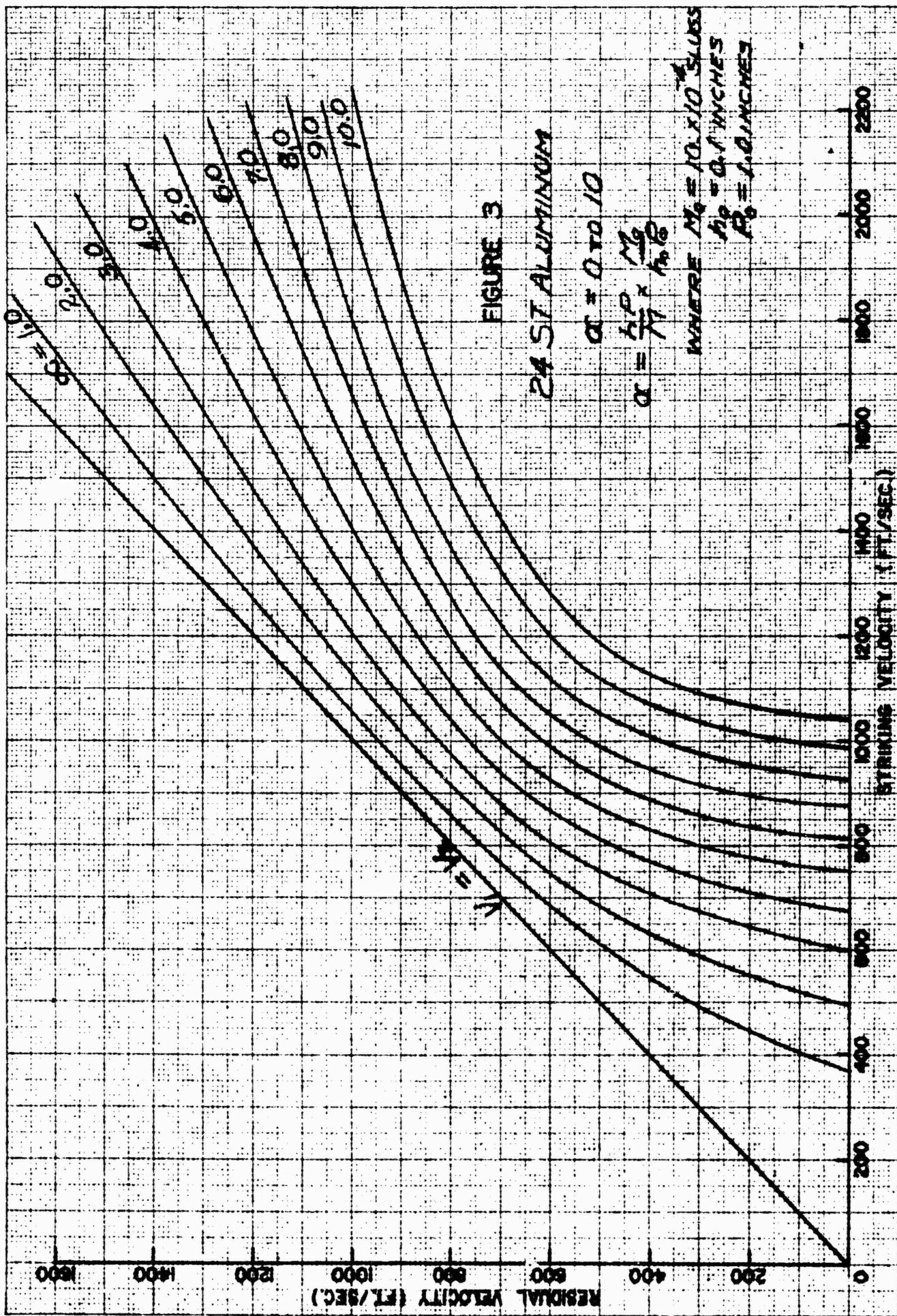
2.50 ALUMINUM

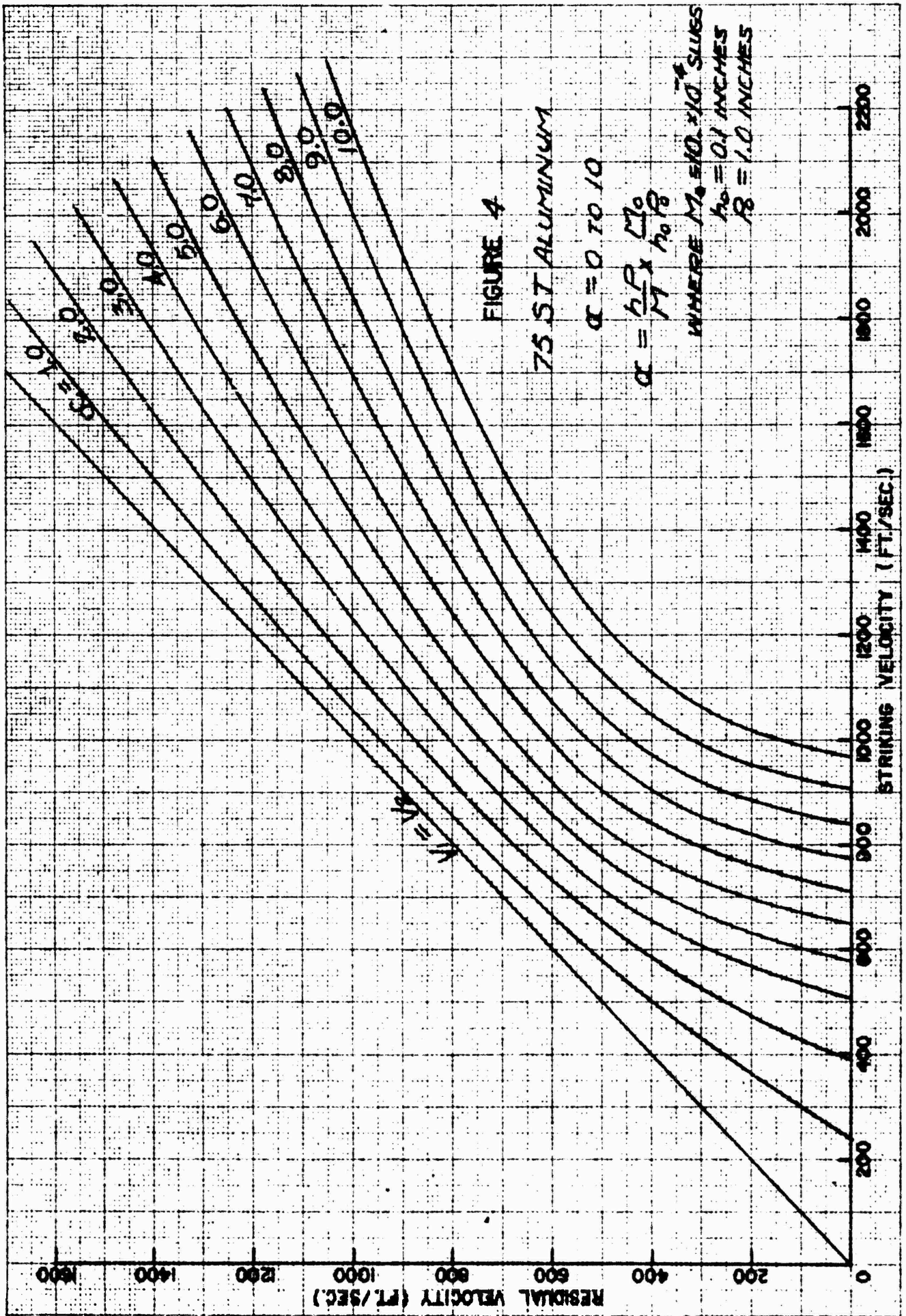
$\alpha = 0 \text{ TO } 1.0$

$$\alpha = \frac{hP}{M} \times \frac{M_0}{h_0 P_0}$$

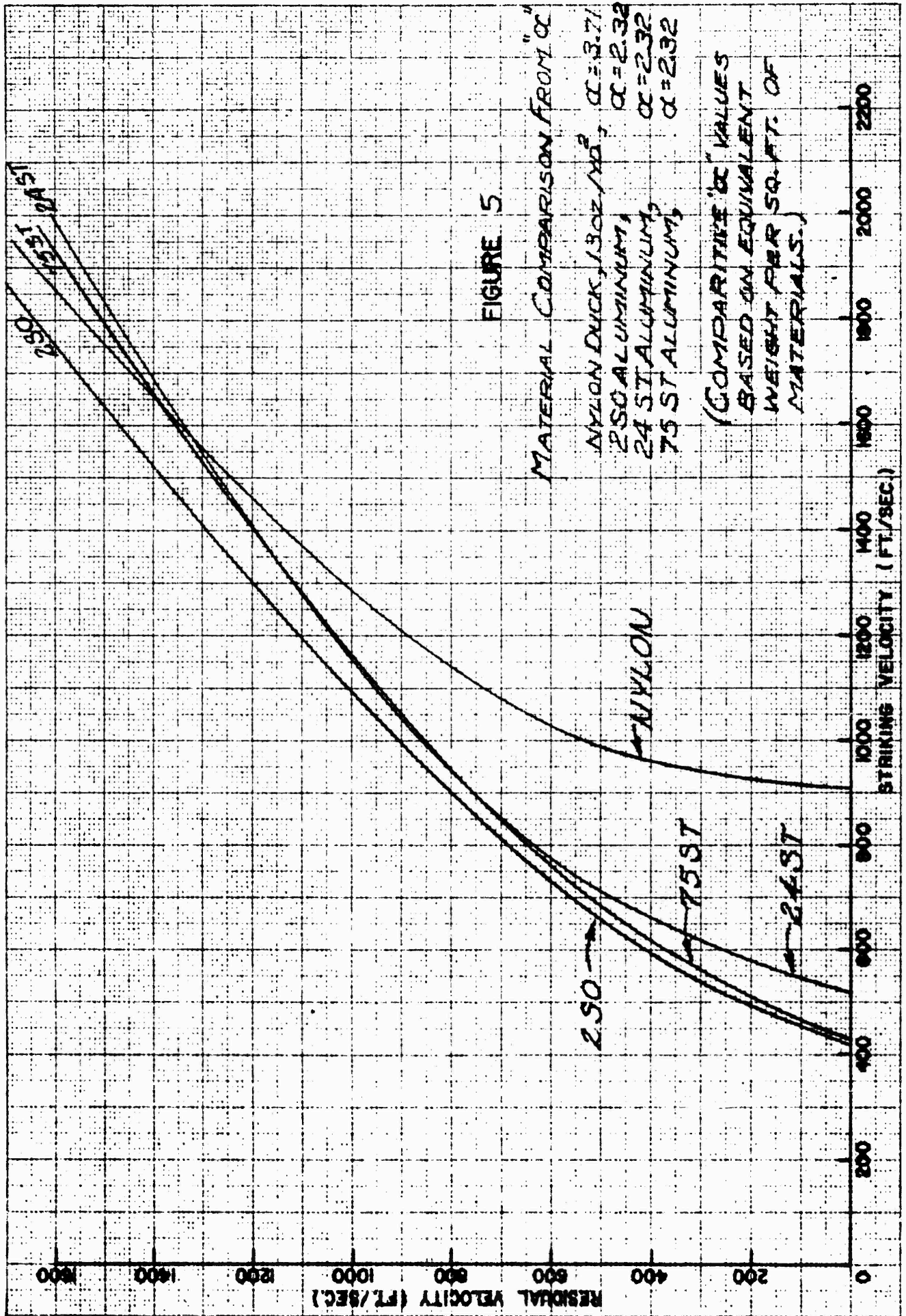
WHERE $M_0 = 10 \times 10^{-4}$ SLUGS
 $h_0 = 1.0$ INCHES
 $P_0 = 0.1$ INCHES

RESTRICTED

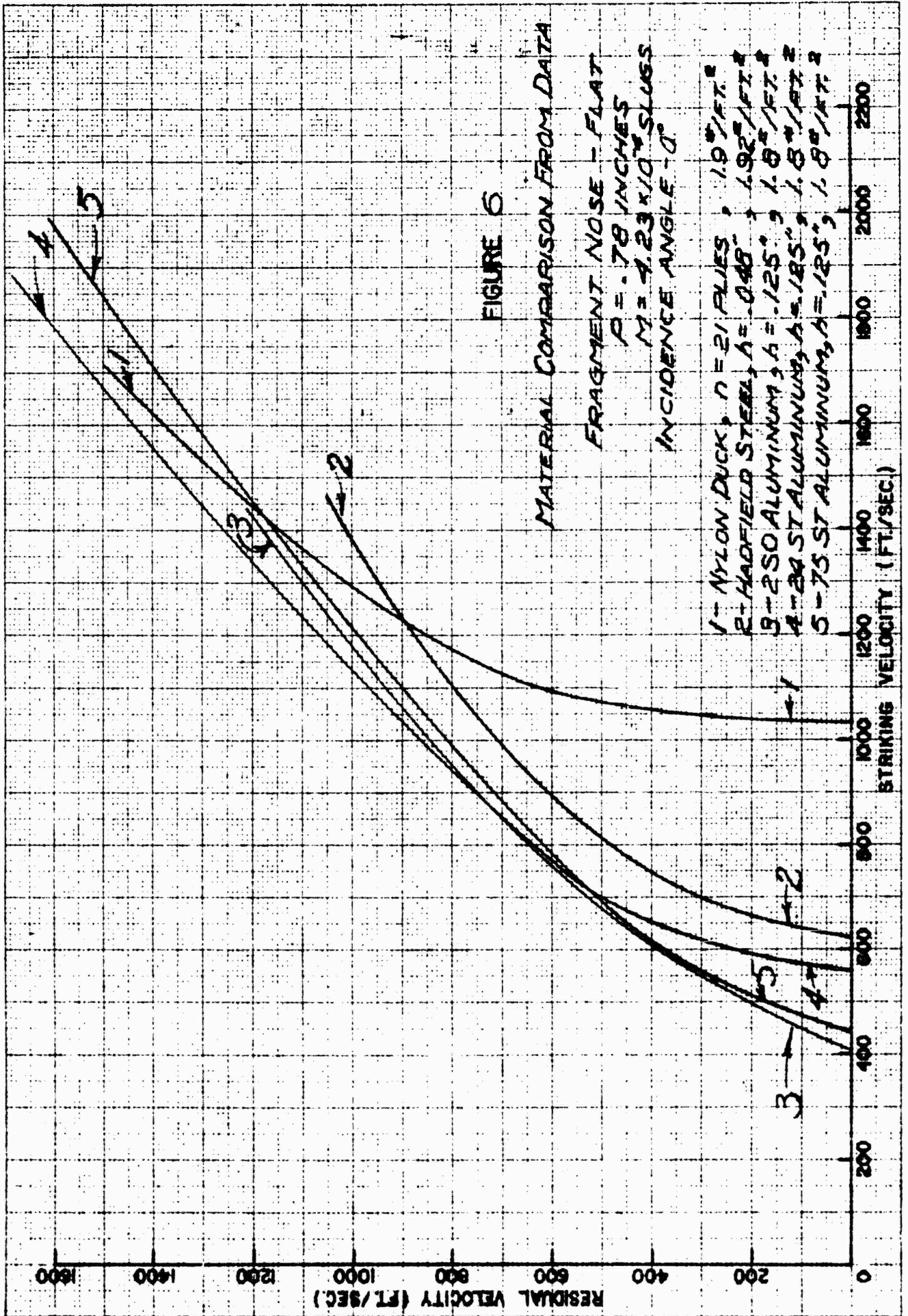


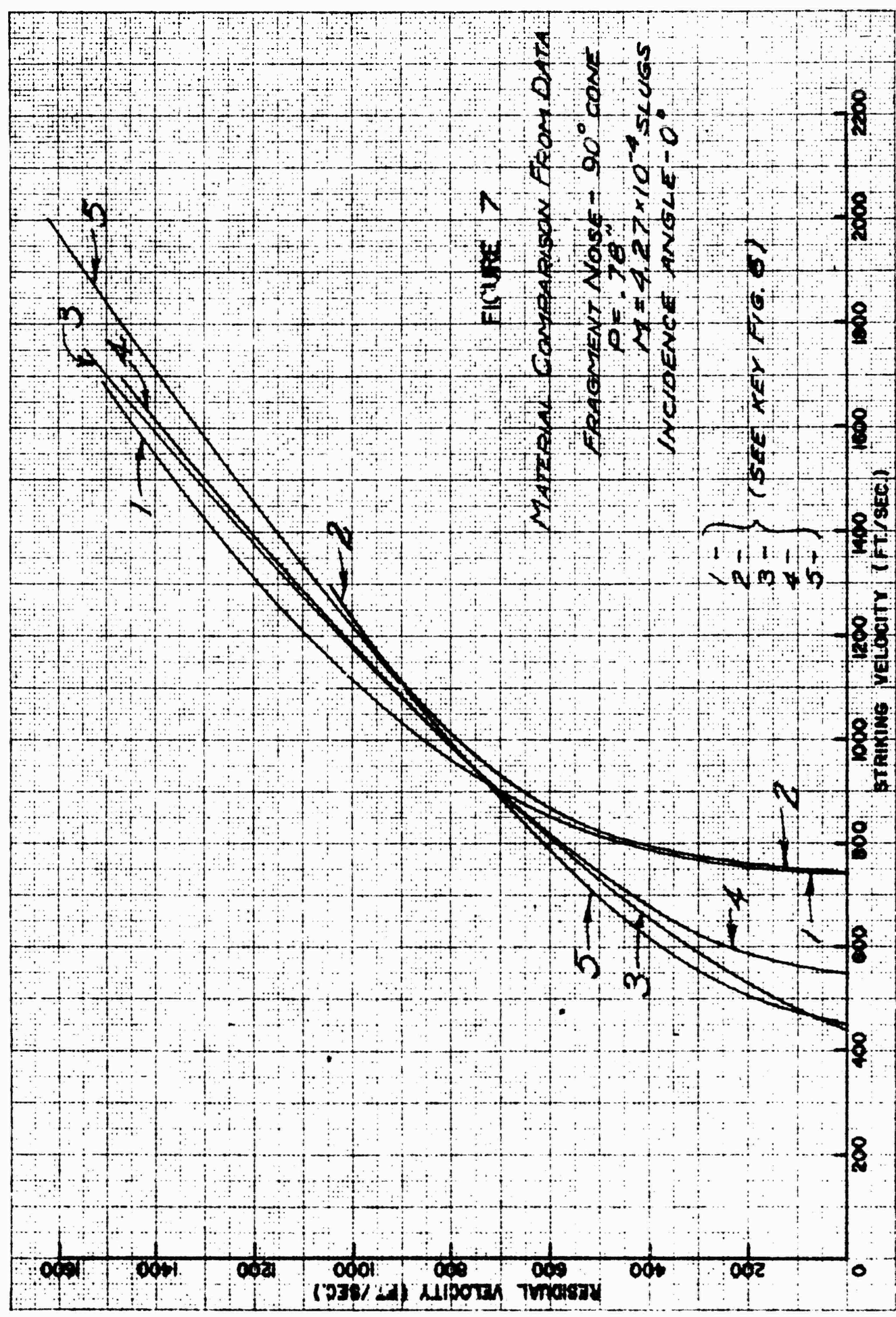


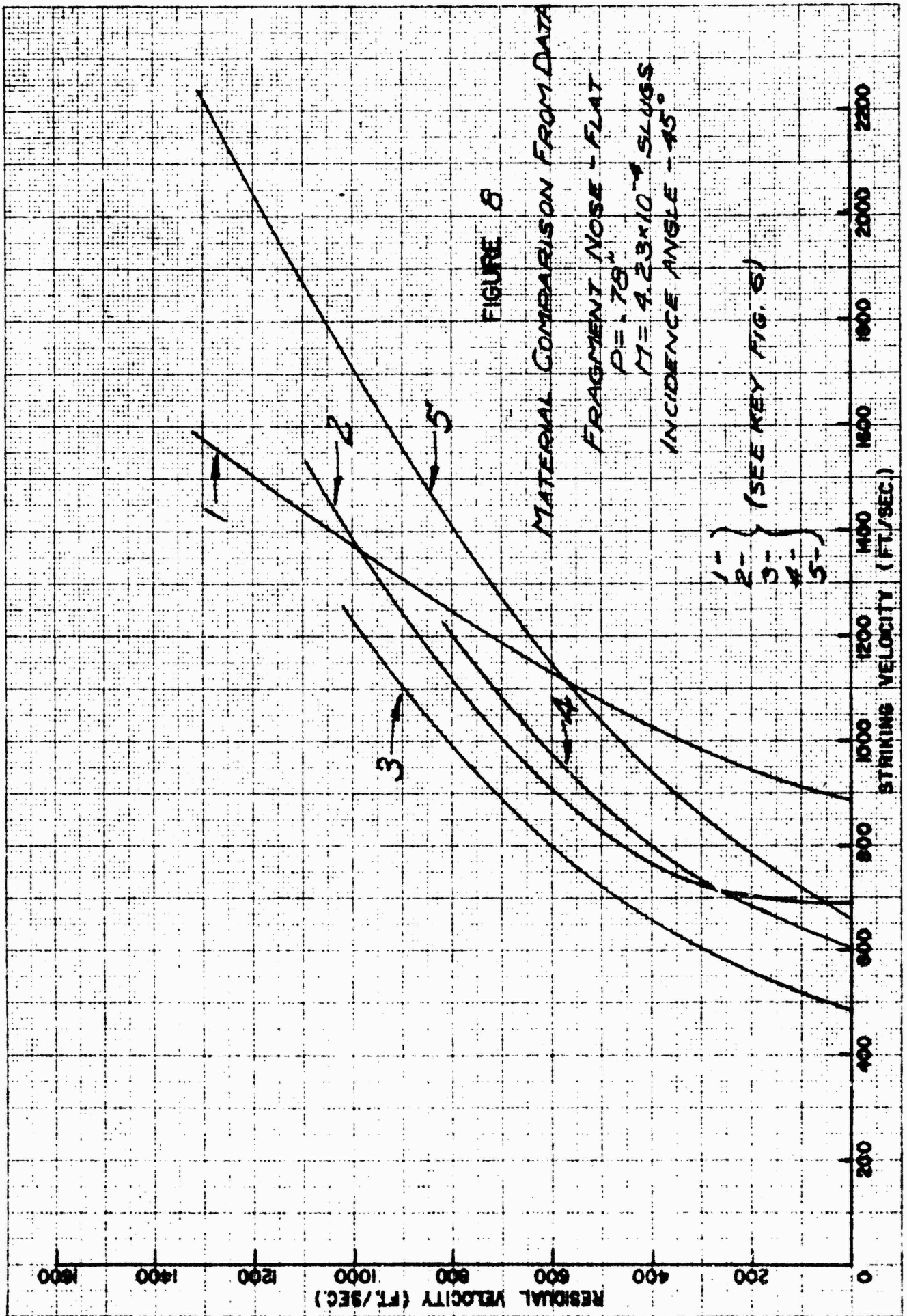
RESTRICTED

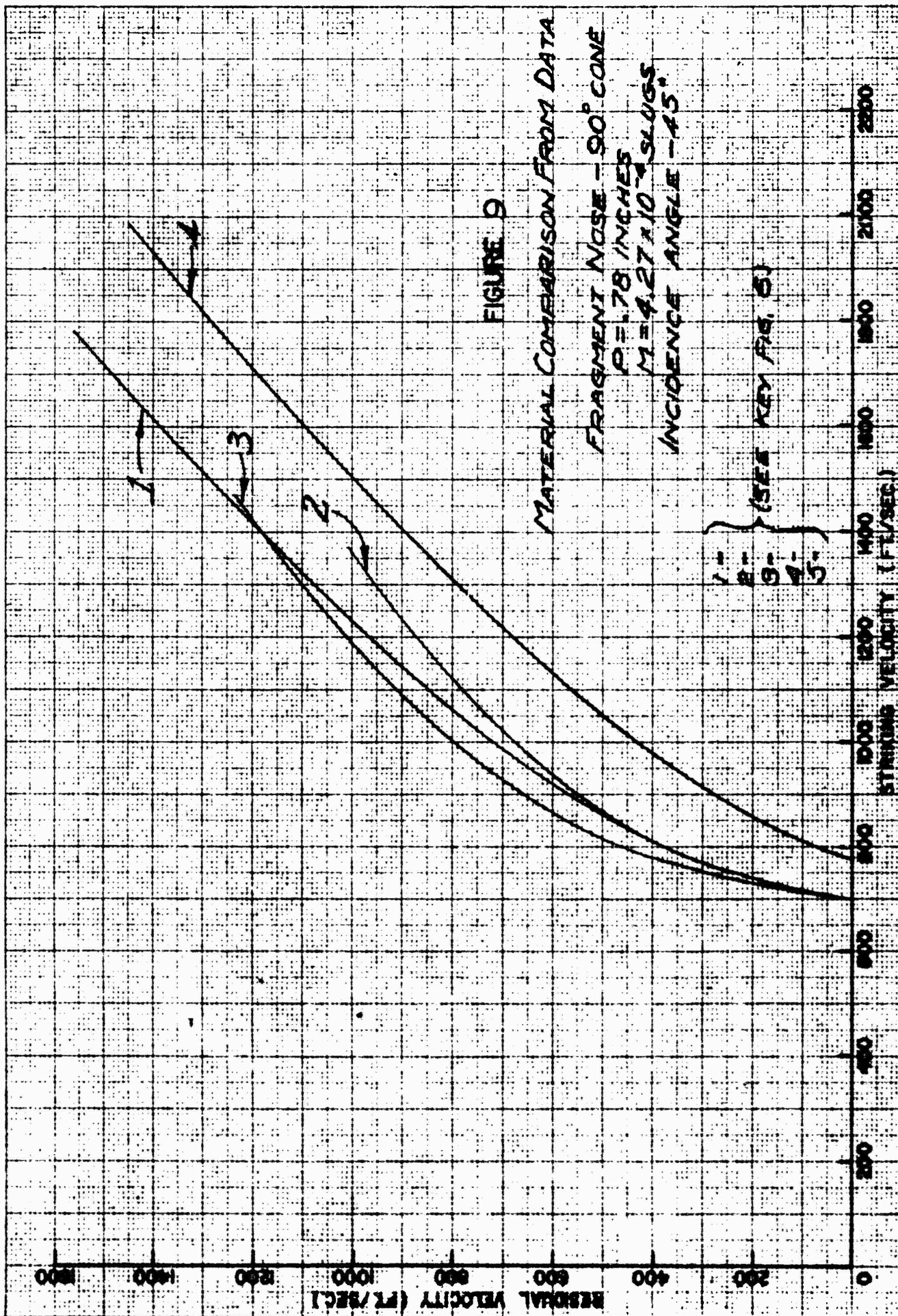


RESTRICTED









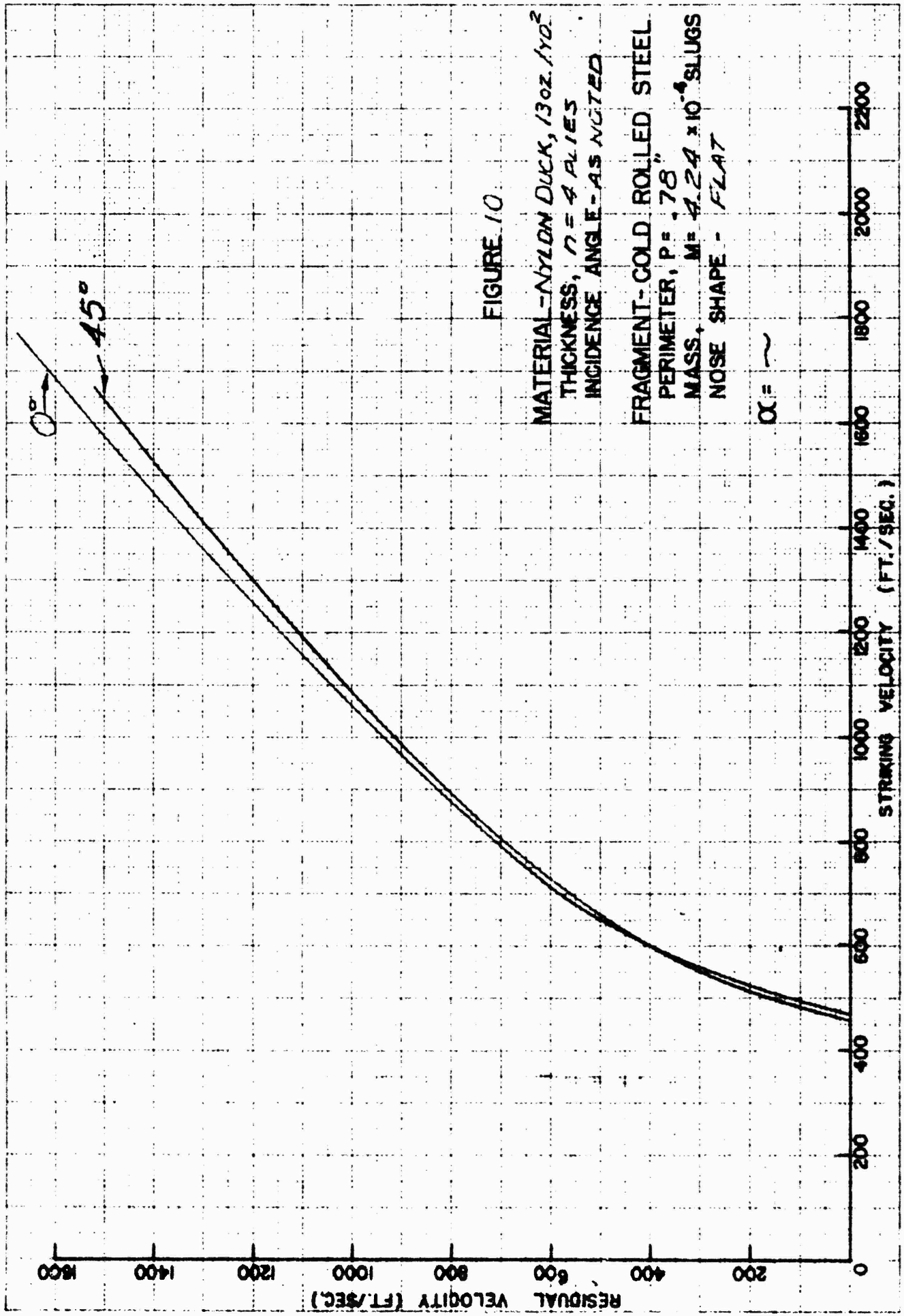


FIGURE 10

MATERIAL - NYLON DUCK, 13oz. 110²
 THICKNESS, $n = 4$ PLIES
 INCIDENCE ANGLE - AS NOTED

FRAGMENT - COLD ROLLED STEEL
 PERIMETER, $P = .78$ "
 MASS, $M = 4.24 \times 10^{-4}$ SLUGS
 NOSE SHAPE - FLAT

$\alpha = \sim$

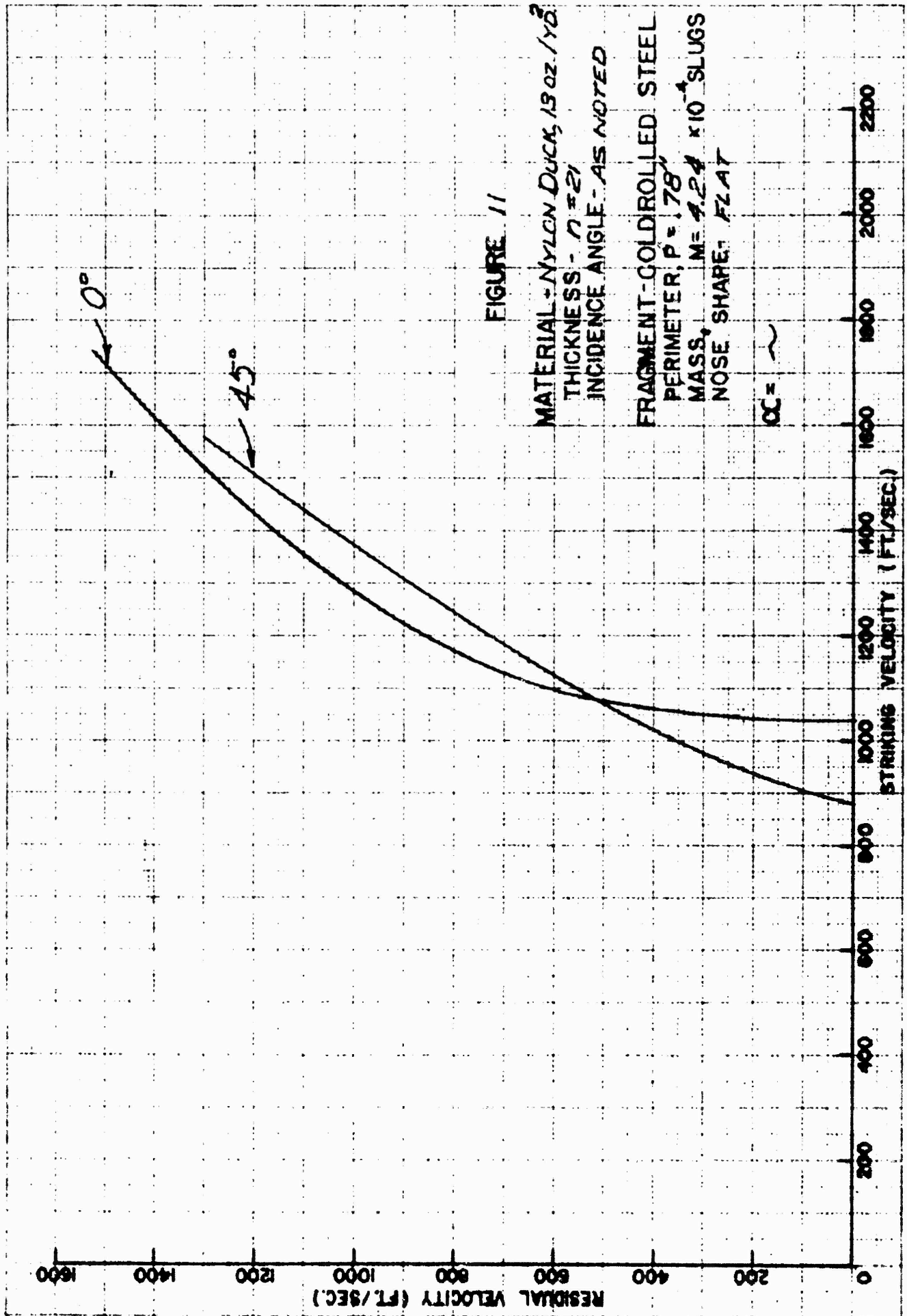
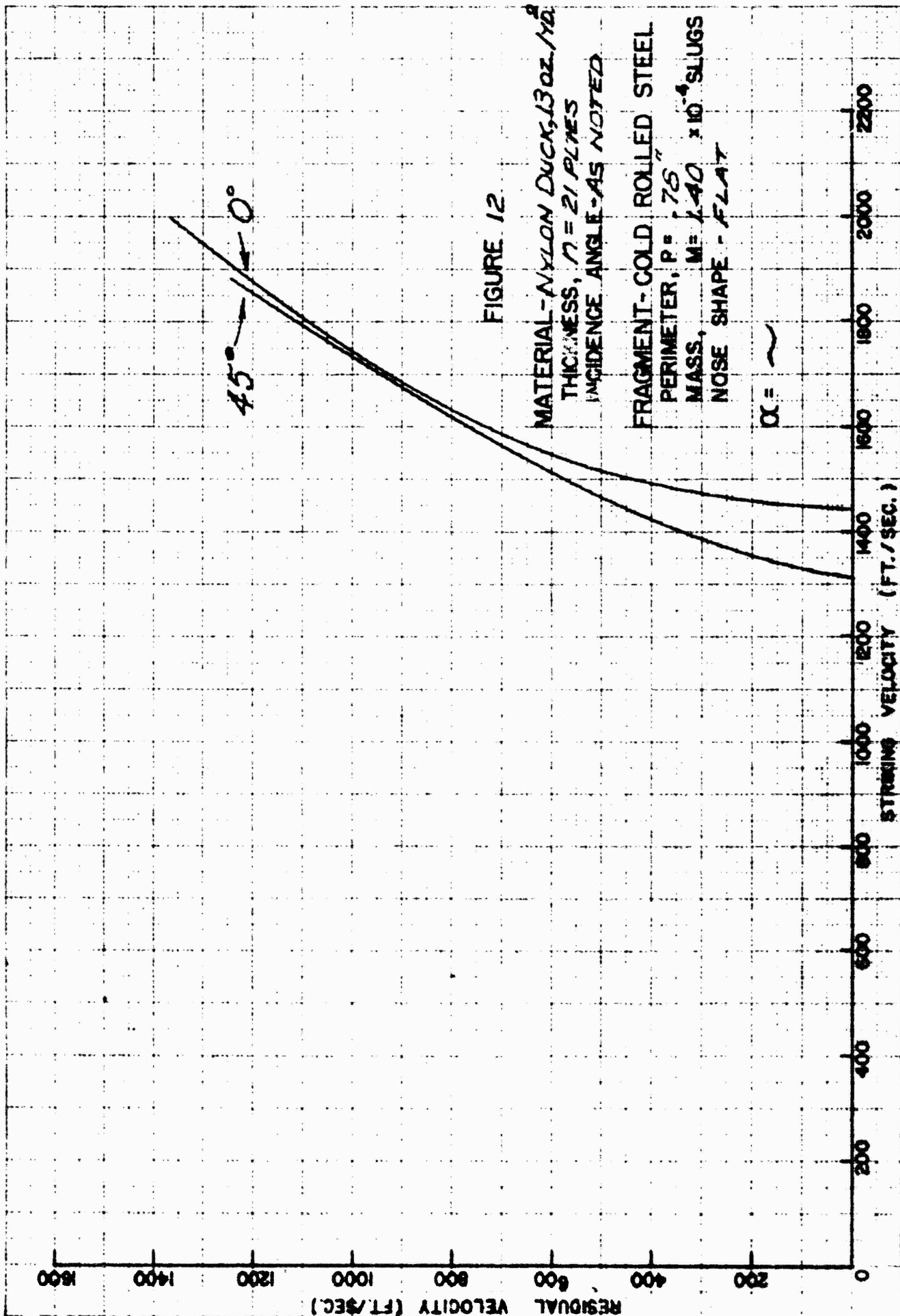


FIGURE 11

MATERIAL - NYLON DUCK, 13 oz./yd.²
 THICKNESS - 0.021"
 INCIDENCE ANGLE - AS NOTED

FRAGMENT - GOLDROLLED STEEL
 PERIMETER, P = 1.78"
 MASS, M = 4.24 x 10⁻⁴ SLUGS
 NOSE SHAPE: FLAT

CC = ~



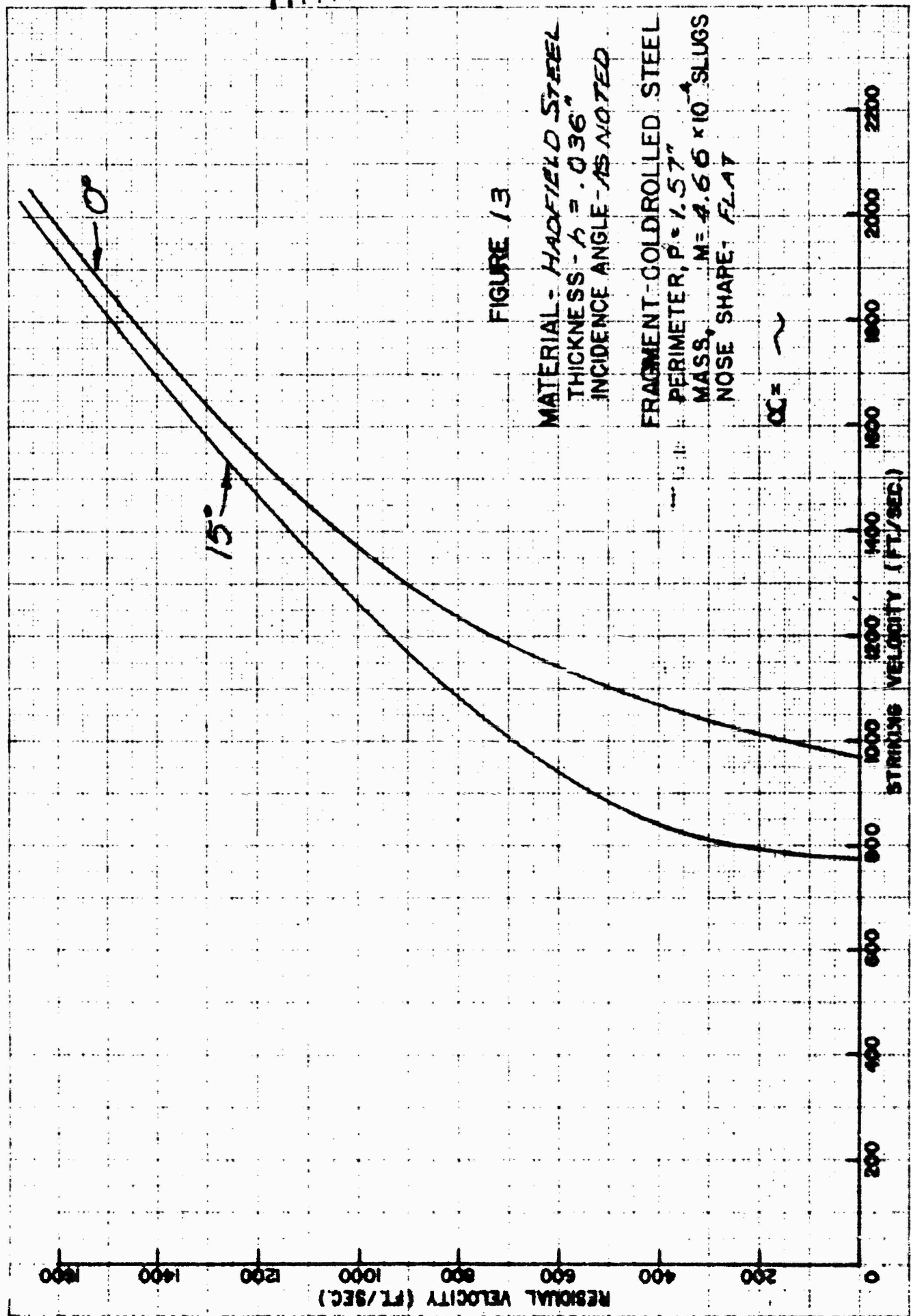


FIGURE 13

MATERIAL: HADFIELD STEEL
 THICKNESS - $t = .036"$
 INCIDENCE ANGLE - AS NOTED

FRAGMENT - COLDROLLED STEEL
 PERIMETER, $P = 1.57"$
 MASS, $M = 4.66 \times 10^{-4}$ SLUGS
 NOSE SHAPE: FLAT

$\alpha = \sim$

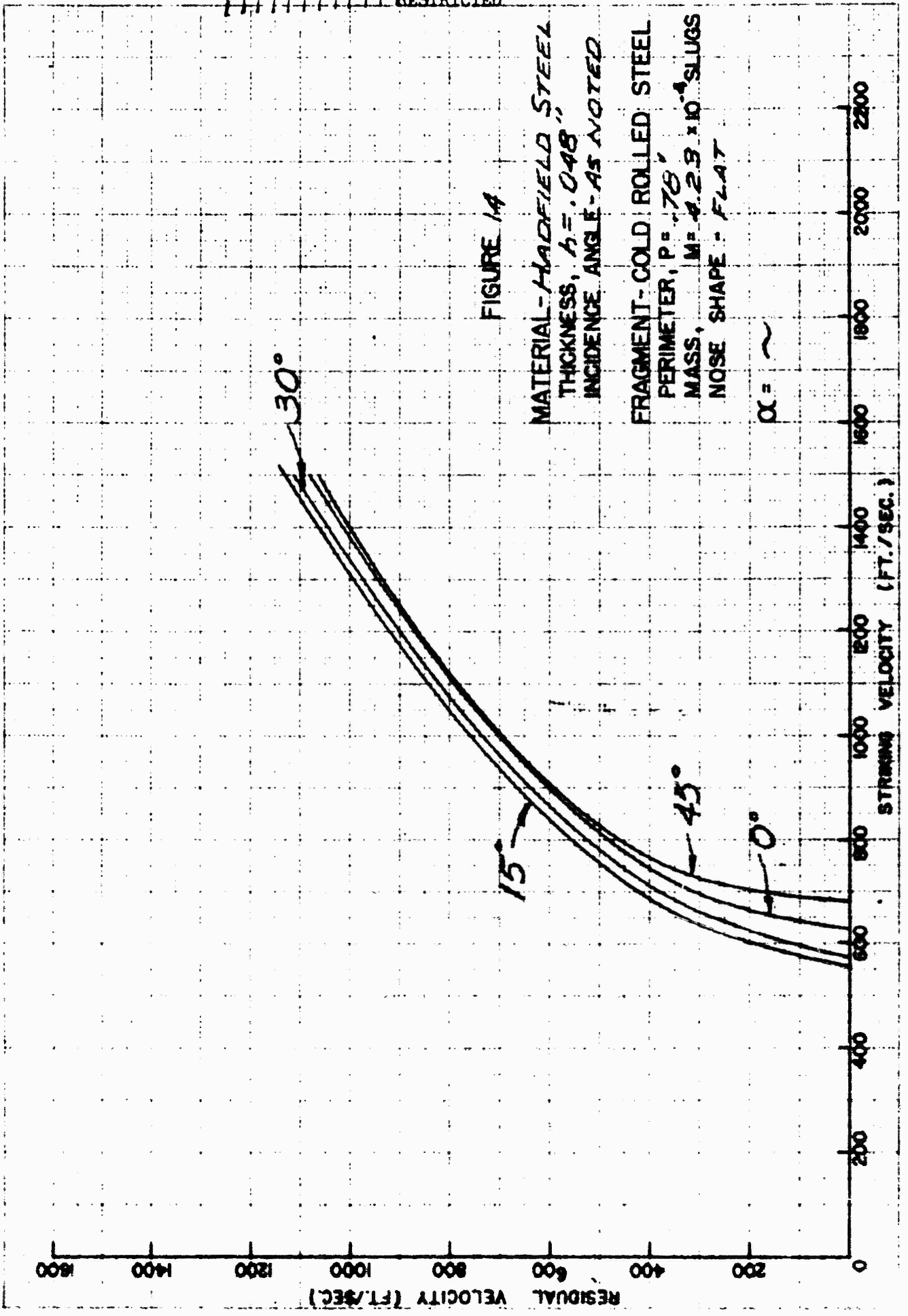


FIGURE 1A

MATERIAL - HADFIELD STEEL
 THICKNESS, $t = .048$ "
 INCIDENCE ANGLE - AS NOTED

FRAGMENT - COLD ROLLED STEEL
 PERIMETER, $P = .76$ "
 MASS, $M = 4.29 \times 10^{-4}$ SLUGS
 NOSE SHAPE - FLAT

$\alpha = \sim$

RESTRICTED

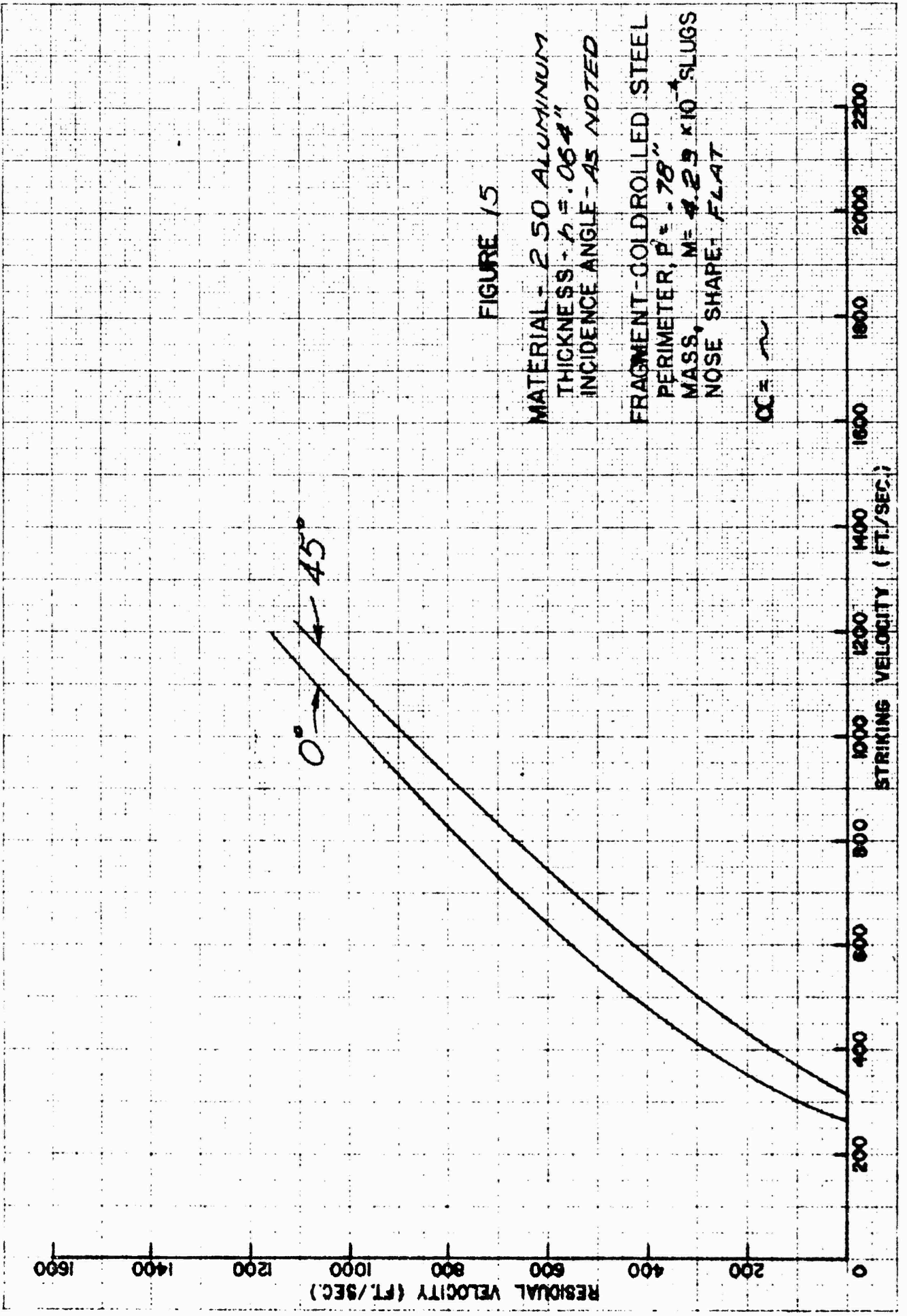


FIGURE 15

MATERIAL - 2.50 ALUMINUM
 THICKNESS - $t = .064"$
 INCIDENCE ANGLE - AS NOTED

FRAGMENT - COLDROLLED STEEL
 PERIMETER, $P = .78"$
 MASS, $M = 4.25 \times 10^{-4}$ SLUGS
 NOSE SHAPE - FLAT

$OC = \sim$

RESTRICTED

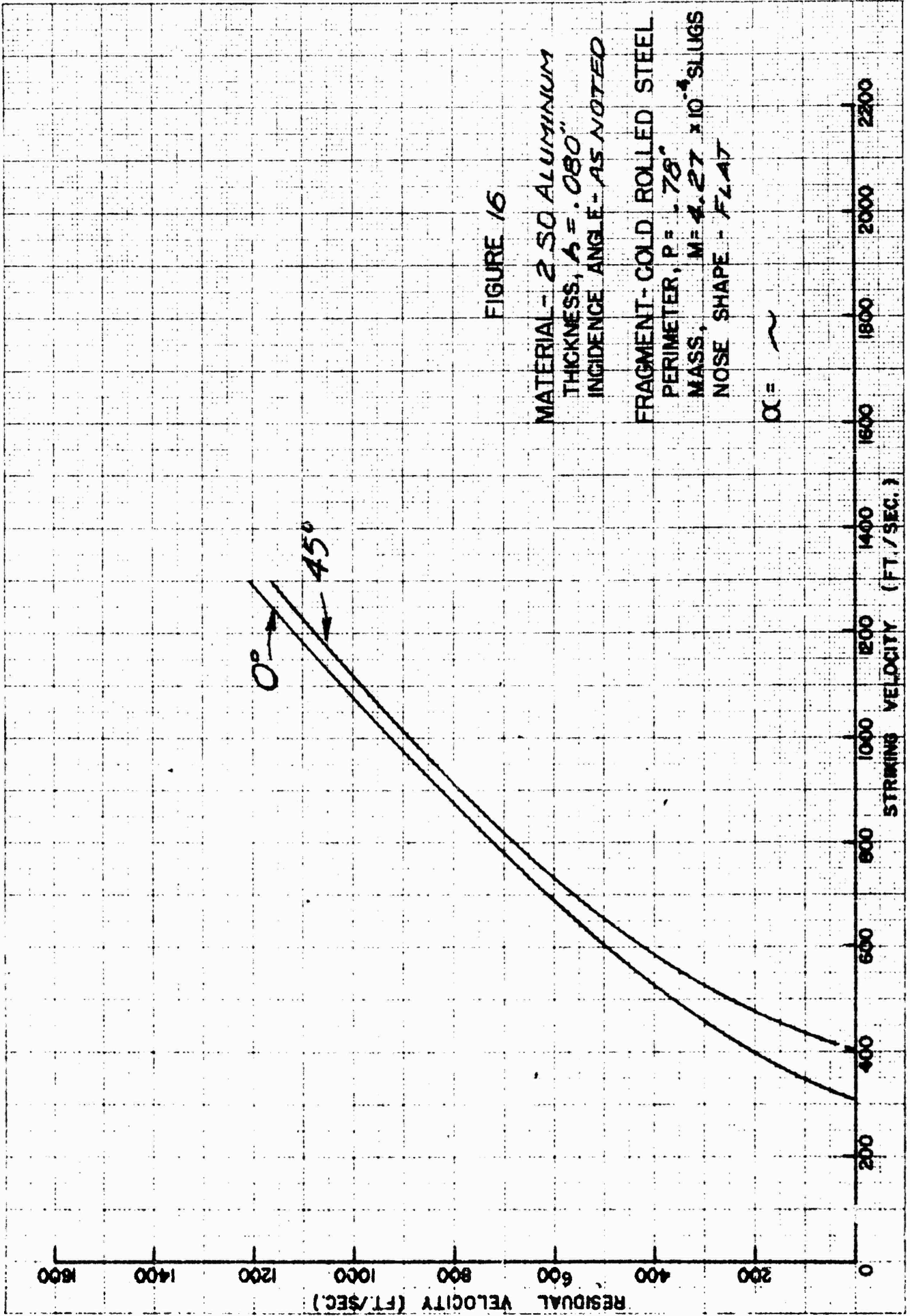


FIGURE 16

MATERIAL - 2 SQ ALUMINUM
THICKNESS, $t = .080$ "
INCIDENCE ANGLE - AS NOTED

FRAGMENT - COLD ROLLED STEEL
PERIMETER, $P = .78$ "
MASS, $M = 4.27 \times 10^{-4}$ SLUGS
NOSE SHAPE - FLAT

$\alpha = \sim$

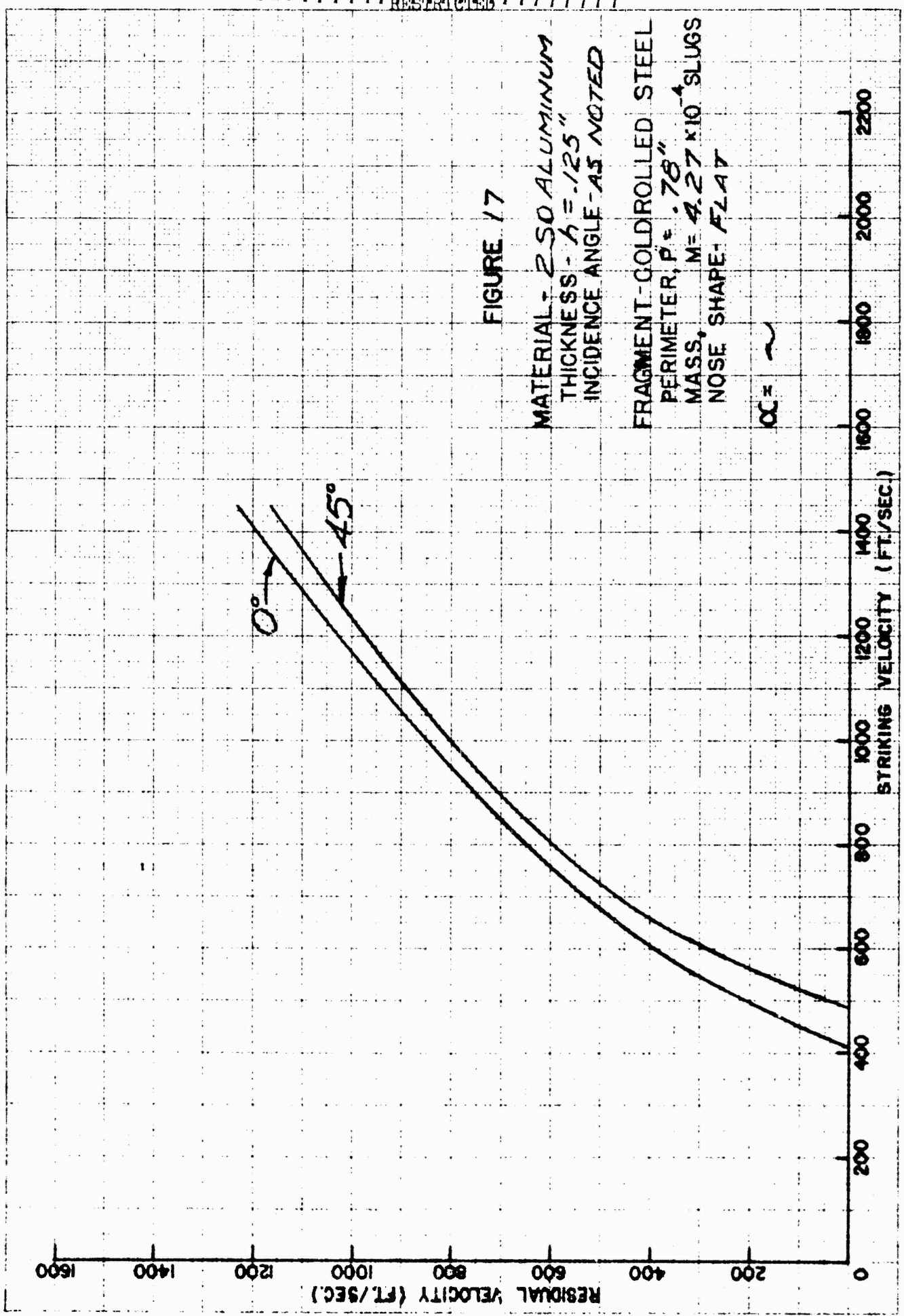


FIGURE 17

MATERIAL: 250 ALUMINUM
 THICKNESS - $t = .125"$
 INCIDENCE ANGLE - AS NOTED

FRAGMENT: GOLDROLLED STEEL
 PERIMETER, $P = .78"$
 MASS, $M = 4.27 \times 10^{-4}$ SLUGS
 NOSE SHAPE: FLAT

$OC = \sim$

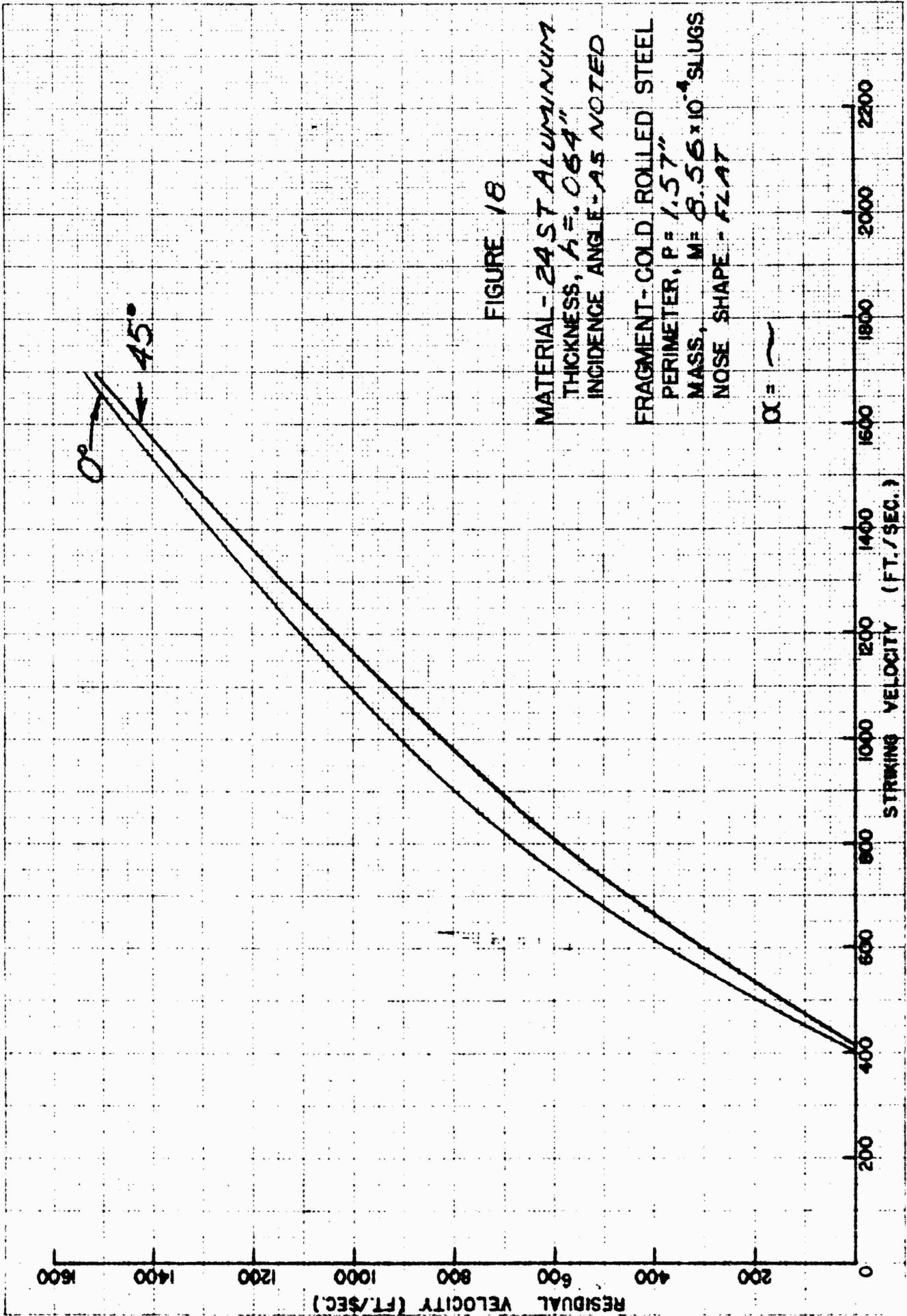


FIGURE 18

MATERIAL - 24 ST ALUMINUM
 THICKNESS, $t = .064"$
 INCIDENCE ANGLE - AS NOTED

FRAGMENT - COLD ROLLED STEEL
 PERIMETER, $P = 1.57"$
 MASS, $M = 8.56 \times 10^{-4}$ SLUGS
 NOSE SHAPE - FLAT

$\alpha =$ ~

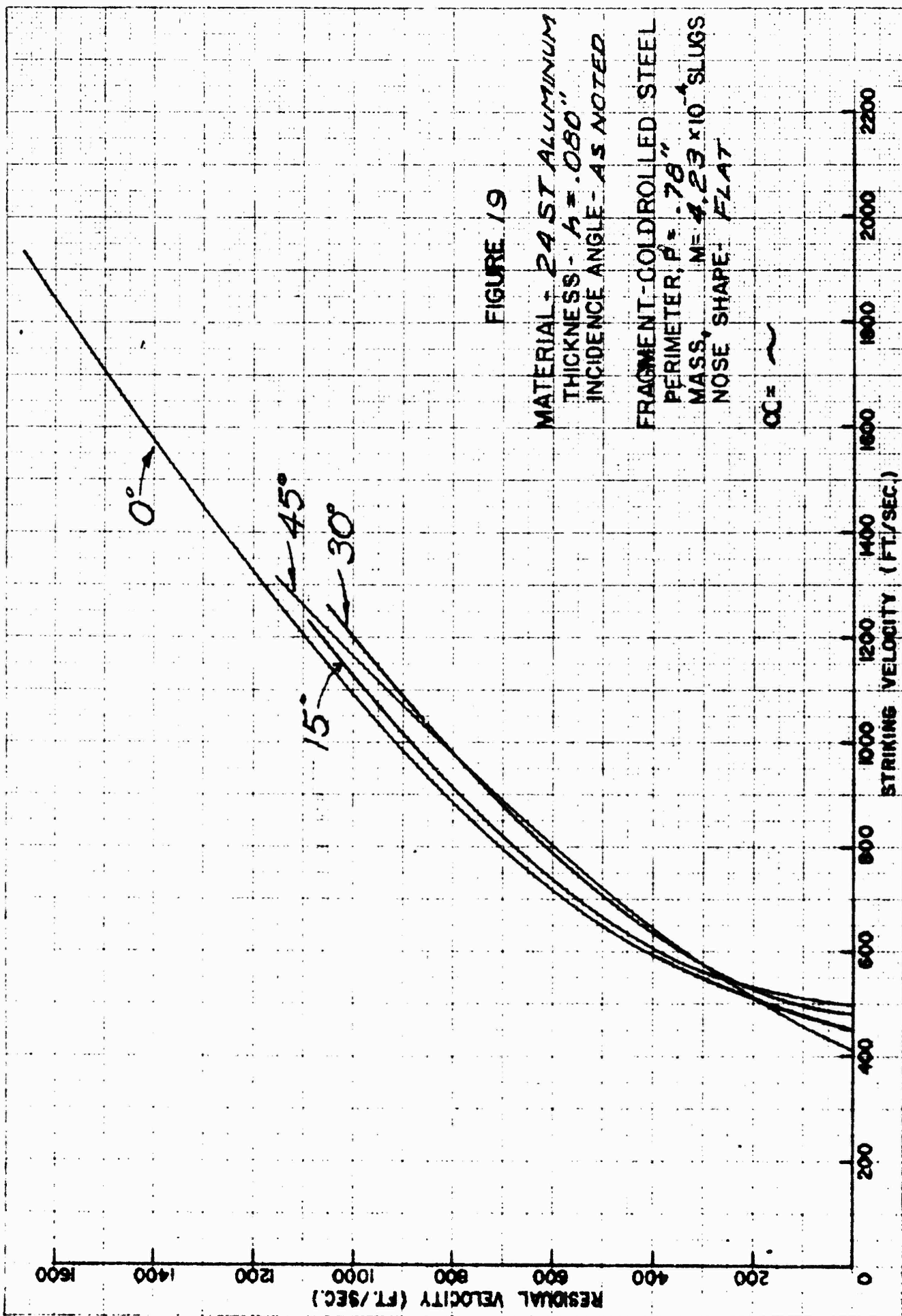


FIGURE 19

MATERIAL - 24 ST ALUMINUM
 THICKNESS - $t = .080$ "
 INCIDENCE ANGLE - AS NOTED
 FRAGMENT - COLDROLLED STEEL
 PERIMETER, $P = .78$ "
 MASS, $M = 4.23 \times 10^{-4}$ SLUGS
 NOSE SHAPE - FLAT

OC = ~

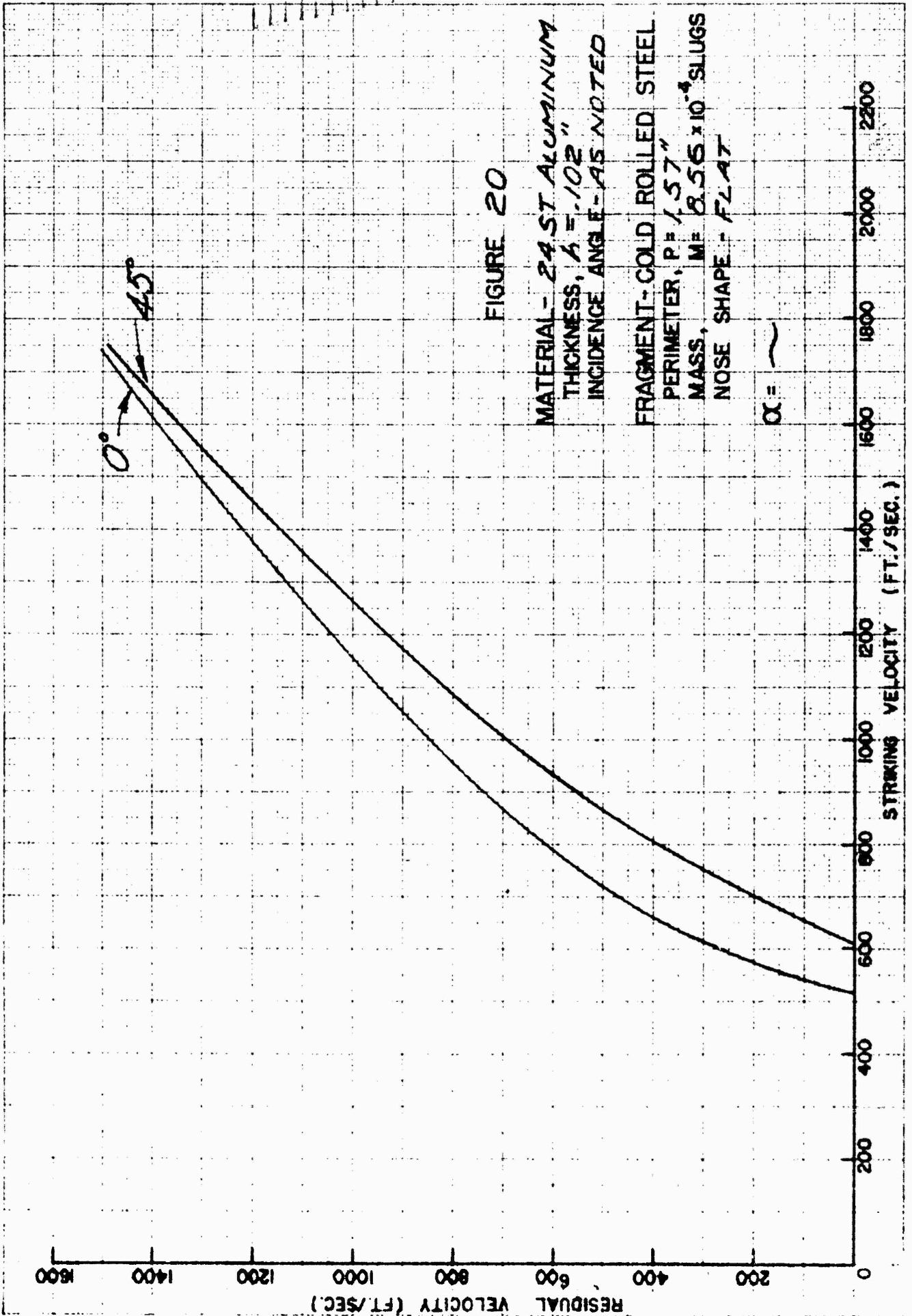
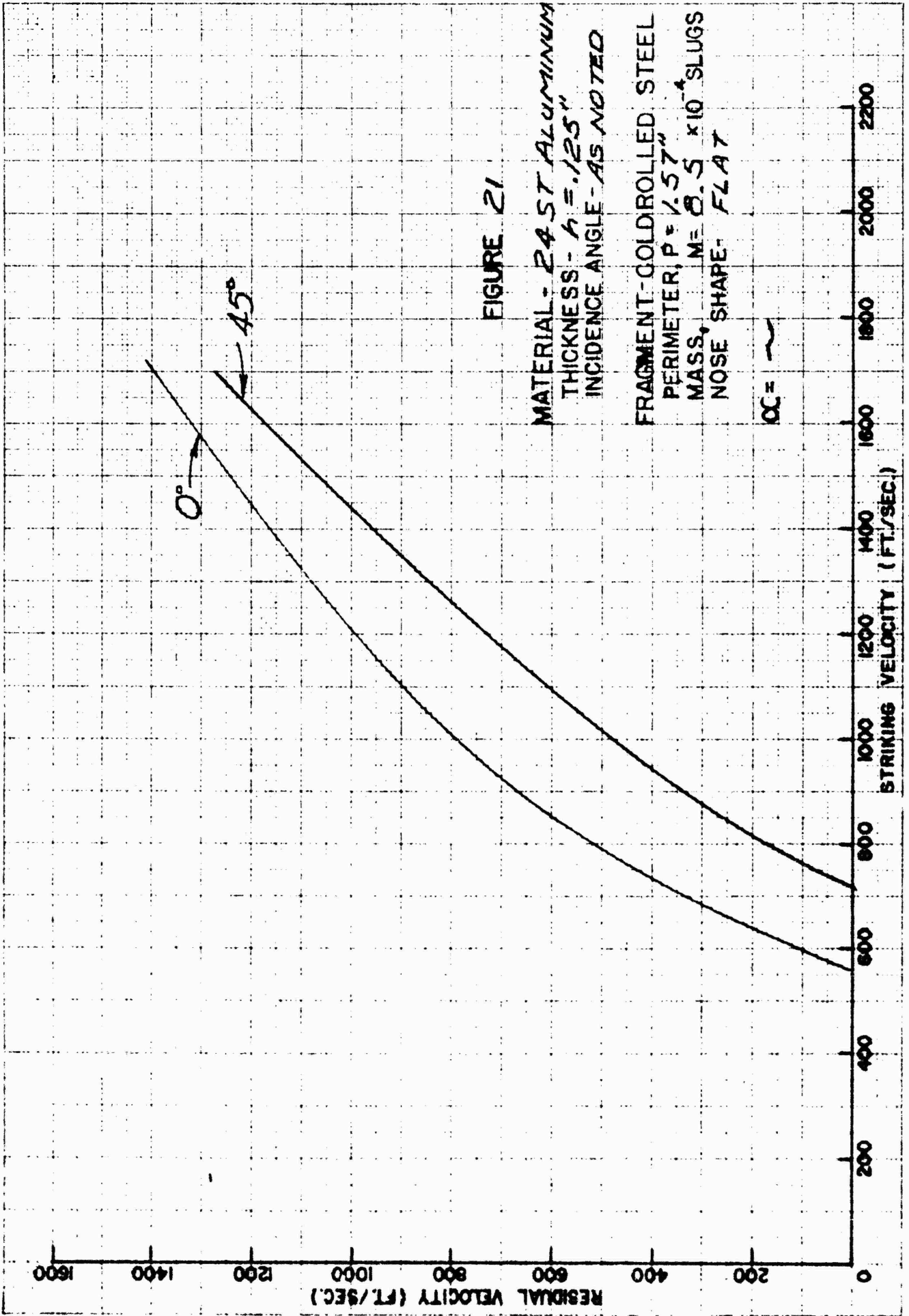


FIGURE 20

MATERIAL - 24 ST ALUMINUM
 THICKNESS, $t = .102$ "
 INCIDENCE ANGLE - AS NOTED

FRAGMENT - COLD ROLLED STEEL
 PERIMETER, $P = 1.57$ "
 MASS, $M = 8.56 \times 10^{-4}$ SLUGS
 NOSE SHAPE - FLAT

$\alpha = \sim$



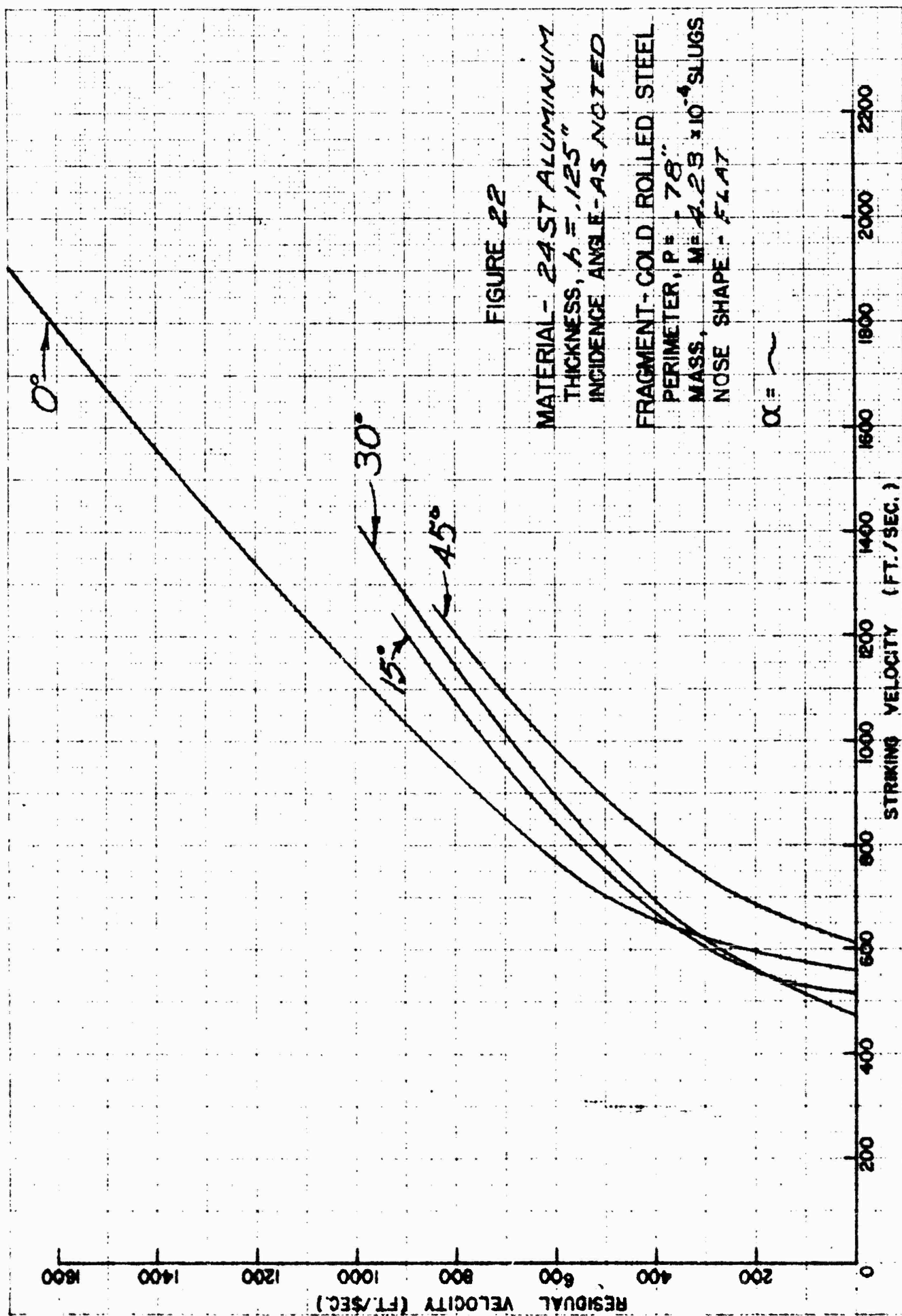


FIGURE 22

MATERIAL - 24 ST ALUMINUM
 THICKNESS, $t = .125"$
 INCIDENCE ANGLE - AS NOTED

FRAGMENT - COLD ROLLED STEEL
 PERIMETER, $P = .78"$
 MASS, $M = 4.23 \times 10^{-4}$ SLUGS
 NOSE SHAPE - FLAT

$\alpha = \sim$

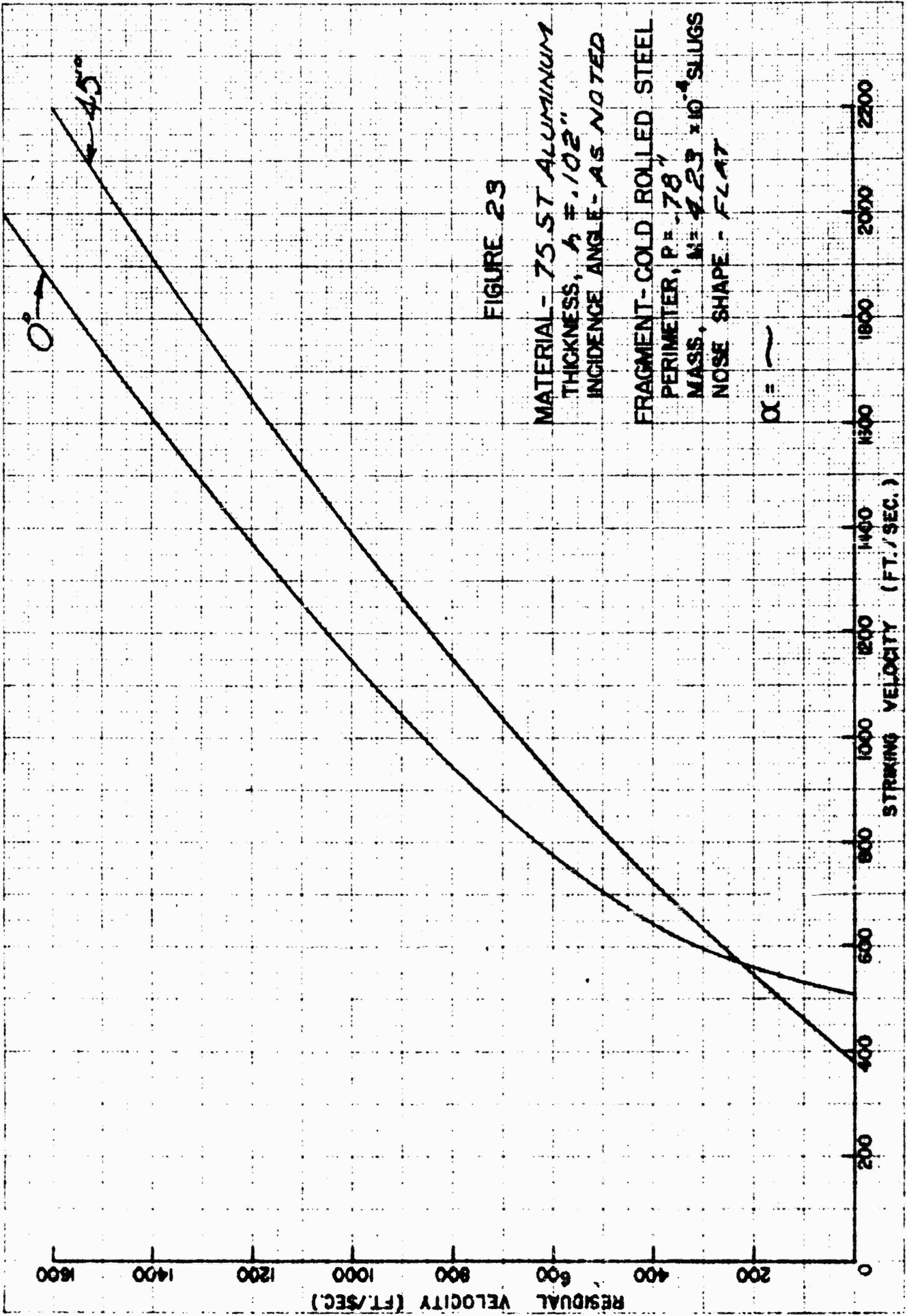


FIGURE 23

MATERIAL - 75 ST ALUMINUM
 THICKNESS, $t = .102"$
 INCIDENCE ANGLE - AS NOTED

FRAGMENT - COLD ROLLED STEEL
 PERIMETER, $P = .78"$
 MASS, $M = 4.23 \times 10^{-4}$ SLUGS
 NOSE SHAPE - FLAT

$\alpha =$ ~

DATA SHEETS

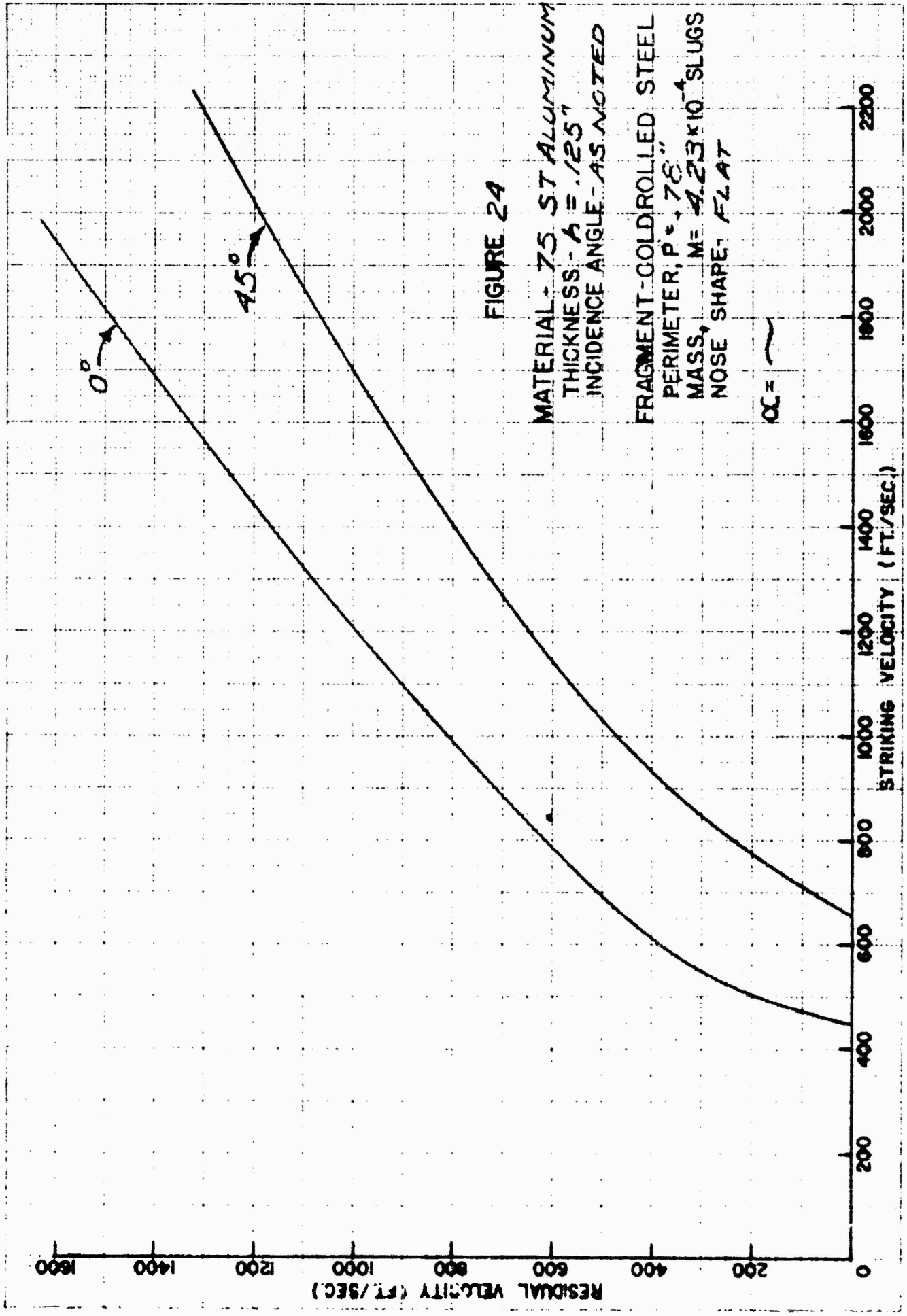


FIGURE 24

MATERIAL - 75 ST ALUMINUM
 THICKNESS - $t = .125"$
 INCIDENCE ANGLE - AS NOTED

FRAGMENT - GOLD ROLLED STEEL
 PERIMETER, $P = 78"$
 MASS, $M = 4.23 \times 10^{-4}$ SLUGS
 NOSE SHAPE: FLAT

$\alpha =$ ~

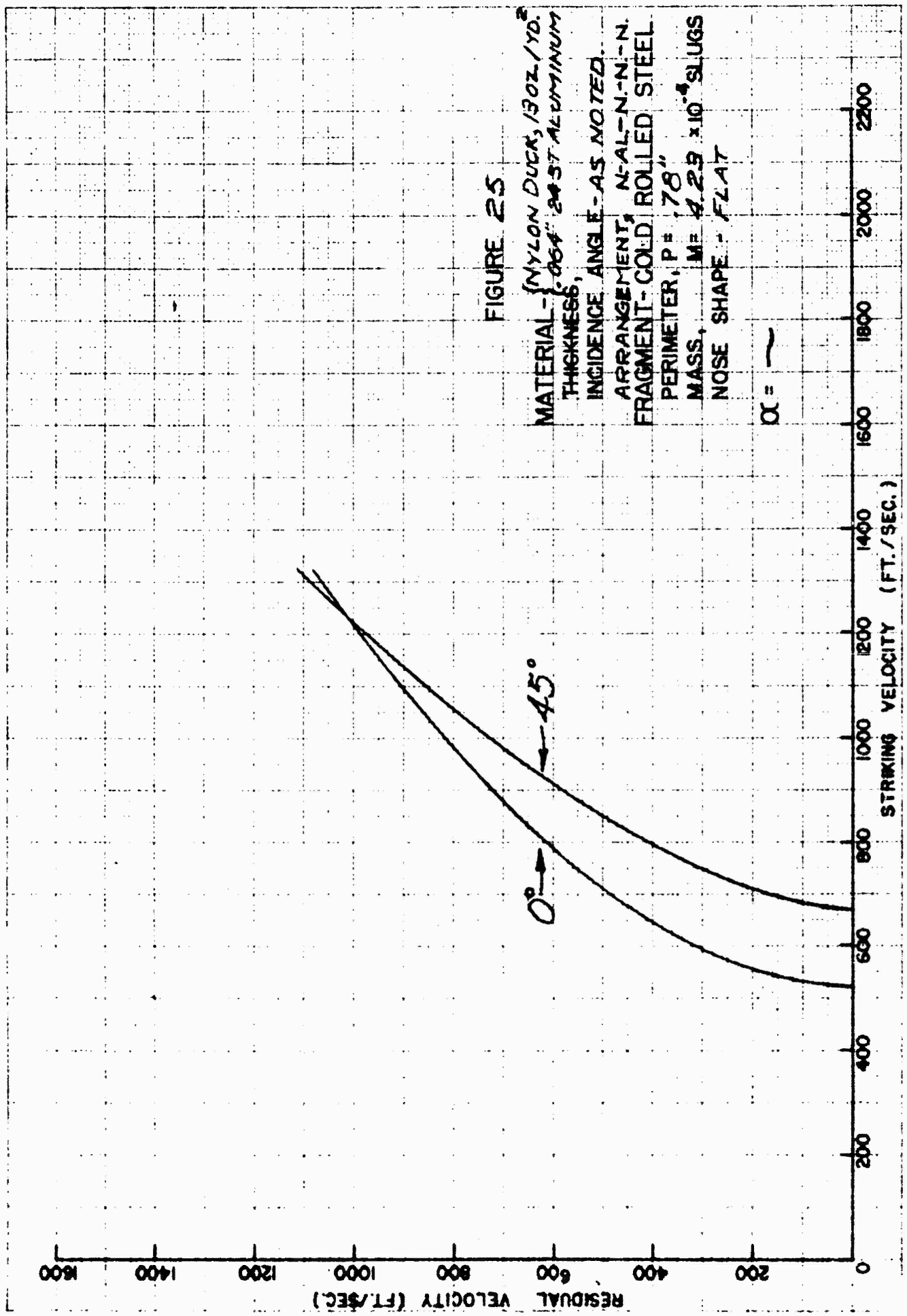
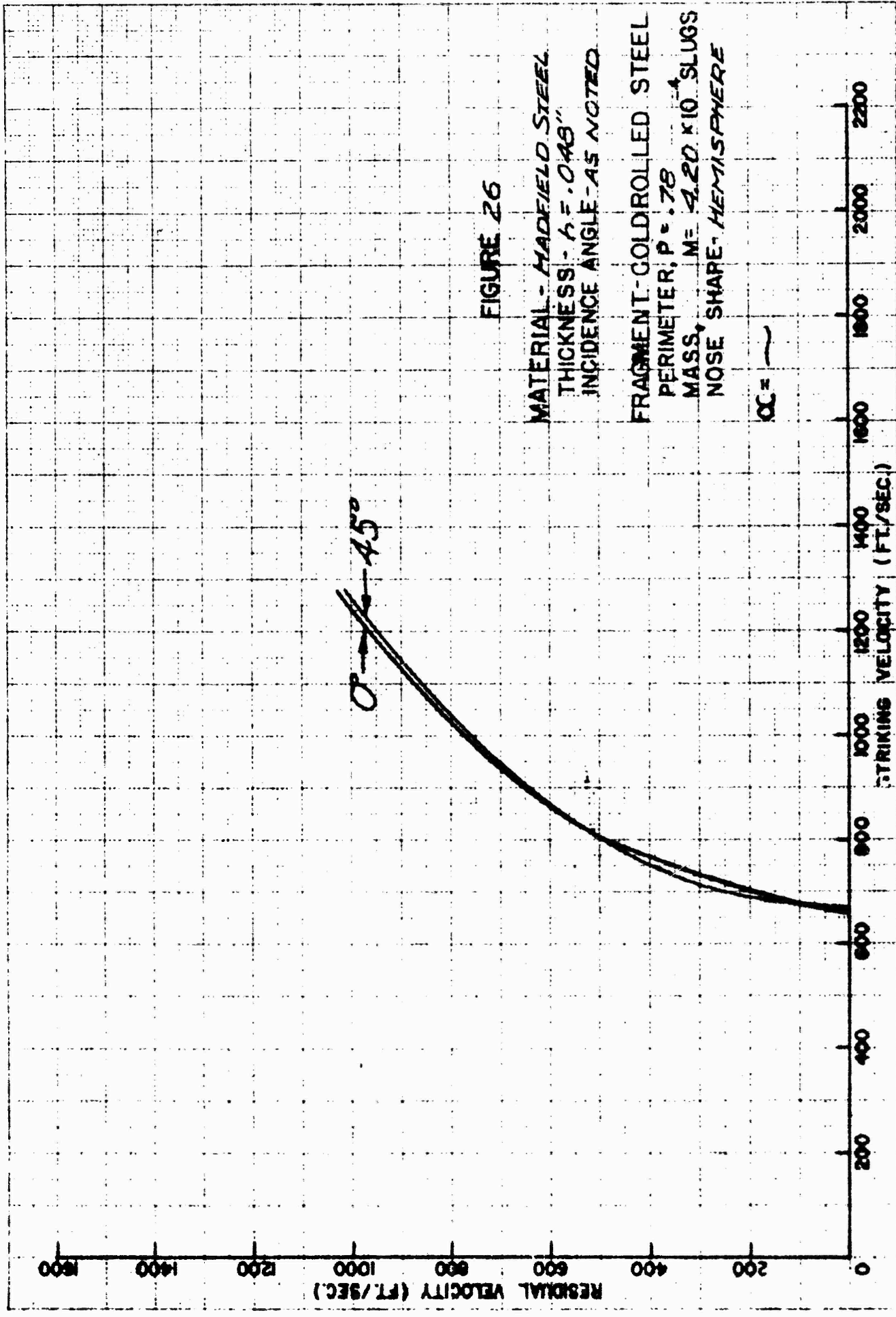


FIGURE 25

MATERIAL - NYLON DUCK, 130Z/YD.²
 THICKNESS, .064" 20 ST ALUMINUM
 INCIDENCE ANGLE - AS NOTED.
 ARRANGEMENT, N-AL-N-N-N.
 FRAGMENT - COLD ROLLED STEEL
 PERIMETER, P = 78"
 MASS, M = 4.29 x 10⁻⁴ SLUGS
 NOSE SHAPE - FLAT

$\alpha = \sim$



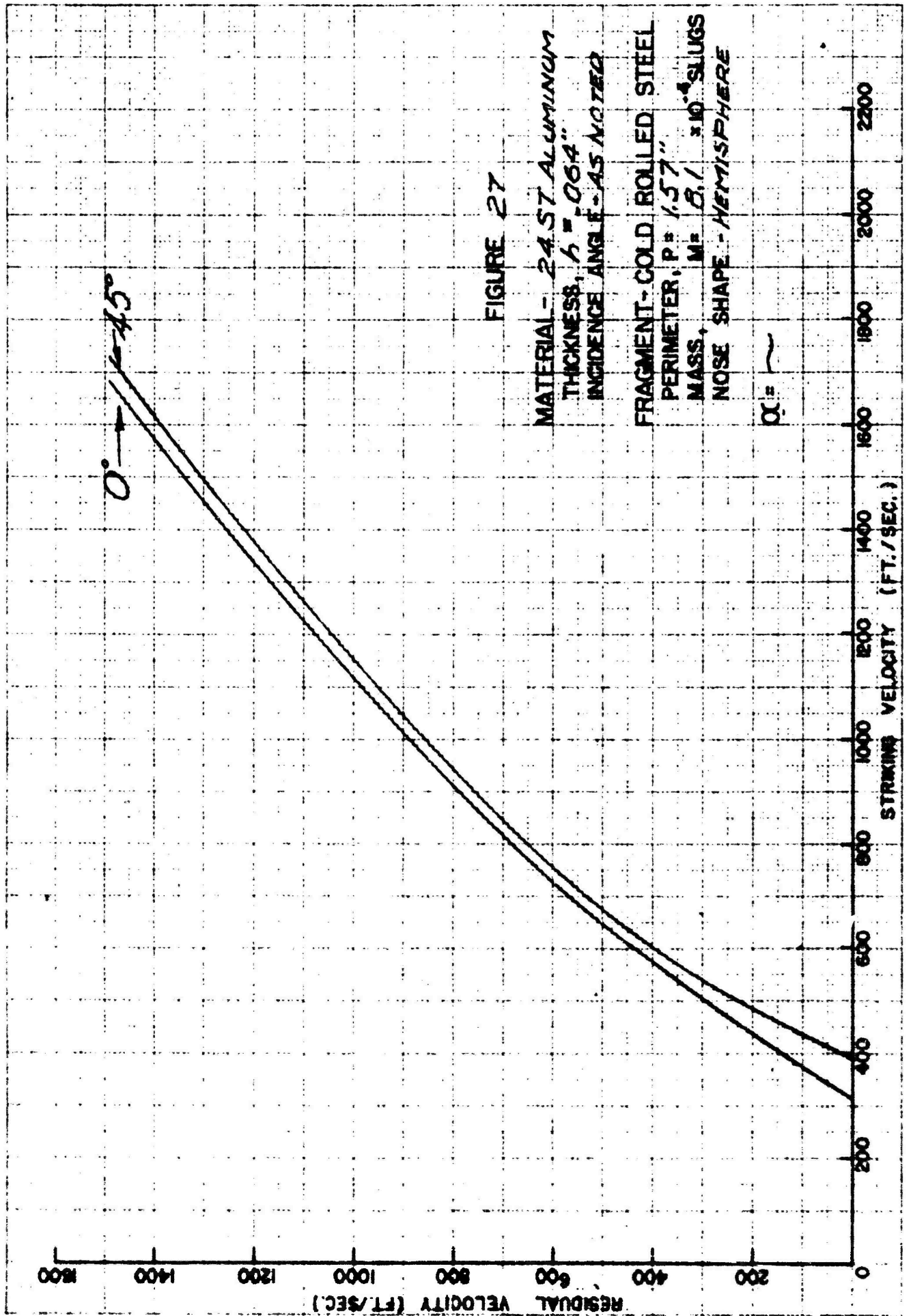


FIGURE 27

MATERIAL - 24 ST ALUMINUM
 THICKNESS, $t = .064"$
 INCIDENCE ANGLE - AS NOTED

FRAGMENT - COLD ROLLED STEEL
 PERIMETER, $P = 1.57"$
 MASS, $M = 5.1 \times 10^{-4}$ SLUGS
 NOSE SHAPE - HEMISPHERE

$\alpha = \sim$

CHARLES W. ... W. ...

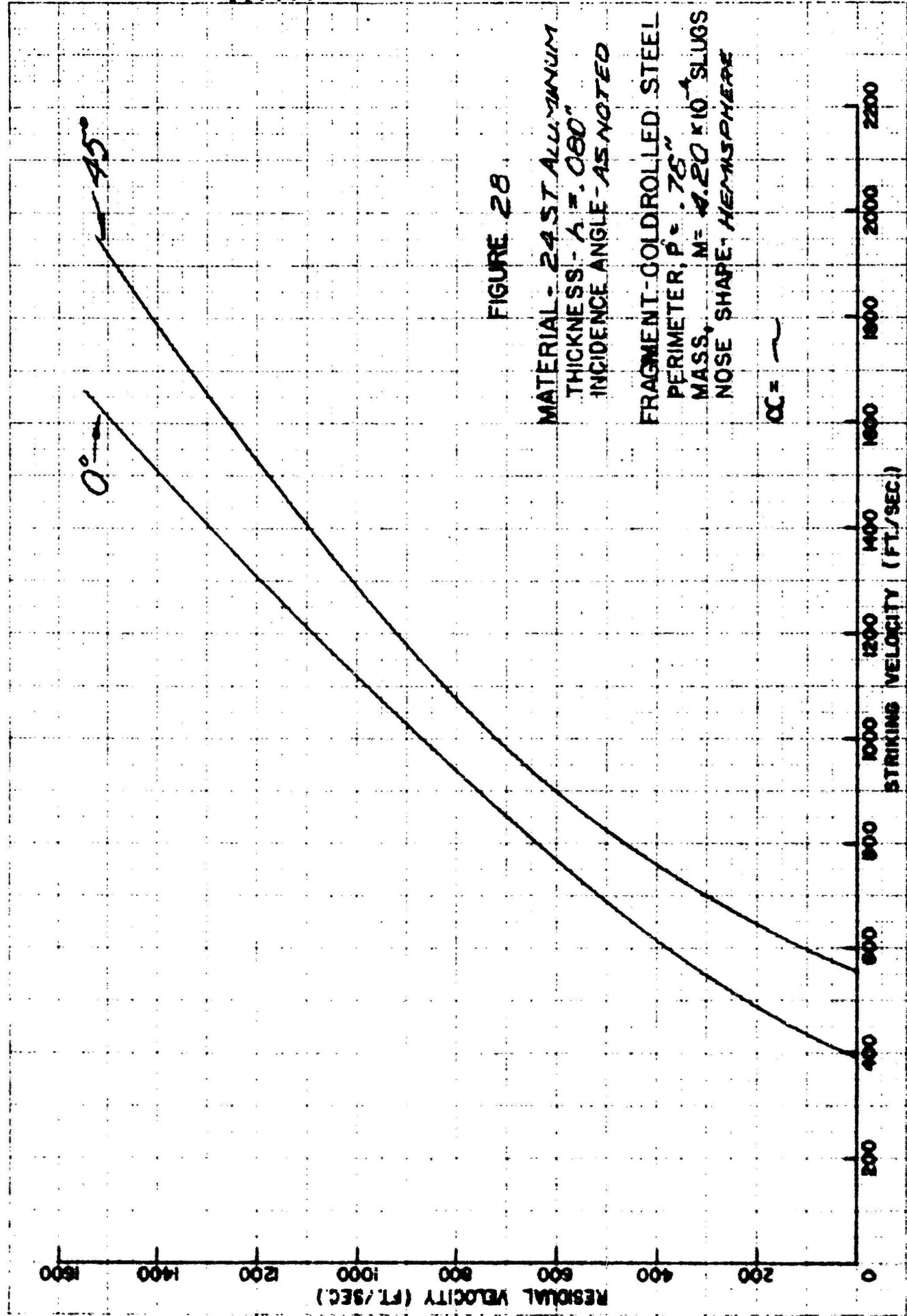


FIGURE 28

MATERIAL - 24 ST. ALUMINUM
 THICKNESS - $t = .060"$
 INCIDENCE ANGLE - AS NOTED

FRAGMENT - GOLD ROLLED STEEL
 PERIMETER, $P = .75"$
 MASS, $M = 0.20 \times 10^{-4}$ SLUGS
 NOSE SHAPE - HEMISPHERE

$OC =$ ~

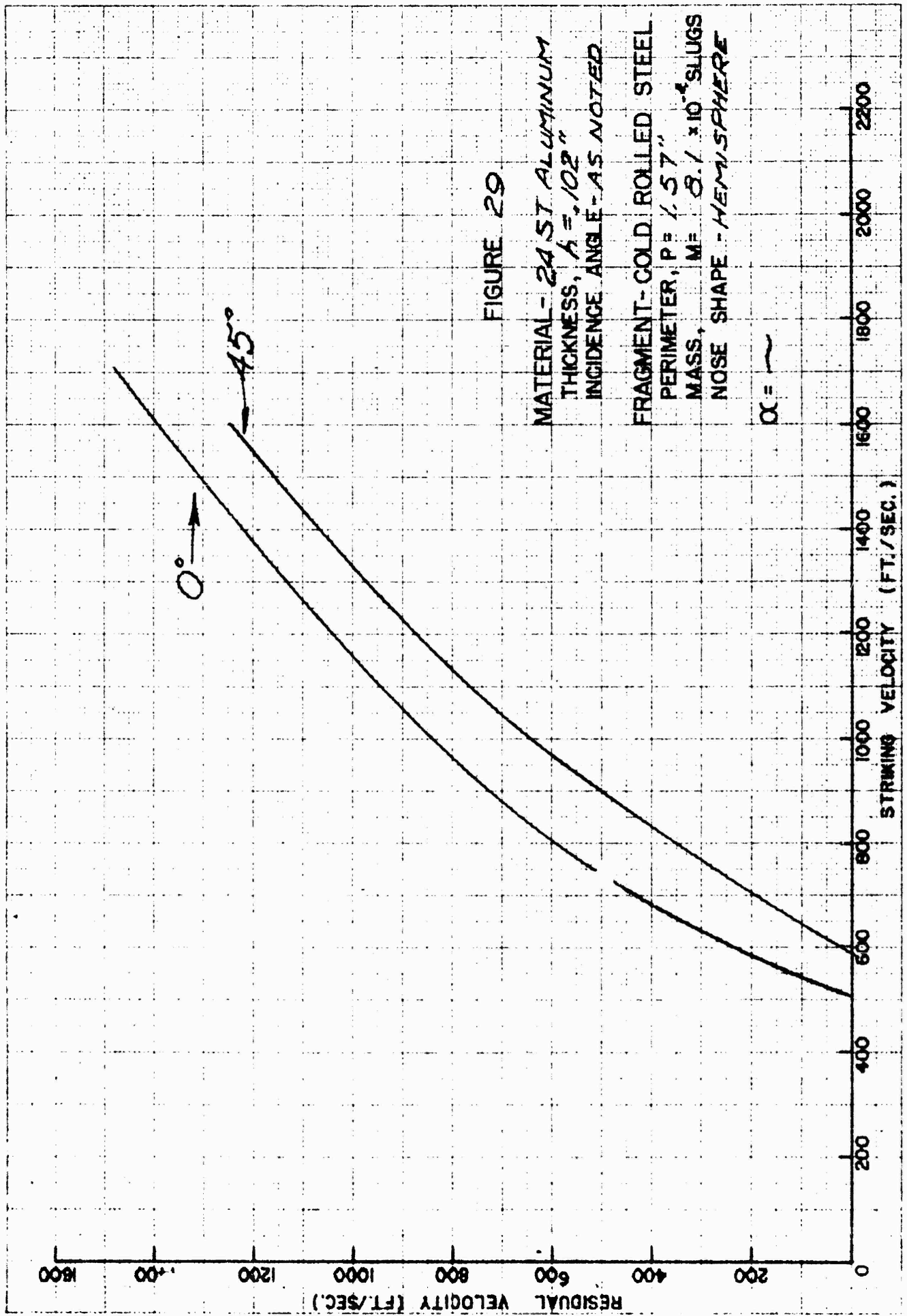


FIGURE 29

MATERIAL - 24 ST ALUMINUM
THICKNESS, $t = .102$ "
INCIDENCE ANGLE - AS NOTED
FRAGMENT - COLD ROLLED STEEL
PERIMETER, $P = 1.57$ "
MASS, $M = 8.1 \times 10^{-4}$ SLUGS
NOSE SHAPE - HEMISPHERE

$\alpha = \sim$

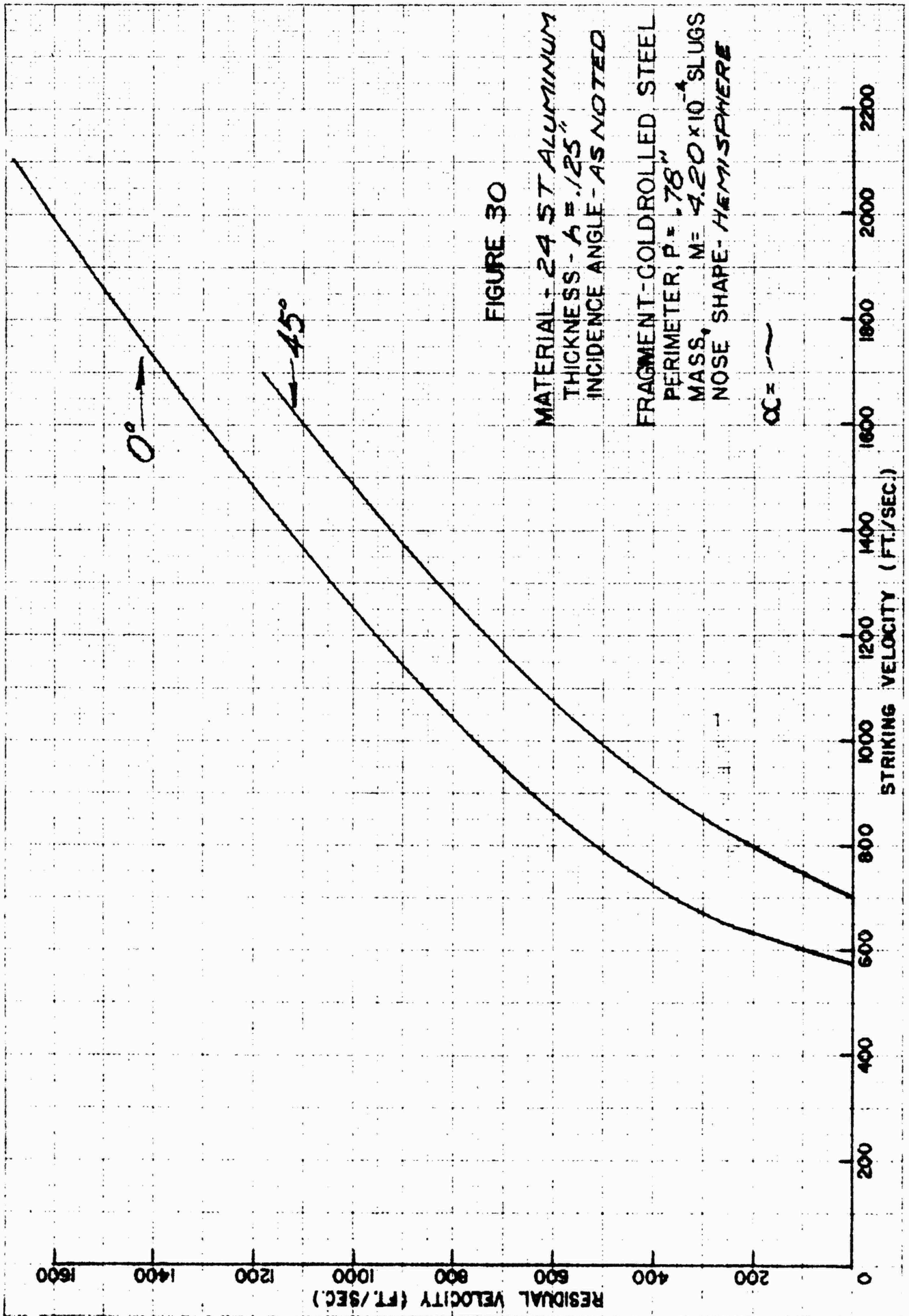


FIGURE 30

MATERIAL - 24 ST ALUMINUM
THICKNESS - $A = .125$ "
INCIDENCE ANGLE - AS NOTED

FRAGMENT - COLD ROLLED STEEL
PERIMETER, $P = .78$ "
MASS, $M = 4.20 \times 10^{-4}$ SLUGS
NOSE SHAPE - HEMISPHERE

$\alpha =$ ~

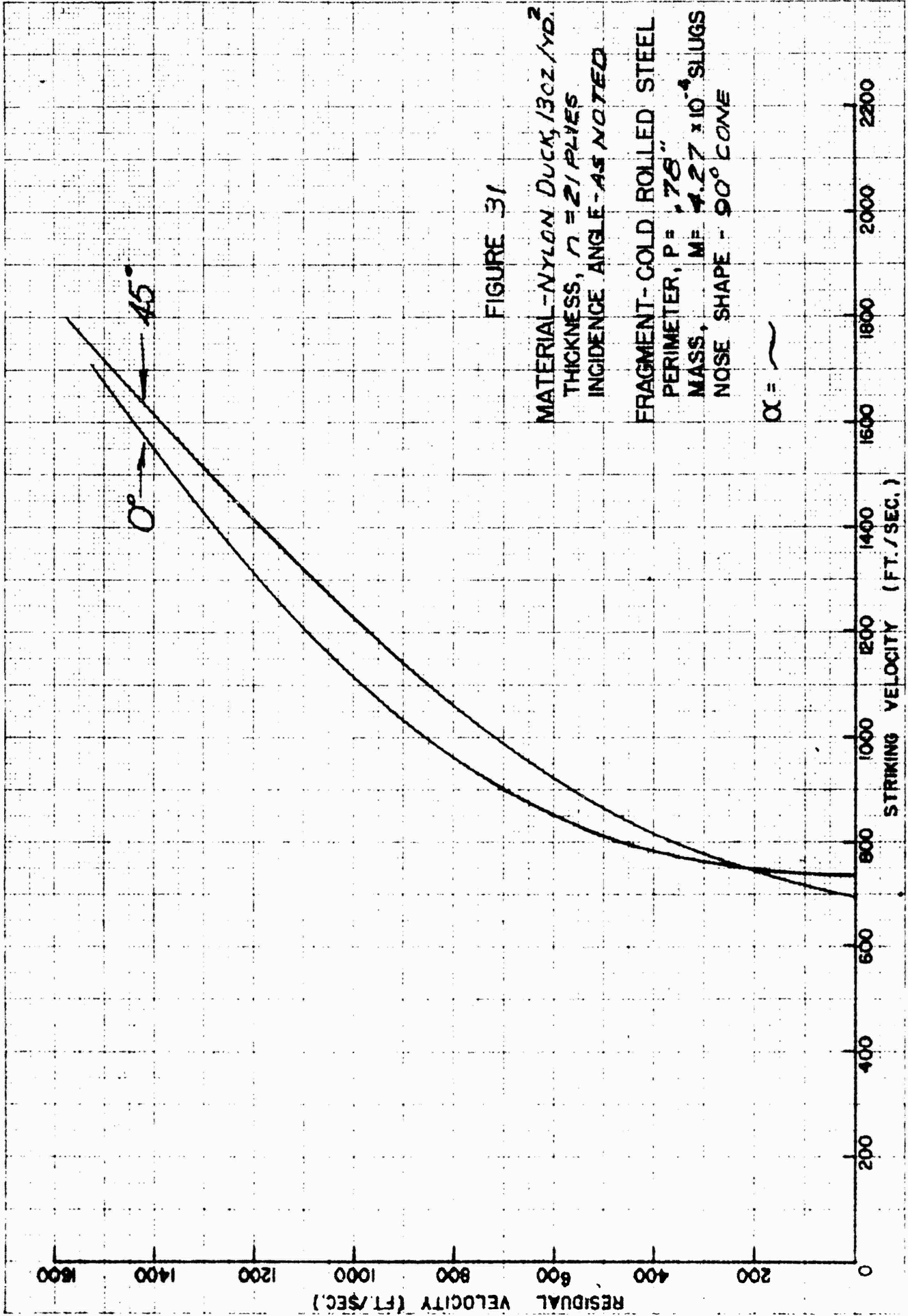


FIGURE 31

MATERIAL - NYLON DUCK, 130Z/YD.²
THICKNESS, $n = 21$ PLYES
INCIDENCE ANGLE - AS NOTED
FRAGMENT - COLD ROLLED STEEL
PERIMETER, $P = .78''$
MASS, $M = 4.27 \times 10^{-4}$ SLUGS
NOSE SHAPE - 90° CONE

$\alpha = \sim$

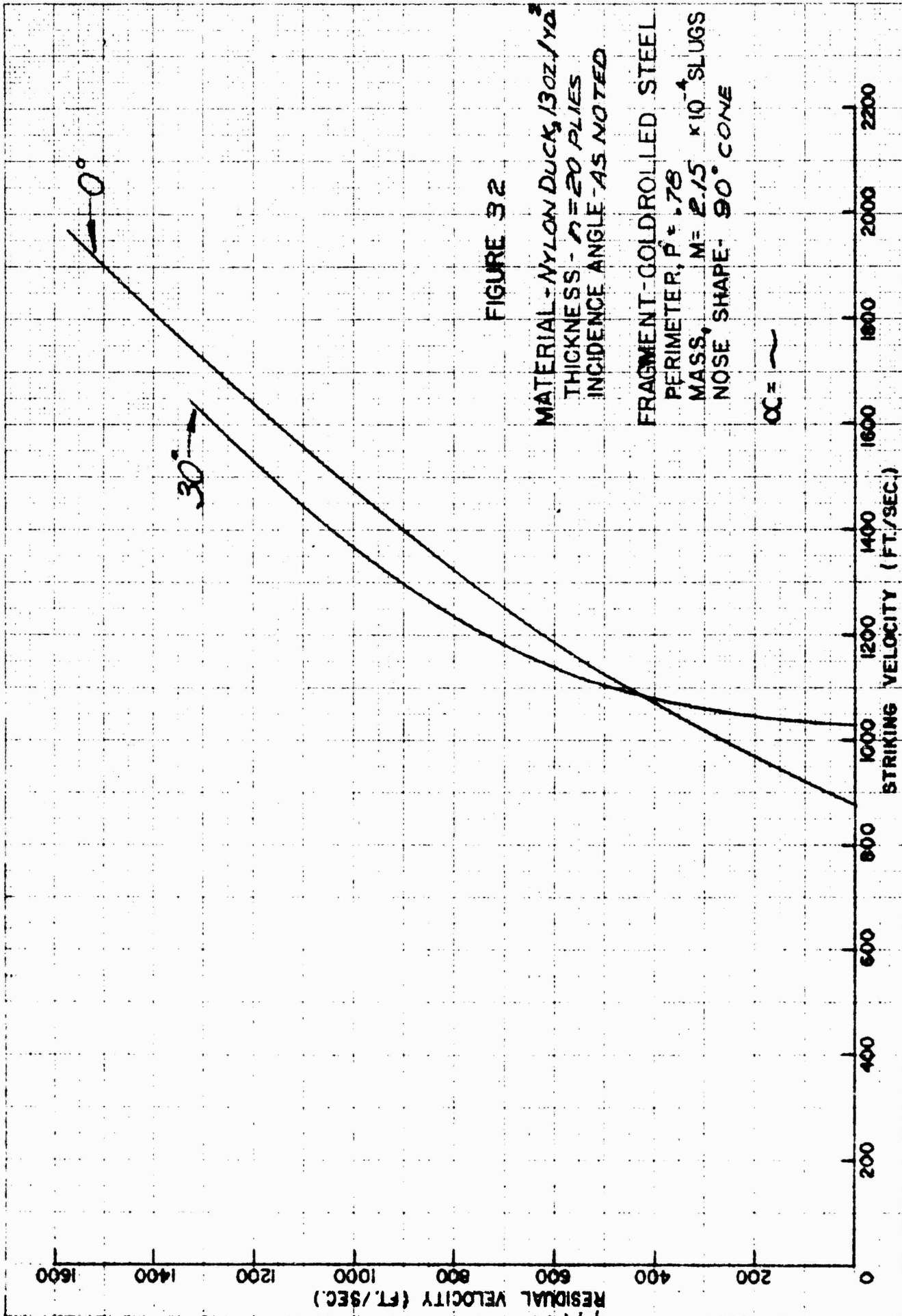


FIGURE 32

MATERIAL - NYLON DUCK, 130Z/YD.²
THICKNESS - $t = 20$ PLIES
INCIDENCE ANGLE - AS NOTED

FRAGMENT - GOLDROLLED STEEL
PERIMETER, $P = 1.78$
MASS, $M = 2.15 \times 10^{-4}$ SLUGS
NOSE SHAPE - 90° CONE

OC = ~

RESTRICTED

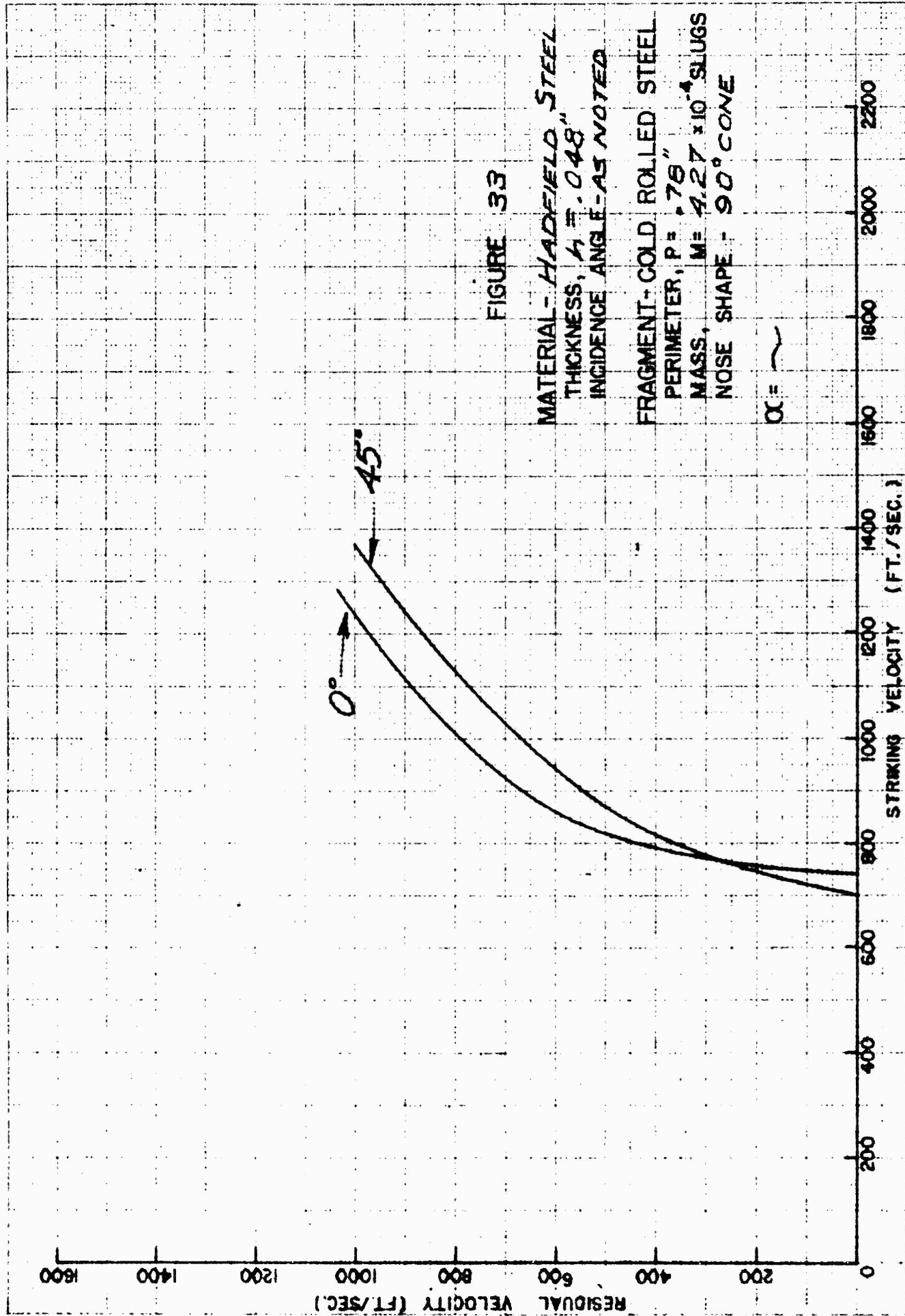


FIGURE 33

MATERIAL - HADFIELD STEEL
THICKNESS, $t = .048$ "
INCIDENCE ANGLE - AS NOTED

FRAGMENT - COLD ROLLED STEEL
PERIMETER, $P = .76$ "
MASS, $M = 4.27 \times 10^{-4}$ SLUGS
NOSE SHAPE - 90° CONE

$\alpha = \sim$

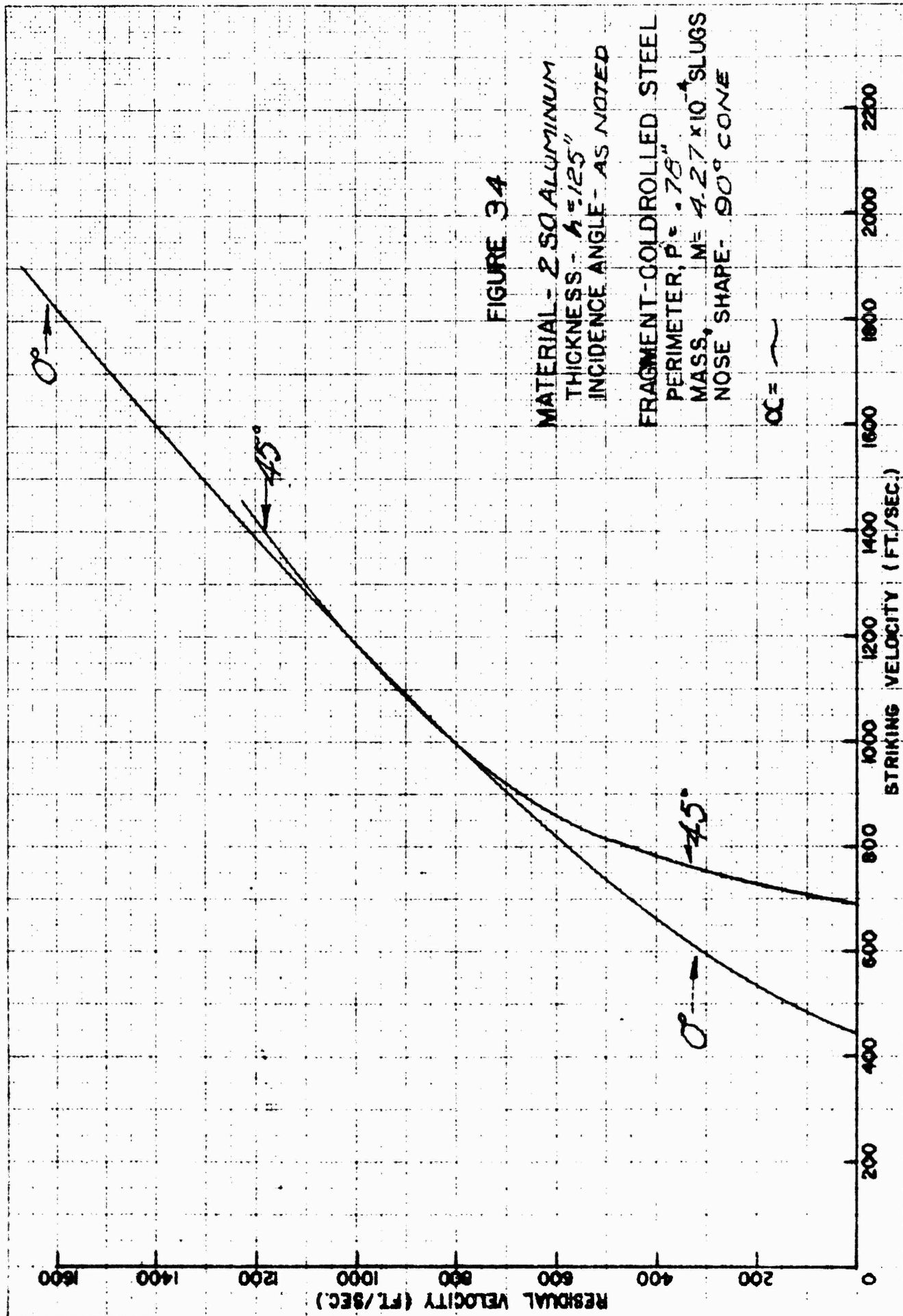


FIGURE 3.4

MATERIAL - 2 SQ ALUMINUM
THICKNESS - $h = .125"$
INCIDENCE ANGLE - AS NOTED
FRAGMENT-COLDROLLED STEEL
PERIMETER, $P = .78"$
MASS, $M = 4.27 \times 10^{-4}$ SLUGS
NOSE SHAPE - 90° CONE

$OC = \sim$

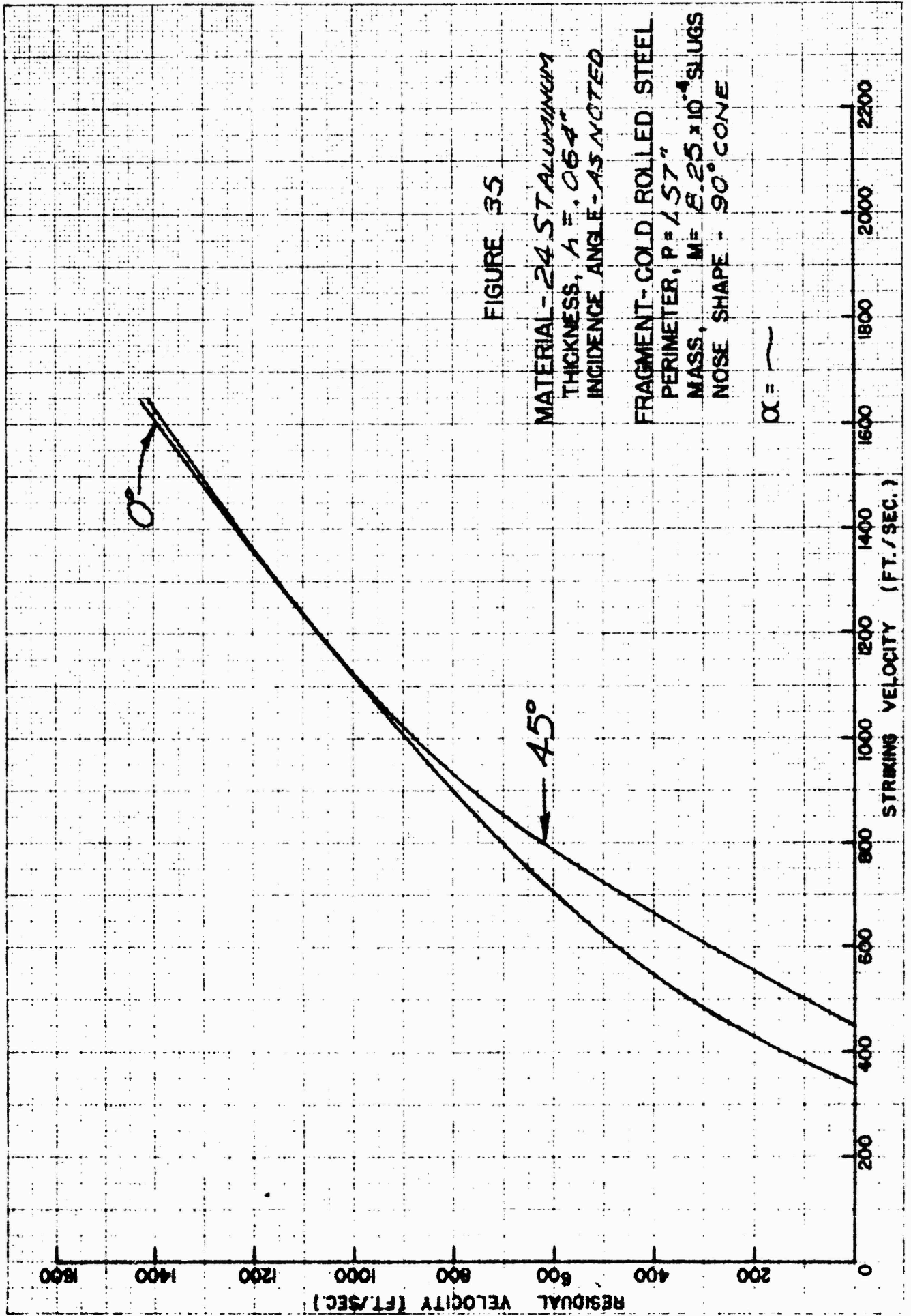


FIGURE 35

MATERIAL - 24 S.T. ALUMINUM
 THICKNESS, $t = .064"$
 INCIDENCE ANGLE - AS NOTED

FRAGMENT - COLD ROLLED STEEL
 PERIMETER, $P = 1.57"$
 MASS, $M = 8.25 \times 10^{-4}$ SLUGS
 NOSE SHAPE - 90° CONE

$\alpha =$ ~

RESTRICTED

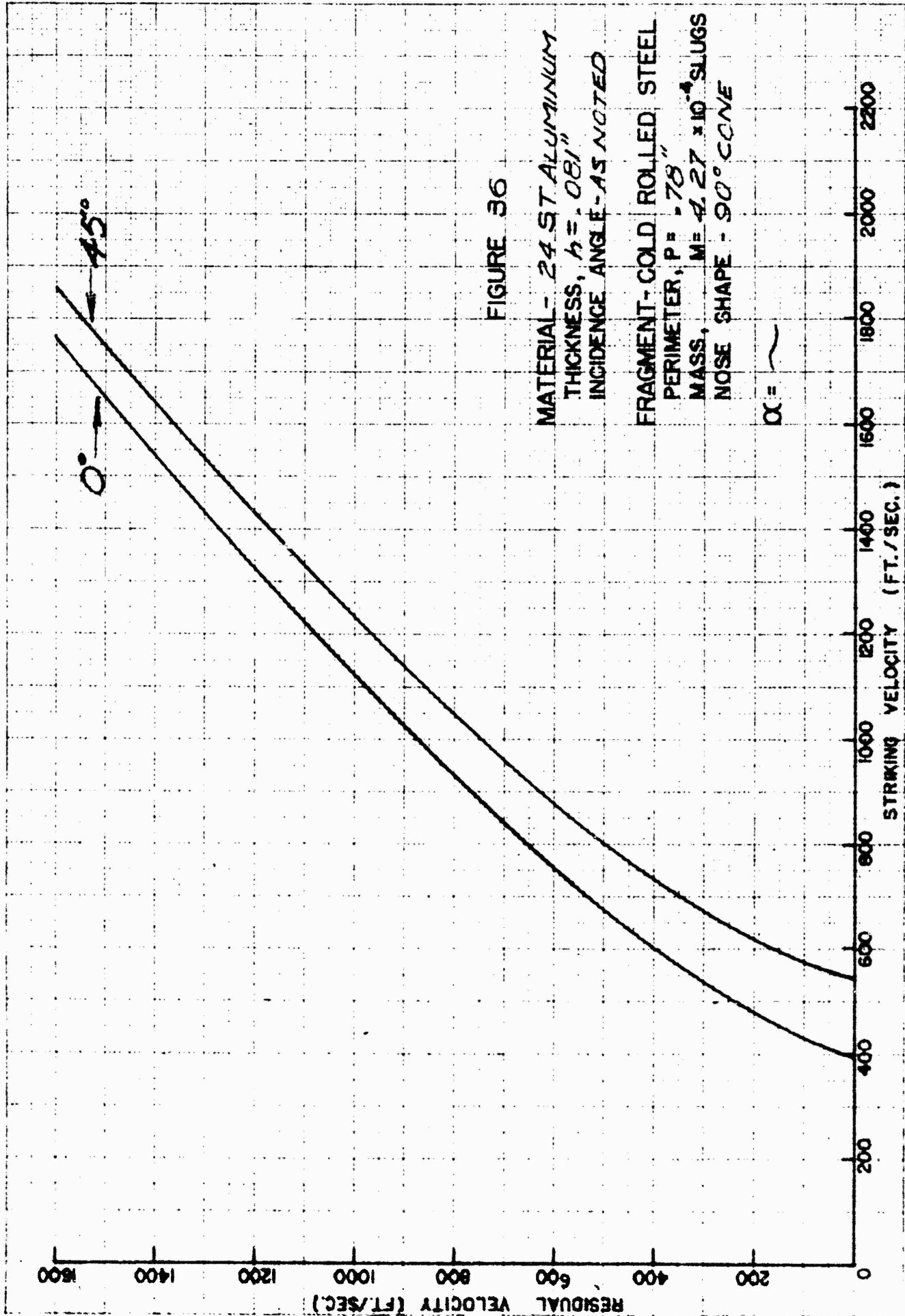


FIGURE 36

MATERIAL - 24 ST ALUMINUM
THICKNESS, $h = .081$ "
INCIDENCE ANGLE - AS NOTED

FRAGMENT - COLD ROLLED STEEL
PERIMETER, $P = .78$ "
MASS, $M = 4.27 \times 10^{-4}$ SLUGS
NOSE SHAPE - 90° CONE

$\alpha = \sim$

RESTRICTED

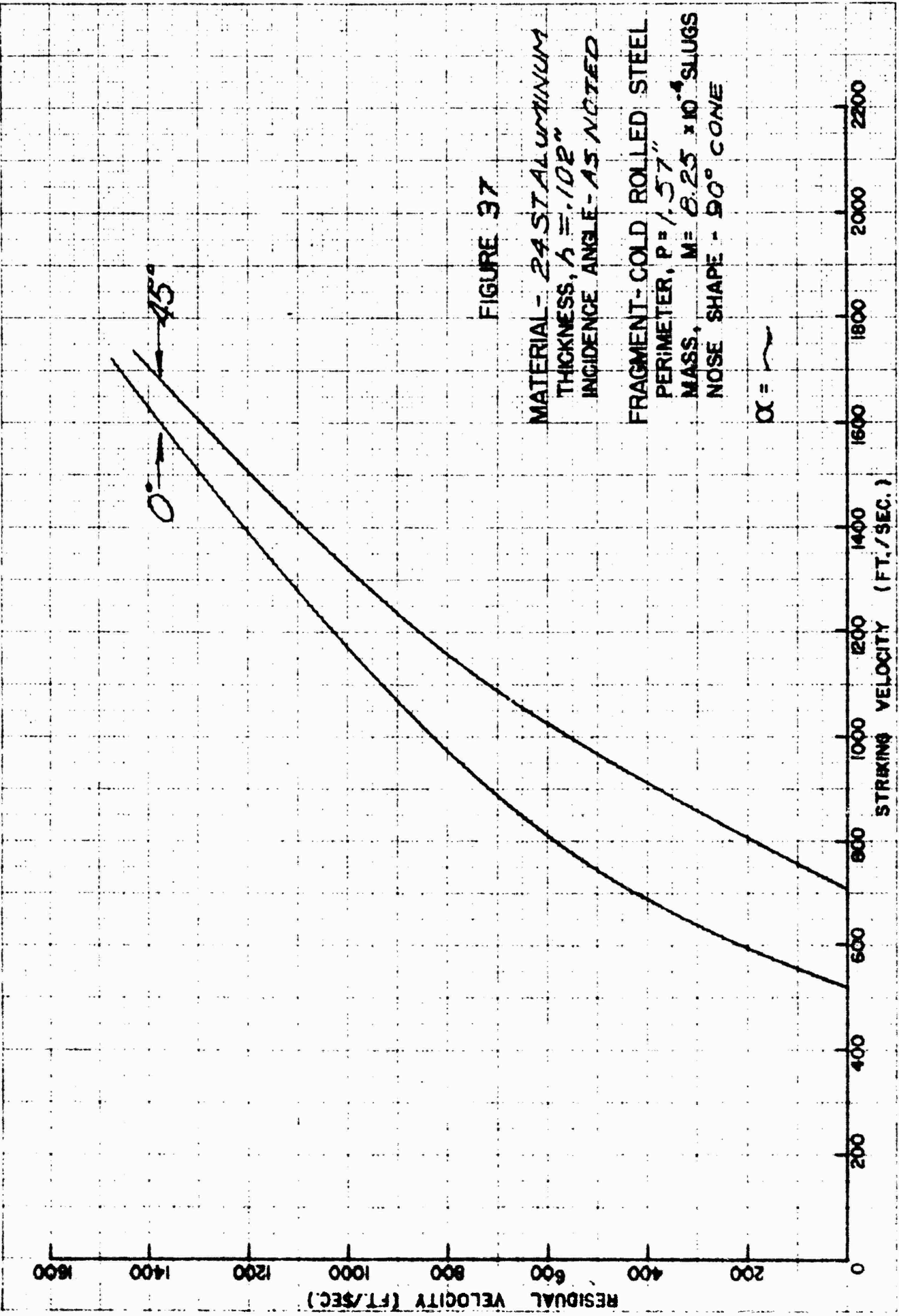


FIGURE 37

MATERIAL - 24S ALUMINUM
 THICKNESS, $t = .102"$
 INCIDENCE ANGLE - AS NOTED

FRAGMENT - COLD ROLLED STEEL
 PERIMETER, $P = 1.57"$
 MASS, $M = 8.25 \times 10^{-4}$ SLUGS
 NOSE SHAPE - 90° CONE

$\alpha =$

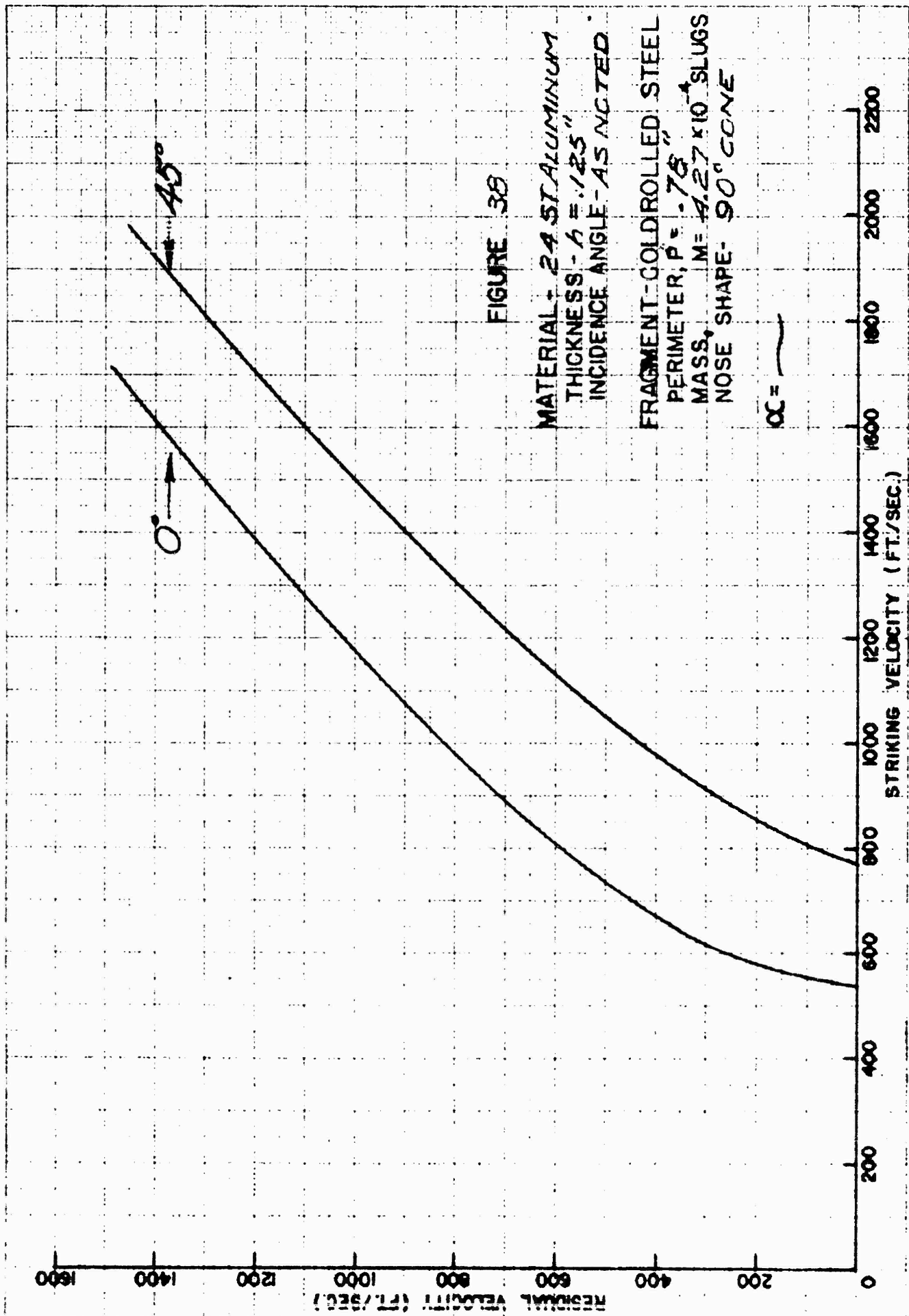
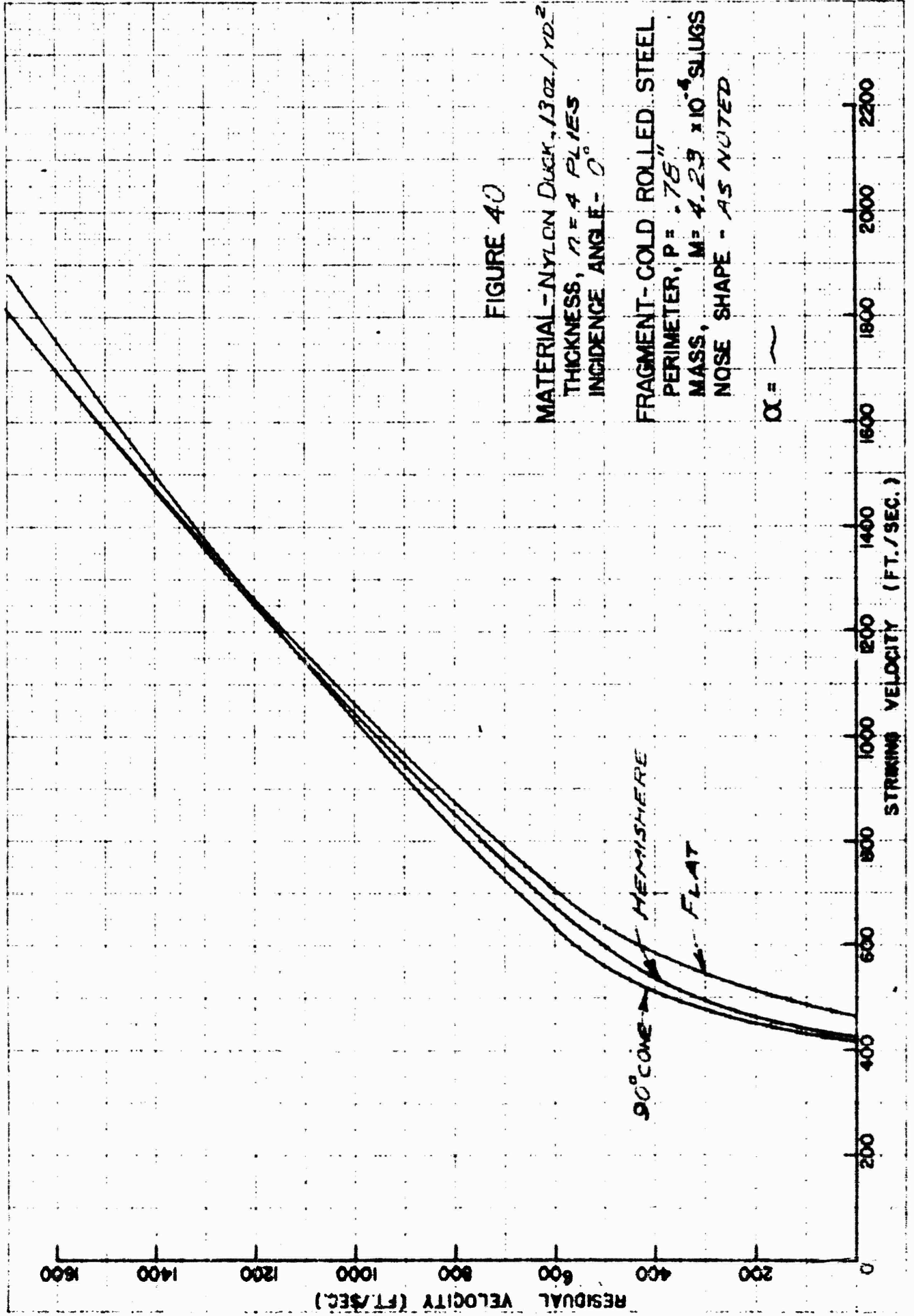


FIGURE 38

MATERIAL - 24 ST ALUMINUM
THICKNESS - $t = .125$ "
INCIDENCE ANGLE - 45 DEGREES

FRAGMENT - COLDROLLED STEEL
PERIMETER, $P = .78$ "
MASS, $M = 4.27 \times 10^{-4}$ SLUGS
NOSE SHAPE - 90 DEGREE

$\alpha =$ [Symbol]



RESTRICTED

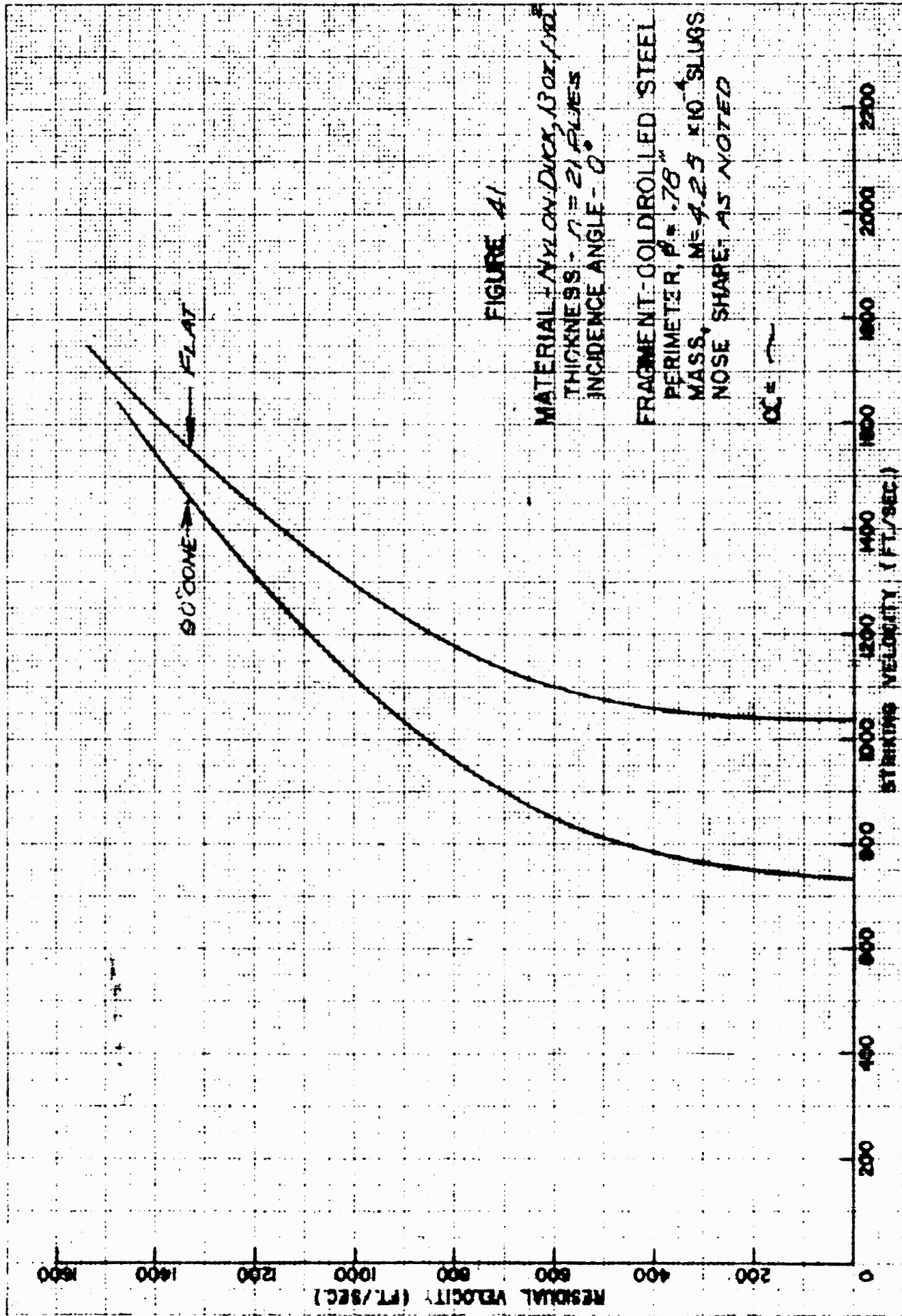


FIGURE 41

MATERIAL - NYLON DUCTS, 30X, 100X
 THICKNESS - $t = 21$ PLIES
 INCIDENCE ANGLE - Q

FRAGMENT - COLD ROLLED STEEL
 PERIMETER, $P = .78$ "
 MASS, $M = 4.25 \times 10^{-4}$ SLUGS
 NOSE SHAPE AS NOTED

OC =

REPRODUCED FROM THE REPORT

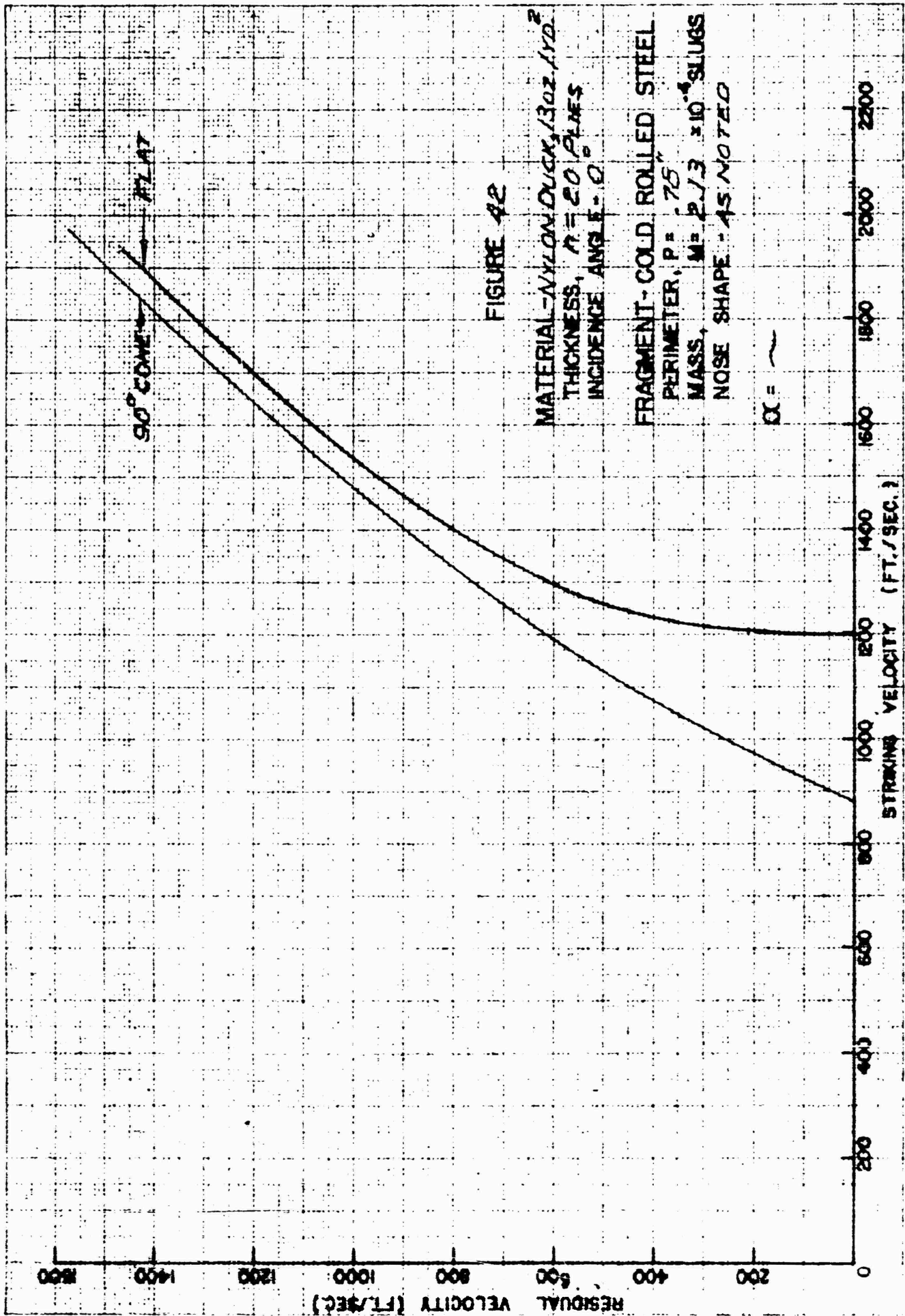


FIGURE 42

MATERIAL - NYLON DUCK, 130Z, 1/16" THICKNESS, $n = 20$ PLATES
INCIDENCE ANGLE - 0

FRAGMENT - COLD ROLLED STEEL
PERIMETER, $P = .75$ "
MASS, $M = 2.13 \times 10^{-4}$ SLUGS
NOSE SHAPE - AS NOTED

$\alpha = \sim$

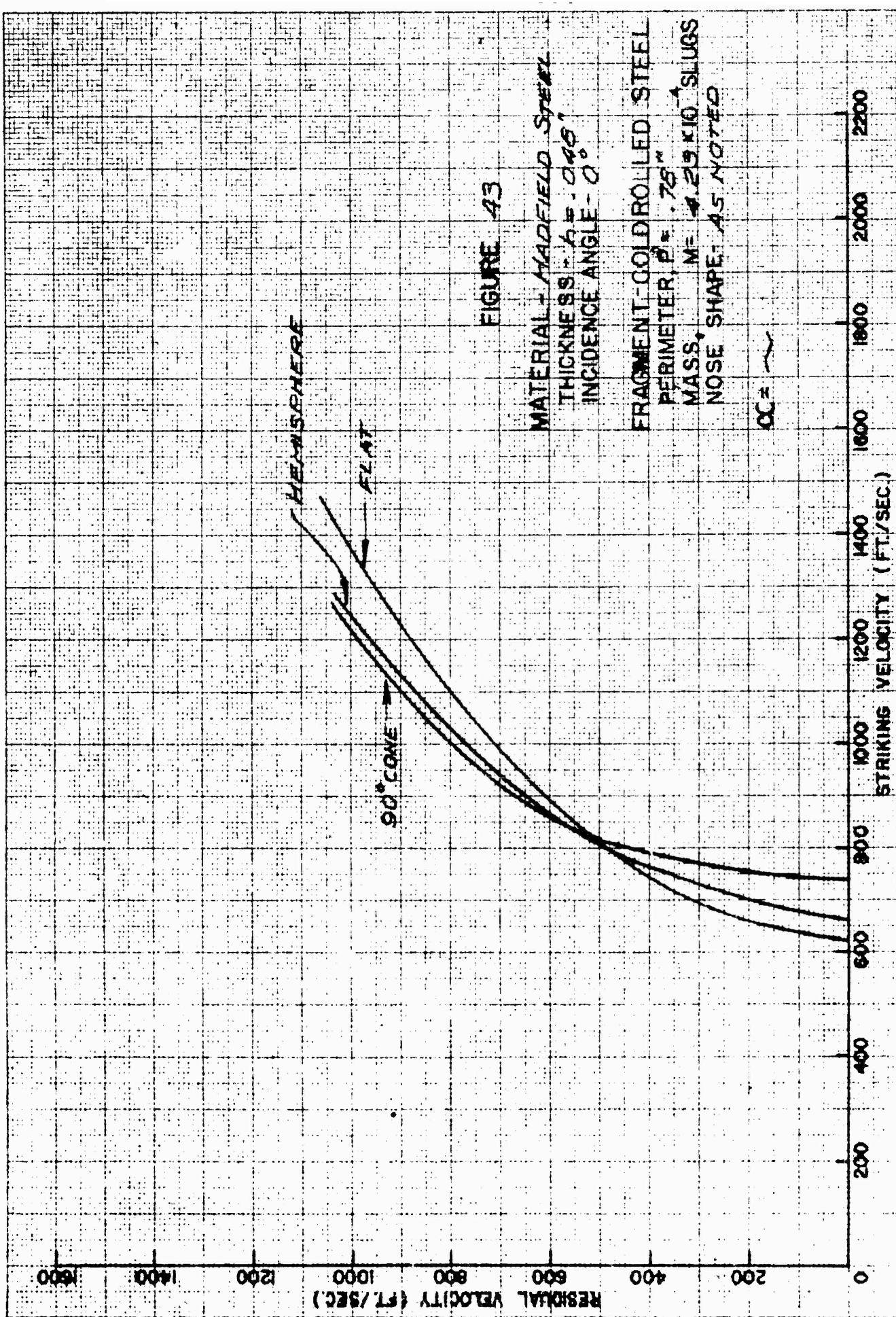


FIGURE 43

MATERIAL - MADFIELD STEEL
THICKNESS - .045"
INCIDENCE ANGLE - 0°
FRAGMENT - COLD ROLLED STEEL
PERIMETER, P = .75"
MASS, M = 4.29 X 10⁻⁴ SLUGS
NOSE SHAPE - AS NOTED

CC = ~

RESTRICTED

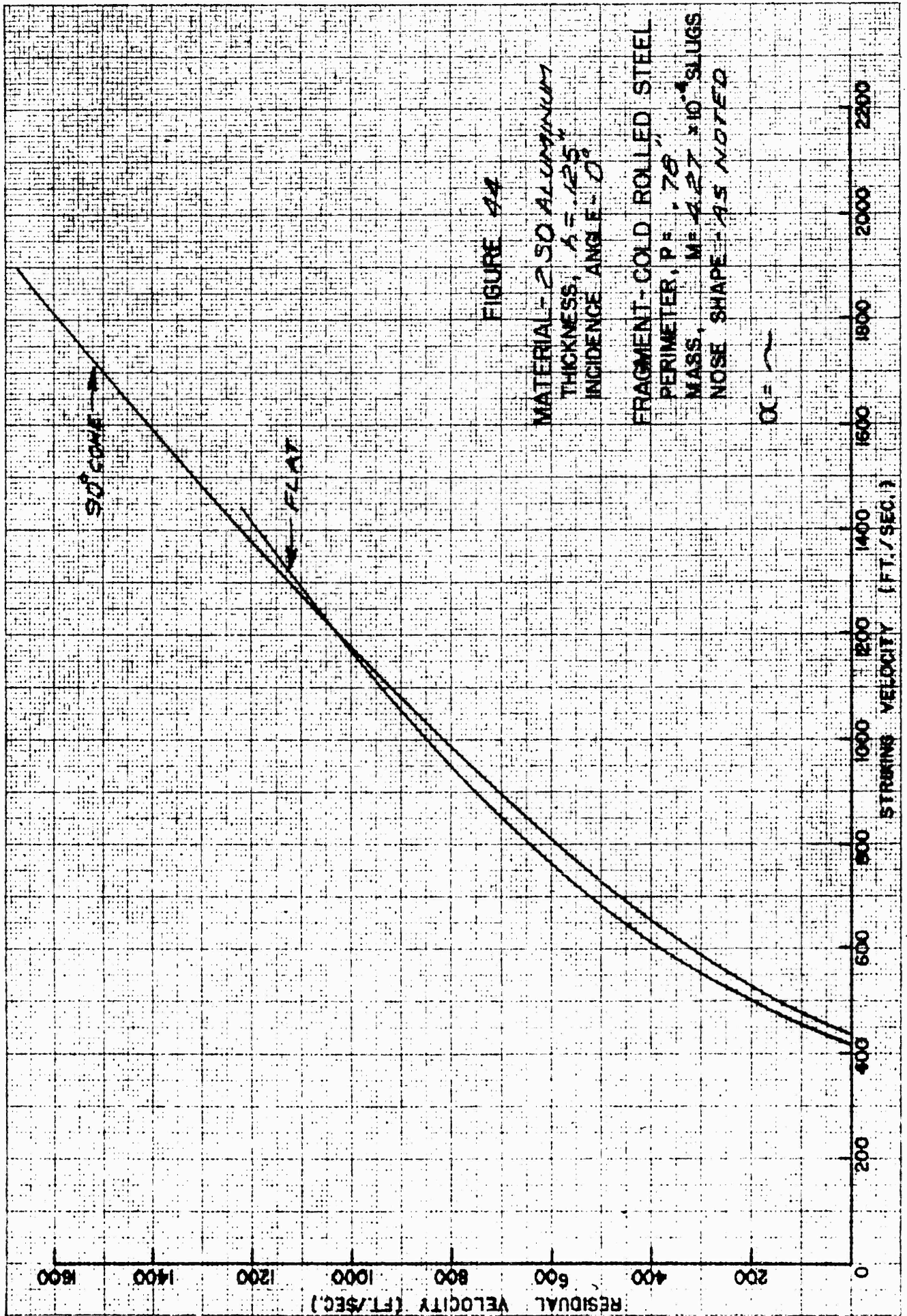
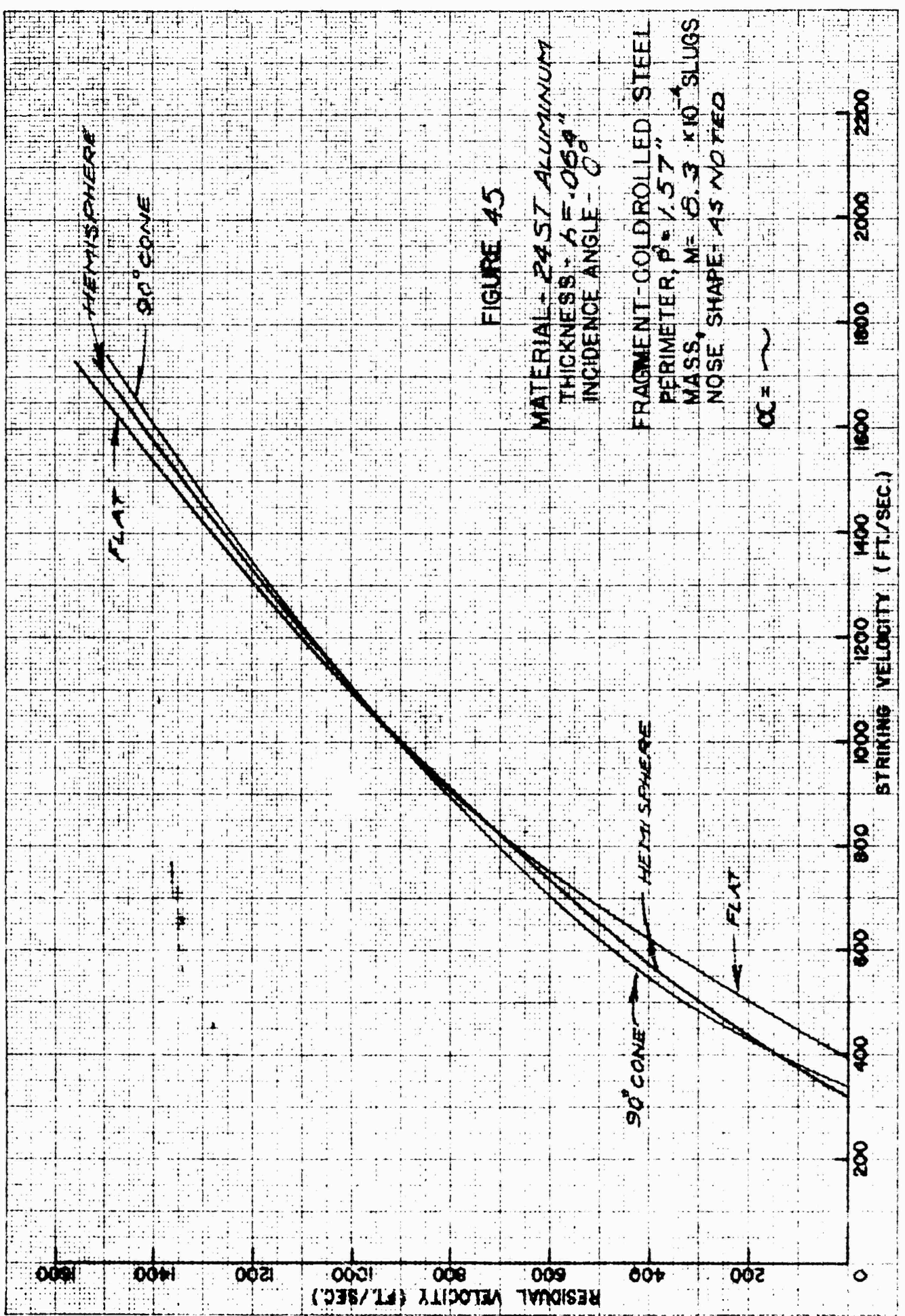


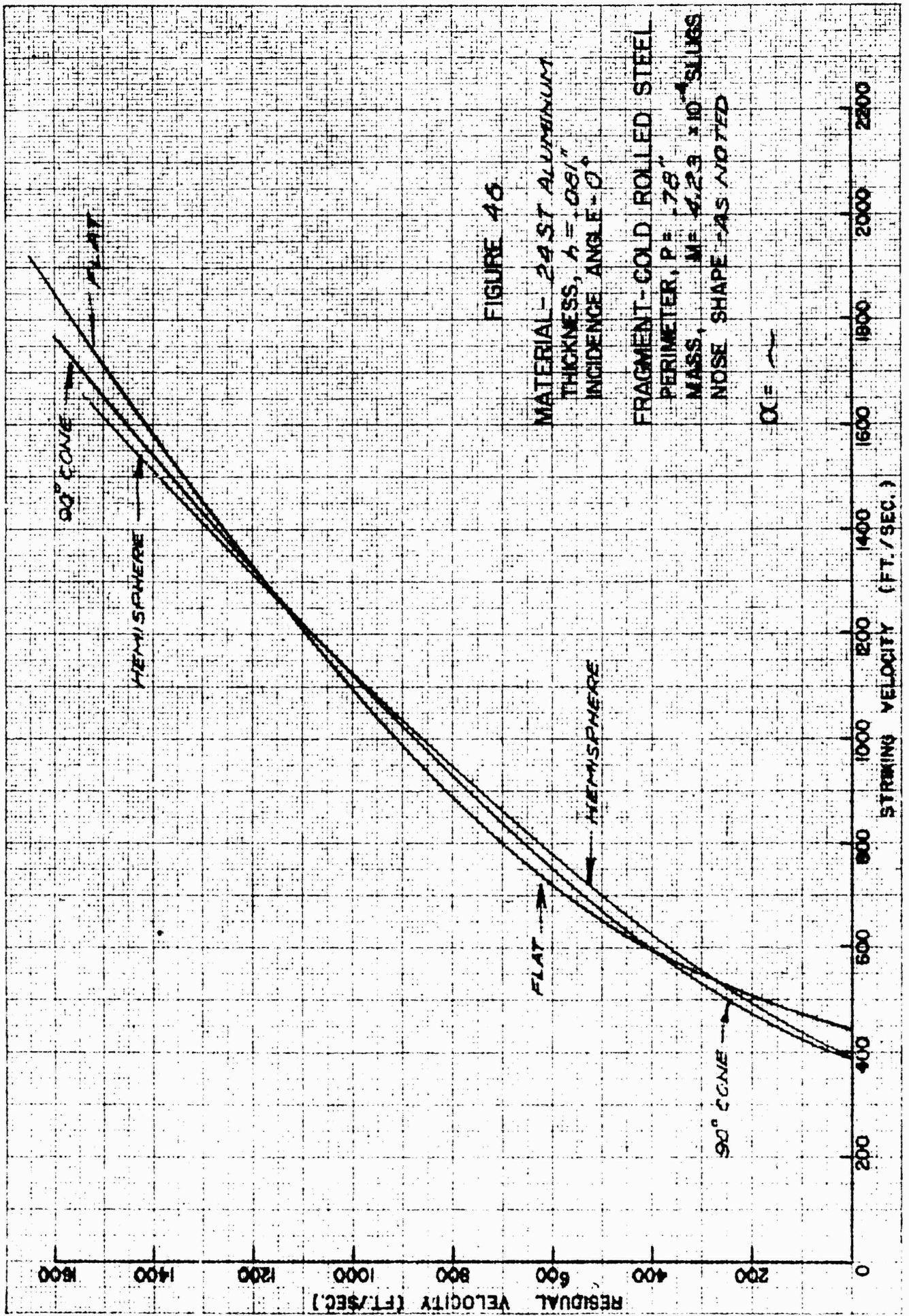
FIGURE 84

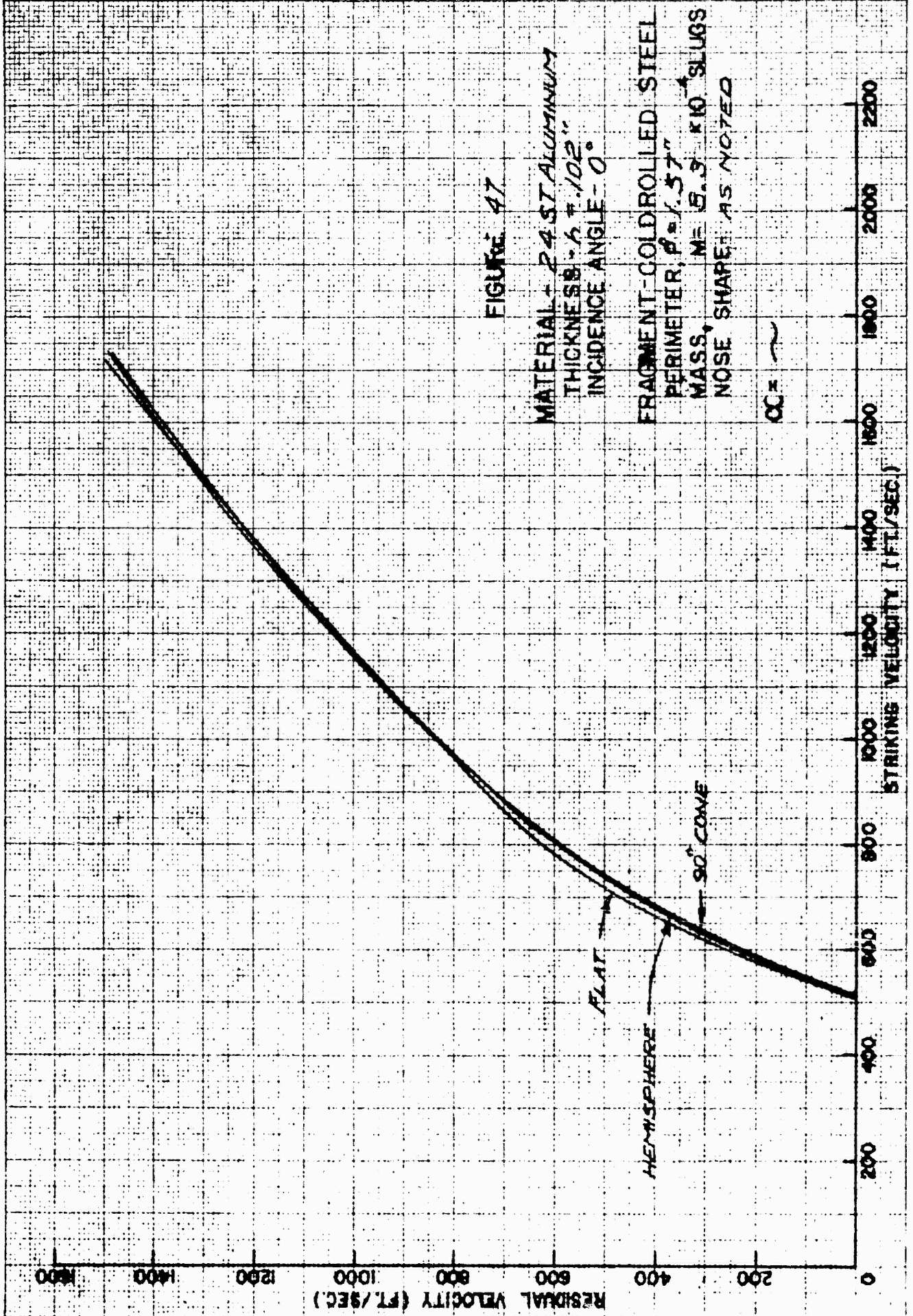
MATERIAL - 250 ALUMINUM
THICKNESS, $t = .125$ "
INCIDENCE ANGLE - 0

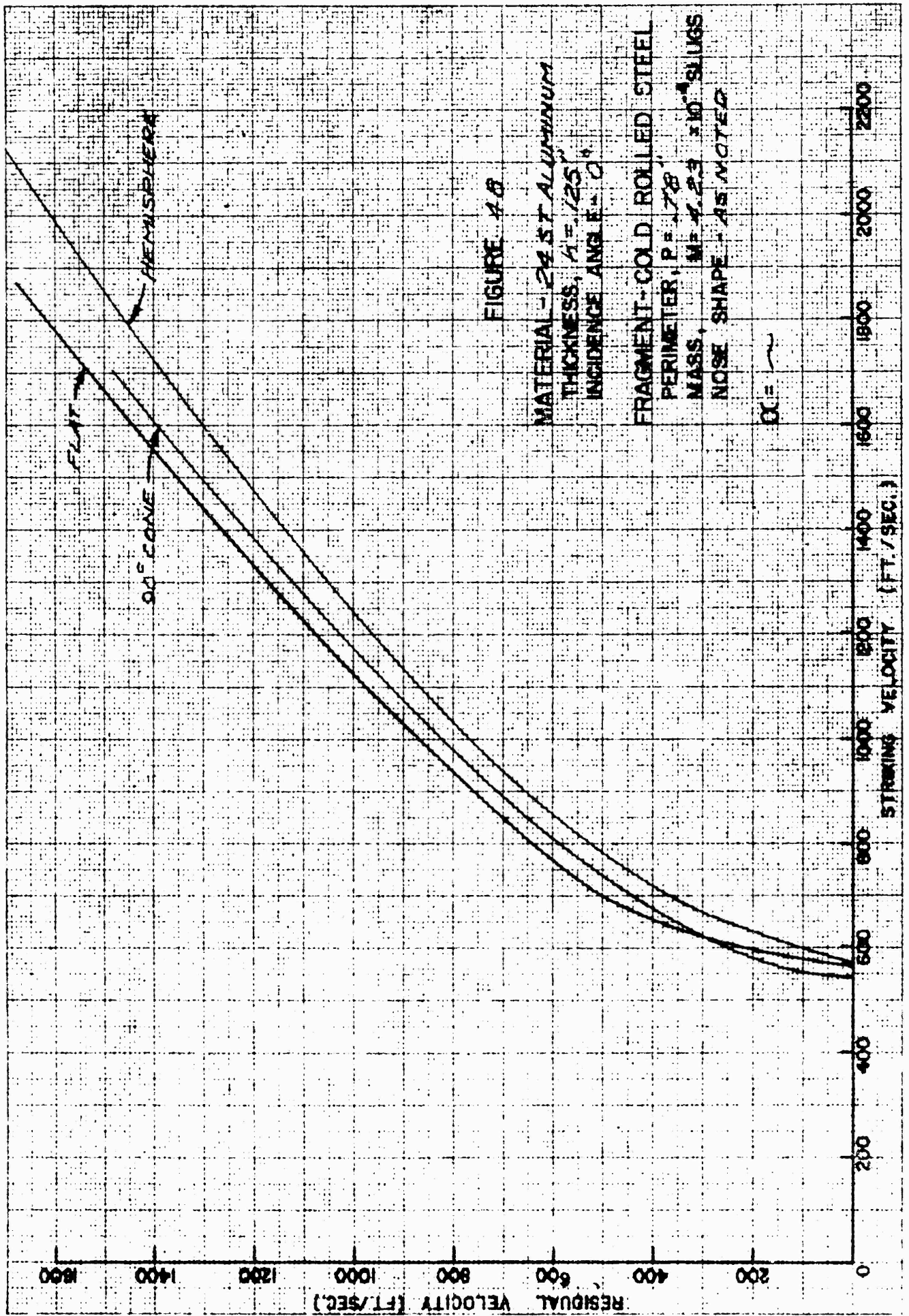
FRAGMENT - COLD ROLLED STEEL
PERIMETER, $P = .78$ "
MASS, $M = 4.27 \times 10^{-4}$ SLUGS
NOSE SHAPE - AS NOTED

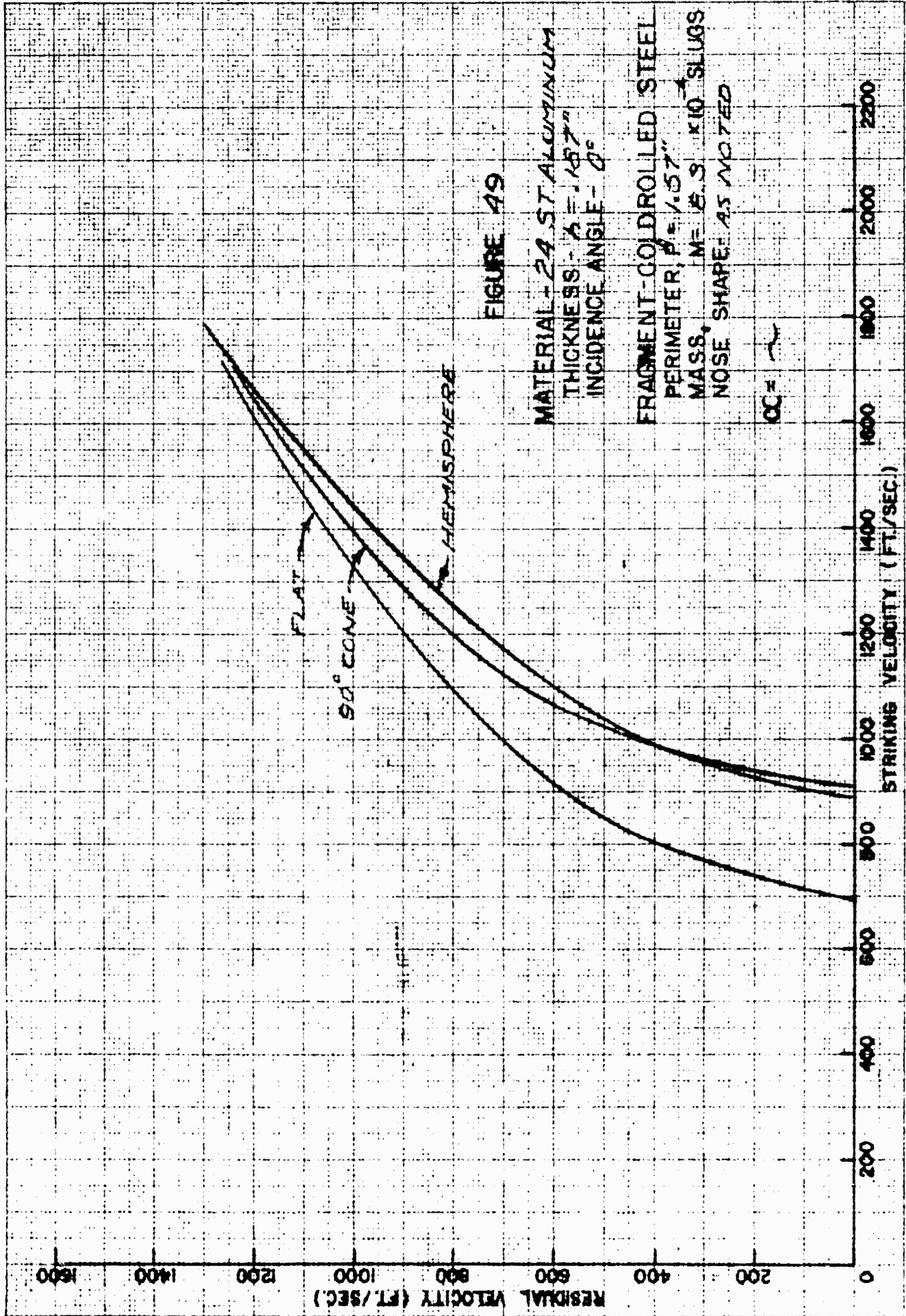


RESTRICTED









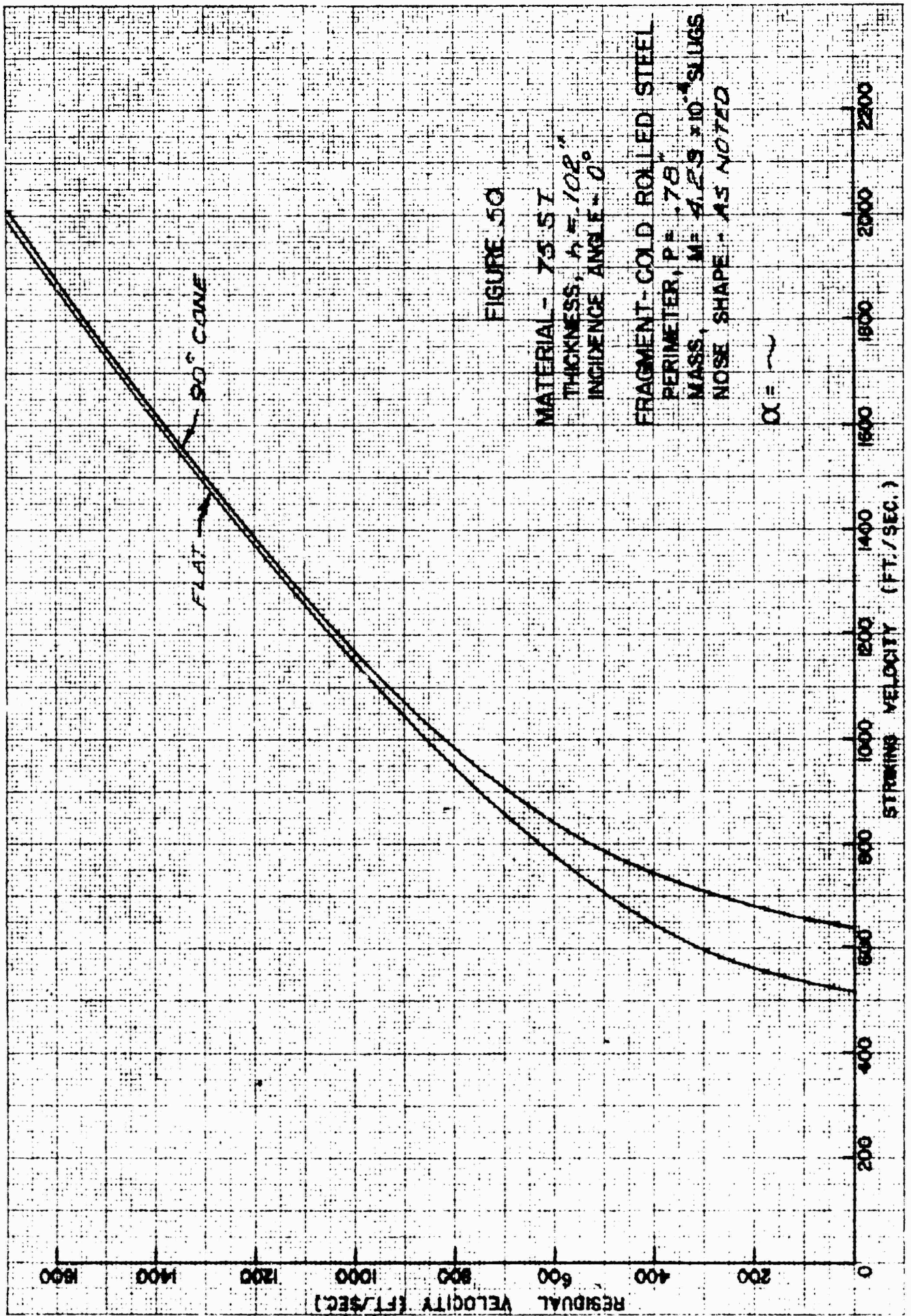


FIGURE 50

MATERIAL - 75 ST
THICKNESS, $t = .108"$
INCIDENCE ANGLE - 0°

FRAGMENT - COLD ROLLED STEEL
PERIMETER, $P = .78"$
MASS, $M = 4.25 \times 10^{-4}$ SLUGS
NOSE SHAPE - AS NOTED

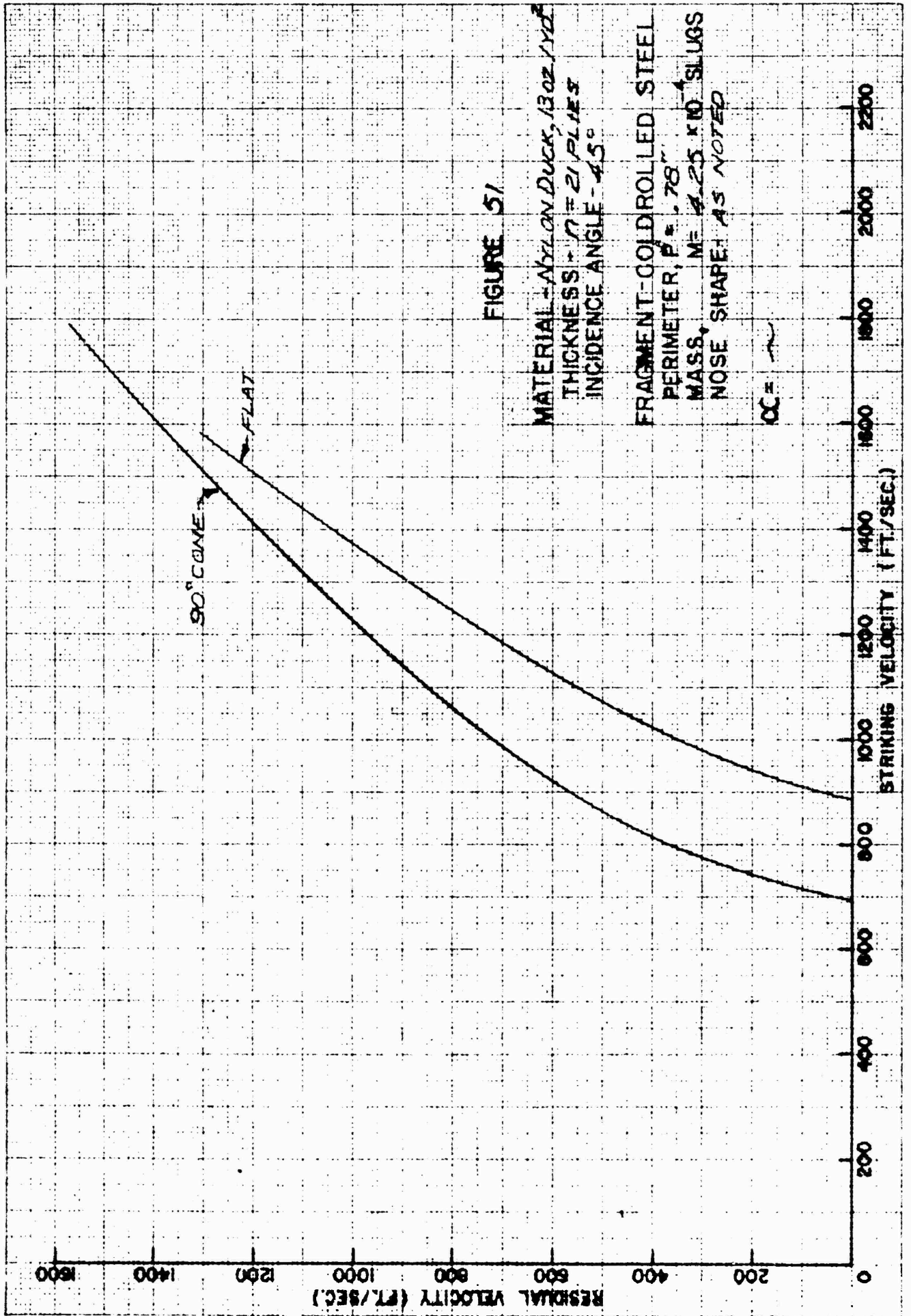


FIGURE 51

MATERIAL - NYLON DUCK, 130Z / YD²
THICKNESS - 1/8" = 21 PLYS
INCIDENCE ANGLE - 45°
FRAGMENT - COLD ROLLED STEEL
PERIMETER, P = .78"
MASS, M = 4.25 KNO SLUGS
NOSE SHAPE AS NOTED

CC =

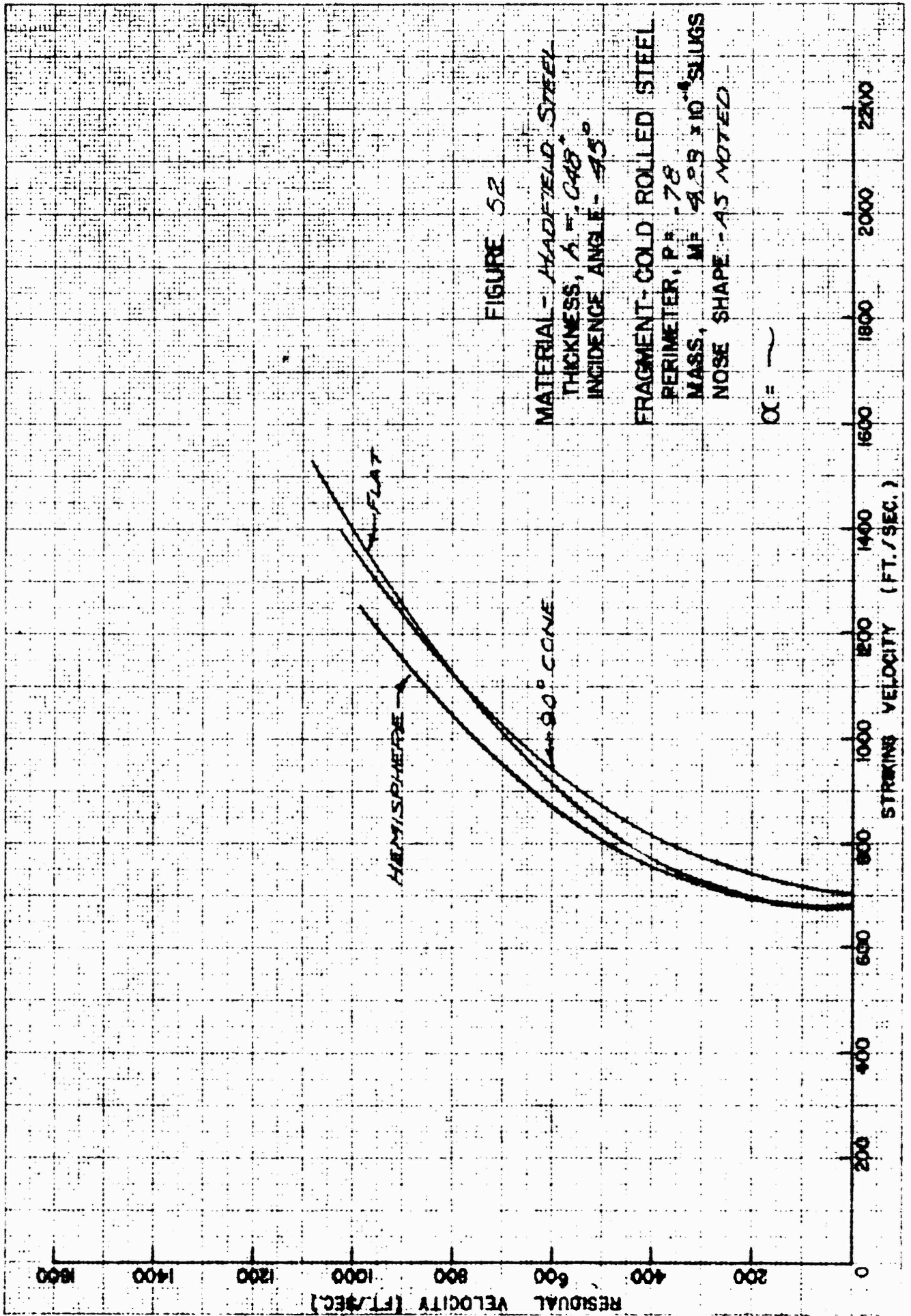
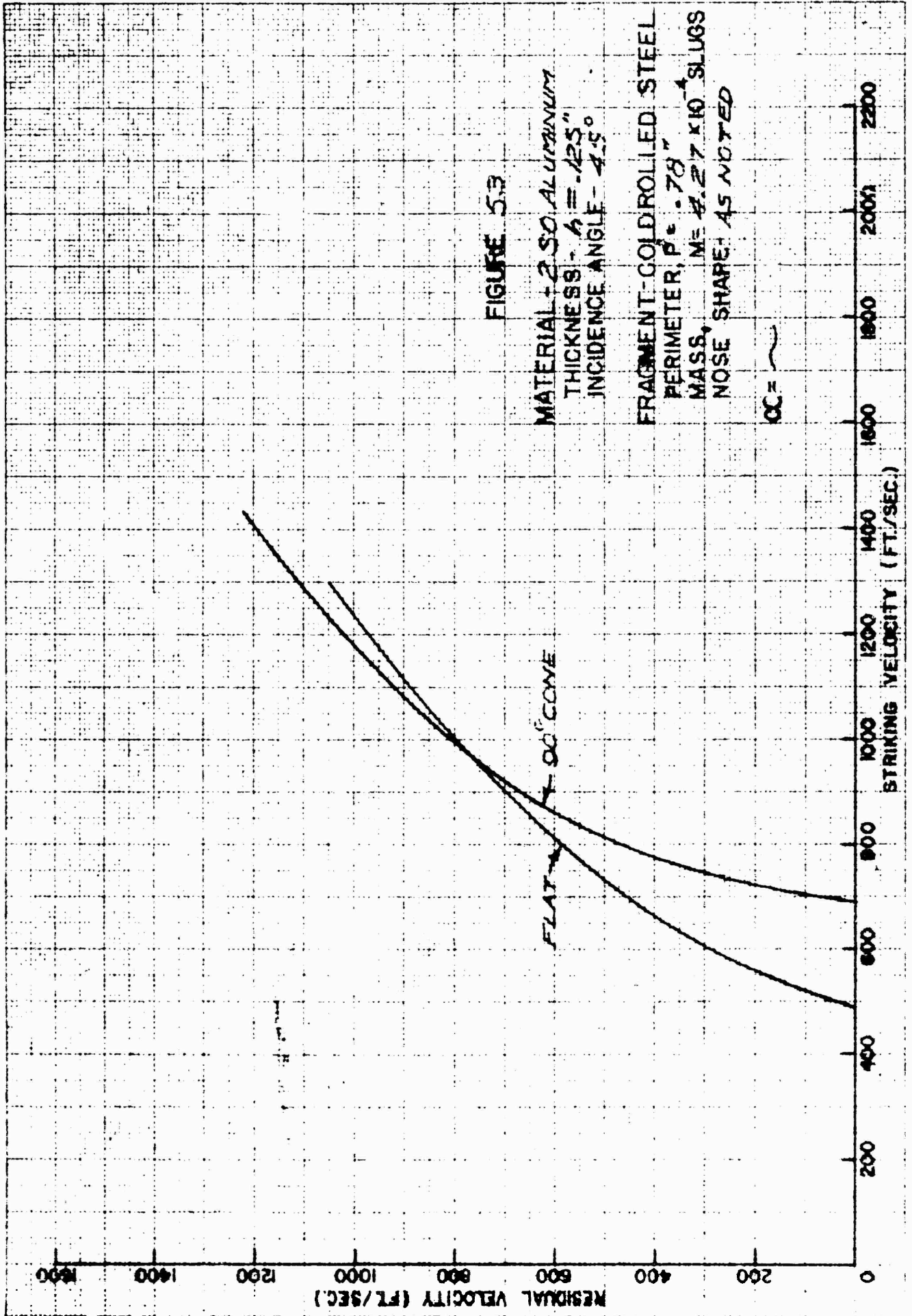


FIGURE 52

MATERIAL - HARDENED STEEL
THICKNESS, $A = 0.48$ "
INCIDENCE ANGLE - 45°

FRAGMENT - COLD ROLLED STEEL
PERIMETER, $P = 78$
MASS, $M = 9.8 \times 10^{-4}$ SLUGS
NOSE SHAPE - AS NOTED

$\alpha =$ ~



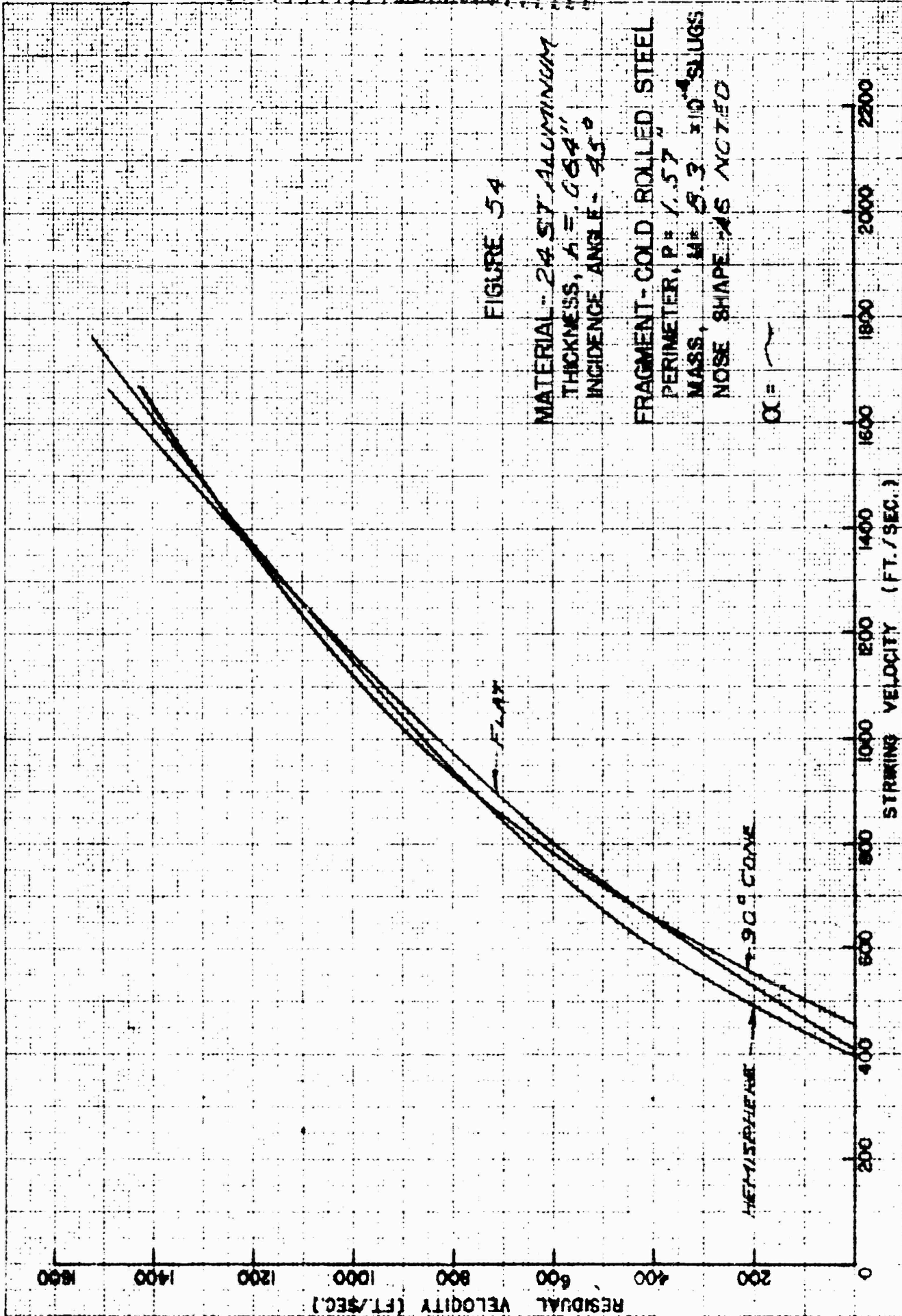


FIGURE 54

MATERIAL - 24 ST. ALUMINUM
THICKNESS, $t = .064"$
INCIDENCE ANGLE - 45°
FRAGMENT - COLD ROLLED STEEL
PERIMETER, $P = 1.57"$
MASS, $M = 5.3 \times 10^{-4}$ SLUGS
NOSE SHAPE - AS NOTED

$\alpha =$

RESIDUAL VELOCITY

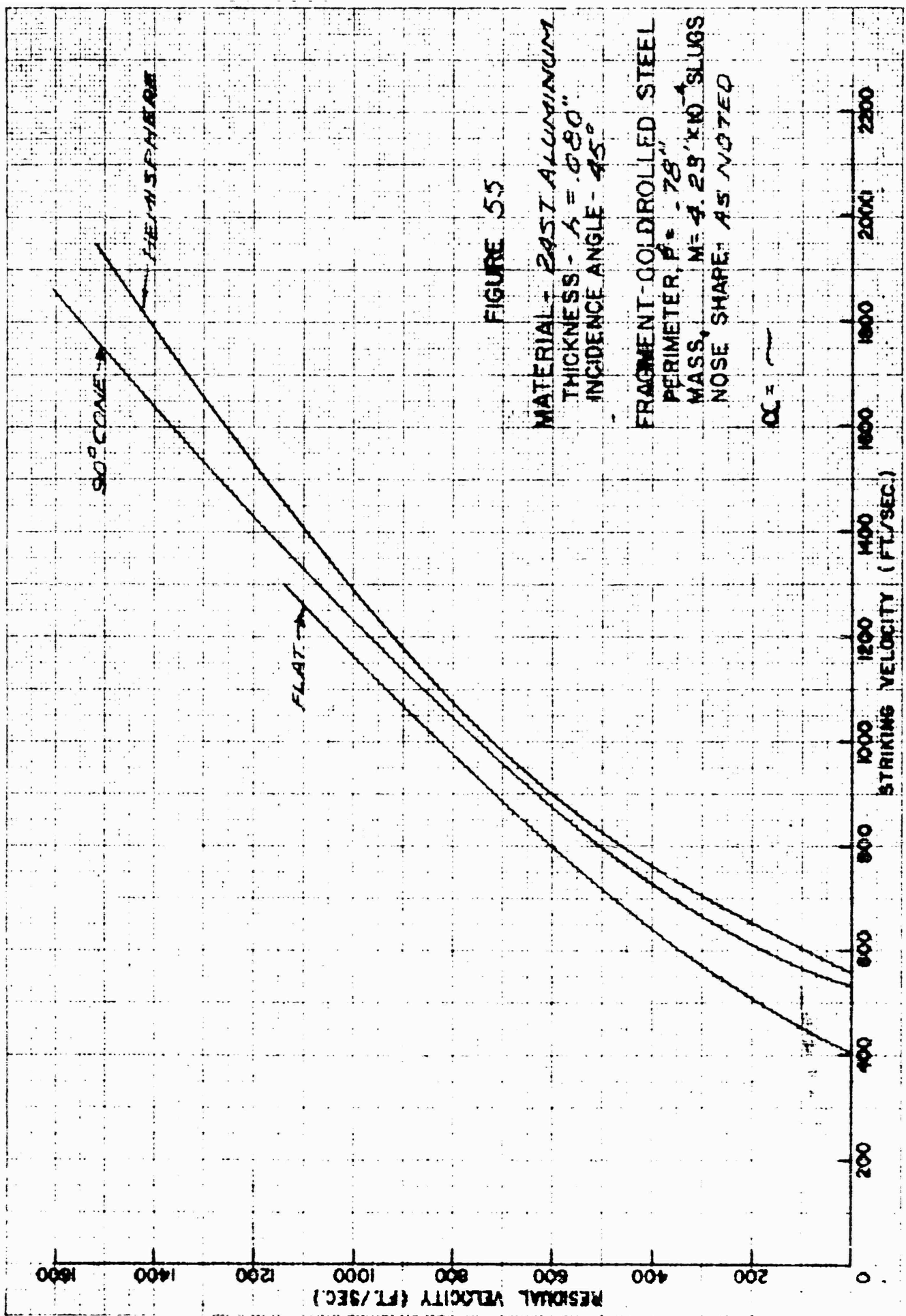


FIGURE 55

MATERIAL - 2024 ALUMINUM
THICKNESS - $t = .080$ "
INCIDENCE ANGLE - 45°

FRAGMENT-GOLDROLLED STEEL
PERIMETER, $P = .78$ "
MASS, $M = 4.29 \times 10^{-4}$ SLUGS
NOSE SHAPE: AS NOTED

OC =

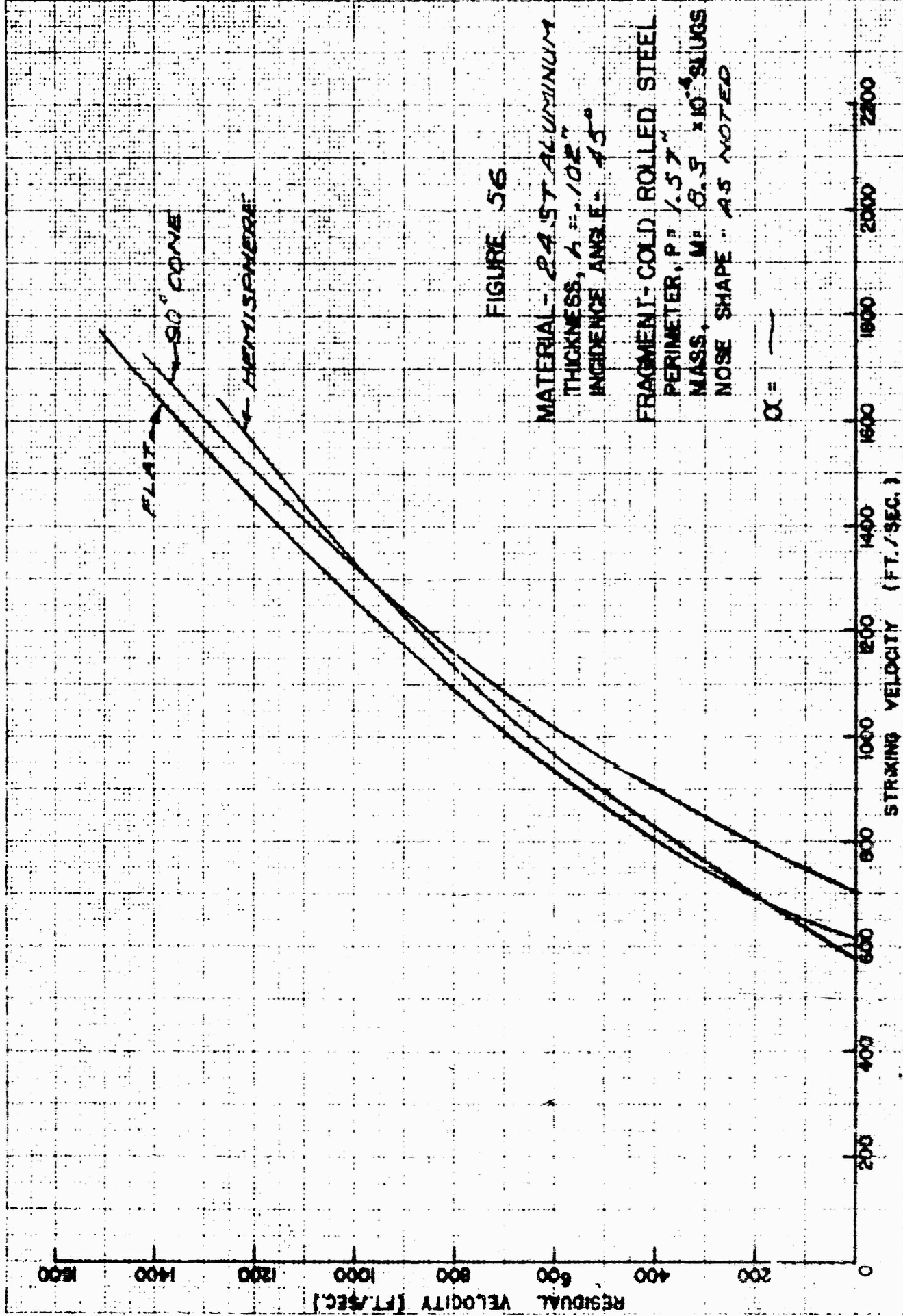
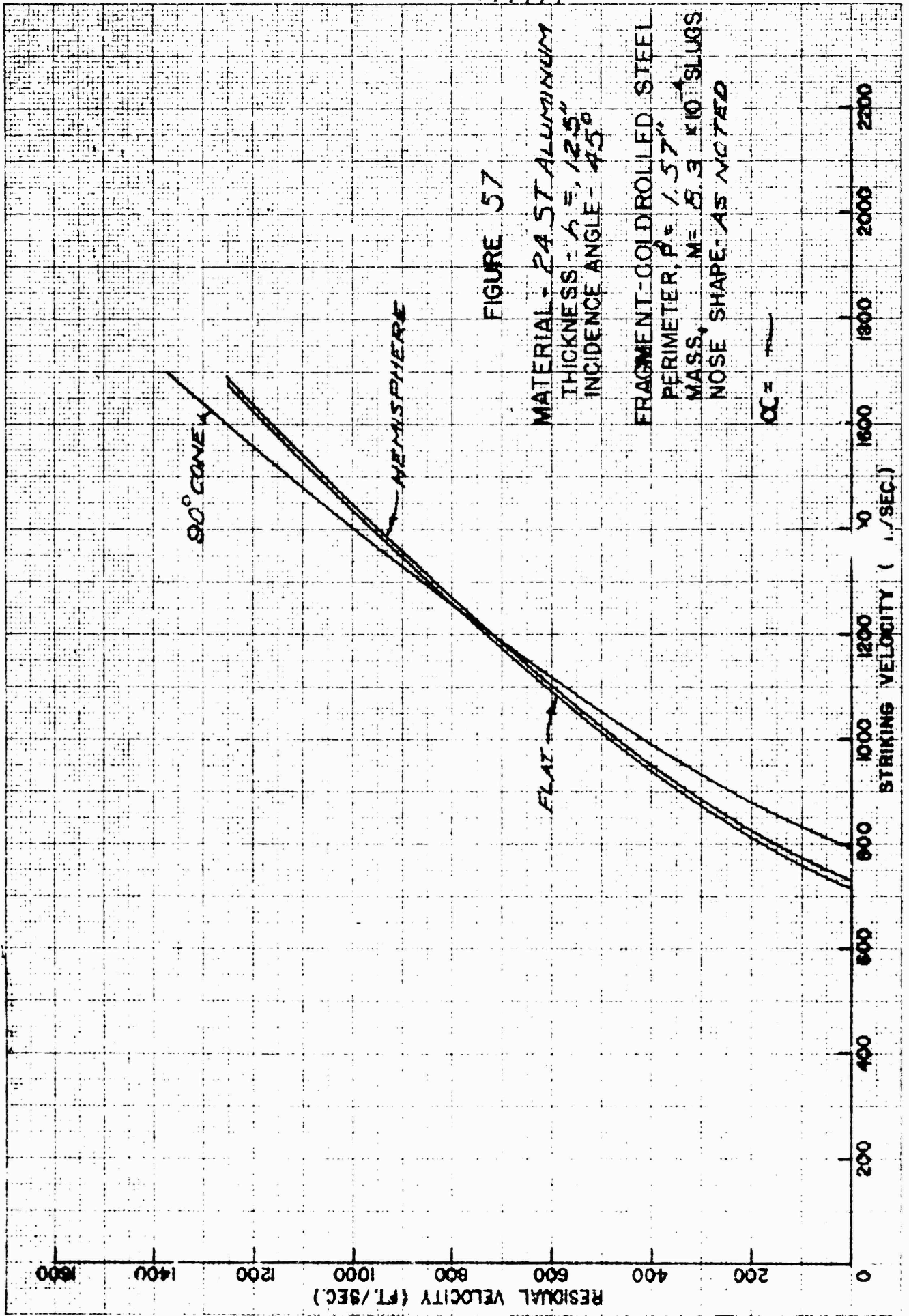
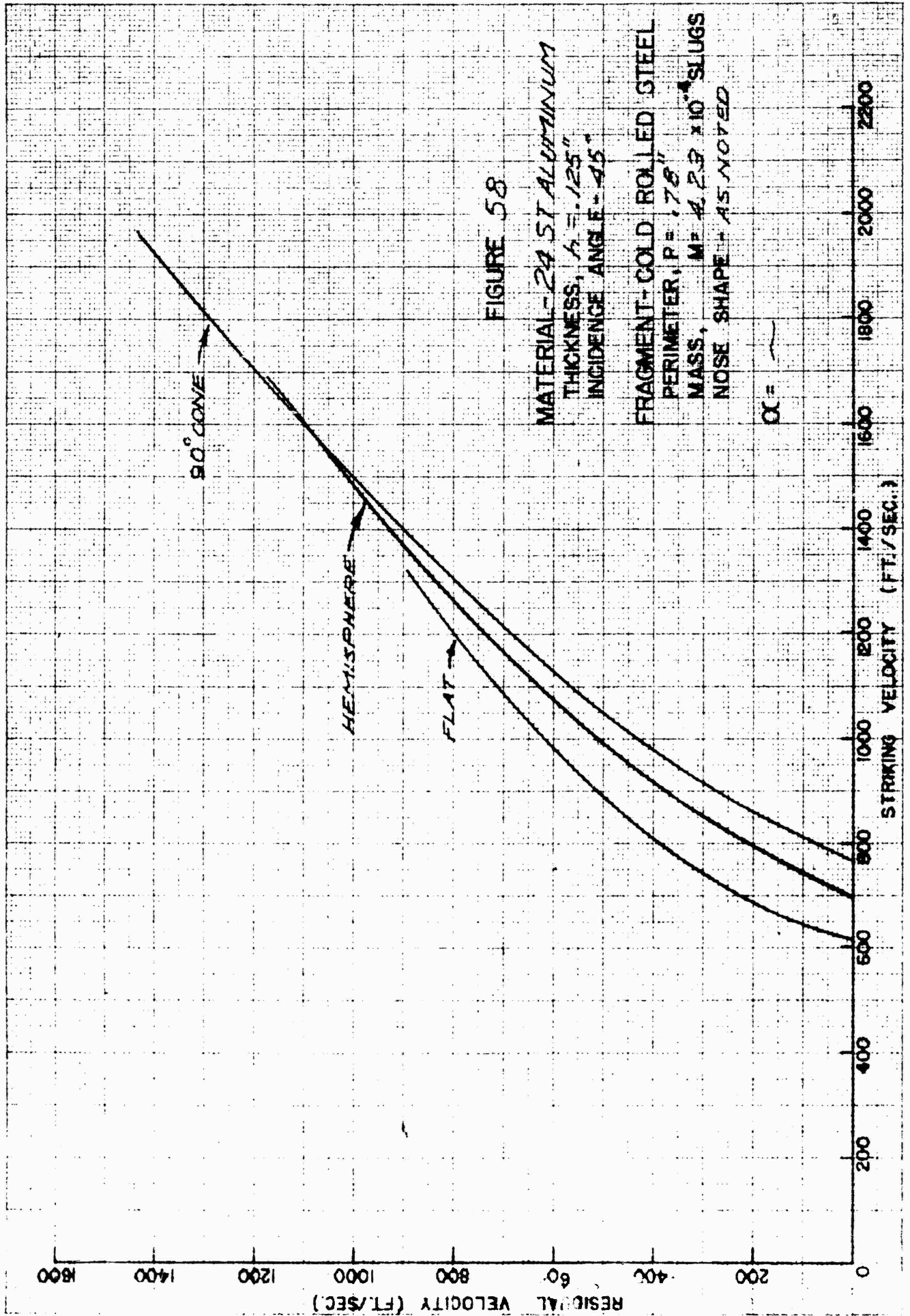


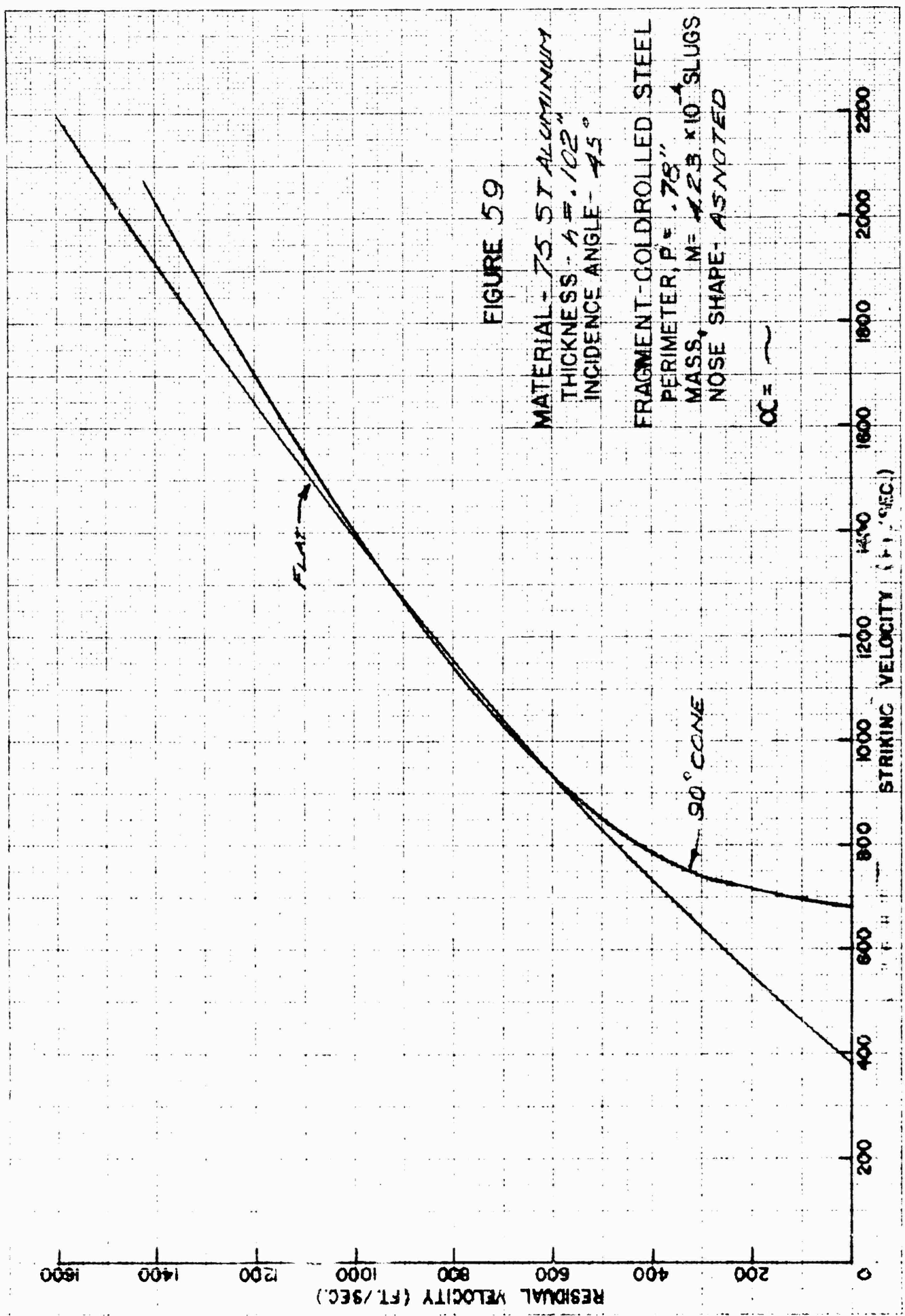
FIGURE 56

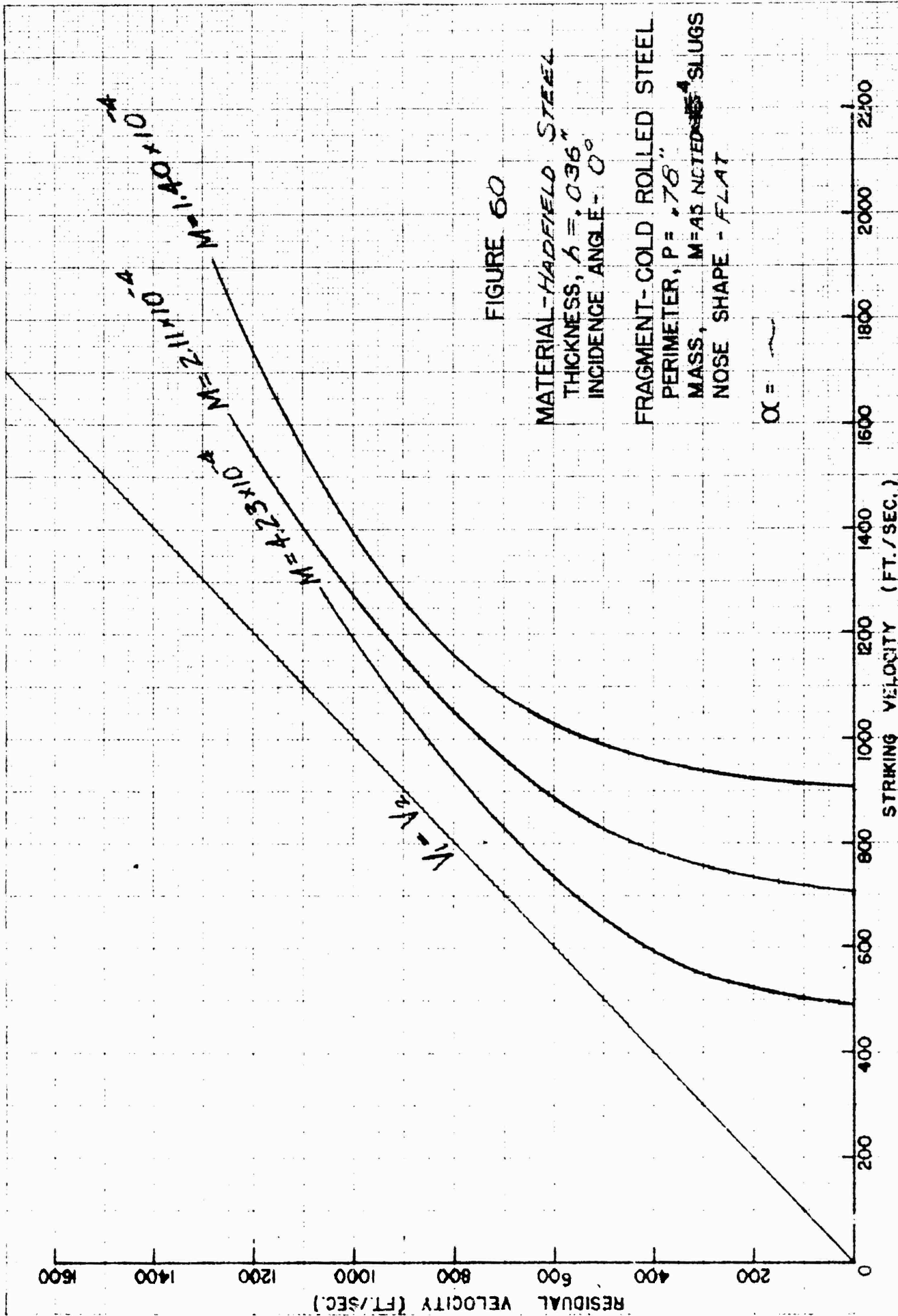
MATERIAL - 24.5T ALUMINUM
THICKNESS, $t = .102"$
INCIDENCE ANGLE - 45°
FRAGMENT - COLD ROLLED STEEL
PERIMETER, $P = 1.57"$
MASS, $M = 8.5 \times 10^{-4}$ SLUGS
NOSE SHAPE - AS NOTED

$\alpha = \text{---}$









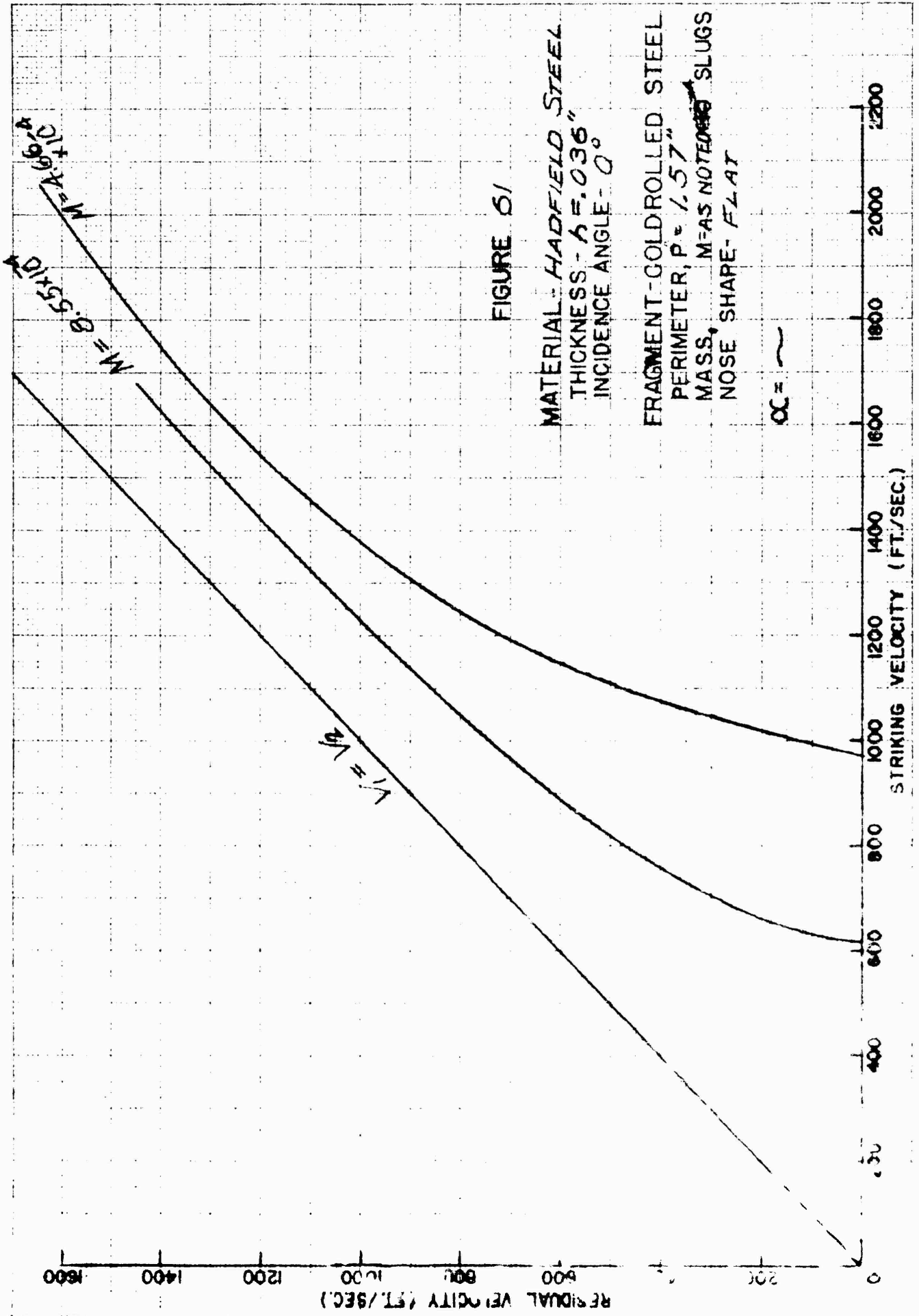


FIGURE 61

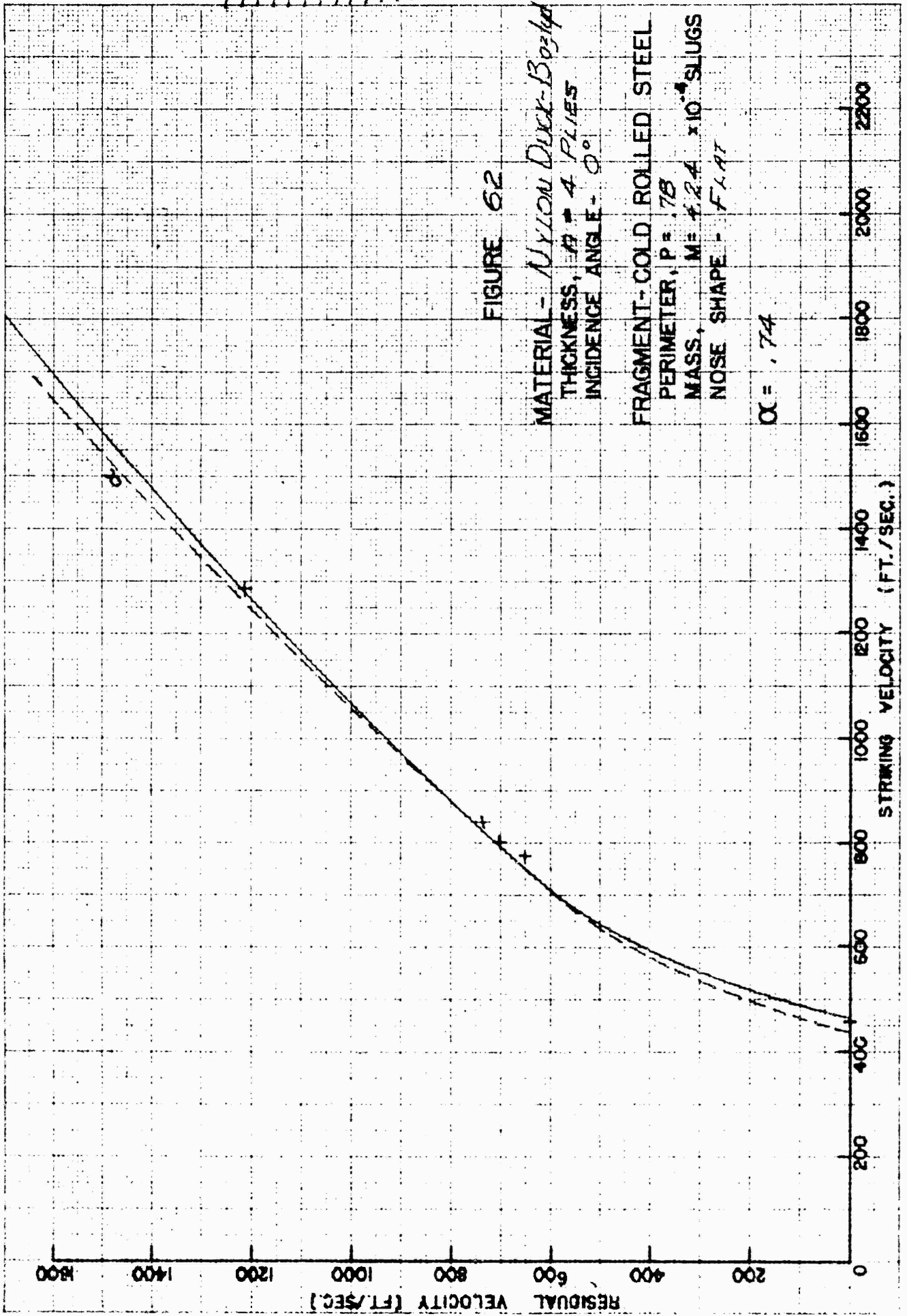


FIGURE 62

MATERIAL - *Nylon Dux-Bond*
THICKNESS, $t = 4$ PLIES
INCIDENCE ANGLE - 0°

FRAGMENT - COLD ROLLED STEEL
PERIMETER, $P = .78$
MASS, $M = 4.24 \times 10^{-4}$ SLUGS
NOSE SHAPE - FLAT

$\alpha = .74$

.....

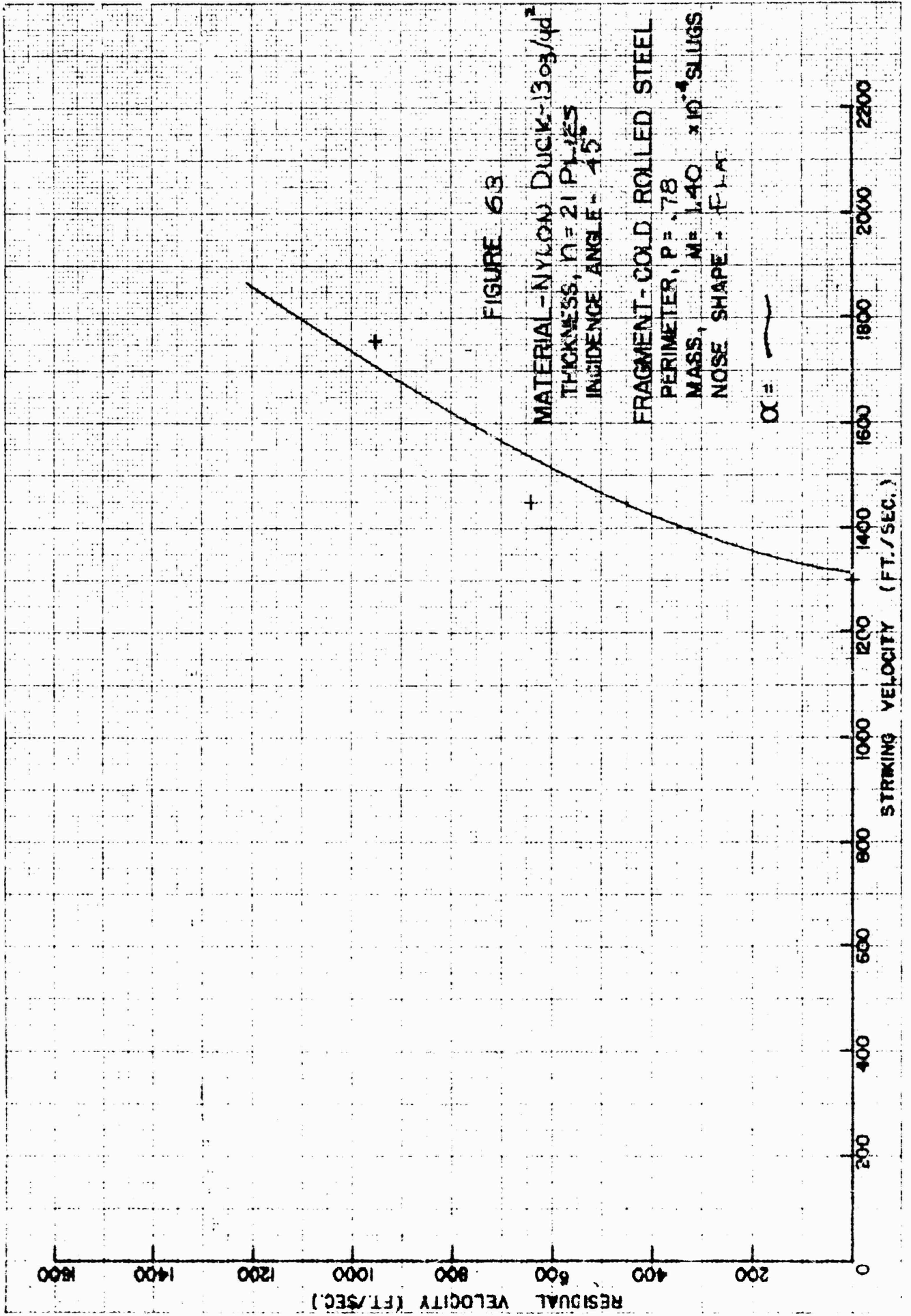


FIGURE 63

MATERIAL - NYLON-DUCIK-1303/4d²
THICKNESS, $n = 21$ PLIES
INCIDENCE ANGLE - 45°

FRAGMENT - COLD ROLLED STEEL
PERIMETER, $P = .78$
MASS, $M = 1.40 \times 10^{-4}$ SLUGS
NOSE SHAPE - FLAT

$\alpha =$

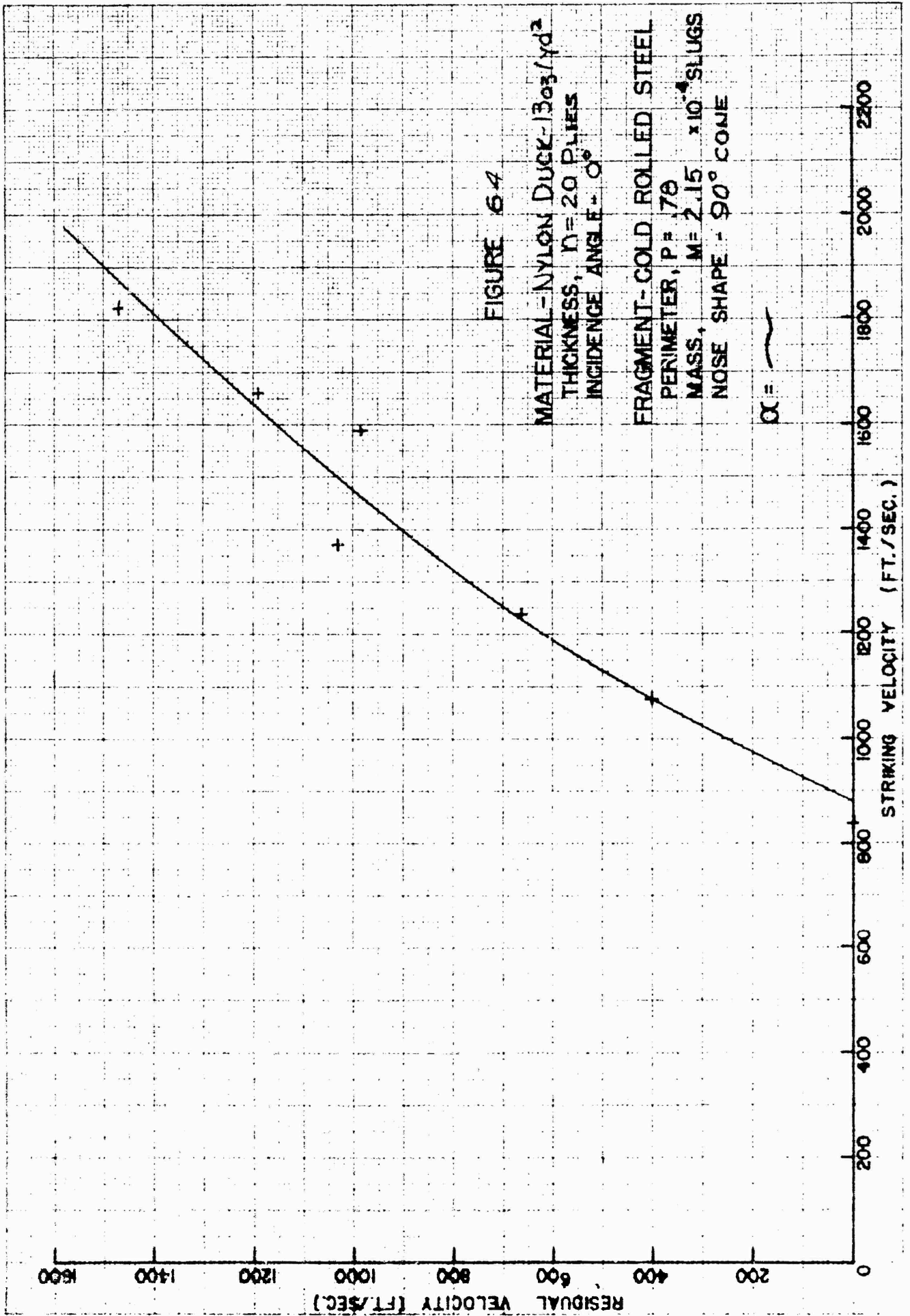


FIGURE 64

MATERIAL - NYLON DUCK - 13oz./yd²
THICKNESS, $\eta = 2.0$ PLIES
INCIDENCE ANGLE - 0°

FRAGMENT - COLD ROLLED STEEL
PERIMETER, $P = .70$
MASS, $M = 2.15 \times 10^{-4}$ SLUGS
NOSE SHAPE - 90° CONE

$\alpha =$

REPRODUCED FROM REPORT

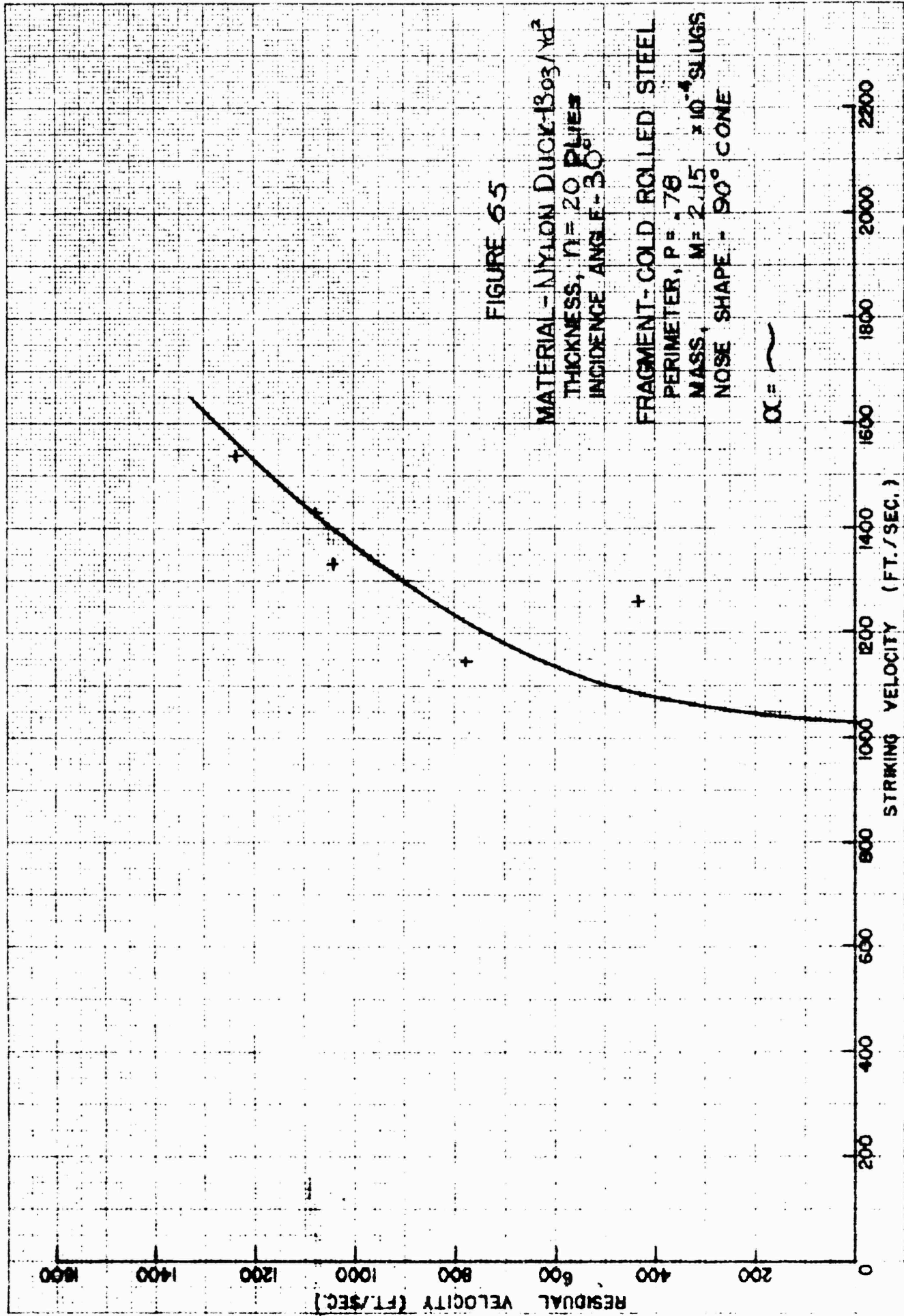


FIGURE 65

MATERIAL - NYLON DUCK-13oz/Yd²
THICKNESS, $n = 20$ PLYES
INCIDENCE ANGLE - 30°

FRAGMENT - COLD ROLLED STEEL
PERIMETER, $P = .76$
MASS, $M = 2.15 \times 10^{-4}$ SLUGS
NOSE SHAPE - 90° CONE

$\alpha = \sim$

RESTRICTED

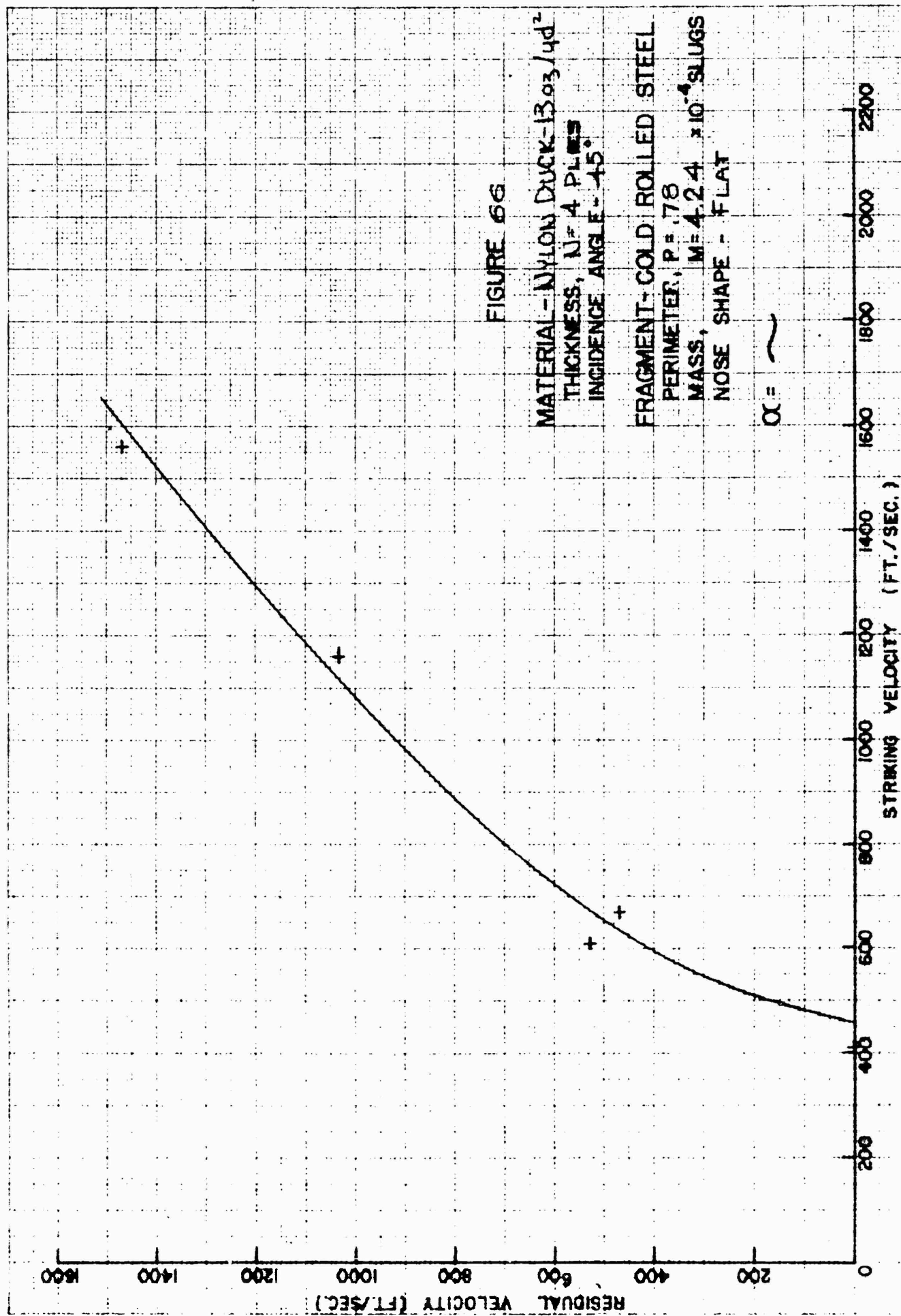


FIGURE 66

MATERIAL - NYLON DUCK-13.03/4d²
 THICKNESS, N = 4 PLYS
 INCIDENCE ANGLE - 45°

FRAGMENT - COLD ROLLED STEEL
 PERIMETER, P = .78
 MASS, M = 4.24 x 10⁻⁴ SLUGS
 NOSE SHAPE - FLAT

$\alpha = \sim$

RESTRICTED

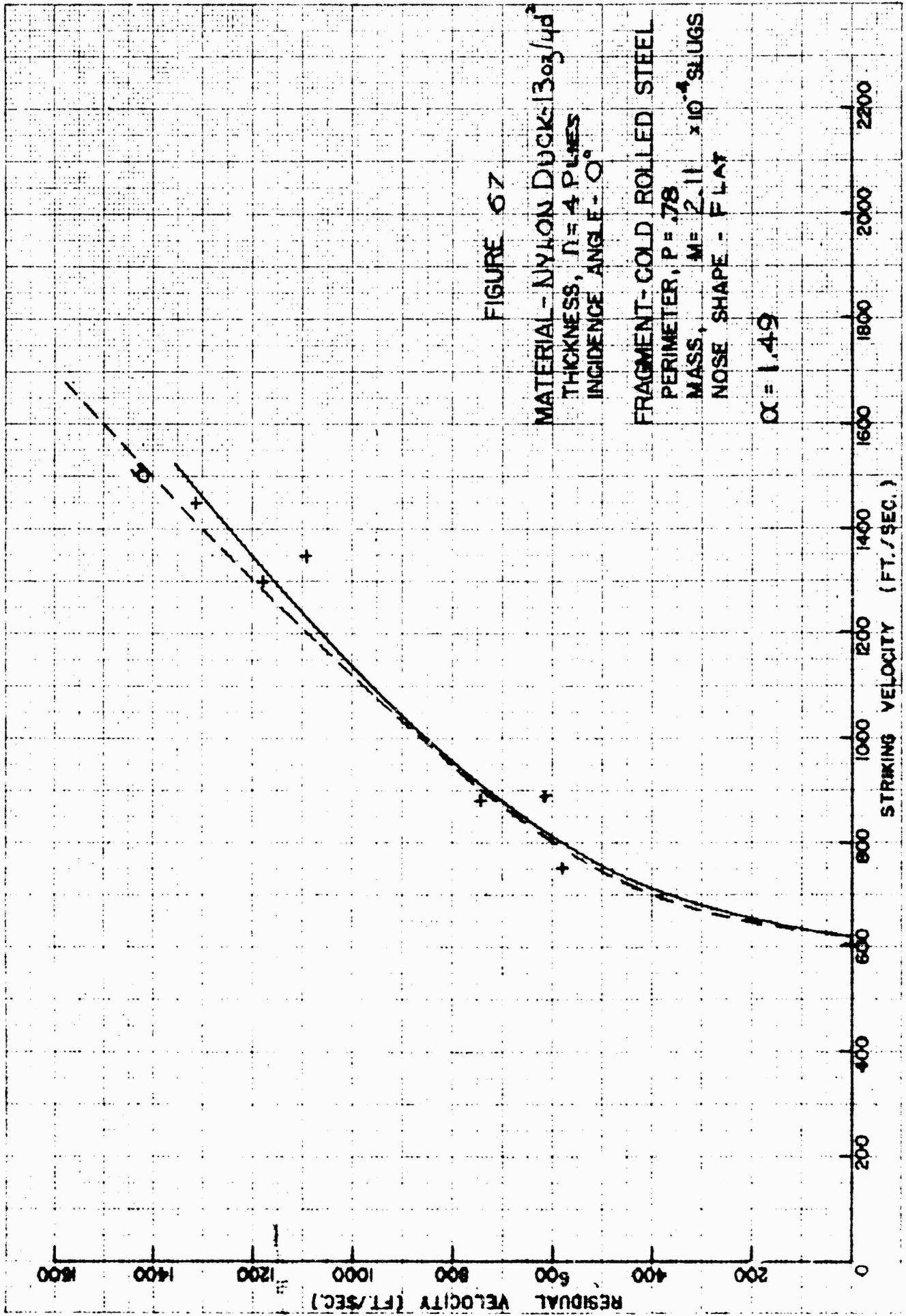
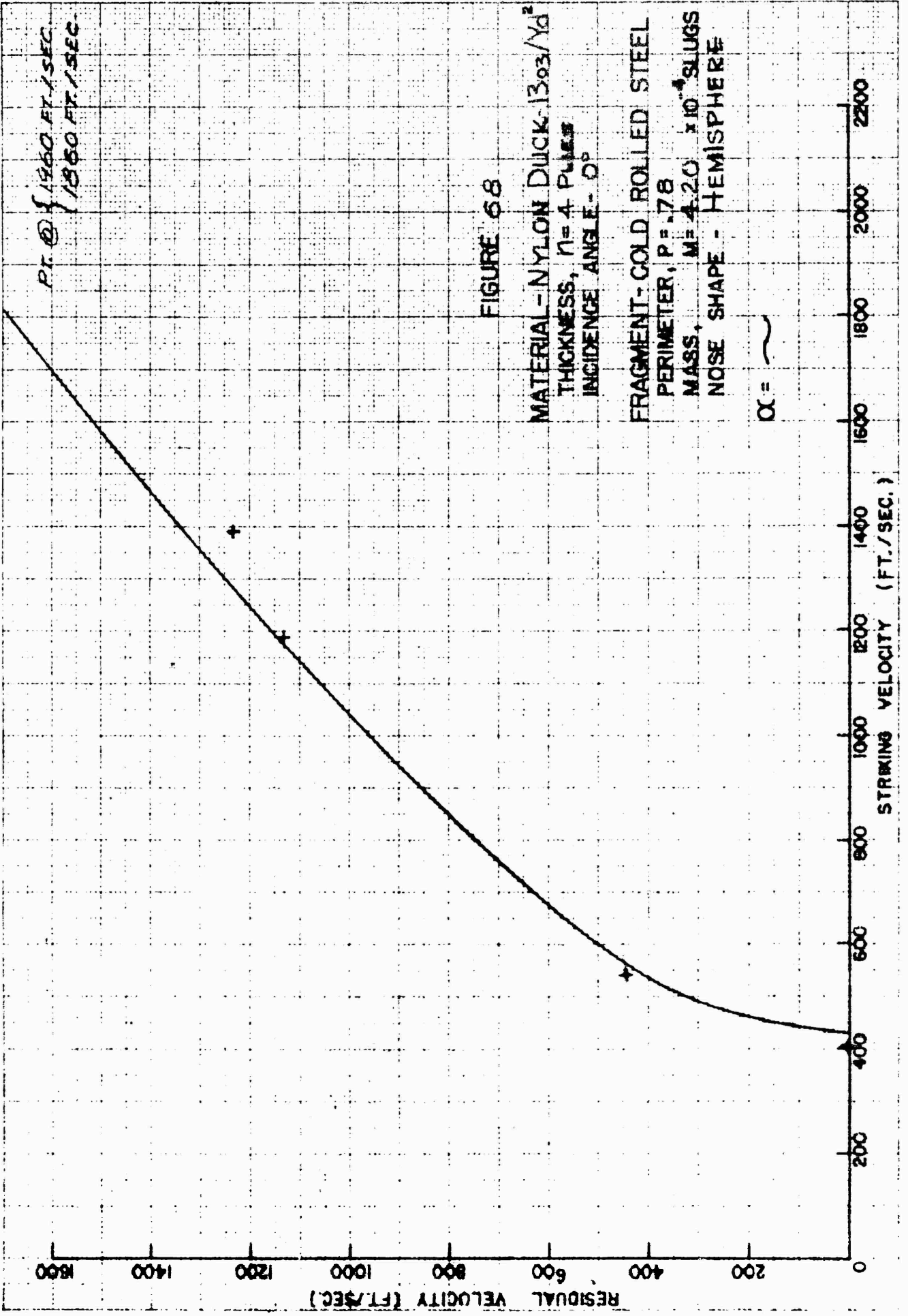


FIGURE 67

MATERIAL - NYLON DUCK - $1303/4d^2$
THICKNESS, $n = 4$ PLYES
INCIDENCE ANGLE - 0°

FRAGMENT - GOLD ROLLED STEEL
PERIMETER, $P = .78$
MASS, $M = 2.11 \times 10^{-4}$ SLUGS
NOSE SHAPE - FLAT

$\alpha = 1.49$



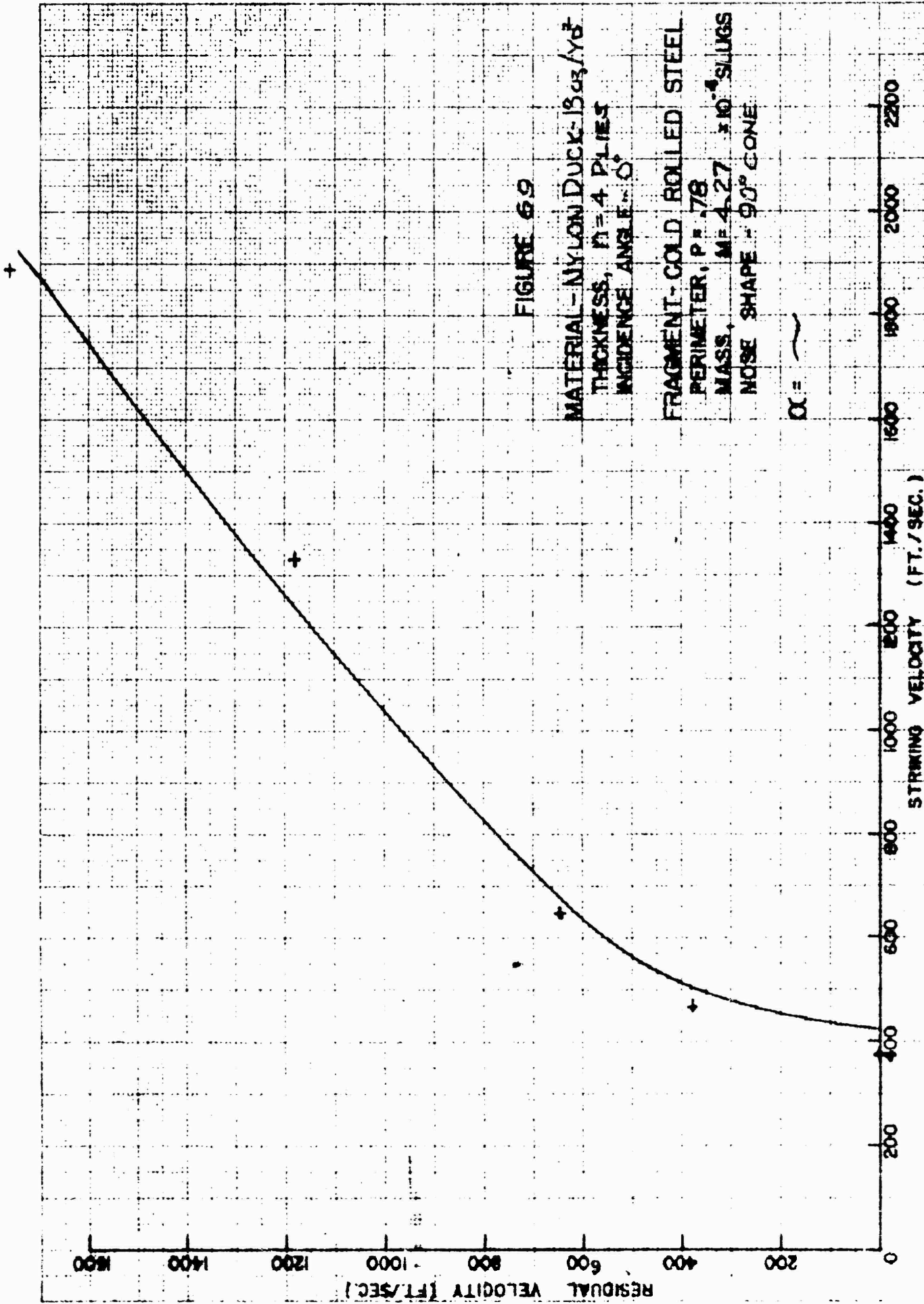


FIGURE 69

MATERIAL - NYLON DUCK - 13 OZ./YD²
THICKNESS, T = 4 P-LIES
INCIDENCE ANGLE - 0°

FRAGMENT - COLD ROLLED STEEL
PERIMETER, P = .78
MASS, M = 4.27 x 10⁻⁶ SLUGS
NOSE SHAPE - 90° CONE

$\alpha = \sim$

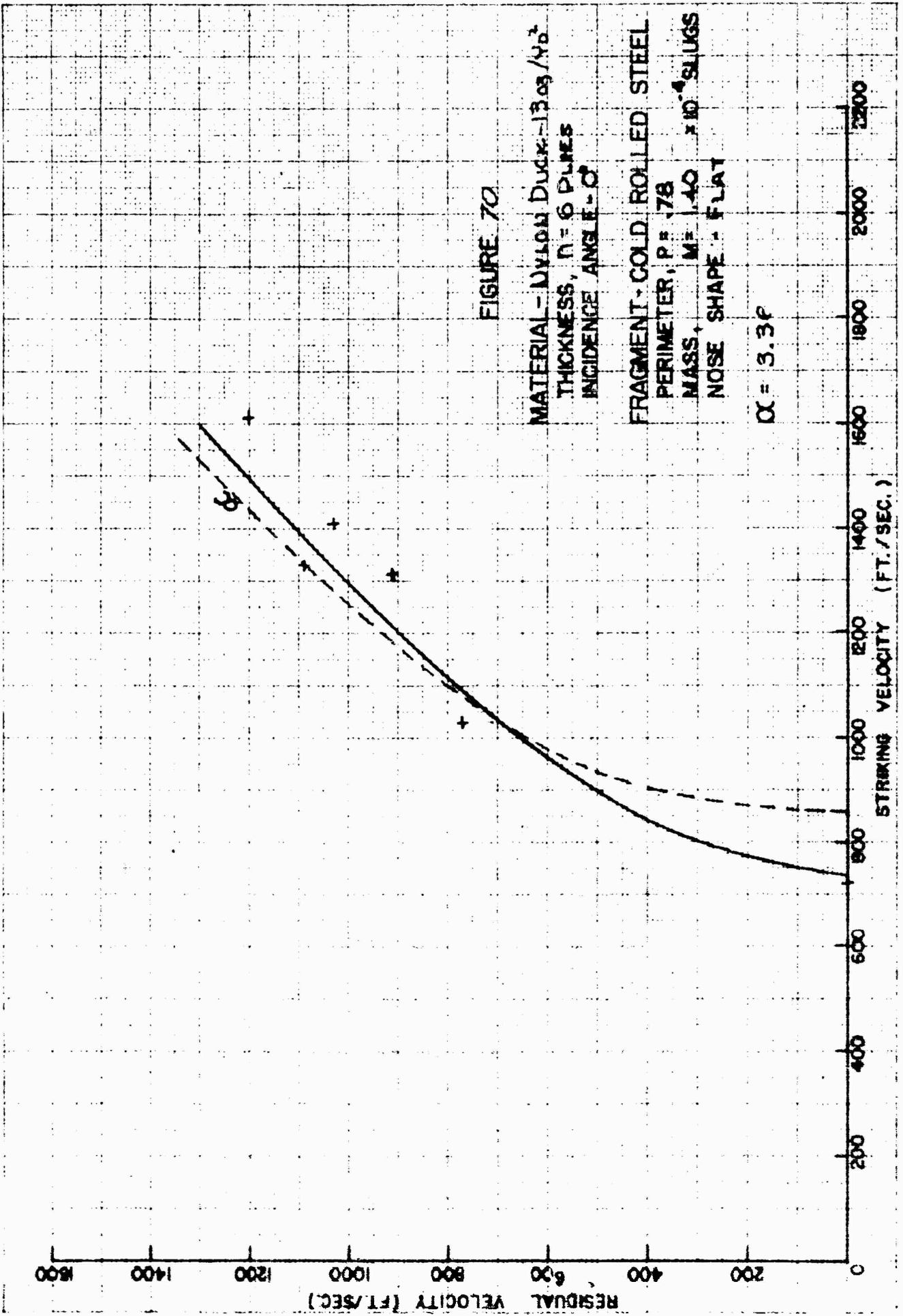
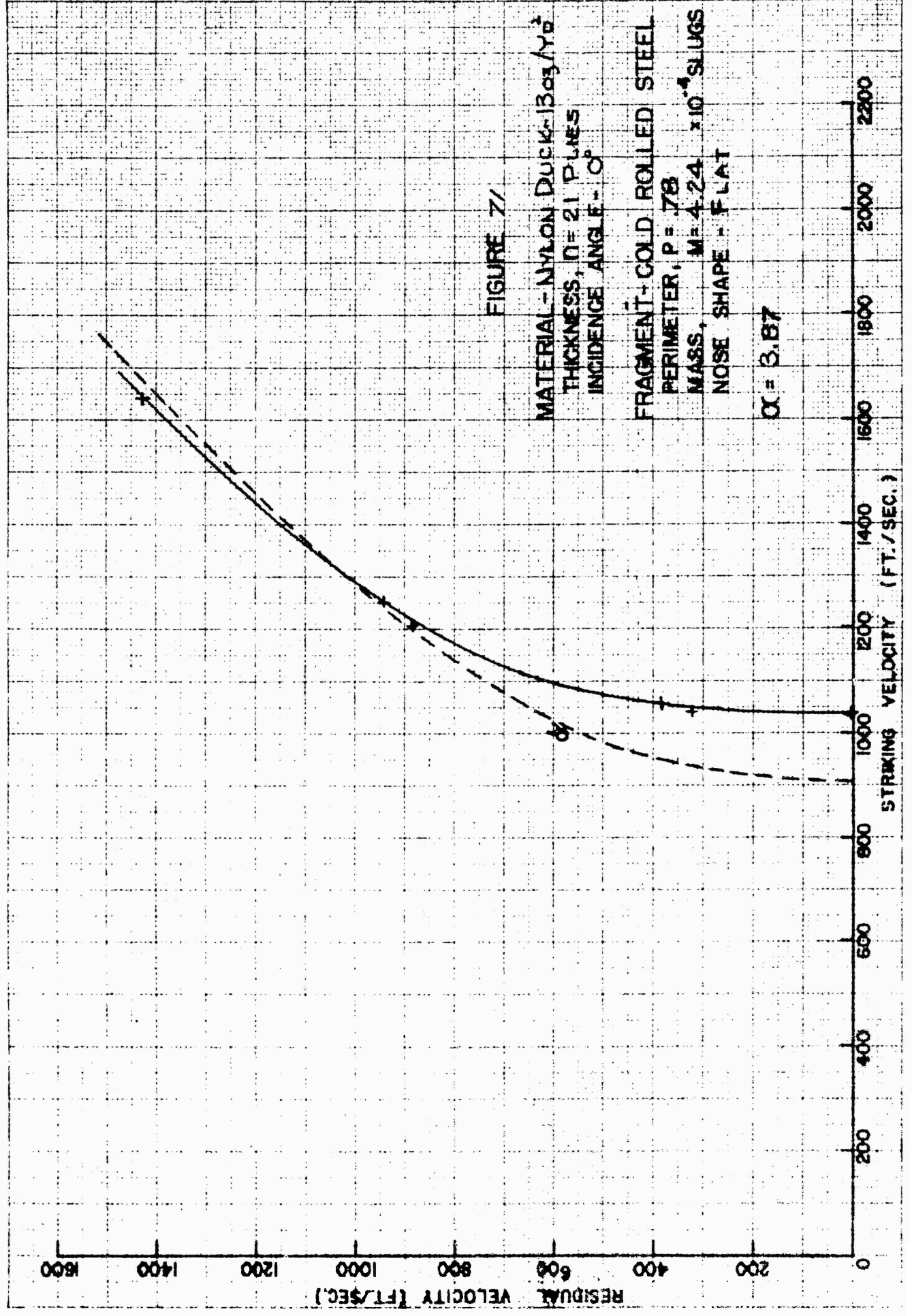


FIGURE 70

MATERIAL - NYLON DUXX-13 O_3/Y_2
THICKNESS, $t = 6$ PLIES
INCIDENCE ANGLE - 0°

FRAGMENT - COLD ROLLED STEEL
PERIMETER, $P = .78$
MASS, $M = 1.40 \times 10^{-4}$ SLUGS
NOSE SHAPE - FLAT

$\alpha = 3.3F$



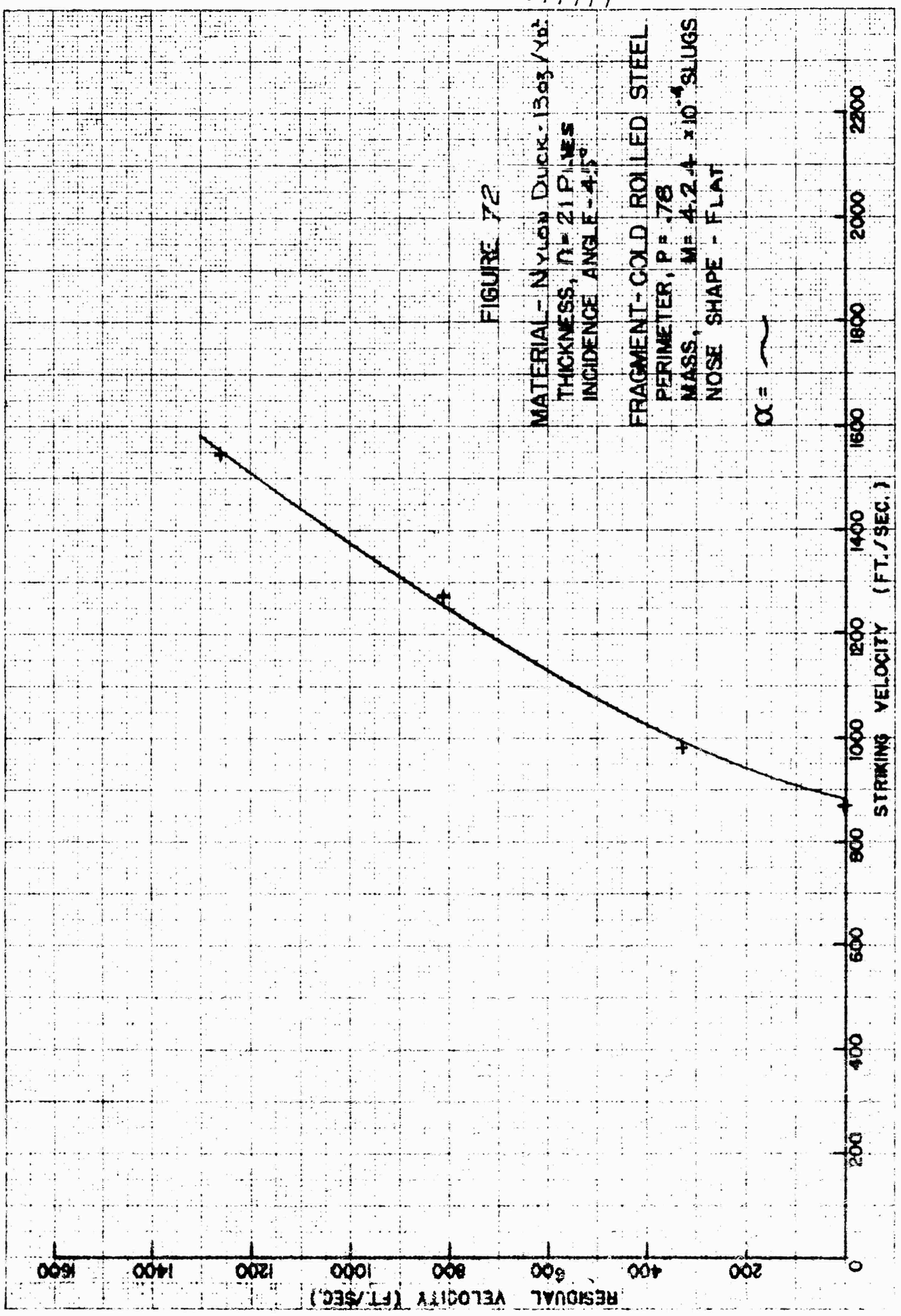


FIGURE 72

MATERIAL - Yellow Duck-1303/Yd.
 THICKNESS, $t = 21$ P.LINES
 INCIDENCE ANGLE - 4.5°

FRAGMENT - COLD ROLLED STEEL
 PERIMETER, $P = .78$
 MASS, $M = 4.24 \times 10^{-4}$ SLUGS
 NOSE SHAPE - FLAT

$\alpha = \sim$

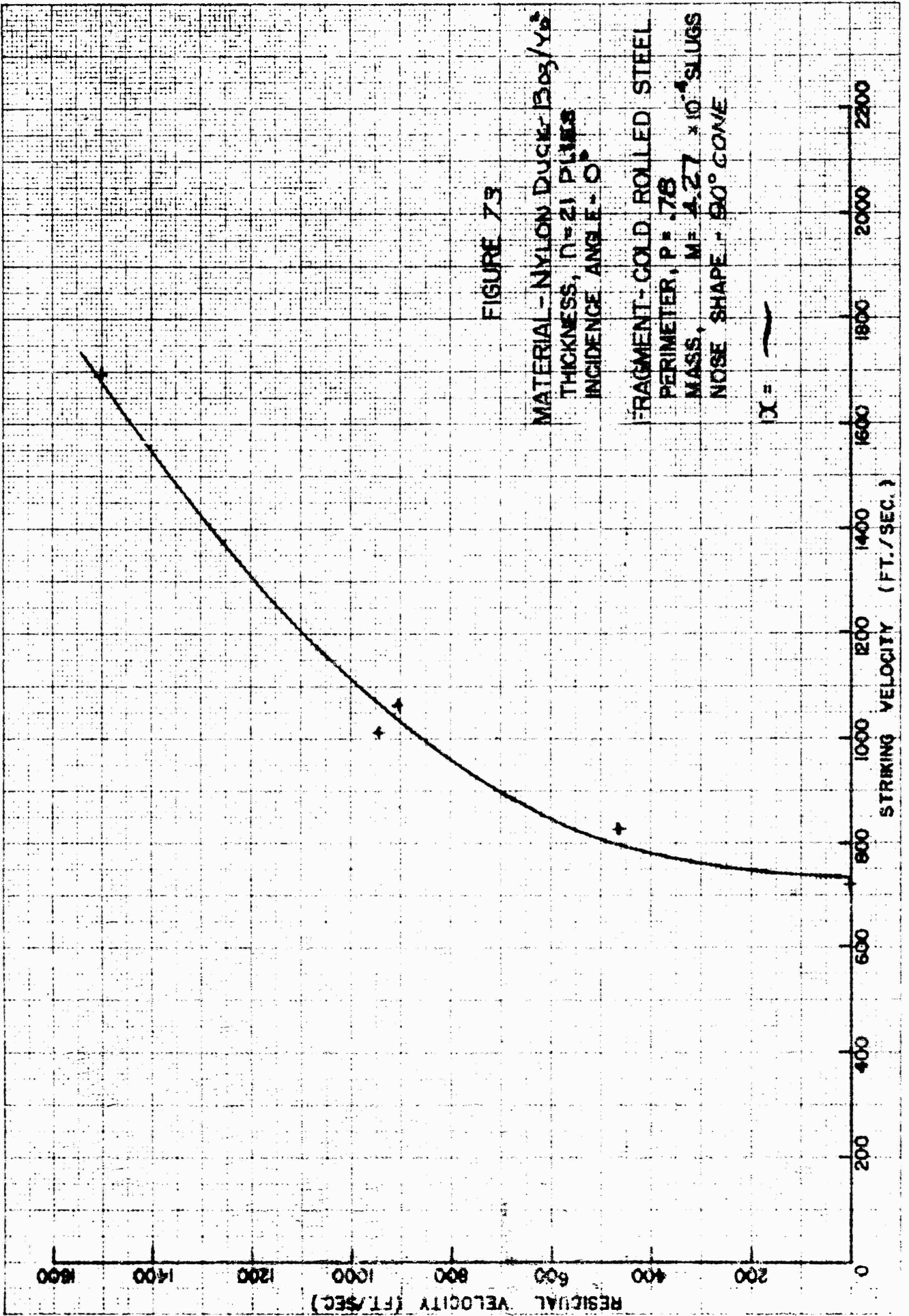


FIGURE 73

MATERIAL - NYLON DUCK-BRONZE/STEEL
THICKNESS, $T = 21$ PLYS
INCIDENCE ANGLE - 0°

FRAGMENT - COLD ROLLED STEEL
PERIMETER, $P = .78$
MASS, $M = 4.27 \times 10^{-4}$ SLUGS
NOSE SHAPE - 90° CONE

$DC =$

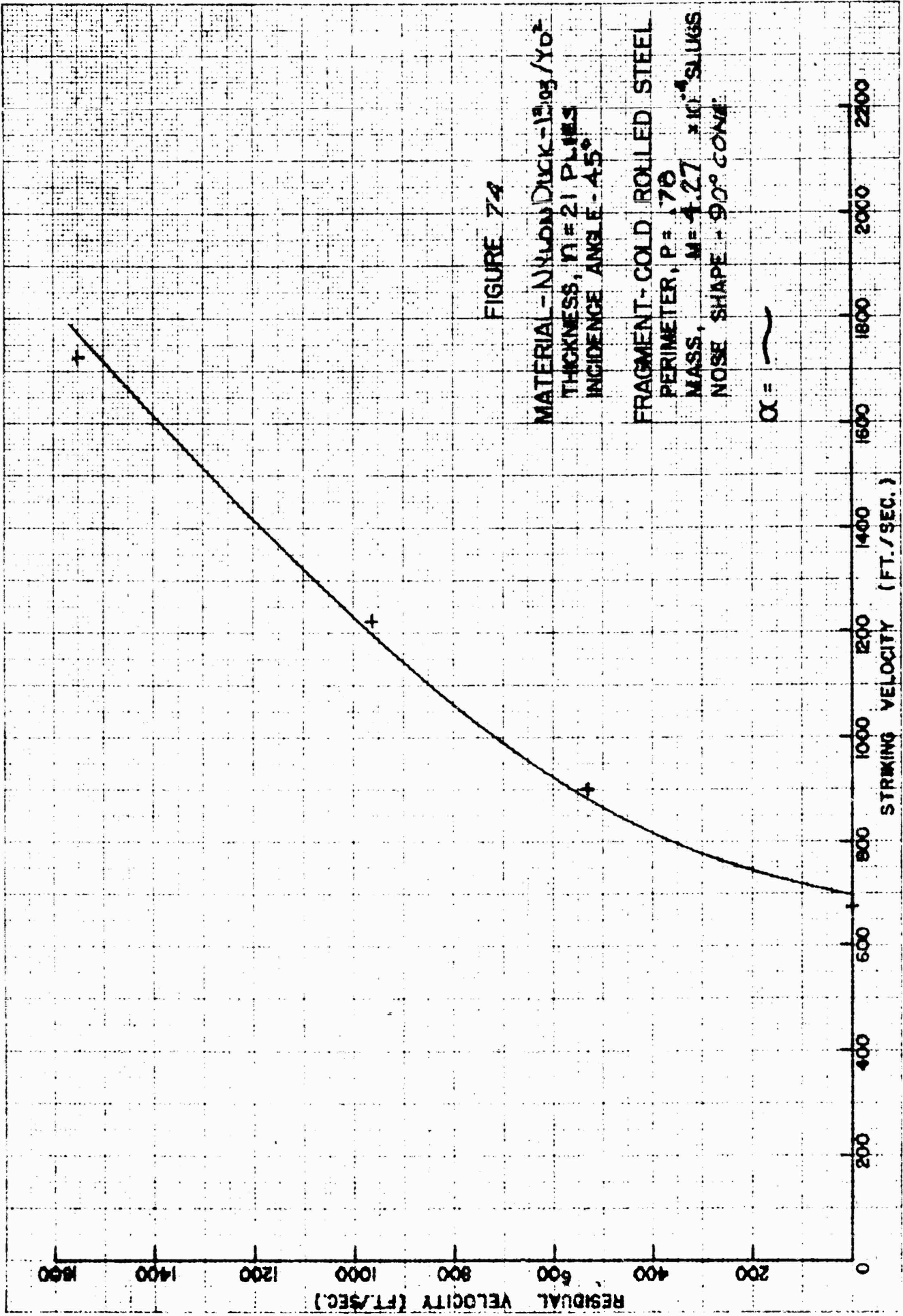
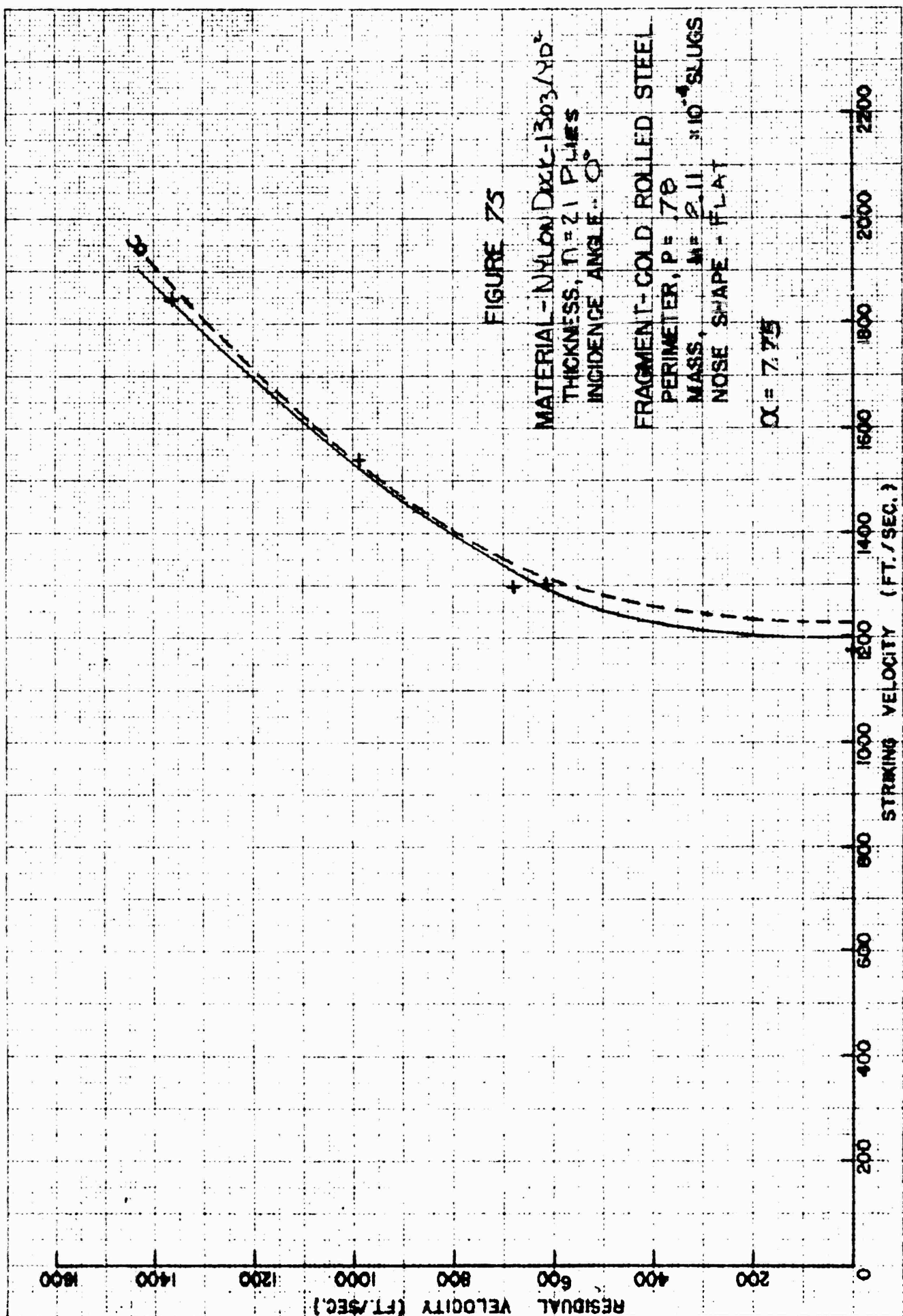


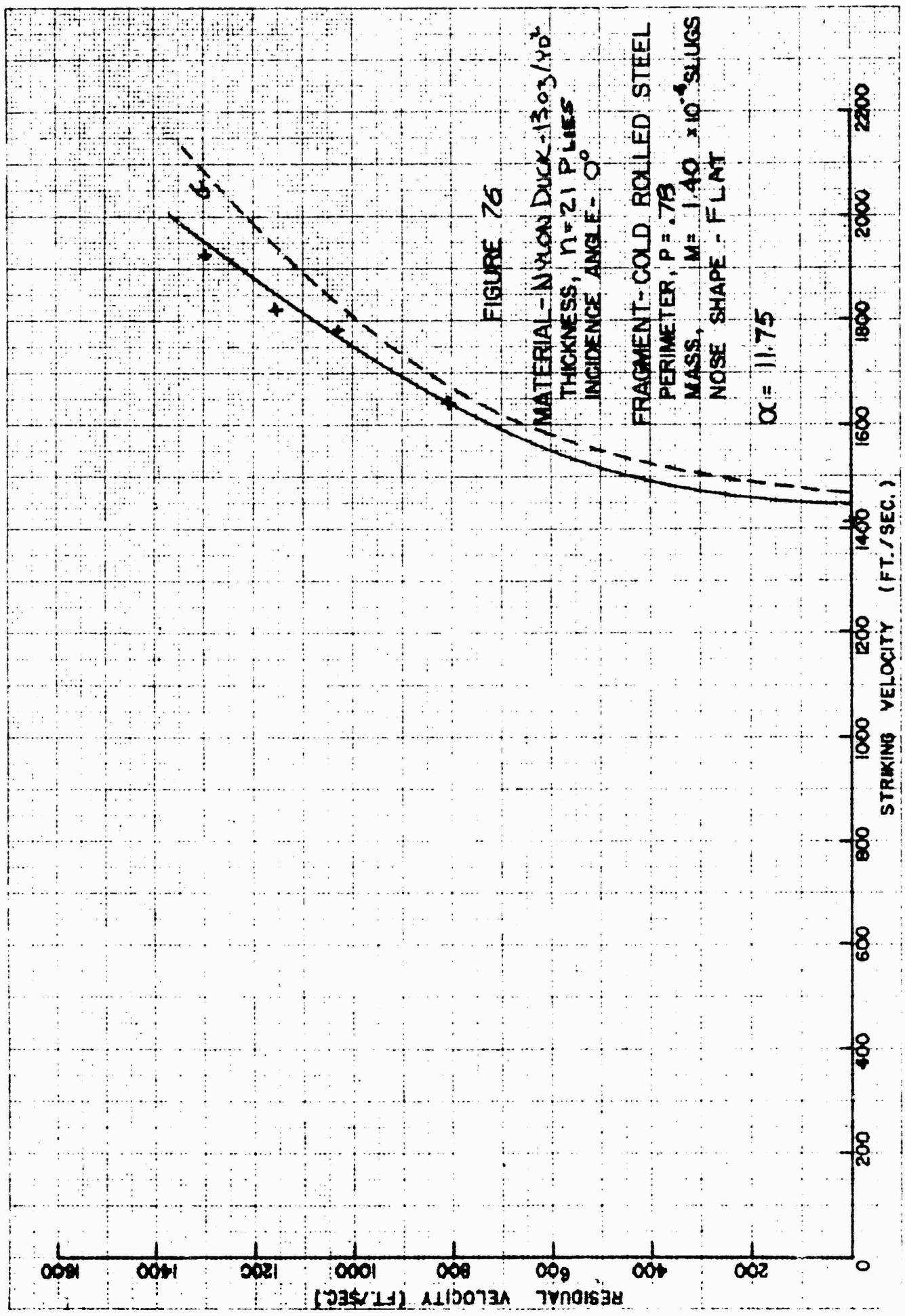
FIGURE 74

MATERIAL - NYLON DUCK-120g/YO²
 THICKNESS, $T = 21$ PLIES
 INCIDENCE ANGLE - 45°

FRAGMENT - COLD ROLLED STEEL
 PERIMETER, $P = 170$
 MASS, $M = 4.27$ KI SLUGS
 NOSE SHAPE - 90° CONE

$\alpha = 0.70$





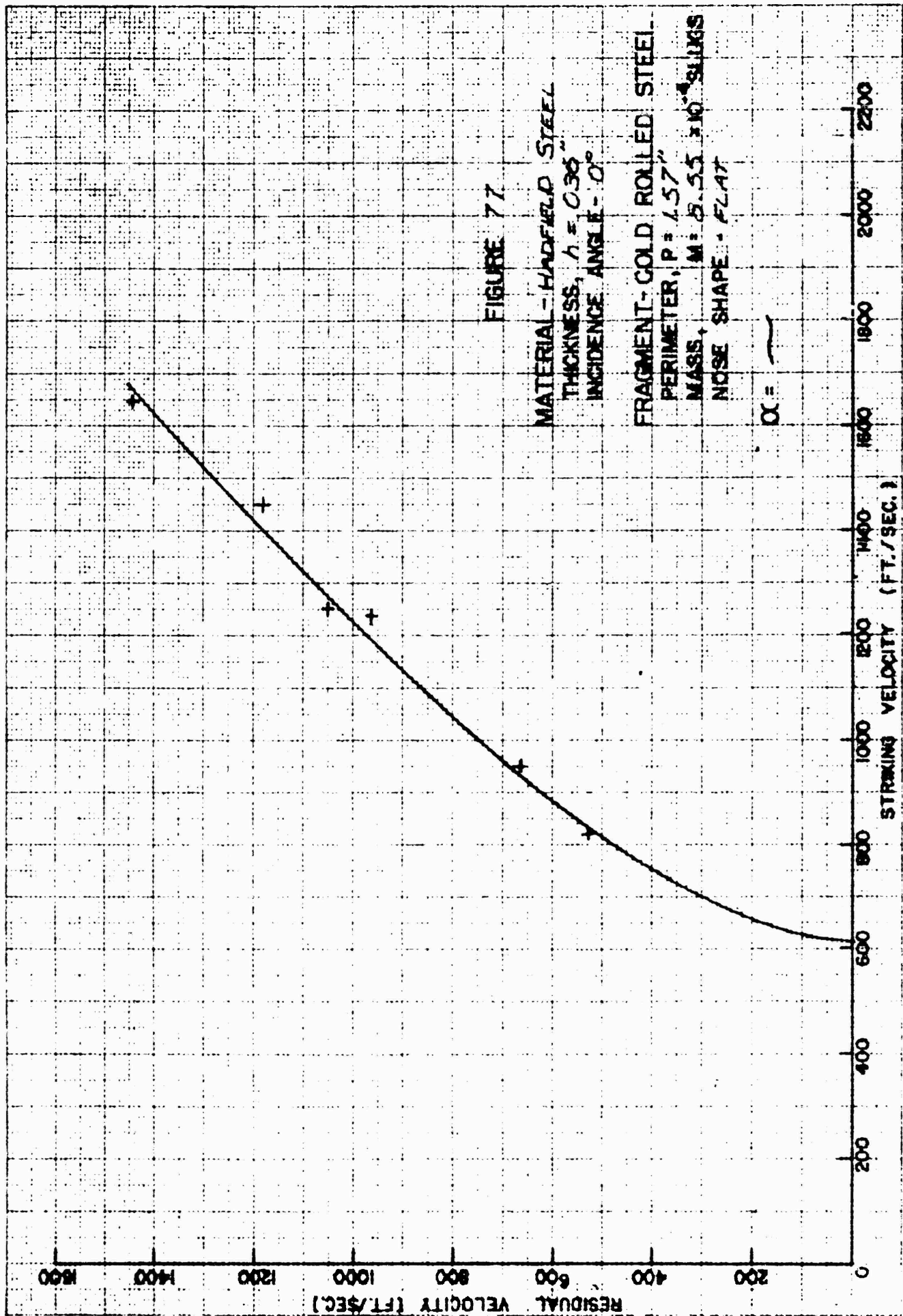


FIGURE 77

MATERIAL - HADFIELD STEEL
 THICKNESS, $t = 0.36$ "
 INCIDENCE ANGLE - 0°
 FRAGMENT - COLD ROLLED STEEL
 PERIMETER, $P = 4.57$ "
 MASS, $M = 2.55 \times 10^{-4}$ SLUGS
 NOSE SHAPE - FLAT

$\alpha =$ _____

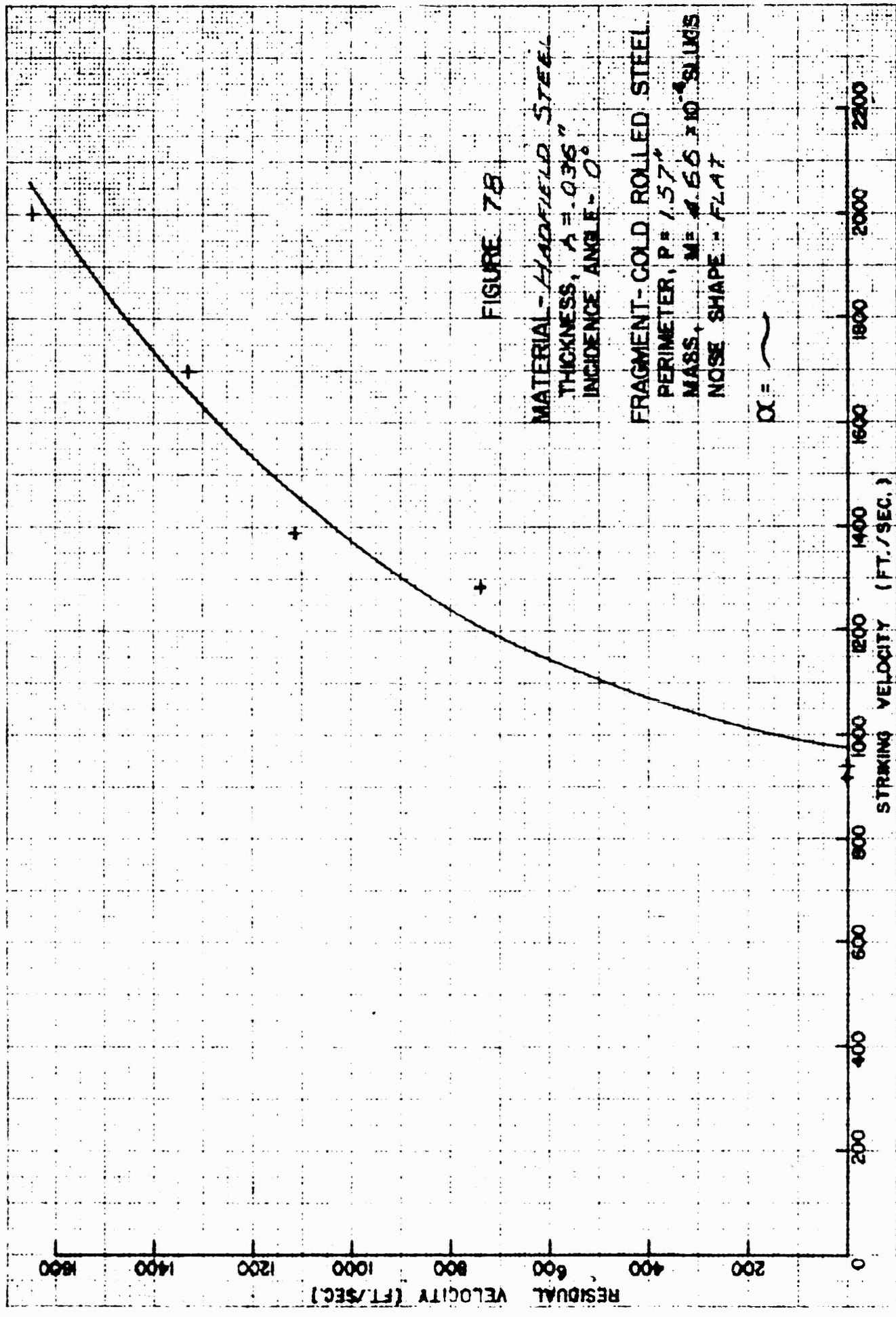


FIGURE 7B

MATERIAL - HADFIELD STEEL
 THICKNESS, $t = 0.036$ "
 INCIDENCE ANGLE - 0°

FRAGMENT - COLD ROLLED STEEL
 PERIMETER, $P = 1.57$ "
 MASS, $M = 0.66 \times 10^{-4}$ SLUGS
 NOSE SHAPE - FLAT

$\alpha = \sim$

RESTRICTED

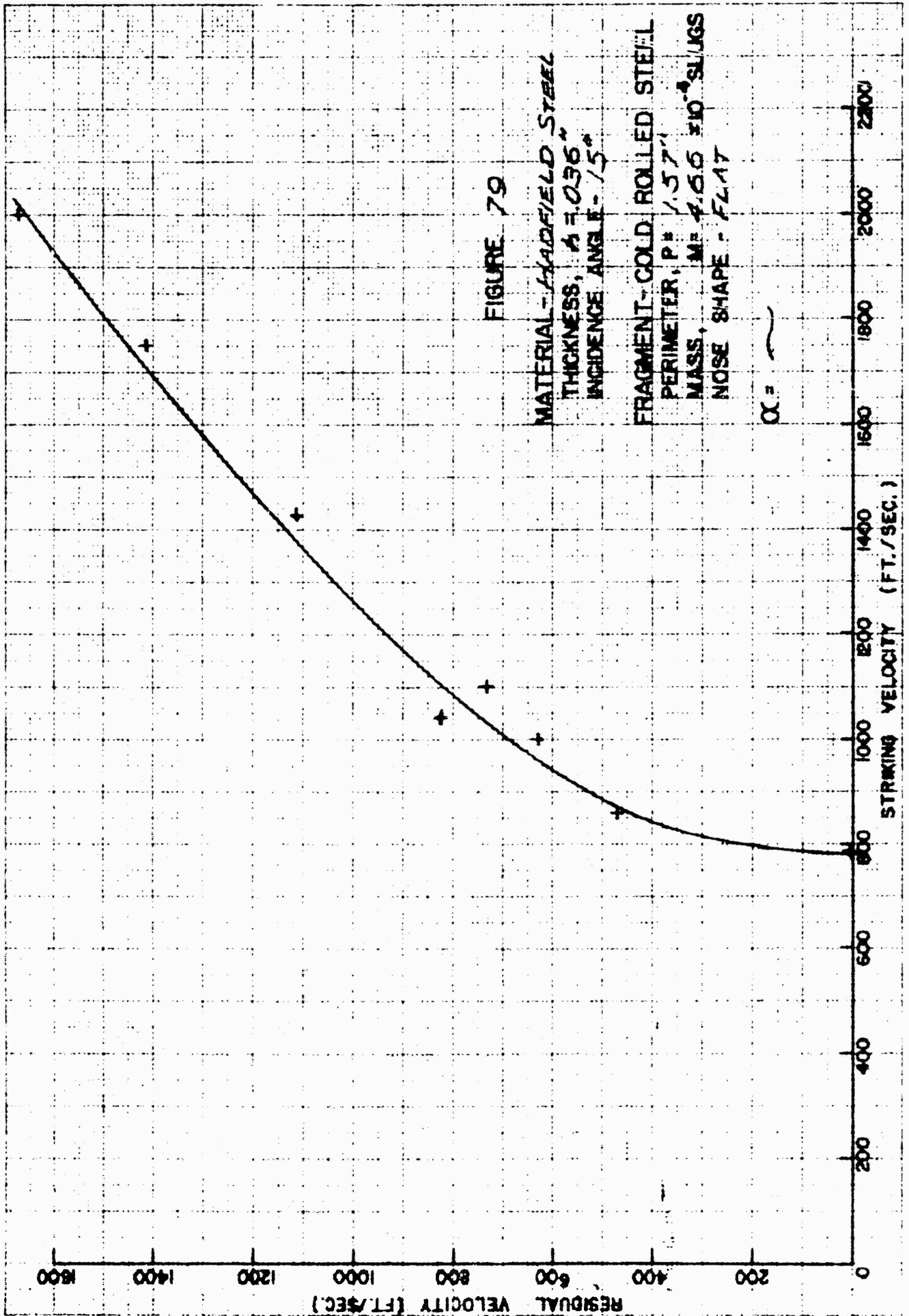


FIGURE 79

MATERIAL - AARFIELD STEEL
THICKNESS, $t = 0.36$ "
INCIDENCE ANGLE - 15°

FRAGMENT - COLD ROLLED STEEL
PERIMETER, $P = 1.57$ "
MASS, $M = 4.66 \times 10^{-4}$ SLUGS
NOSE SHAPE - FLAT

$\alpha = \sim$

RESTRICTED

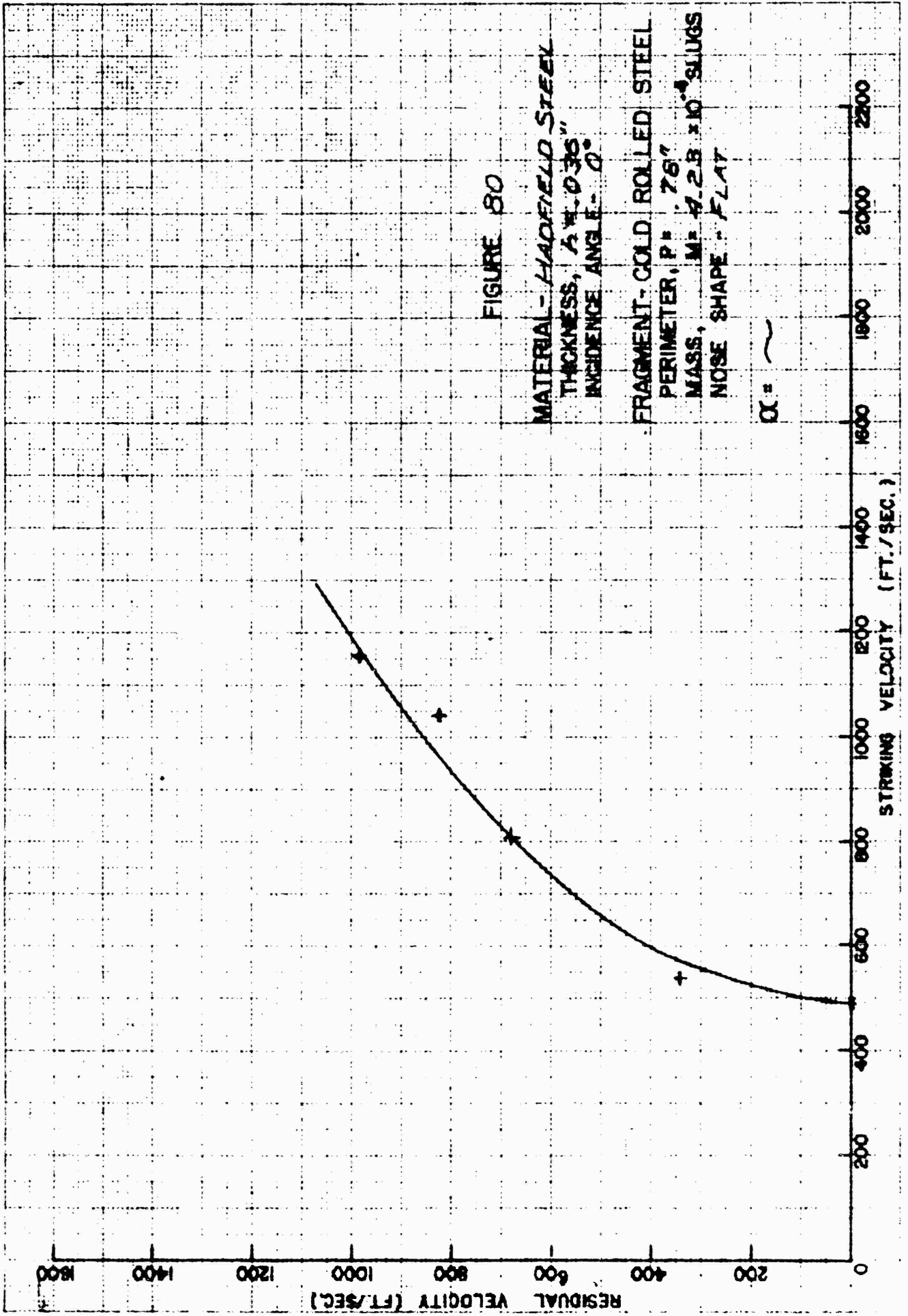


FIGURE 80

MATERIAL - HADFIELD STEEL
THICKNESS, $\frac{1}{2}$ IN. ± 0.036 "
INCIDENCE ANGLE - 0°

FRAGMENT - COLD ROLLED STEEL
PERIMETER, P = 7.6"
MASS, M = 4.28×10^{-4} SLUGS
NOSE SHAPE - FLAT

$\alpha = \sim$

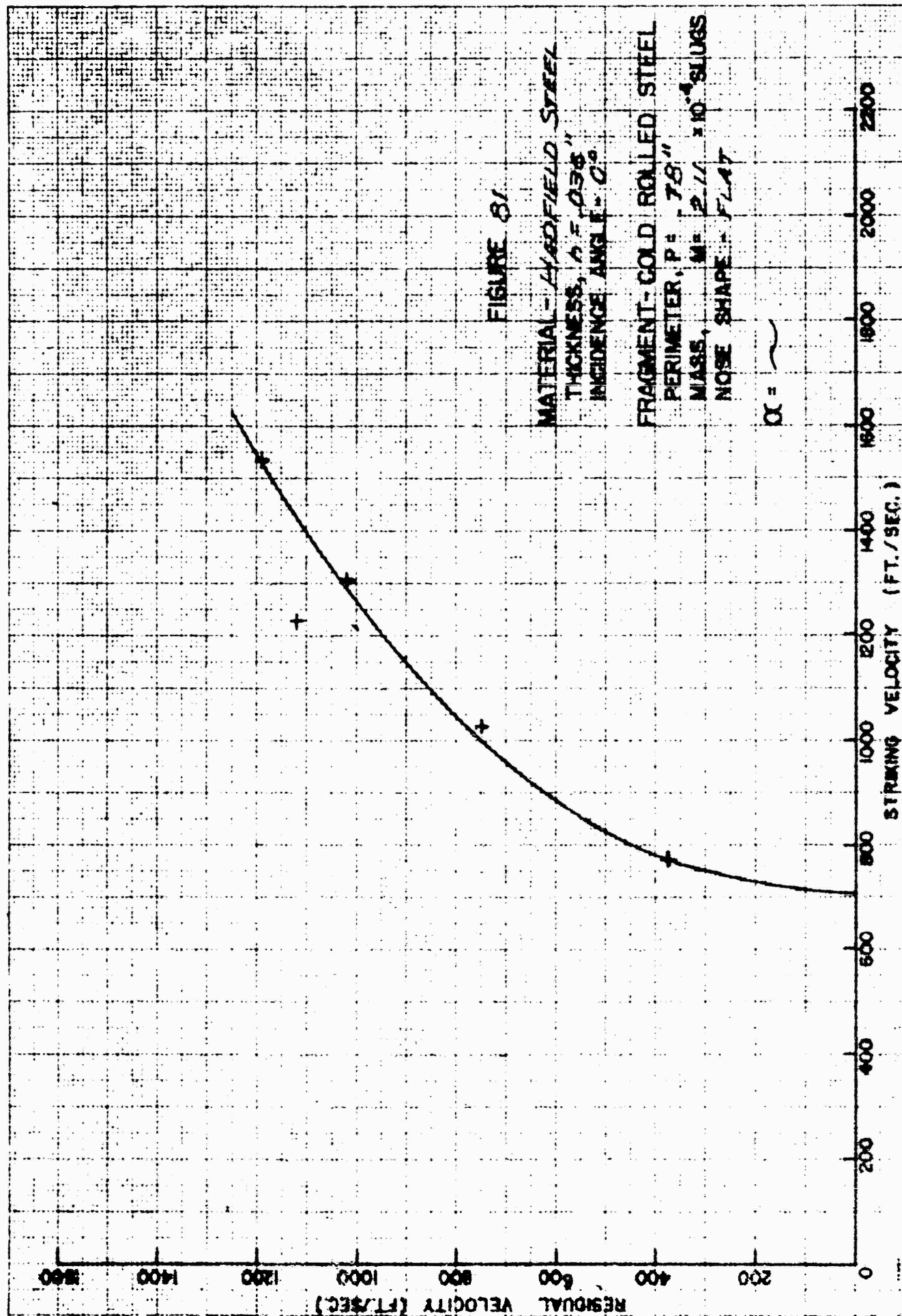
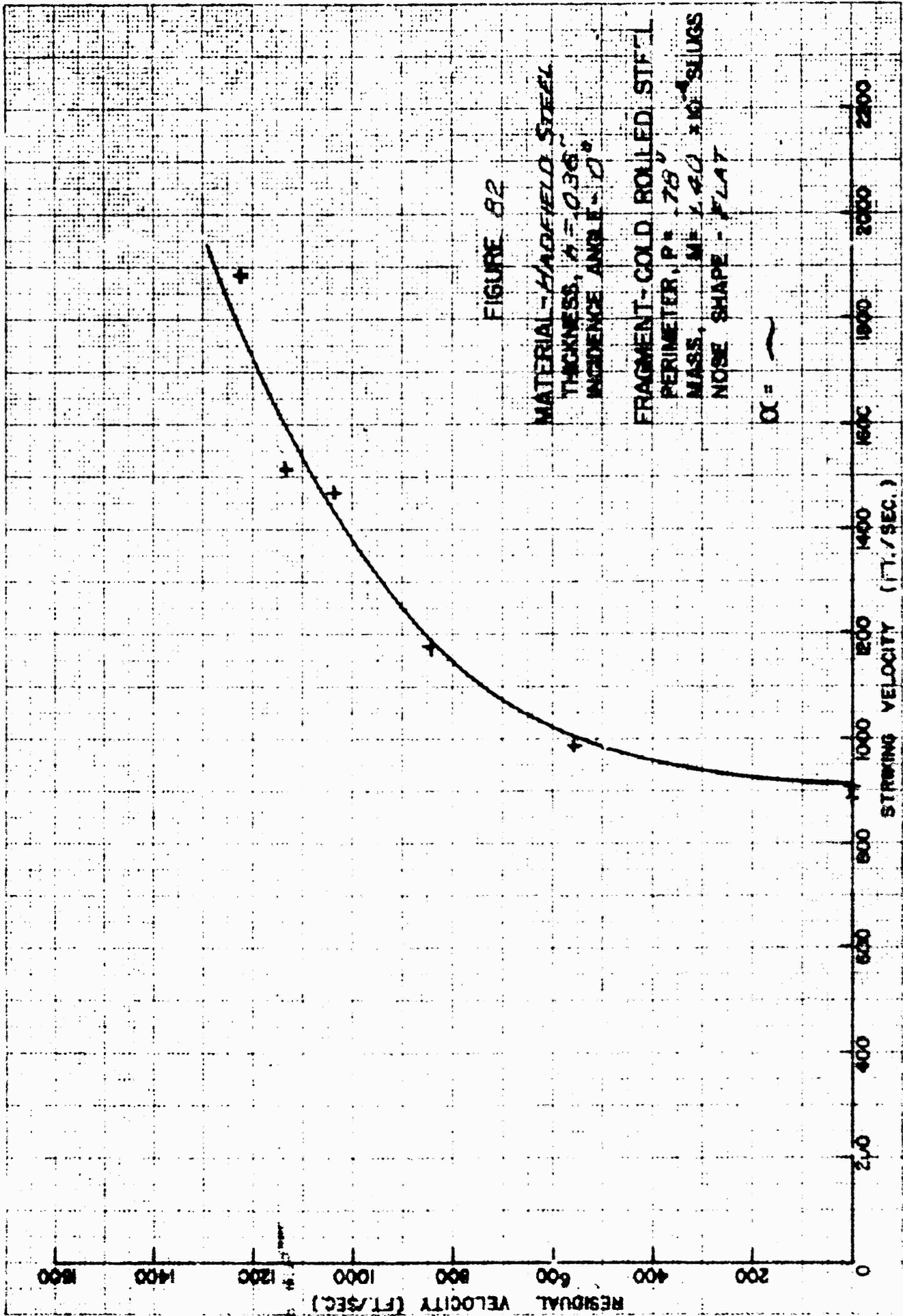


FIGURE 81

MATERIAL - HYADFIELD STEEL
 THICKNESS, $t = 0.036$ "
 INCIDENCE ANGLE - 0°

FRAGMENT - COLD ROLLED STEEL
 PERIMETER, $P = 7.8$ "
 MASS, $M = 2.71 \times 10^{-4}$ SLUGS
 NOSE SHAPE - FLAT

$\alpha = \sim$



RESTRICTED

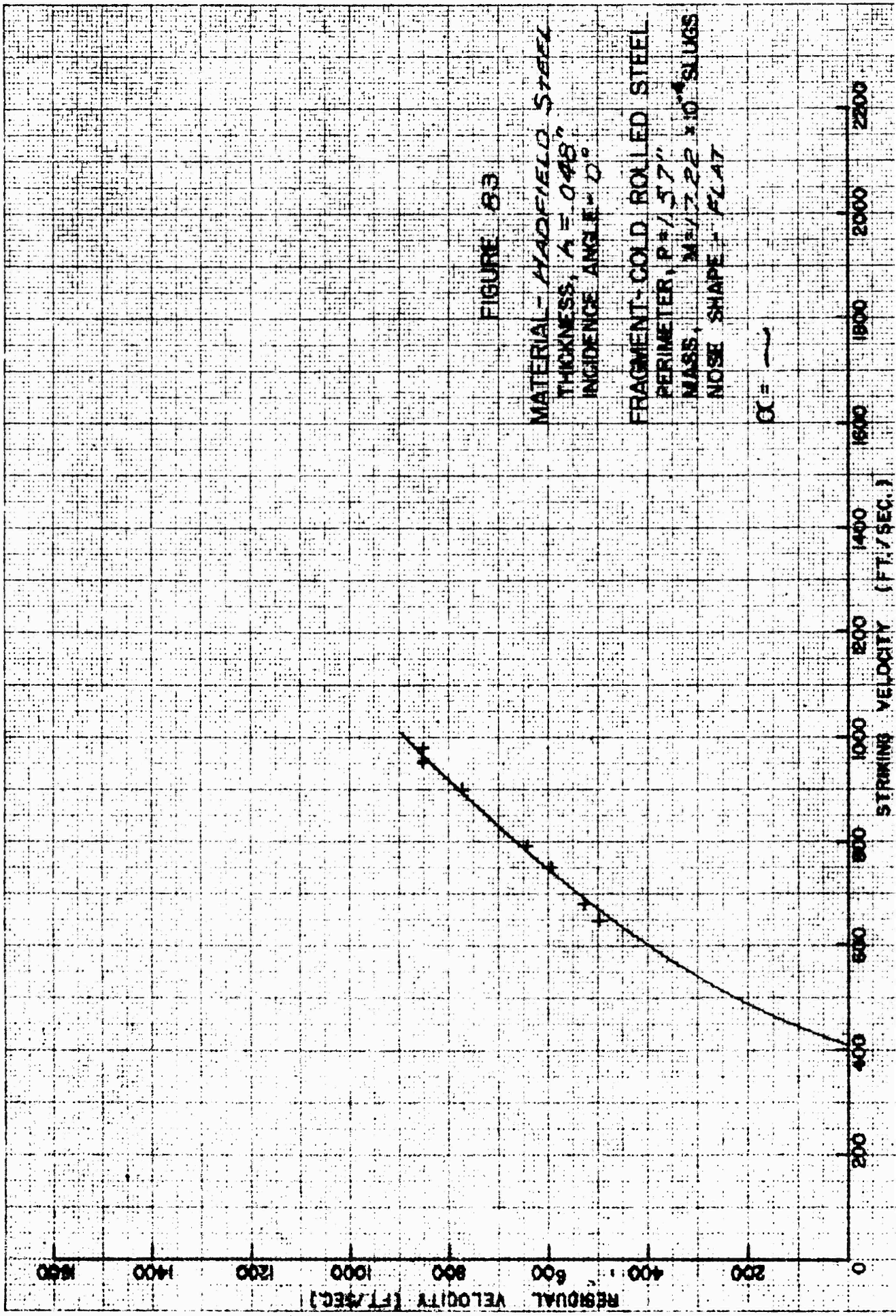


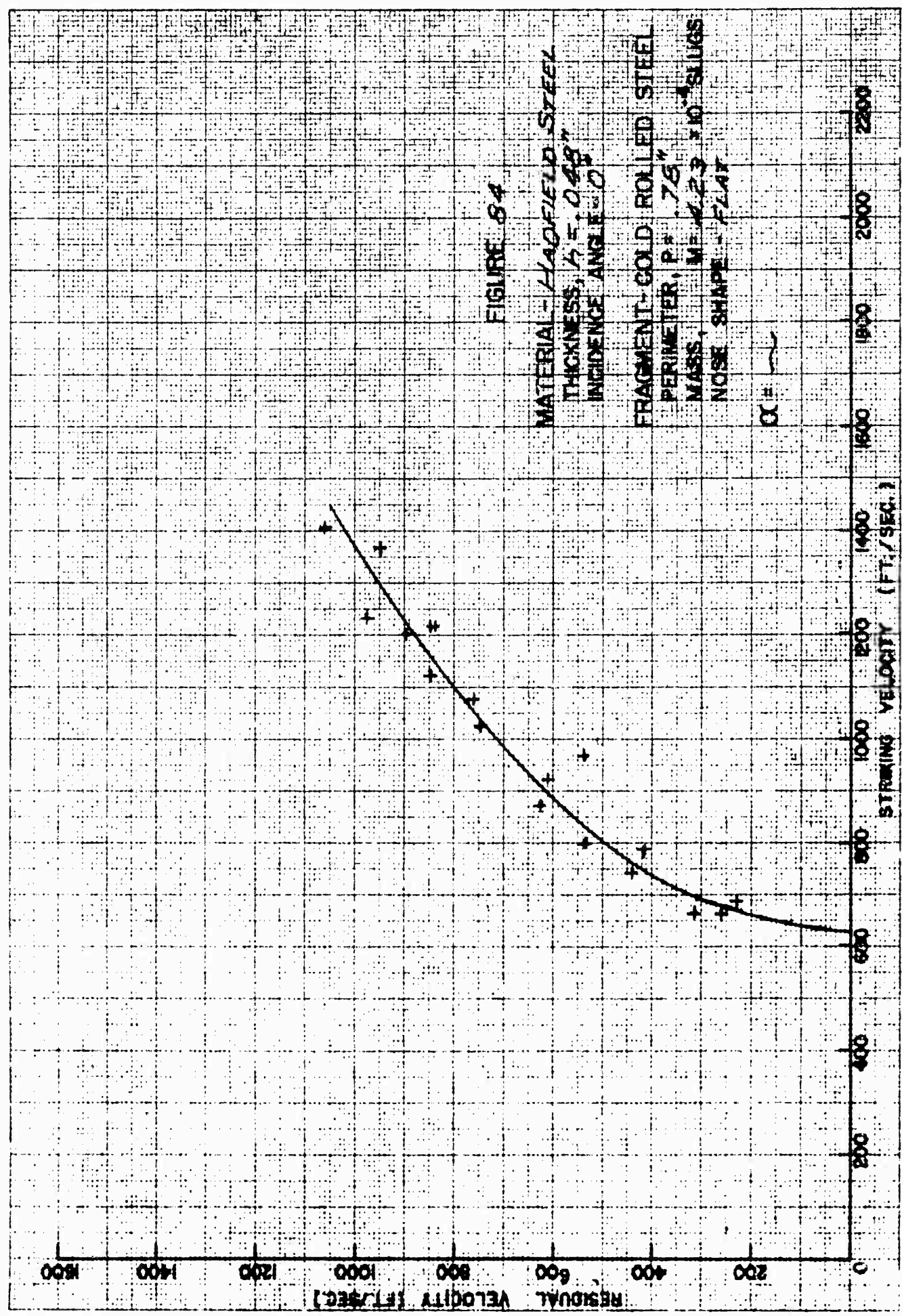
FIGURE 83

MATERIAL - AADFIELD STEEL
THICKNESS, $t = 0.48"$
INCIDENCE ANGLE = 0°

FRAGMENT - COLD ROLLED STEEL
PERIMETER, $P = 1.57"$
MASS, $M = 7.22 \times 10^{-4}$ SLUGS
NOSE SHAPE - FLAT

$\alpha = \text{---}$

RESTRICTED



RESTRICTED

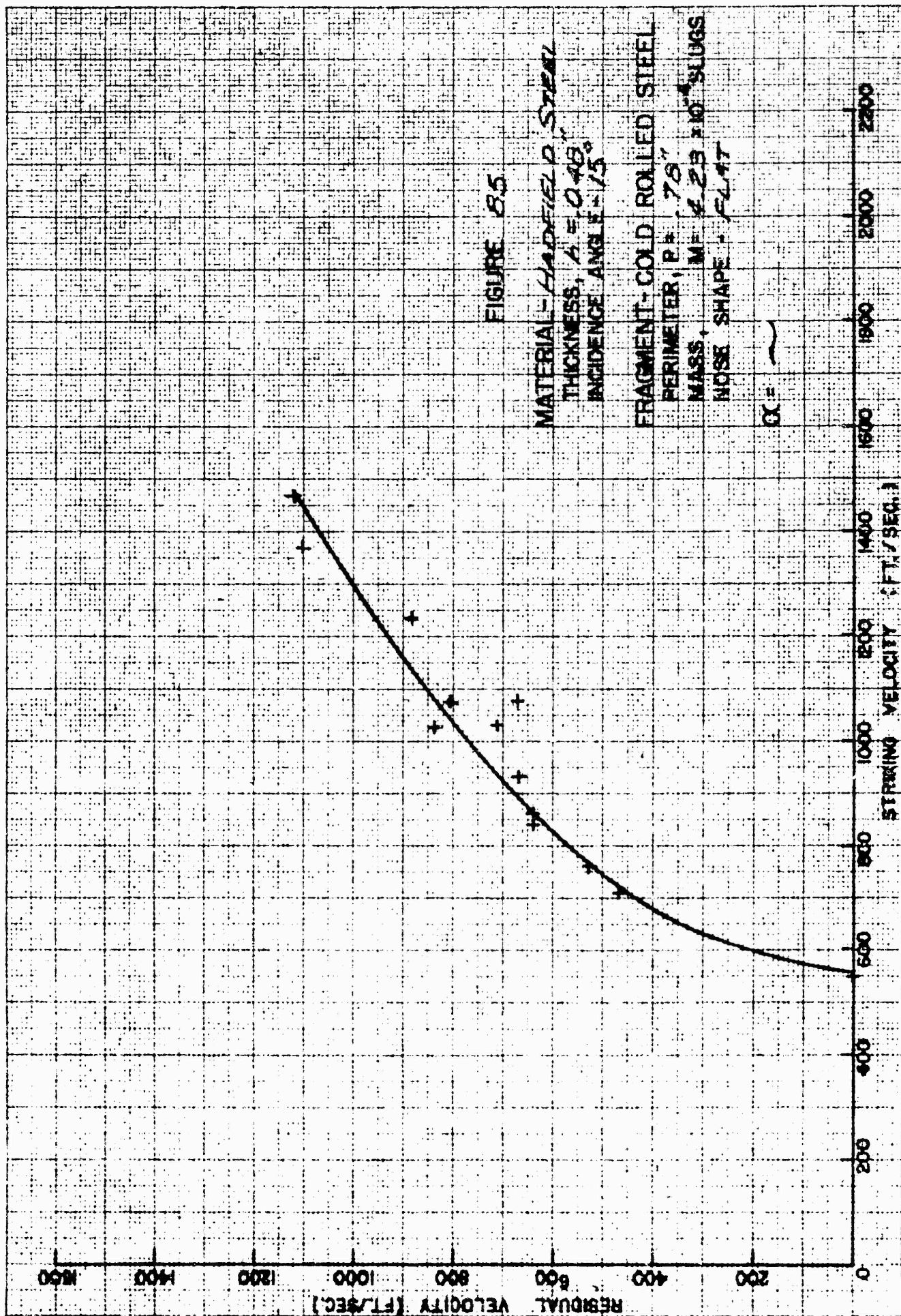


FIGURE 85

MATERIAL - HARDFIELD P. STEEL

THICKNESS, $t = 0.48"$

INCIDENCE ANGLE $= 15^\circ$

FRAGMENT - COLD ROLLED STEEL

PERIMETER, $P = .78"$

MASS, $M = 4.25 \times 10^{-4}$ SLUGS

NOSE SHAPE - FLAT

$\alpha =$ ~

RESTRICTED

DATA SHEETS
CHARLES NILES WRIGHT, JR. RE-1000K
Y. 11. 10. 1947

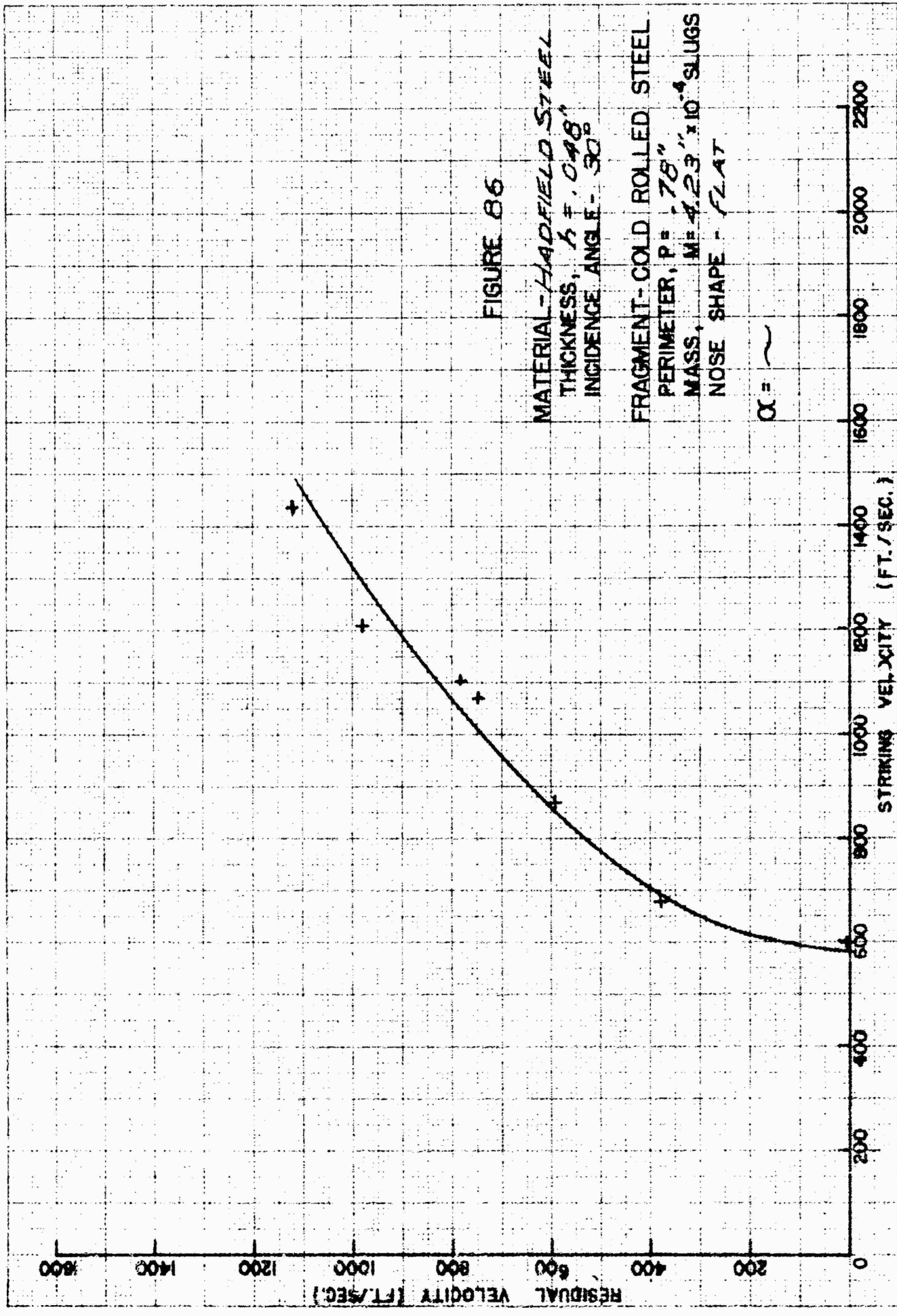


FIGURE 86

MATERIAL - HADFIELD STEEL
THICKNESS, $t = .048$ "
INCIDENCE ANGLE - 30°

FRAGMENT - COLD ROLLED STEEL
PERIMETER, $P = .78$ "
MASS, $M = 4.23 \times 10^{-4}$ SLUGS
NOSE SHAPE - FLAT

$\alpha = \sim$

RESTRICTED

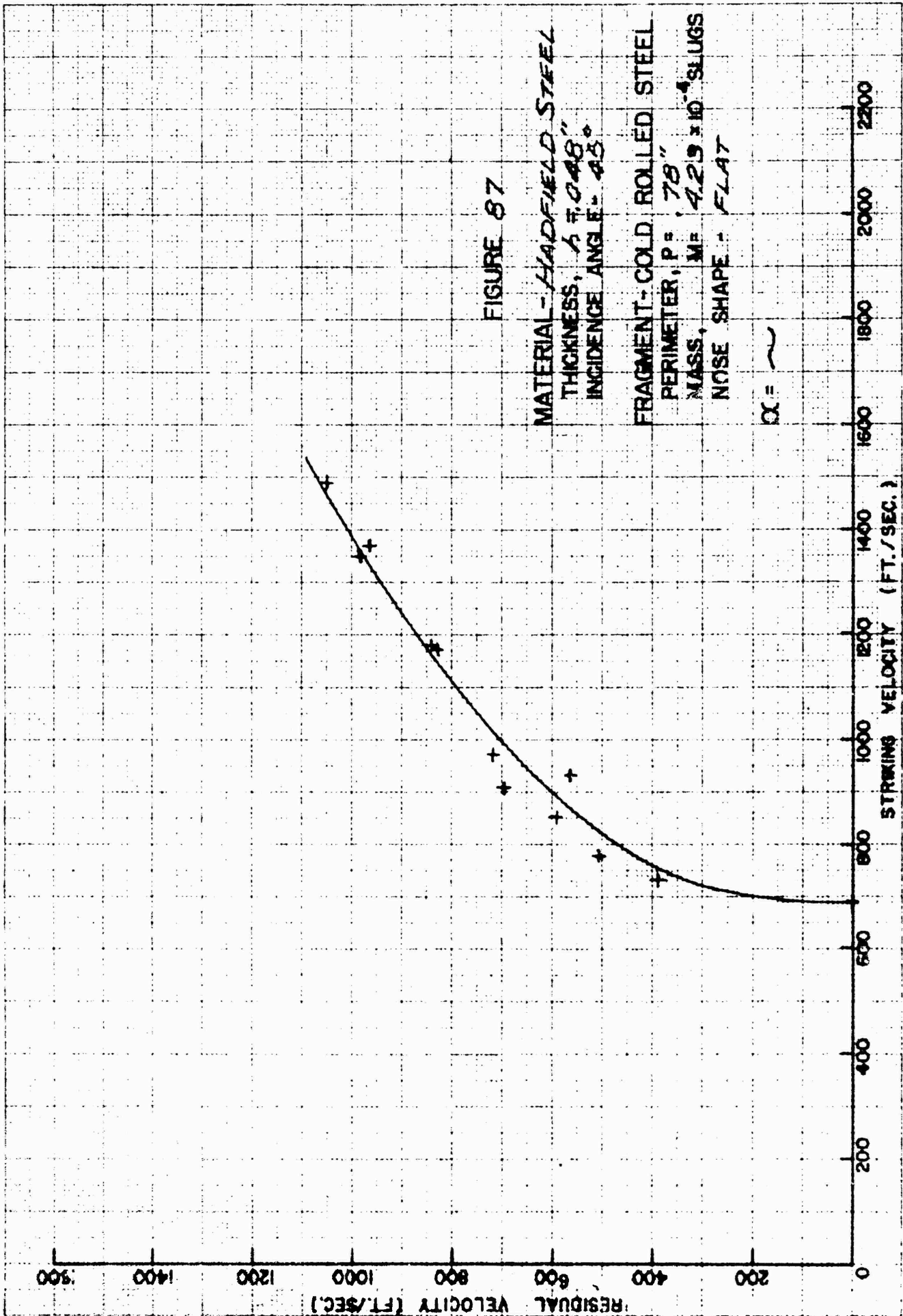


FIGURE 87

MATERIAL - HADFIELD STEEL
 THICKNESS, 5.7048"
 INCIDENCE ANGLE - 45°

FRAGMENT - COLD ROLLED STEEL
 PERIMETER, P = .78"
 MASS, M = 4.29 x 10⁻⁴ SLUGS
 NOSE SHAPE - FLAT

$\alpha = \sim$

RESTRICTED

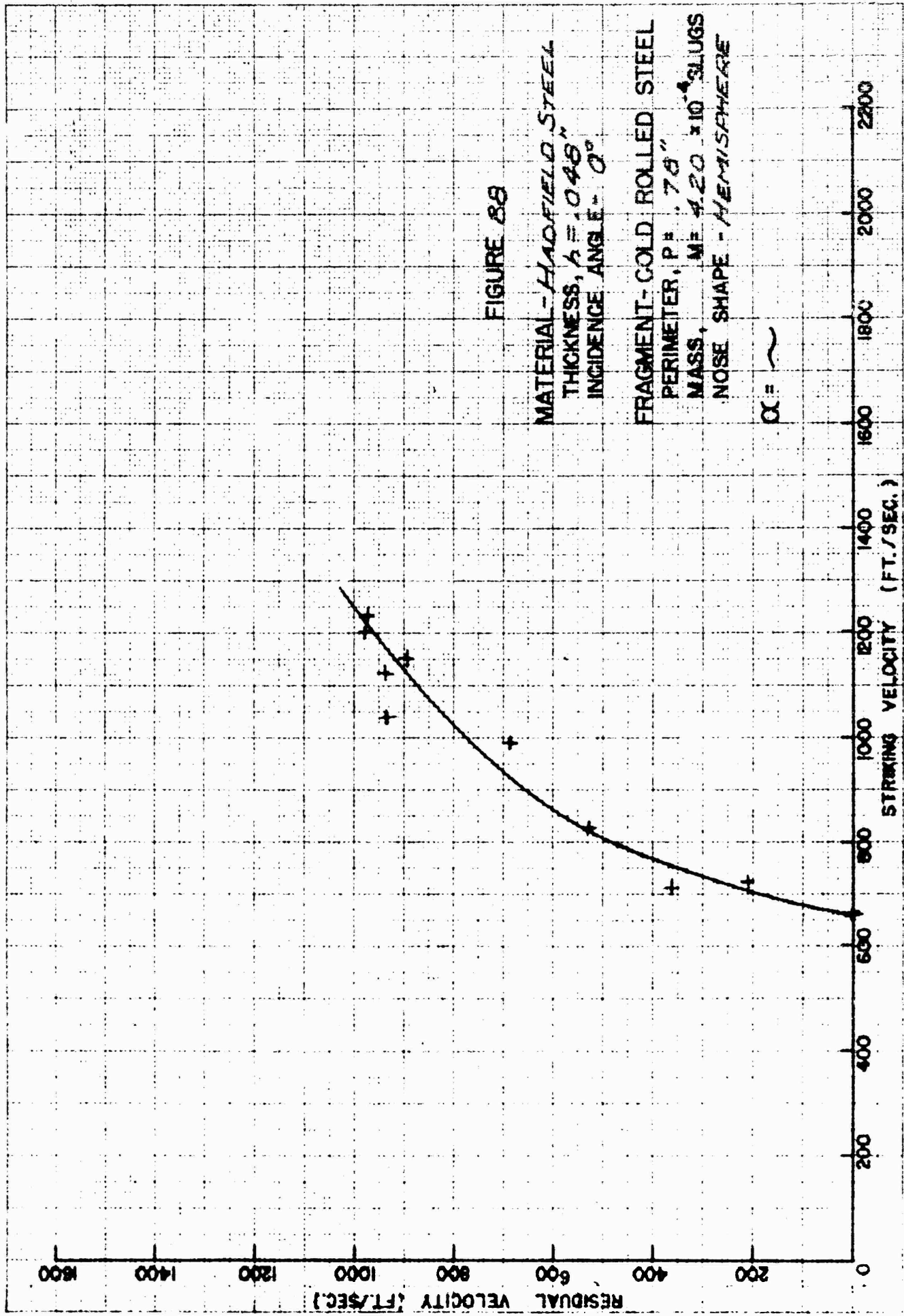


FIGURE 88

MATERIAL - HADFIELD STEEL
THICKNESS, $t = .048$ "
INCIDENCE ANGLE - 0°

FRAGMENT - COLD ROLLED STEEL
PERIMETER, $P = .78$ "
MASS, $M = 4.20 \times 10^{-4}$ SLUGS
NOSE SHAPE - HEMISPHERE

$\alpha = \sim$

RESTRICTED

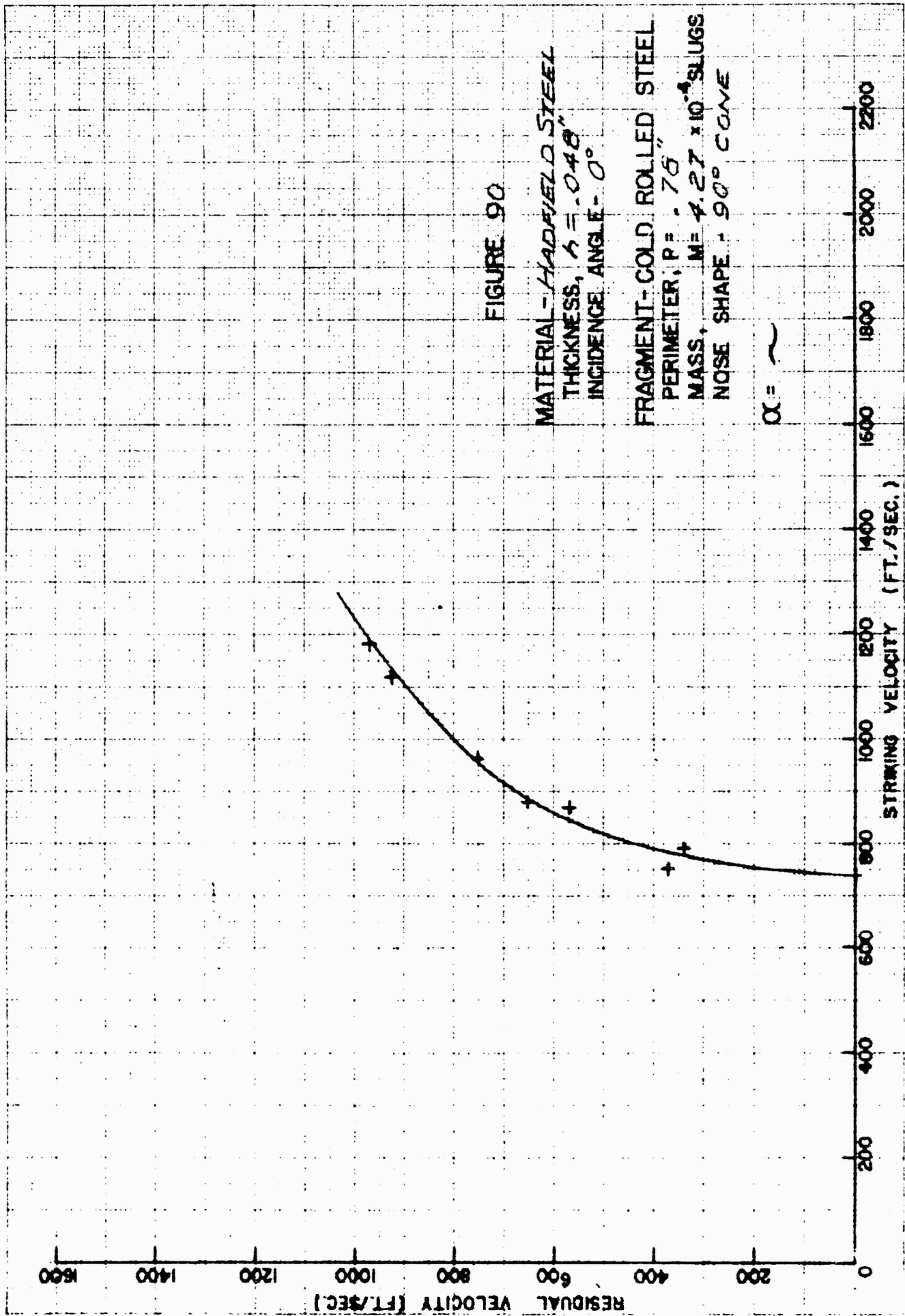


FIGURE 90

MATERIAL - HADFIELD STEEL
 THICKNESS, $t = .048$ "
 INCIDENCE ANGLE - 0°

FRAGMENT - COLD ROLLED STEEL
 PERIMETER, $P = .76$ "
 MASS, $M = 4.27 \times 10^{-4}$ SLUGS
 NOSE SHAPE - 90° CONE

$\alpha = \sim$

RESTRICTED

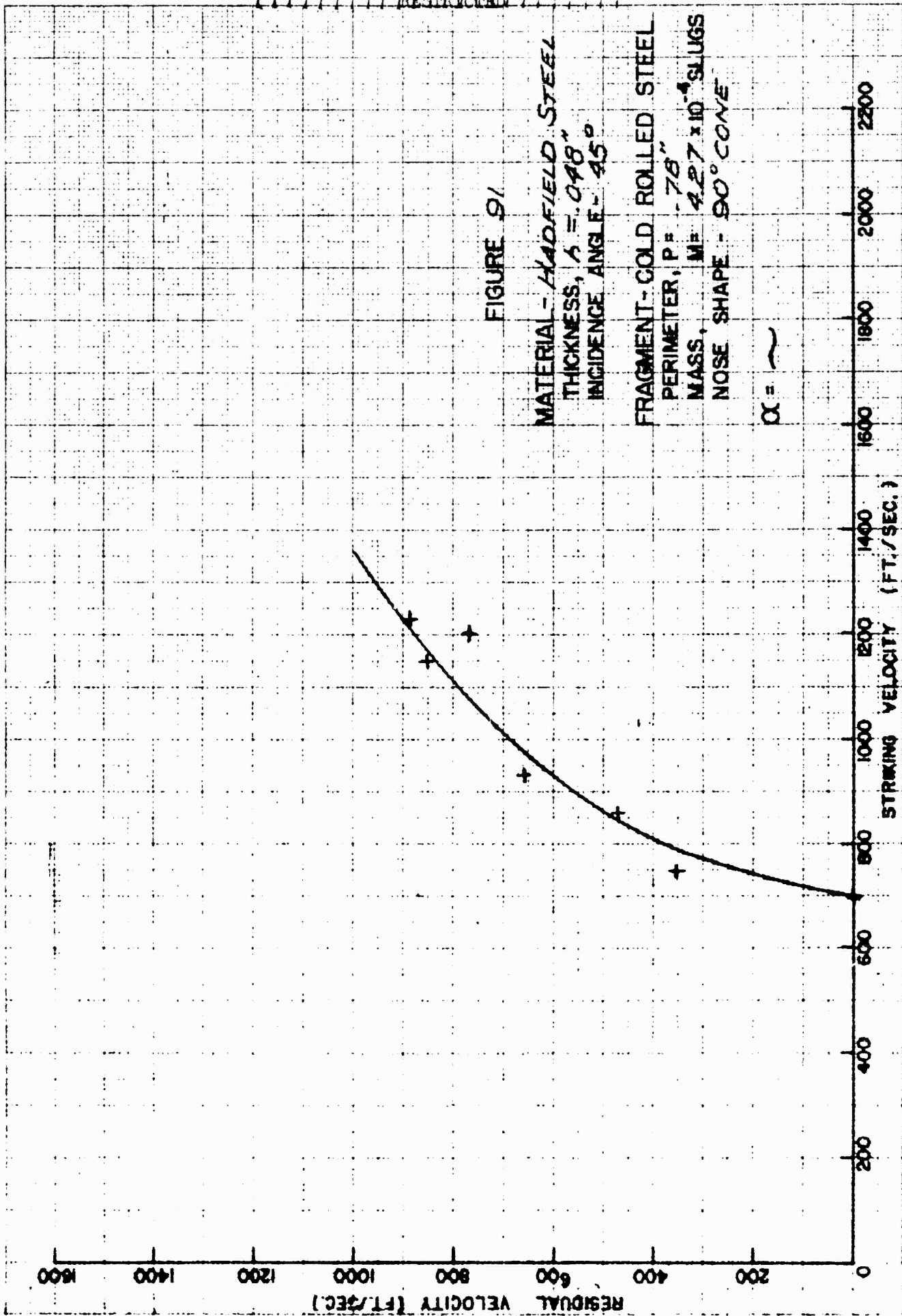


FIGURE 91

MATERIAL - HADFIELD STEEL

THICKNESS, $t = .048"$

INCIDENCE ANGLE - 45°

FRAGMENT - COLD ROLLED STEEL

PERIMETER, $P = .78"$

MASS, $M = 4.27 \times 10^{-4}$ SLUGS

NOSE SHAPE - 90° CONE

$\alpha = \sim$

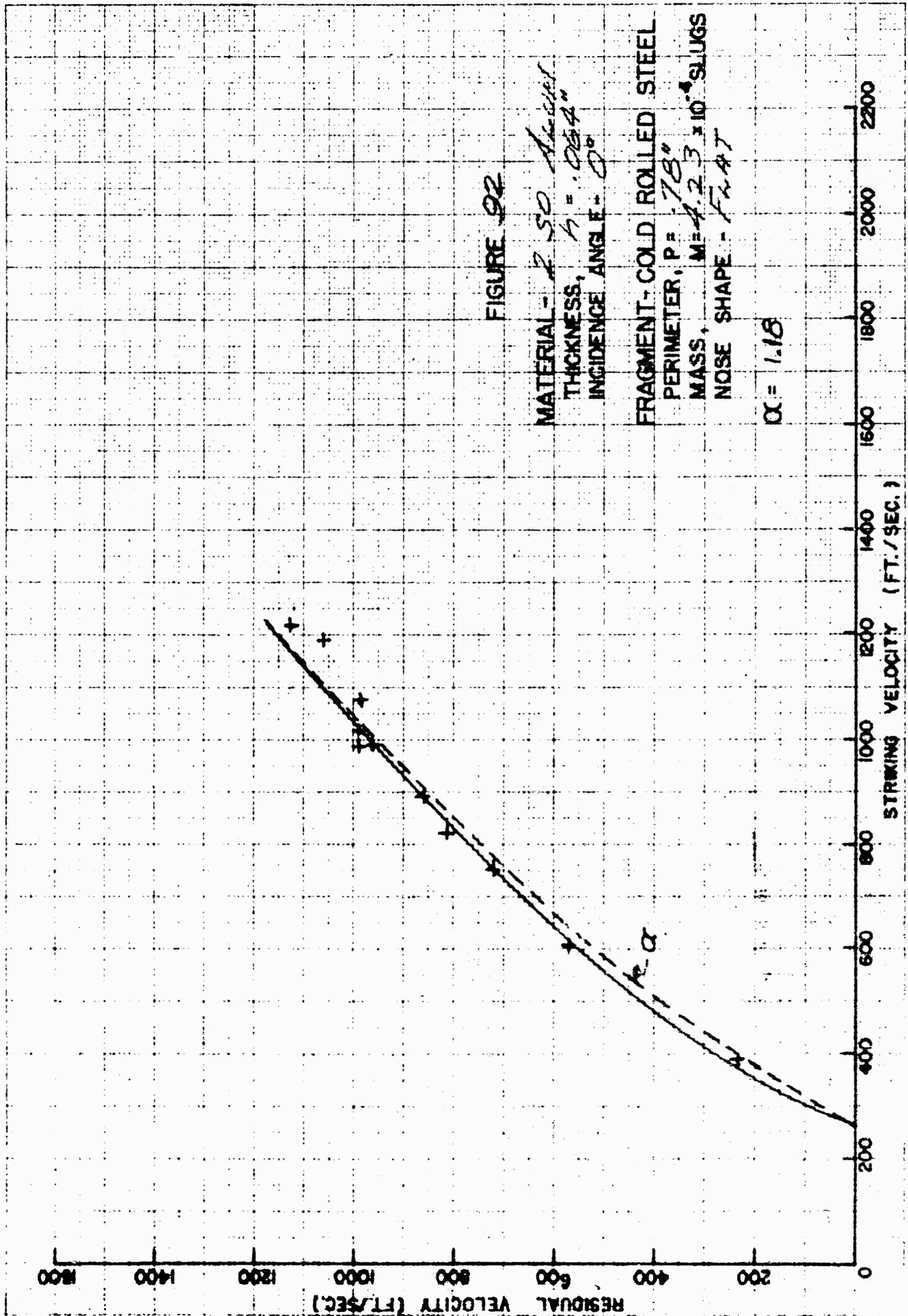
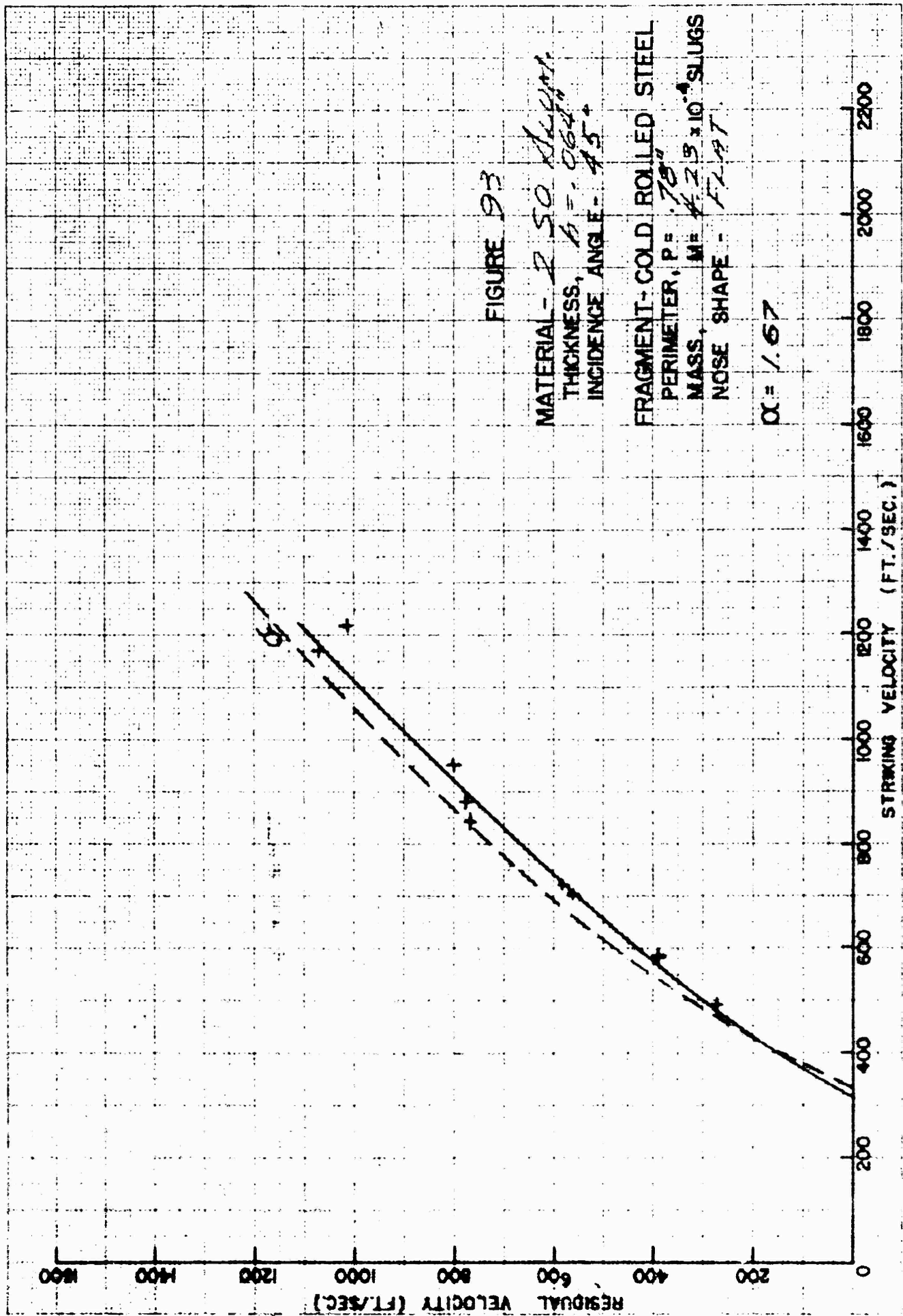


FIGURE 92

MATERIAL - 2.50 Alsteel
 THICKNESS, $t = .064"$
 INCIDENCE ANGLE - 0°
 FRAGMENT - COLD ROLLED STEEL
 PERIMETER, $P = .78"$
 MASS, $M = 4.23 \times 10^{-4}$ SLUGS
 NOSE SHAPE - FLAT
 $\alpha = 1.18$



DATA SHEETS

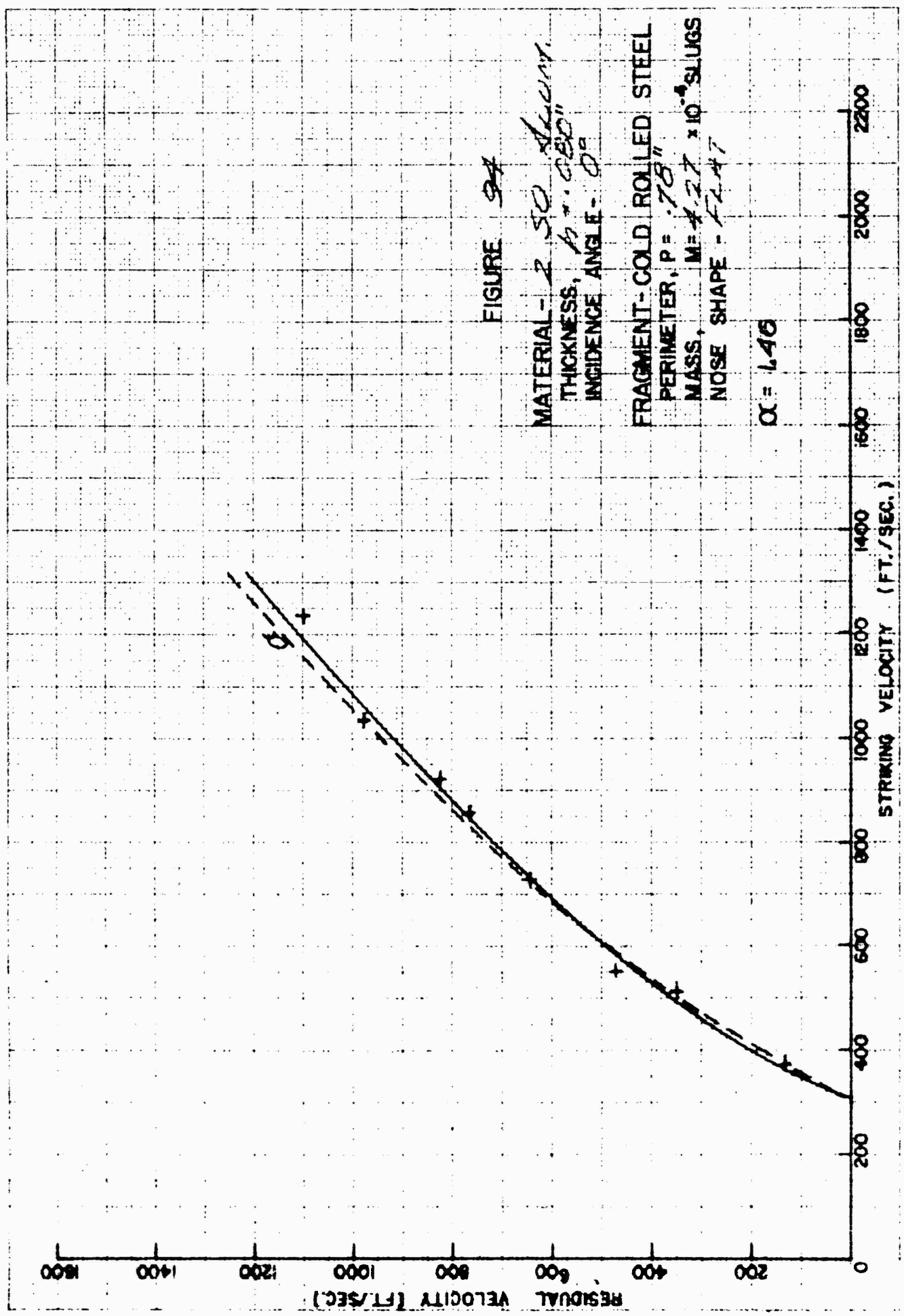


FIGURE 9A

MATERIAL - 2.50 ALUMINUM.
 THICKNESS, $t = .080"$
 INCIDENCE ANGLE - 0°

FRAGMENT - COLD ROLLED STEEL
 PERIMETER, $P = .78"$
 MASS, $M = .27 \times 10^{-3}$ SLUGS
 NOSE SHAPE - FLAT

$\alpha = 1.46$

CALIF. ELECTRA

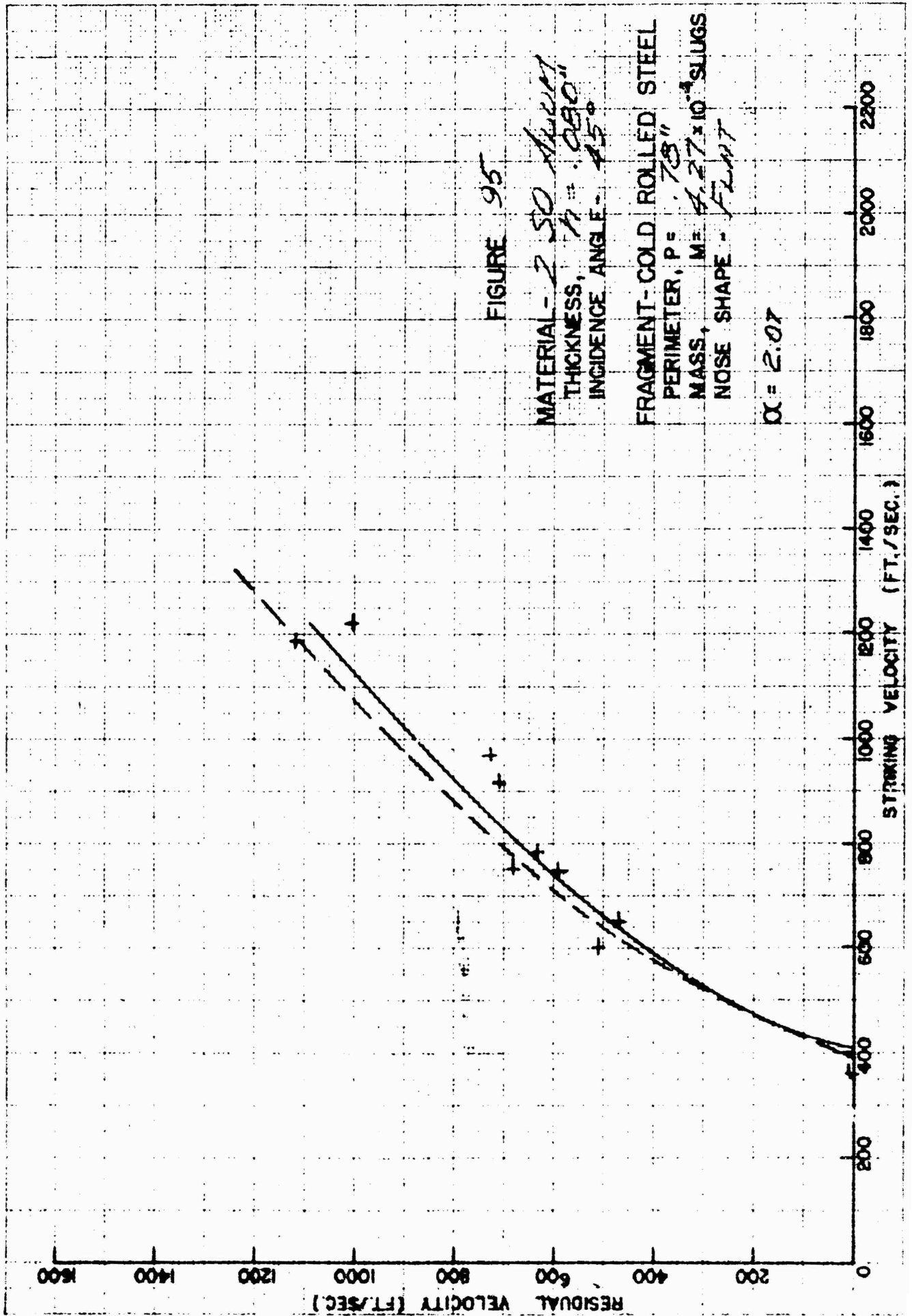


FIGURE 95

MATERIAL - 2.50 ALUMINUM
 THICKNESS, $t = .080"$
 INCIDENCE ANGLE - 45°
 FRAGMENT - COLD ROLLED STEEL
 PERIMETER, $P = .78"$
 MASS, $M = 4.27 \times 10^{-4}$ SLUGS
 NOSE SHAPE - FLAT

$\alpha = 2.07$

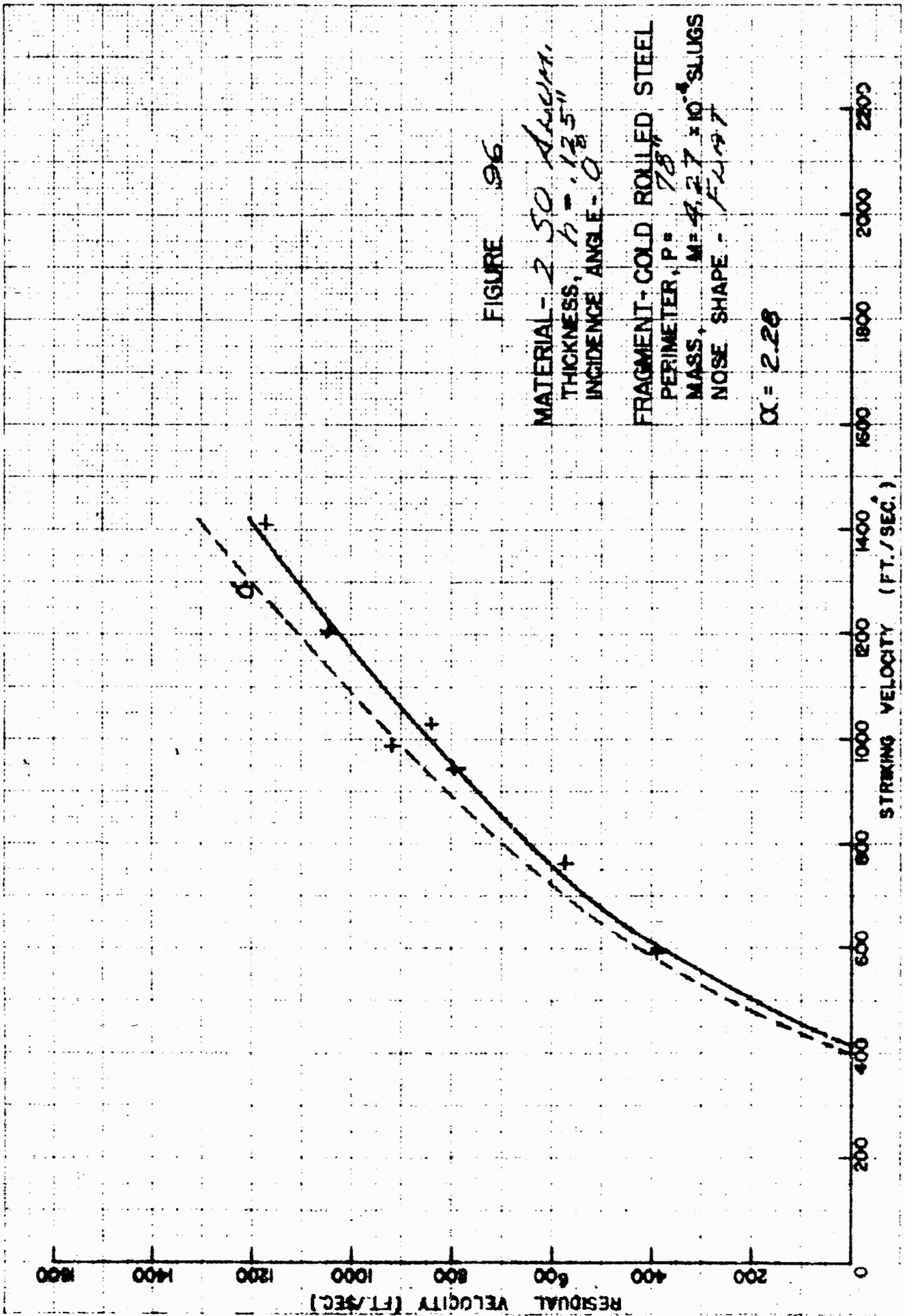


FIGURE 96

MATERIAL - 2.50 INCH.
 THICKNESS, $h = .125$ "
 INCIDENCE ANGLE - 0

FRAGMENT - COLD ROLLED STEEL
 PERIMETER, $P = 78$ "
 MASS, $M = 4.27 \times 10^{-4}$ SLUGS
 NOSE SHAPE - F417

$\alpha = 2.28$

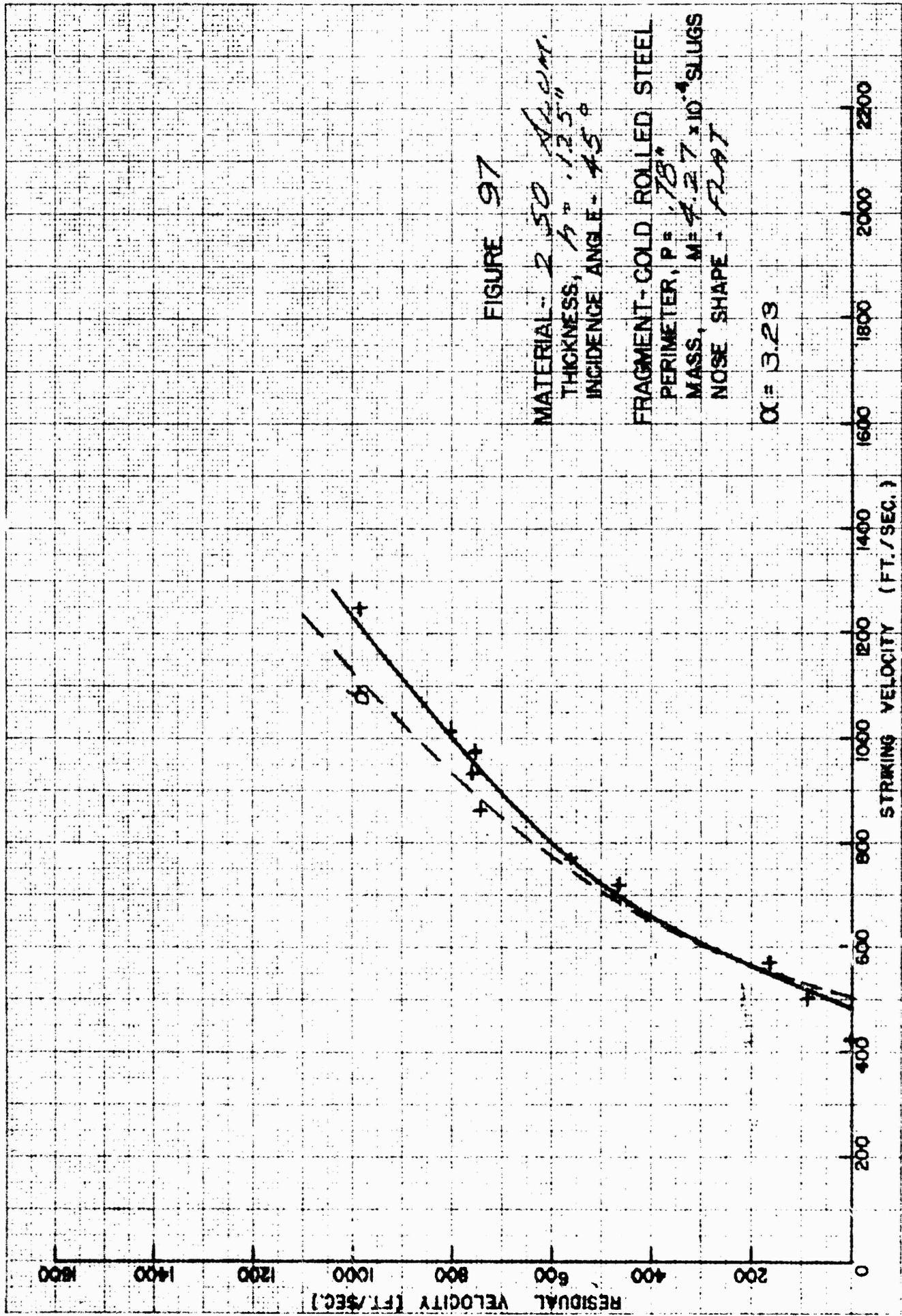


FIGURE 97

MATERIAL - 2.50 ALUM.
 THICKNESS, $t = .125"$
 INCIDENCE ANGLE - 45°
 FRAGMENT - COLD ROLLED STEEL
 PERIMETER, $P = .78"$
 MASS, $M = 4.27 \times 10^{-4}$ SLUGS
 NOSE SHAPE - FLAT

$\alpha = 3.23$

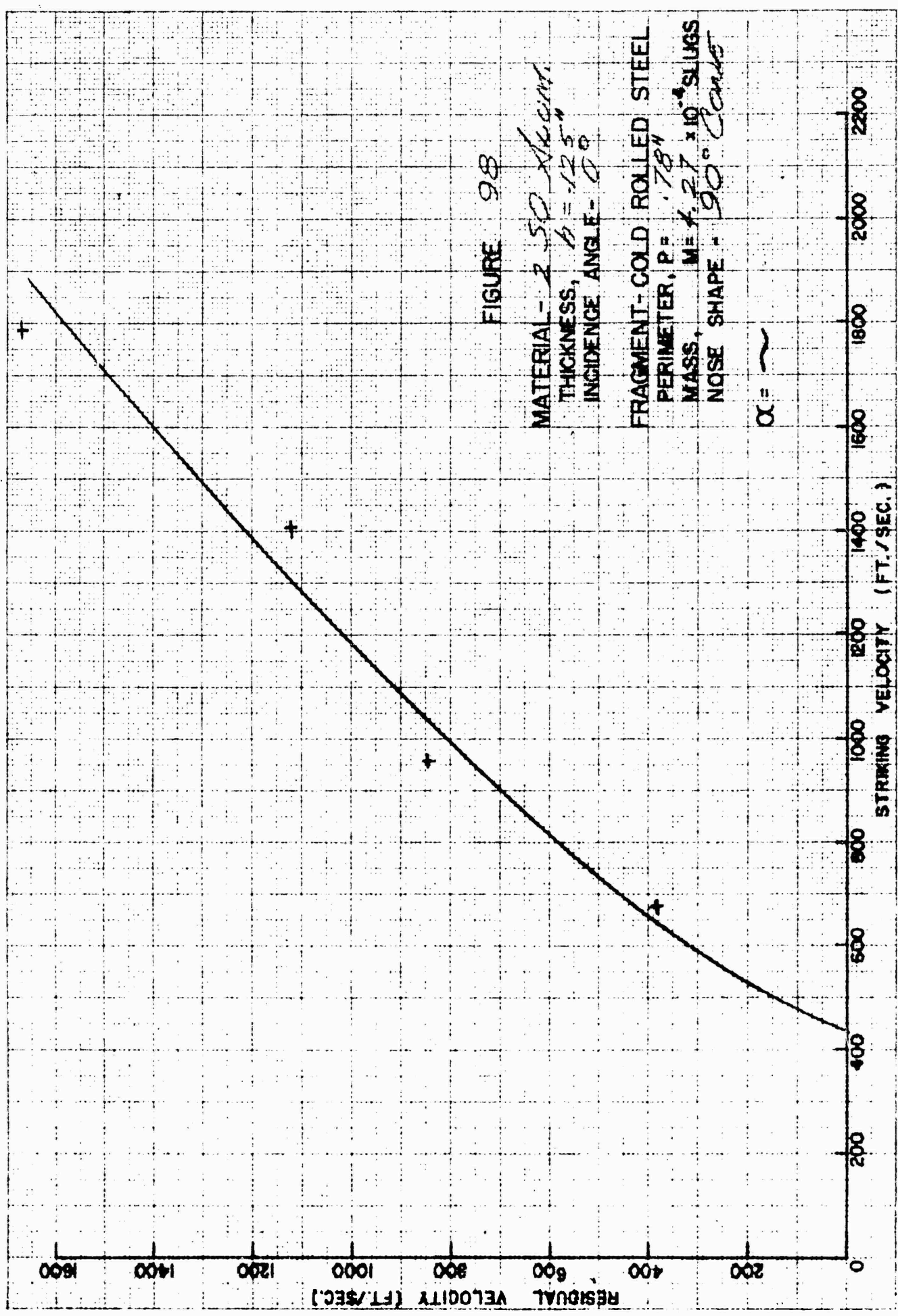


FIGURE 98

MATERIAL - 2 50 ALUMIN.
 THICKNESS, $t = .125''$
 INCIDENCE ANGLE - 0°

FRAGMENT - COLD ROLLED STEEL
 PERIMETER, $P = .78''$
 MASS, $M = 4.27 \times 10^{-4}$ SLUGS
 NOSE SHAPE - 90° CONE

$\alpha = \sim$

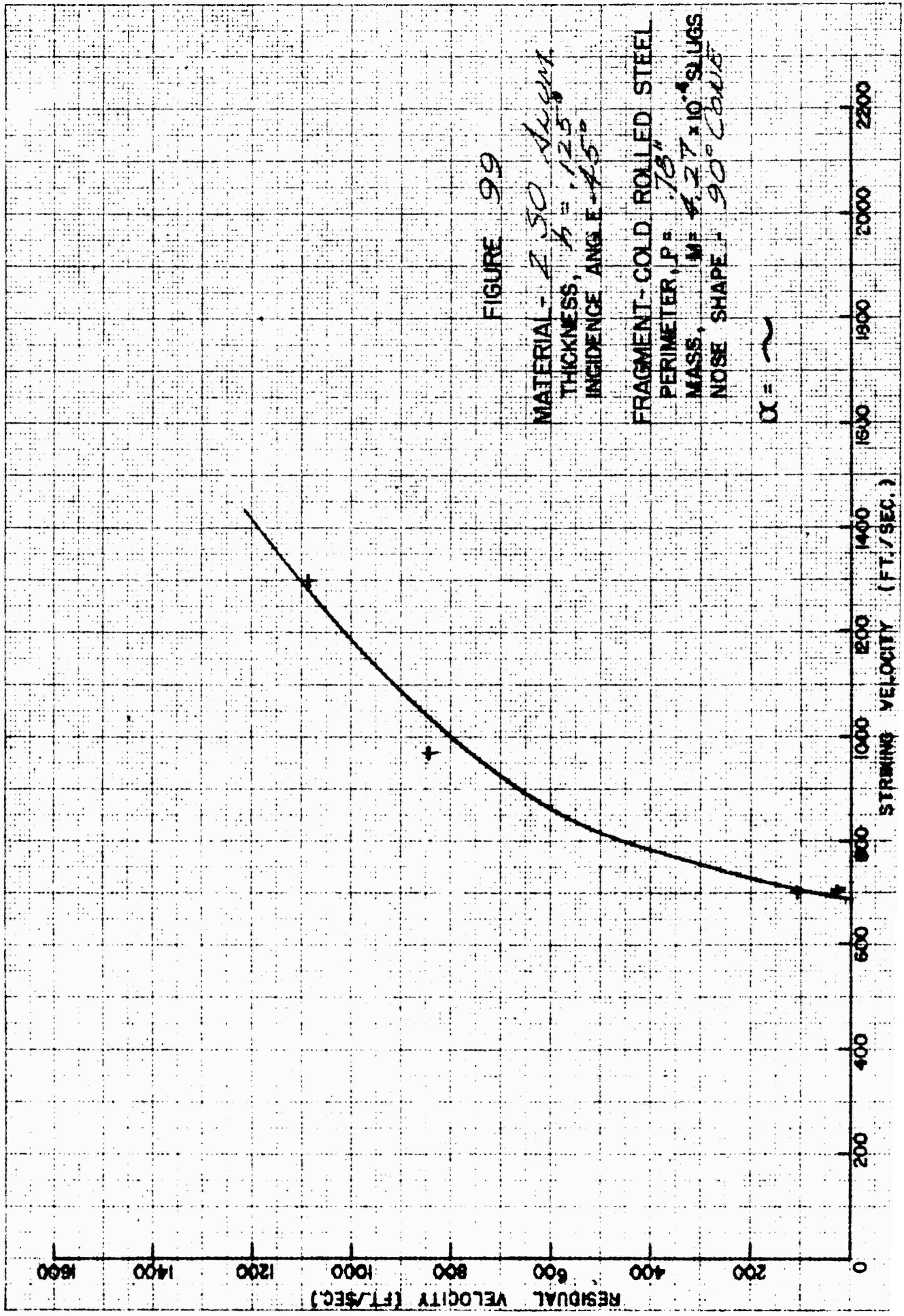


FIGURE 99

MATERIAL - *A-50 Alcant*
 THICKNESS, *t = .125"*
 INCIDENCE ANGLE *45°*

FRAGMENT - COLD ROLLED STEEL
 PERIMETER, *P = .18"*
 MASS, *M = 4.27 x 10⁻⁴ SLUGS*
 NOSE SHAPE *90° CONE*

$\alpha = \sim$

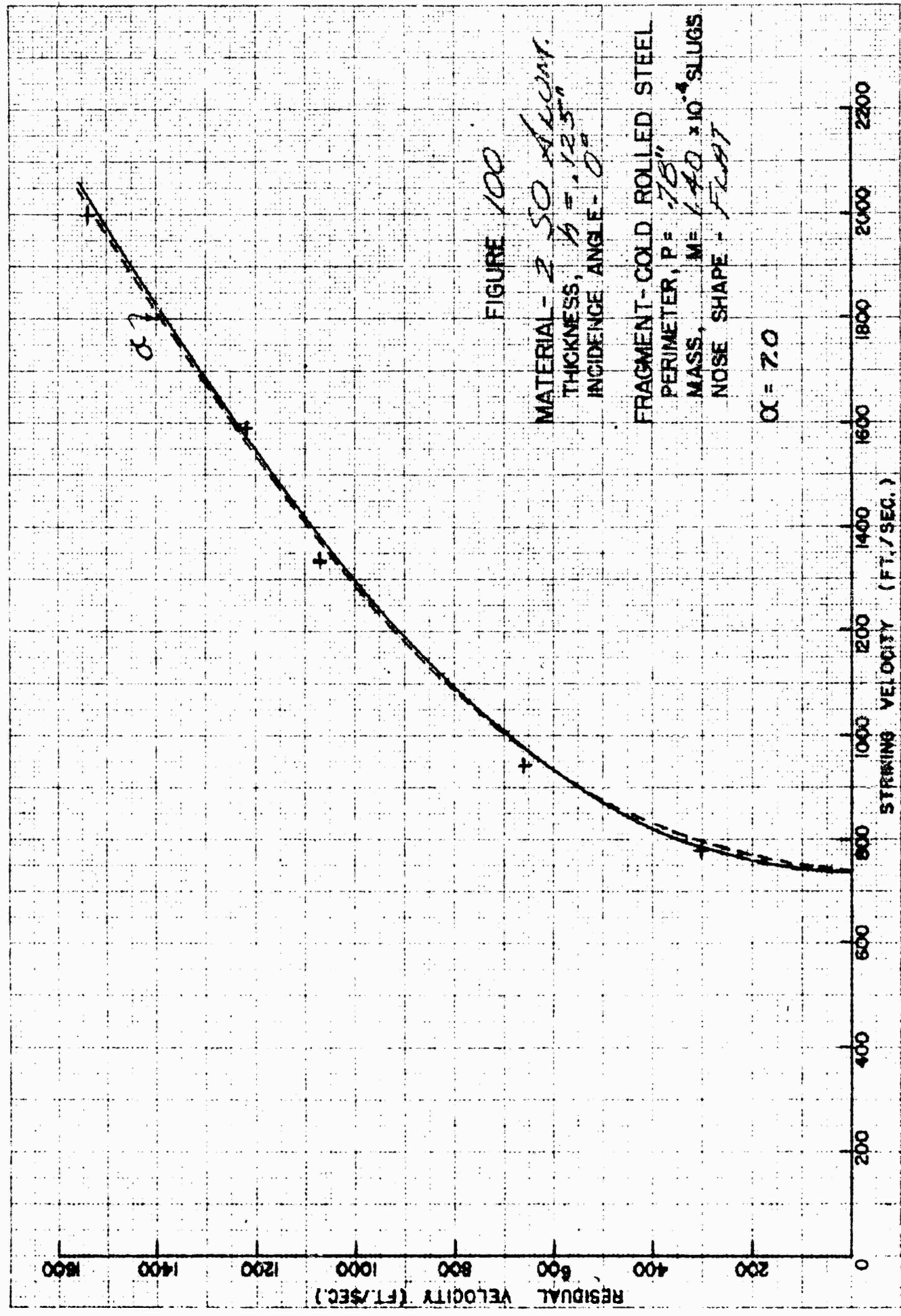
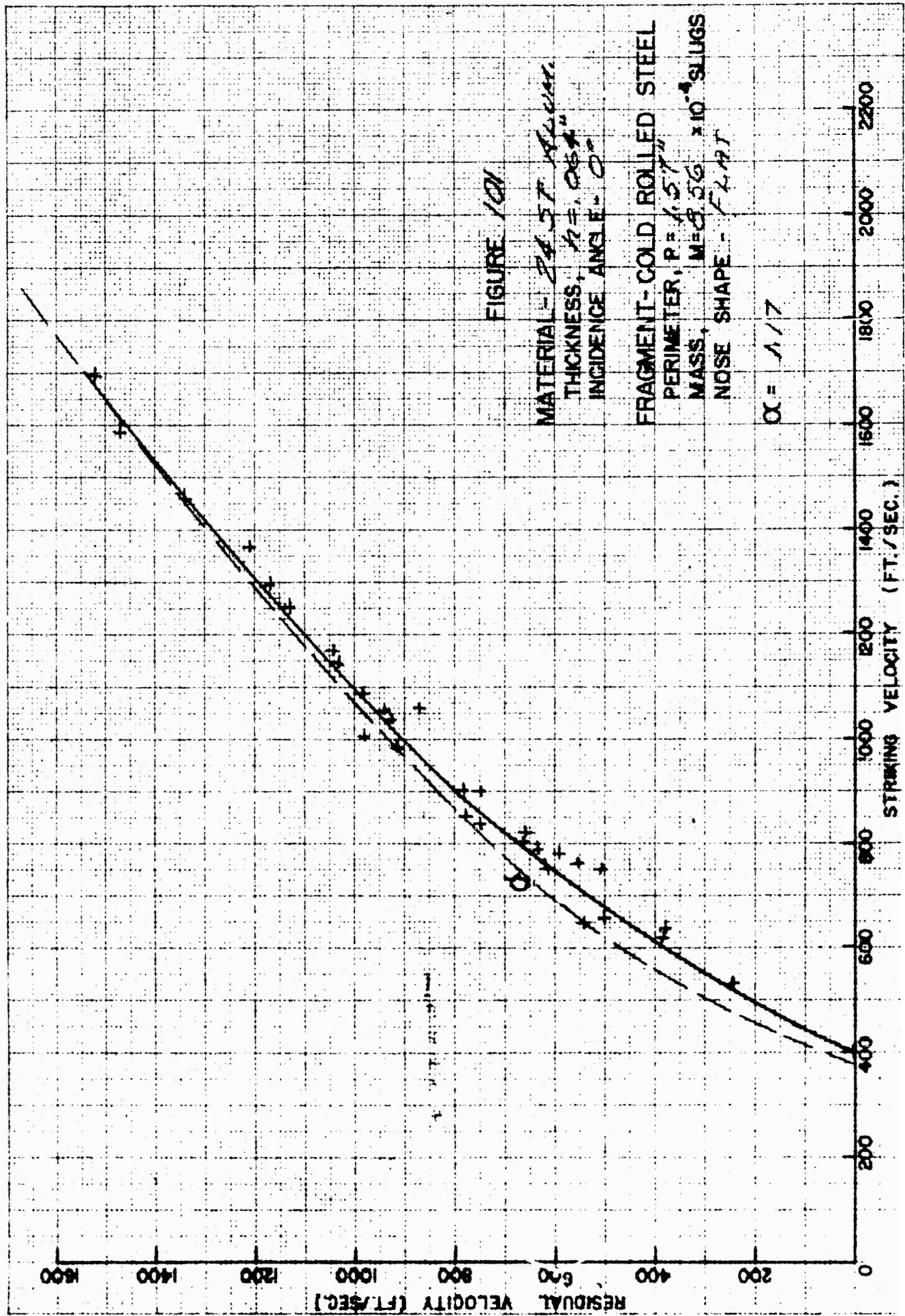


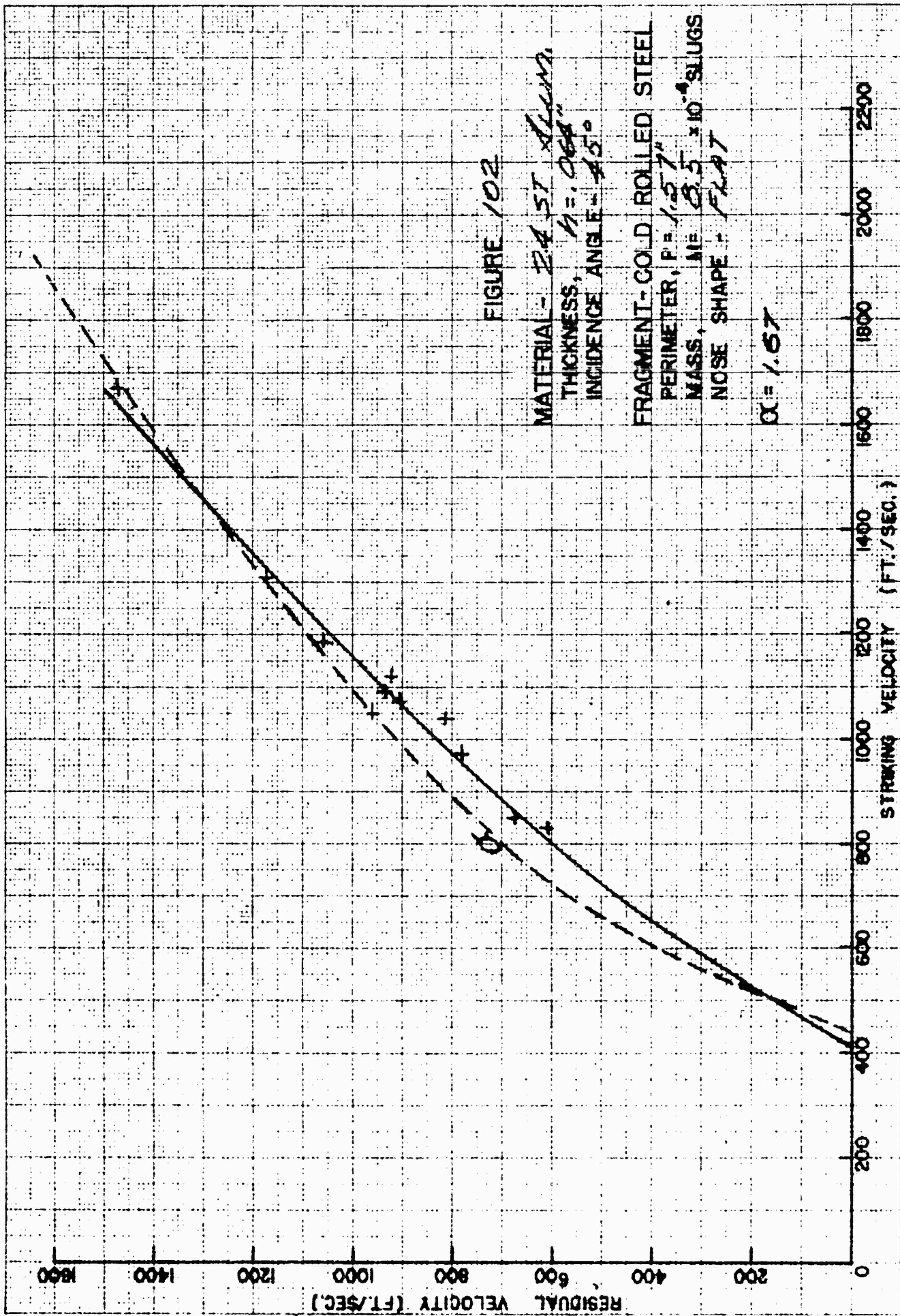
FIGURE 100

MATERIAL - 2 50 ALUM.
 THICKNESS, $b = .125"$
 INCIDENCE ANGLE - 0°
 FRAGMENT - COLD ROLLED STEEL
 PERIMETER, $P = .75"$
 MASS, $M = 1.40 \times 10^{-4}$ SLUGS
 NOSE SHAPE - FLAT

$\alpha = 70$

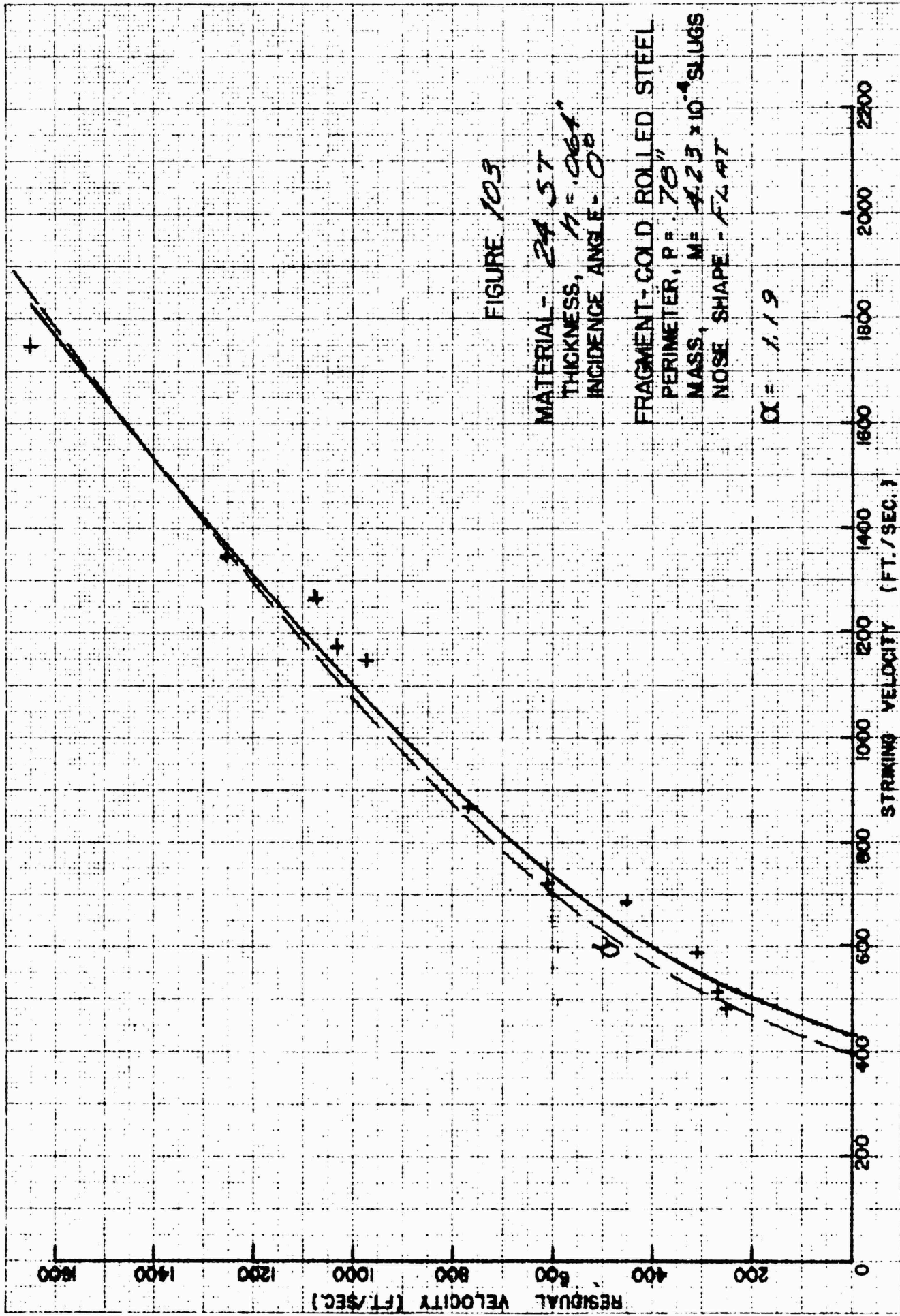


RESTRICTED

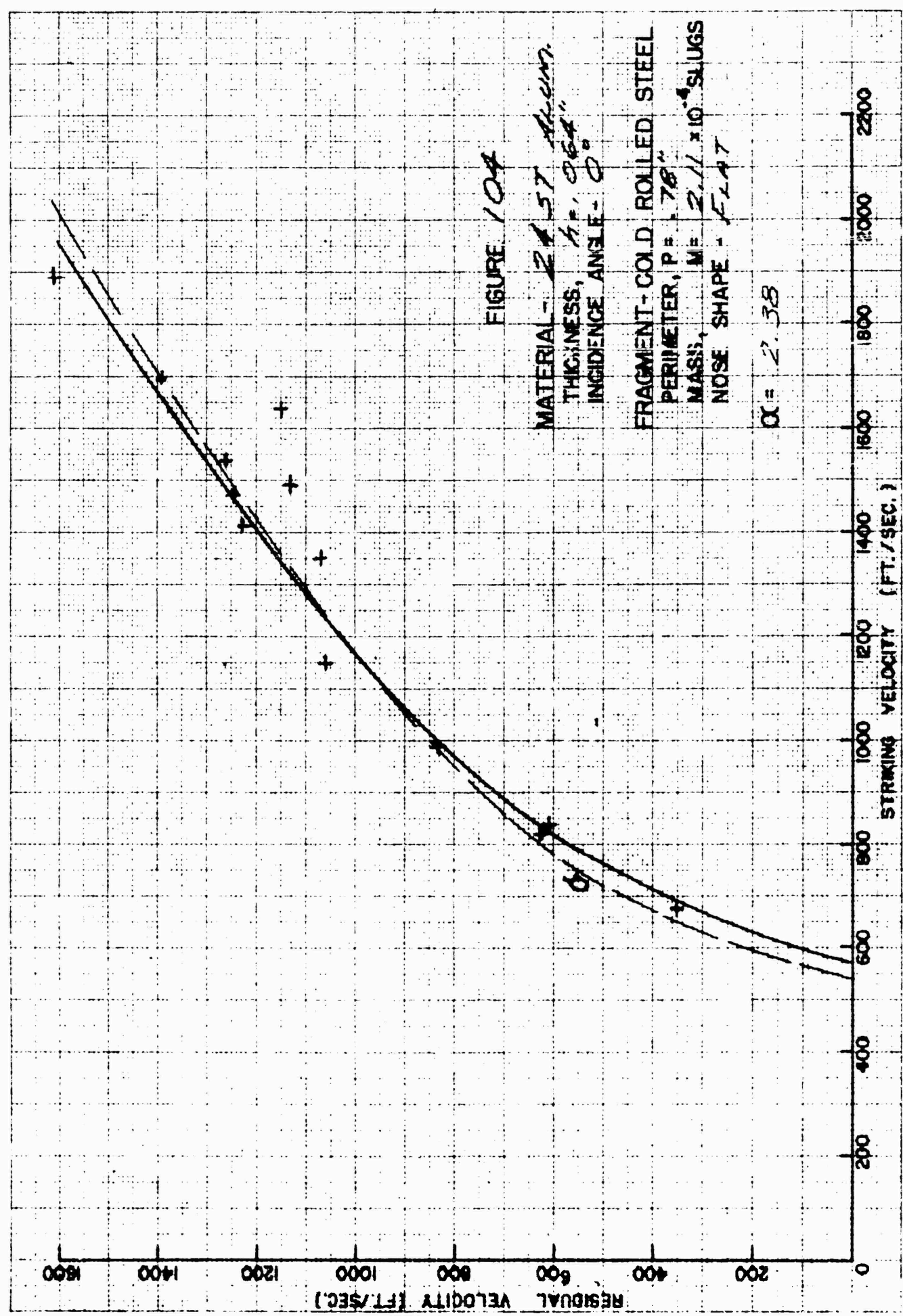


RESTRICTED

RESTRICTED



RESTRICTED



RESTRICTED

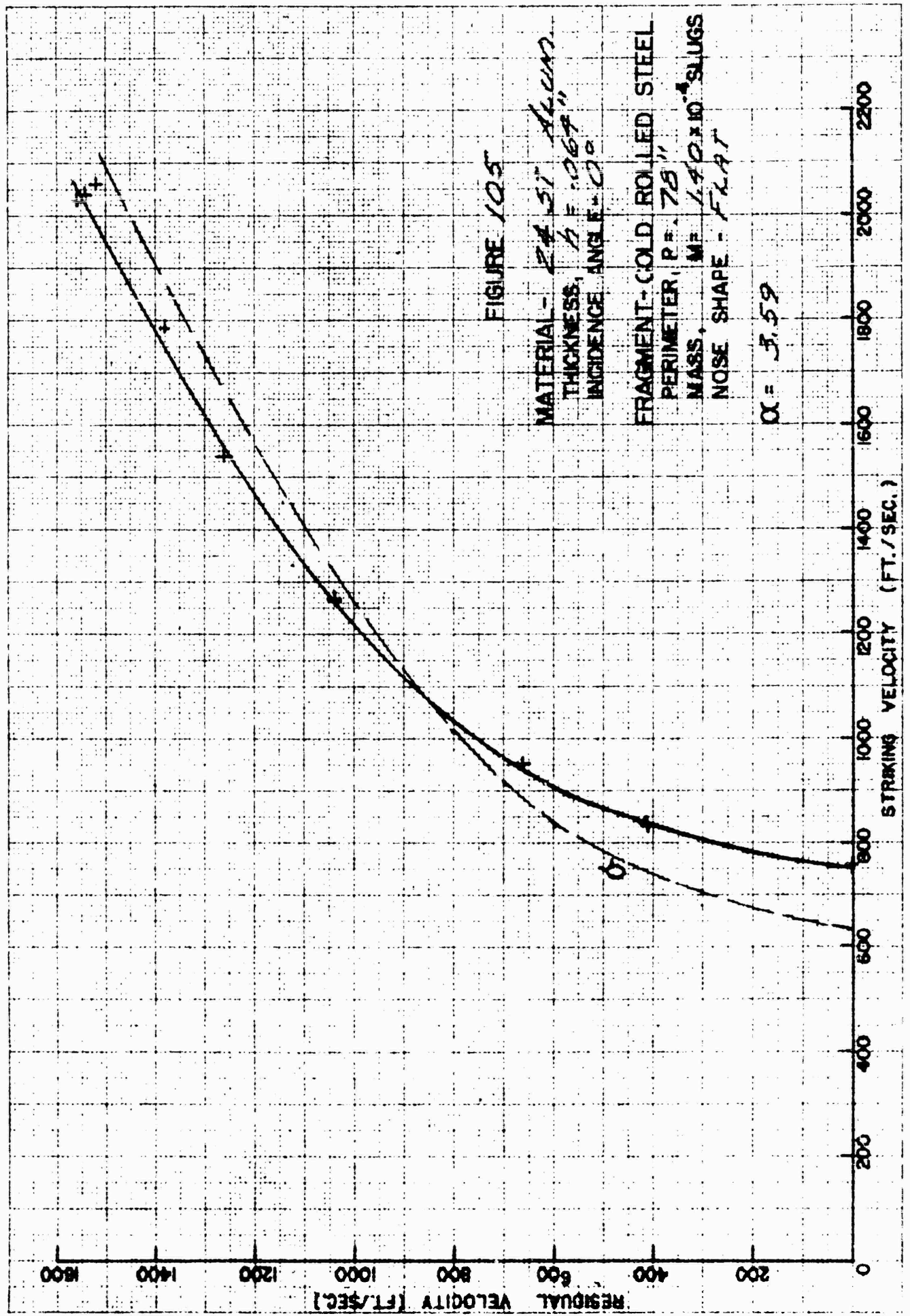


FIGURE 105

MATERIAL - *24 51 ALUM.*
 THICKNESS, $t = .067$ "
 INCIDENCE ANGLE - 20°
 FRAGMENT - COLD ROLLED STEEL
 PERIMETER, $P = .75$ "
 MASS, $M = 1.4 \times 10^{-4}$ SLUGS
 NOSE SHAPE - FLAT

$\alpha = 3.59$

RESTRICTED

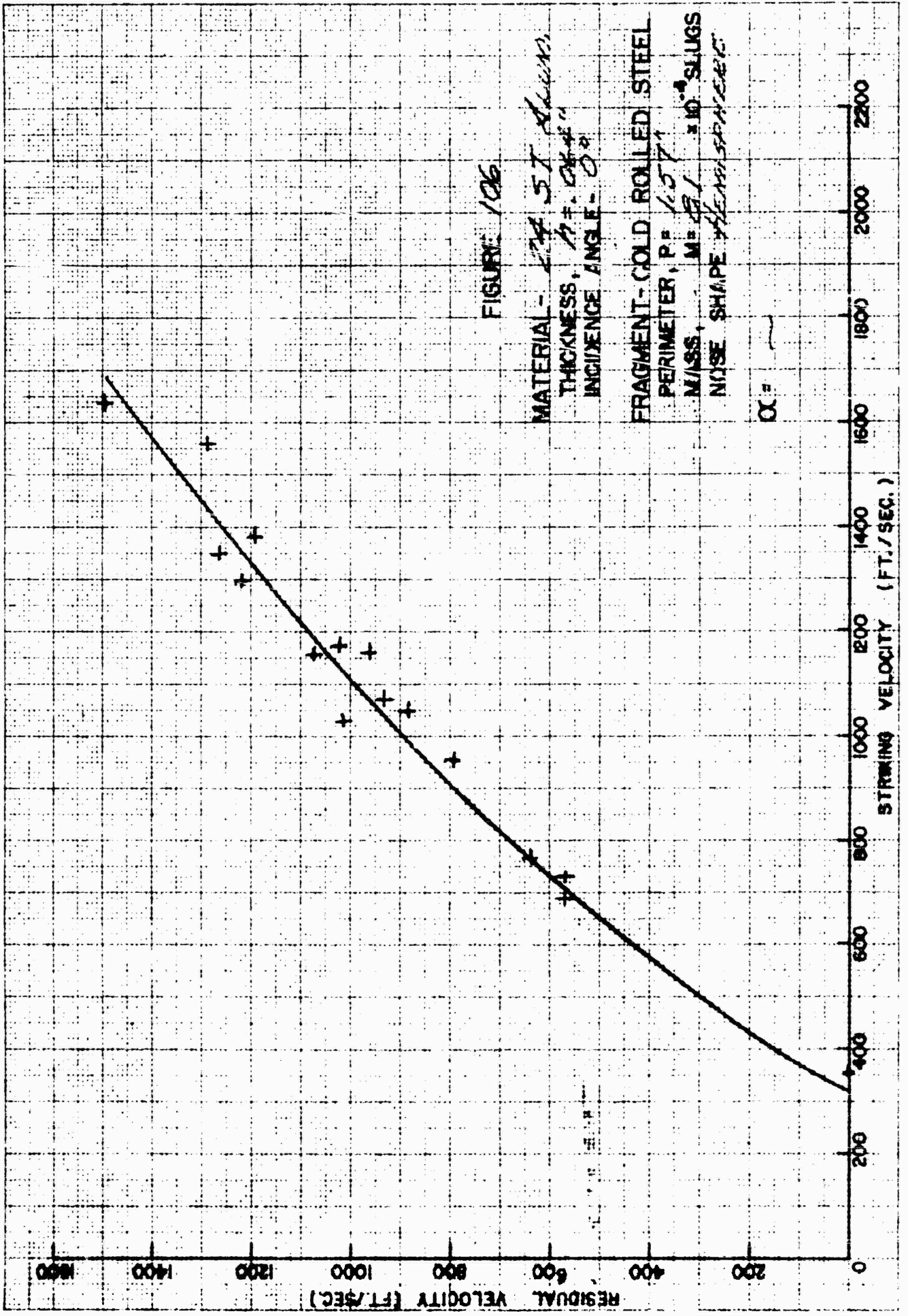


FIGURE 106

MATERIAL - 27 5T ALUMINUM
 THICKNESS, $1/8$ "
 INCIDENCE ANGLE - 0°
 FRAGMENT - COLD ROLLED STEEL
 PERIMETER, $P = 1.571$
 MASS, $M = 51$ SLUGS
 NOISE SHAPE $1/10$ SPAN/SEC

$\alpha =$

|||||

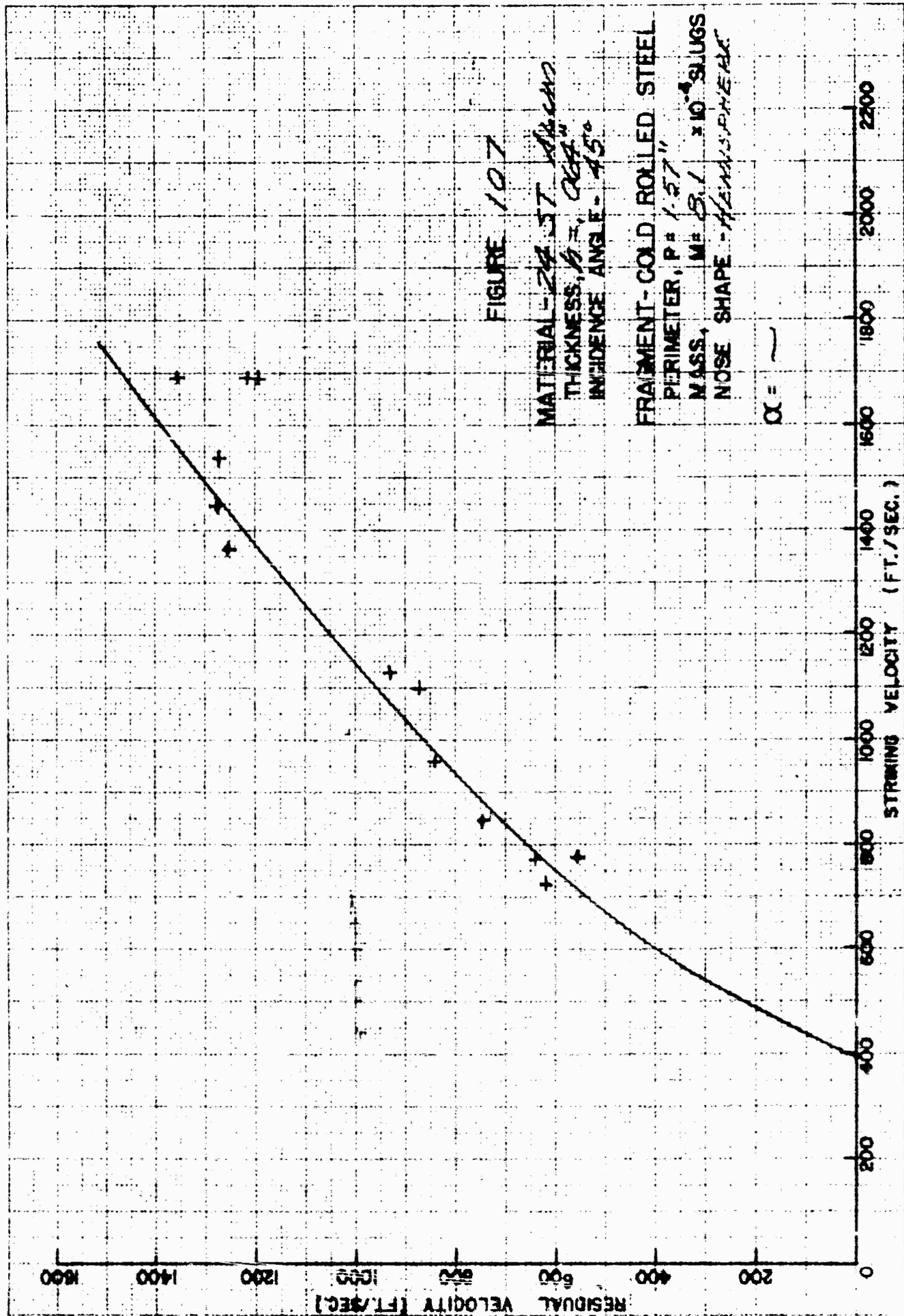


FIGURE 107

MATERIAL - *24 ST. 10000*
 THICKNESS, *1/8", 0.044"*
 INCIDENCE ANGLE - *45°*
 FRAGMENT - COLD ROLLED STEEL
 PERIMETER, *P = 1.27"*
 MASS, *M = 3.1 x 10⁻⁴ SLUGS*
 NOSE SHAPE - *HEMISPHERICAL*

$\alpha = \sim$

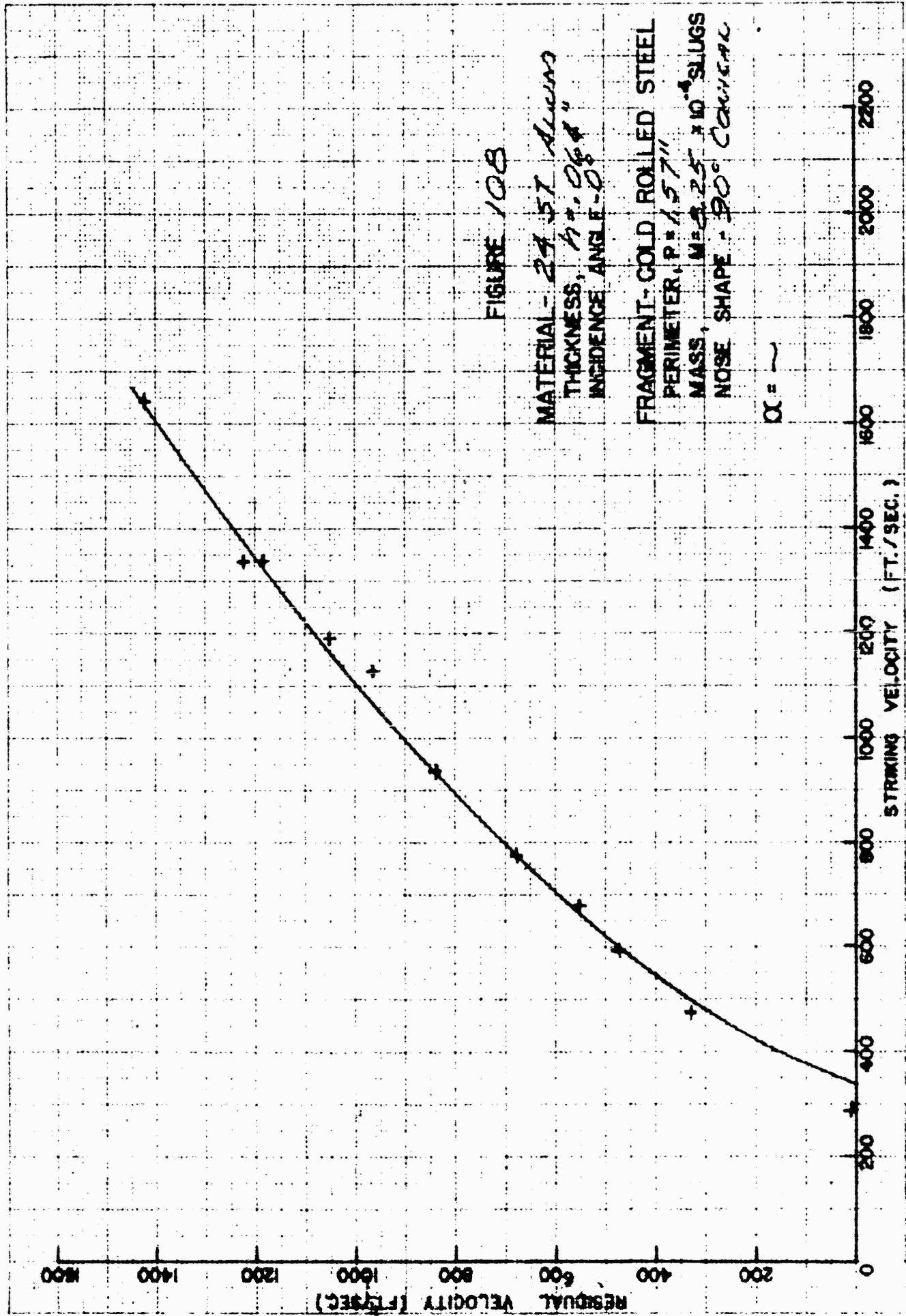


FIGURE 108

MATERIAL - 24 57 ALUMINUM
THICKNESS, $h = 0.064$ "
INCIDENCE ANGLE - 0°

FRAGMENT - COLD ROLLED STEEL
PERIMETER, $P = 1.57$ "
MASS, $M = 2.25 \times 10^{-4}$ SLUGS
NOSE SHAPE - 90° CONICAL

$\alpha = \sim$

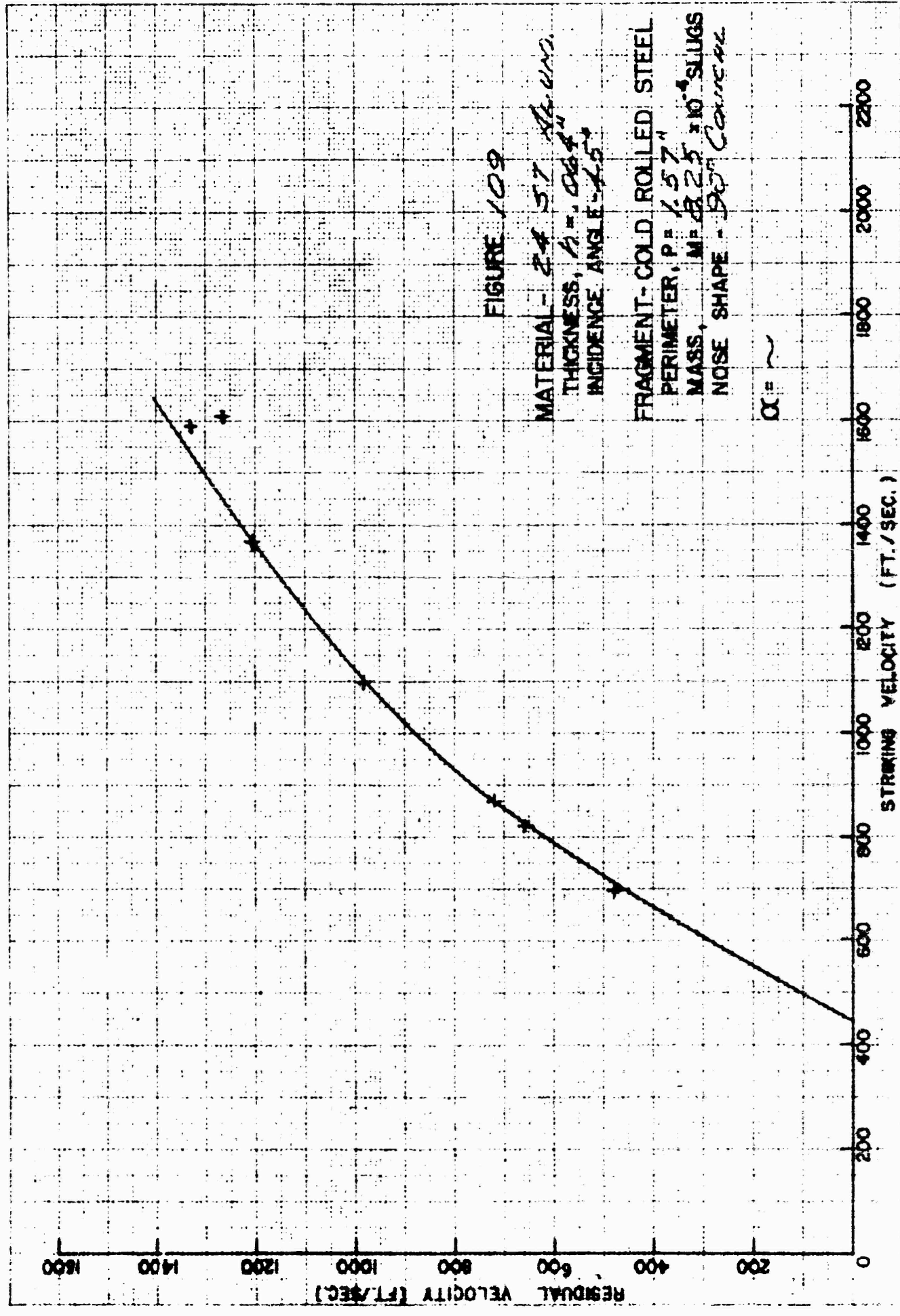


FIGURE 109

MATERIAL - 24 57 ALUMINUM

THICKNESS, $t = .0664"$

INCIDENCE ANGLE - 45°

FRAGMENT - COLD ROLLED STEEL

PERIMETER, $P = 1.57"$

MASS, $M = 2.5 \times 10^{-4}$ SLUGS

NOSE SHAPE - 30° CONICAL

$\alpha = \sim$

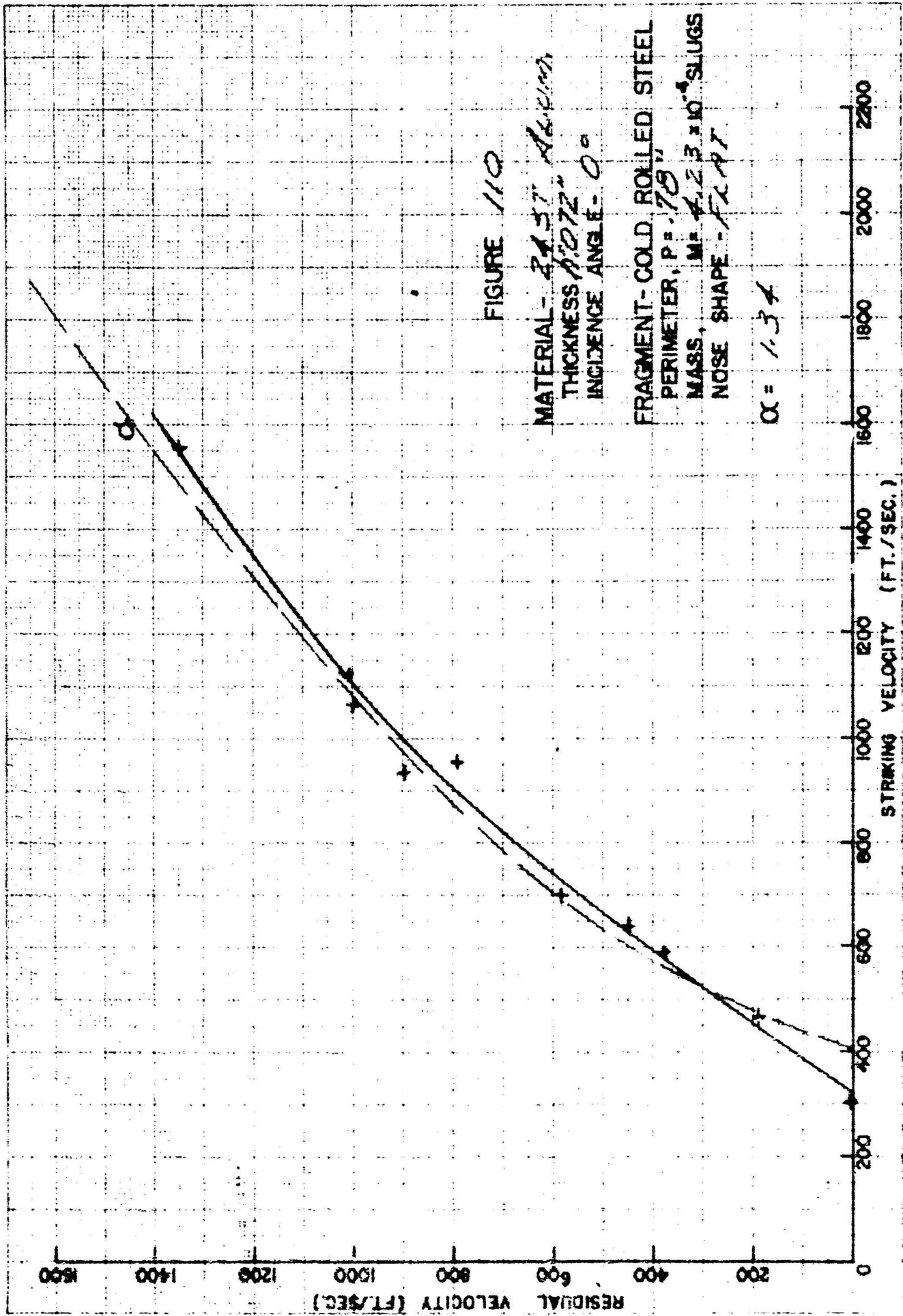


FIGURE 110

MATERIAL - *2457 A617*
 THICKNESS *0.072"*
 INCIDENCE ANGLE - *0°*

FRAGMENT - COLD ROLLED STEEL
 PERIMETER, *P = .78"*
 MASS, *M = 4.23 x 10⁻⁴ SLUGS*
 NOSE SHAPE - *FLAT*

$\alpha = 1.34$

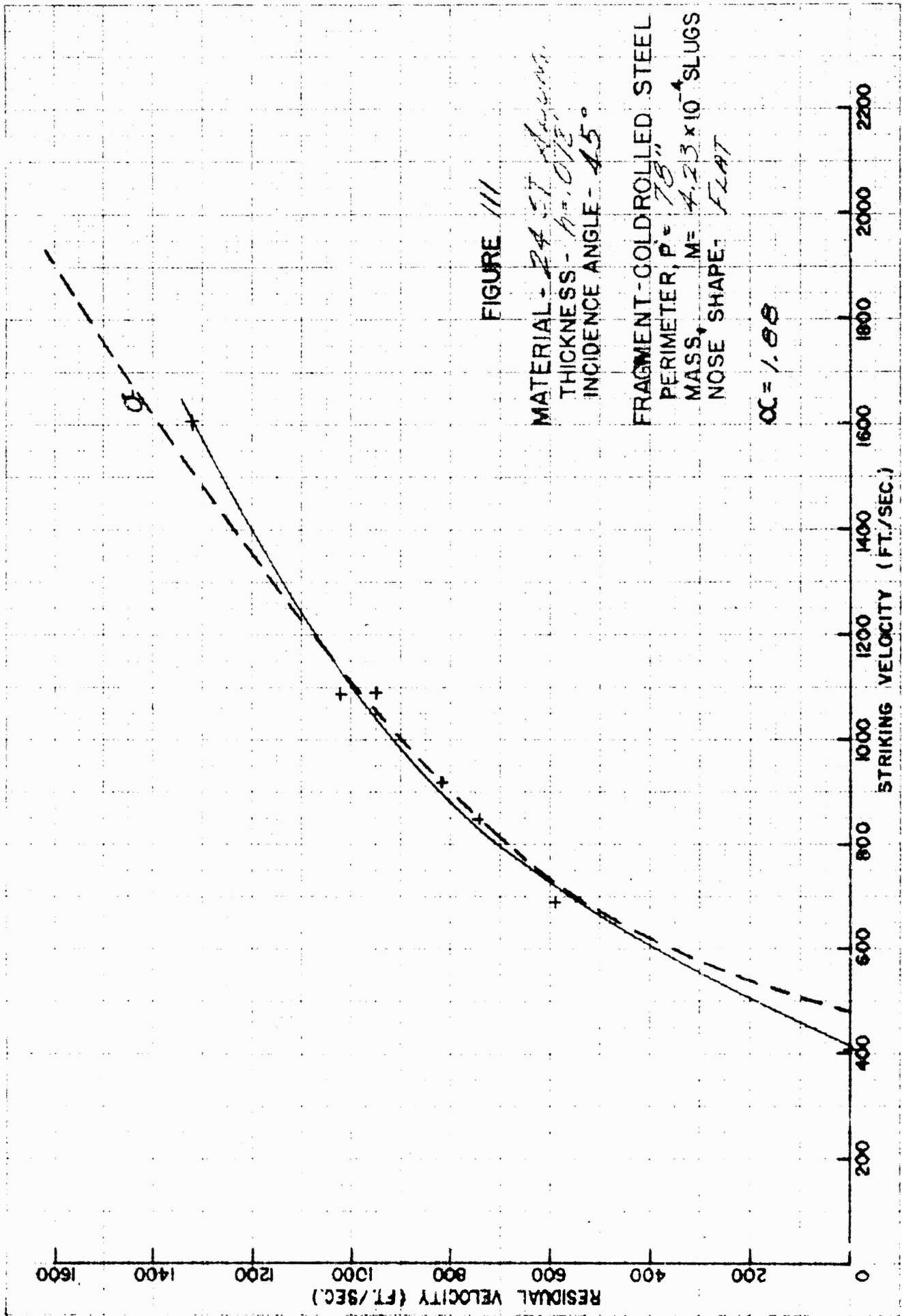


FIGURE III

MATERIAL - 24 ST. *Aluminum*
 THICKNESS - *1/2" OVE*
 INCIDENCE ANGLE - 45°

FRAGMENT - GOLD ROLLED STEEL
 PERIMETER, P = 78"
 MASS, M = 4.23 x 10⁻⁴ SLUGS
 NOSE SHAPE - FLAT

$\alpha = 1.98$

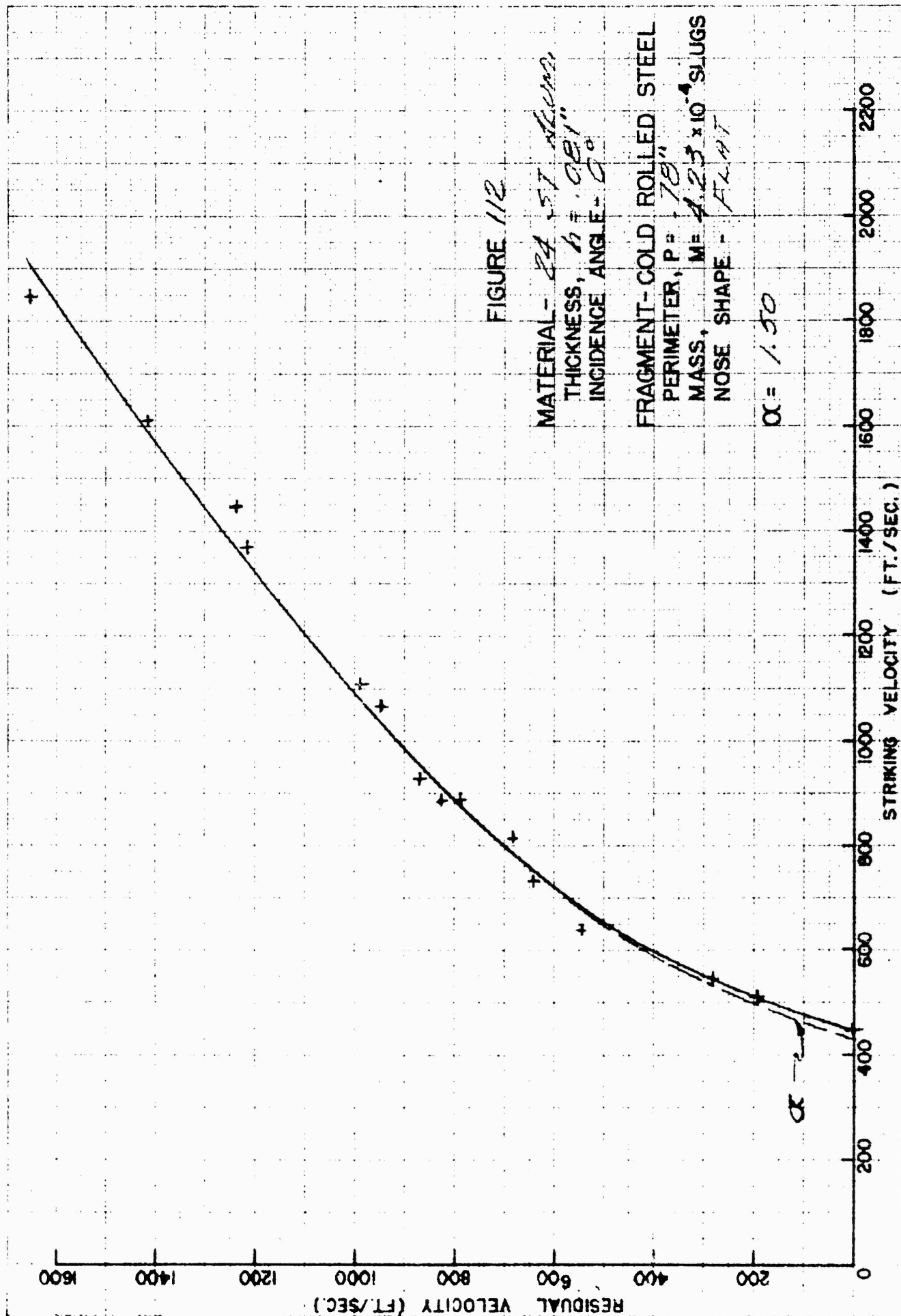


FIGURE 112

MATERIAL - 24 x 57 SLUGS
THICKNESS, $h = .081"$
INCIDENCE ANGLE - 0°
FRAGMENT - COLD ROLLED STEEL
PERIMETER, $P = 78"$
MASS, $M = 4.23 \times 10^{-4}$ SLUGS
NOSE SHAPE - FLAT

$\alpha = 1.30$

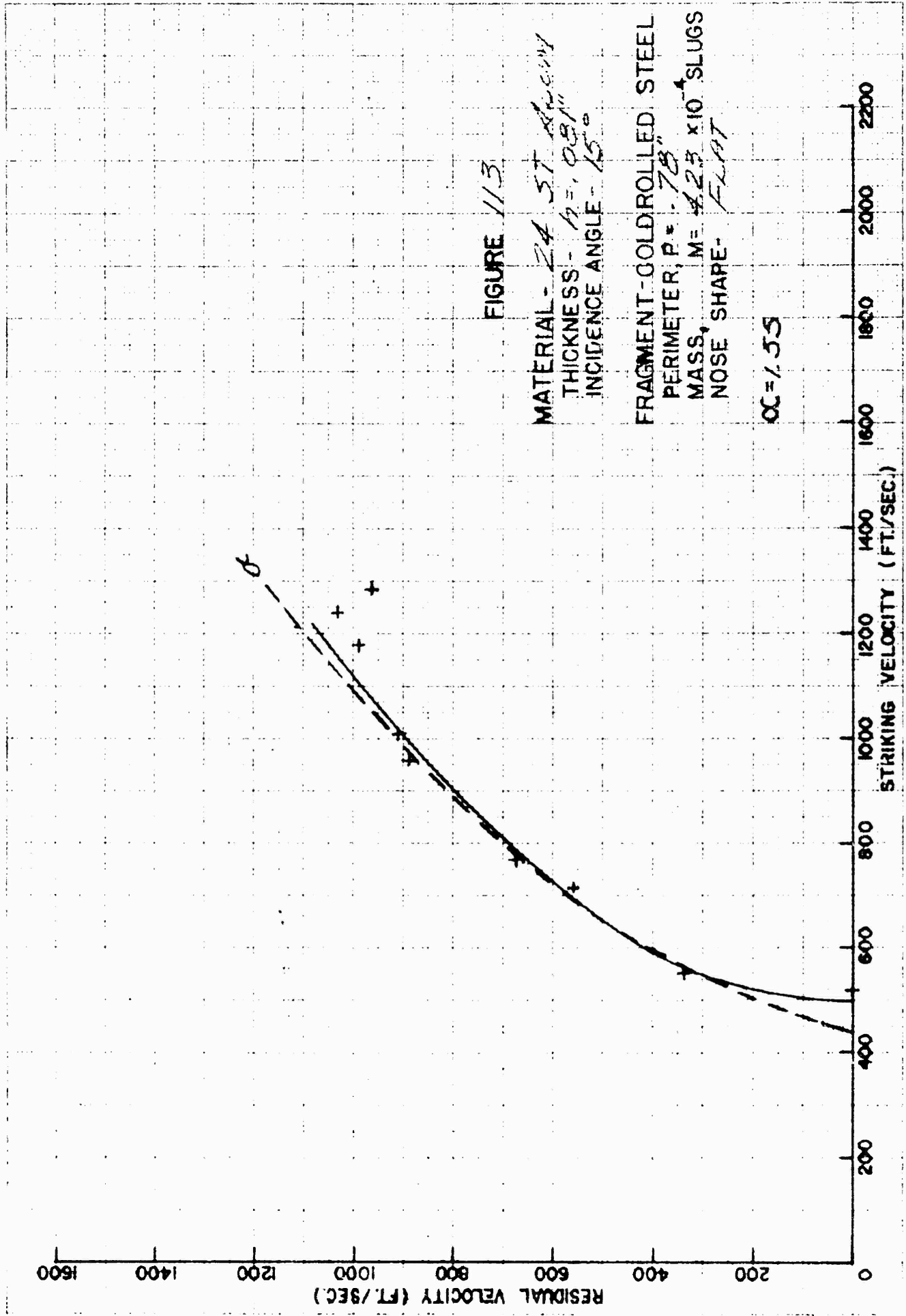


FIGURE 113

MATERIAL - 24 ST. AUSTENITE
 THICKNESS - $t = .081$ "
 INCIDENCE ANGLE - 15°

FRAGMENT - GOLD ROLLED STEEL
 PERIMETER, $P = .78$ "
 MASS, $M = 4.23 \times 10^{-4}$ SLUGS
 NOSE SHAPE - FLAT

$\alpha = 1.55$

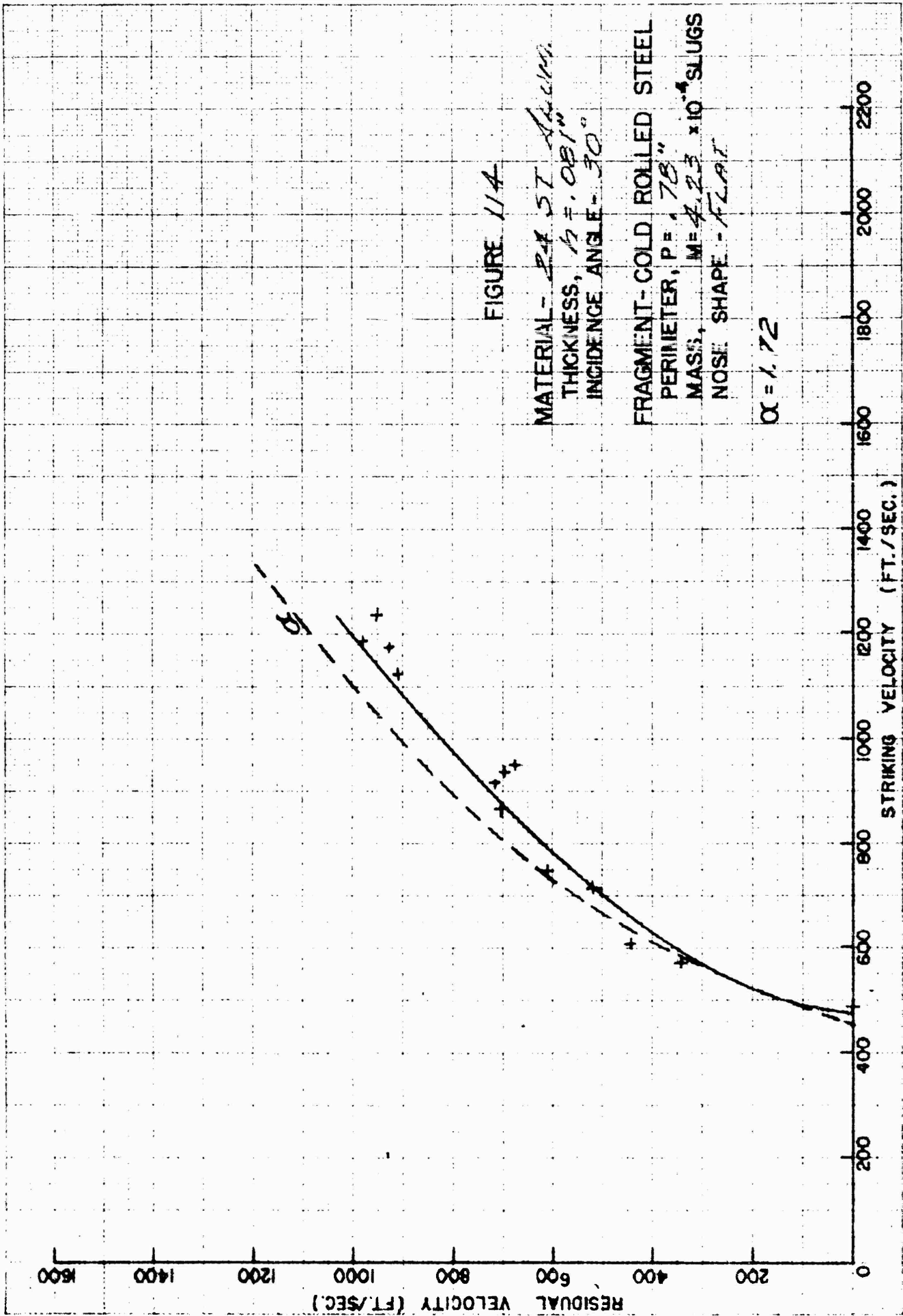


FIGURE 11A

MATERIAL - *SA 57 ALCAM*
THICKNESS, $t = 0.081"$
INCIDENCE ANGLE - 30°

FRAGMENT - COLD ROLLED STEEL
PERIMETER, $P = 1.78"$
M.A.S.I., $M = 4.23 \times 10^{-4}$ SLUGS
NOSE SHAPE - *FLAT*

$\alpha = 1.72$

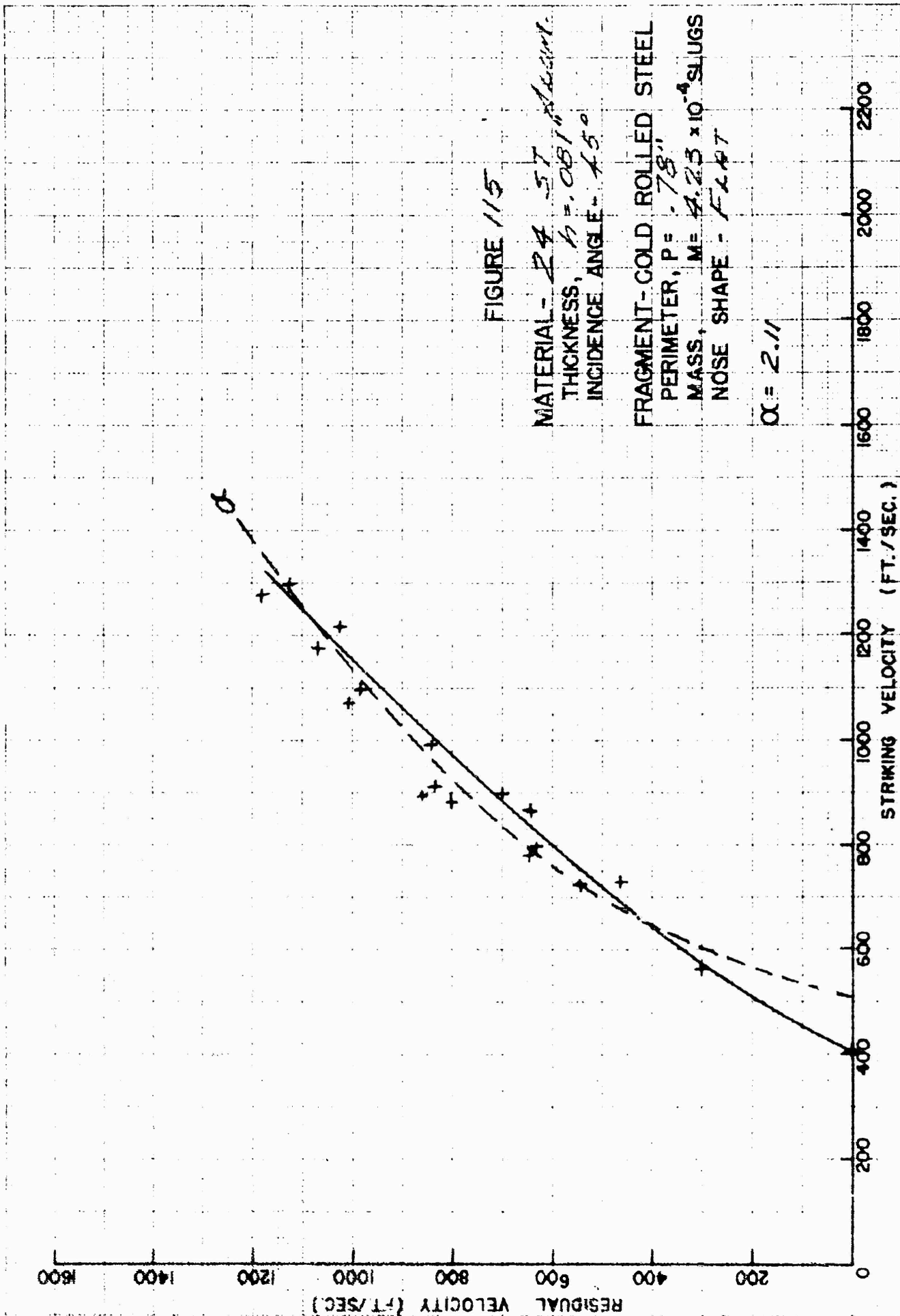


FIGURE 115

MATERIAL - 24 57 ¹⁶/₁₆ ALUM.
 THICKNESS, $h = .081$
 INCIDENCE ANGLE - 45°

FRAGMENT - COLD ROLLED STEEL
 PERIMETER, $P = .78$
 MASS, $M = 4.23 \times 10^{-4}$ SLUGS
 NOSE SHAPE - $F_{4.67}$

$\alpha = 2.11$

RESIDUAL VELOCITY (FT/SEC)

STRIKING VELOCITY (FT./SEC.)

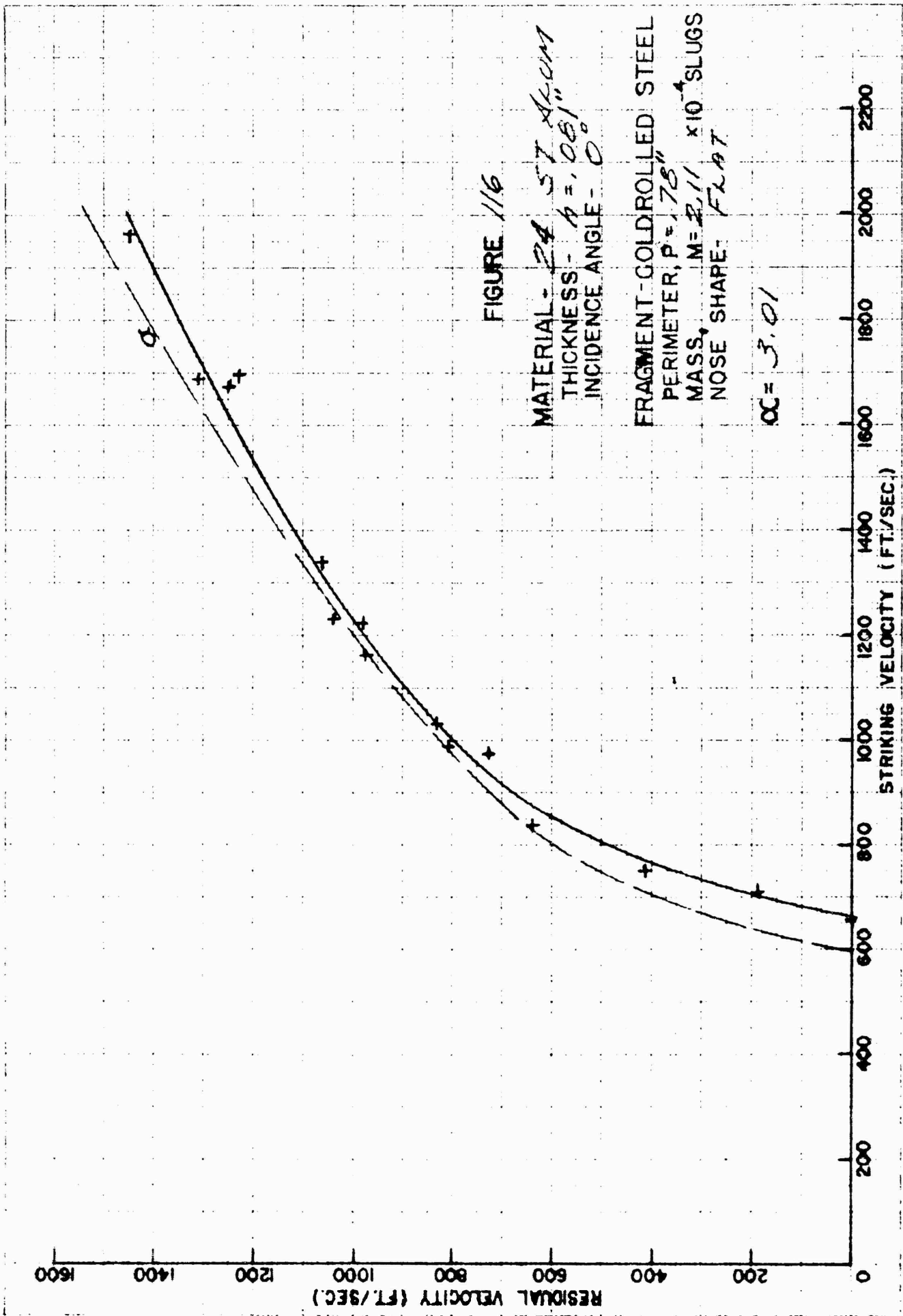


FIGURE 116

MATERIAL - 24 ST A30M
 THICKNESS - $t = .081$ "
 INCIDENCE ANGLE - 0°

FRAGMENT - GOLDROLLED STEEL
 PERIMETER, $P = .78$ "
 MASS, $M = 2.11 \times 10^{-4}$ SLUGS
 NOSE SHAPE - FLAT

$OC = 3.01$

RESTRICTED

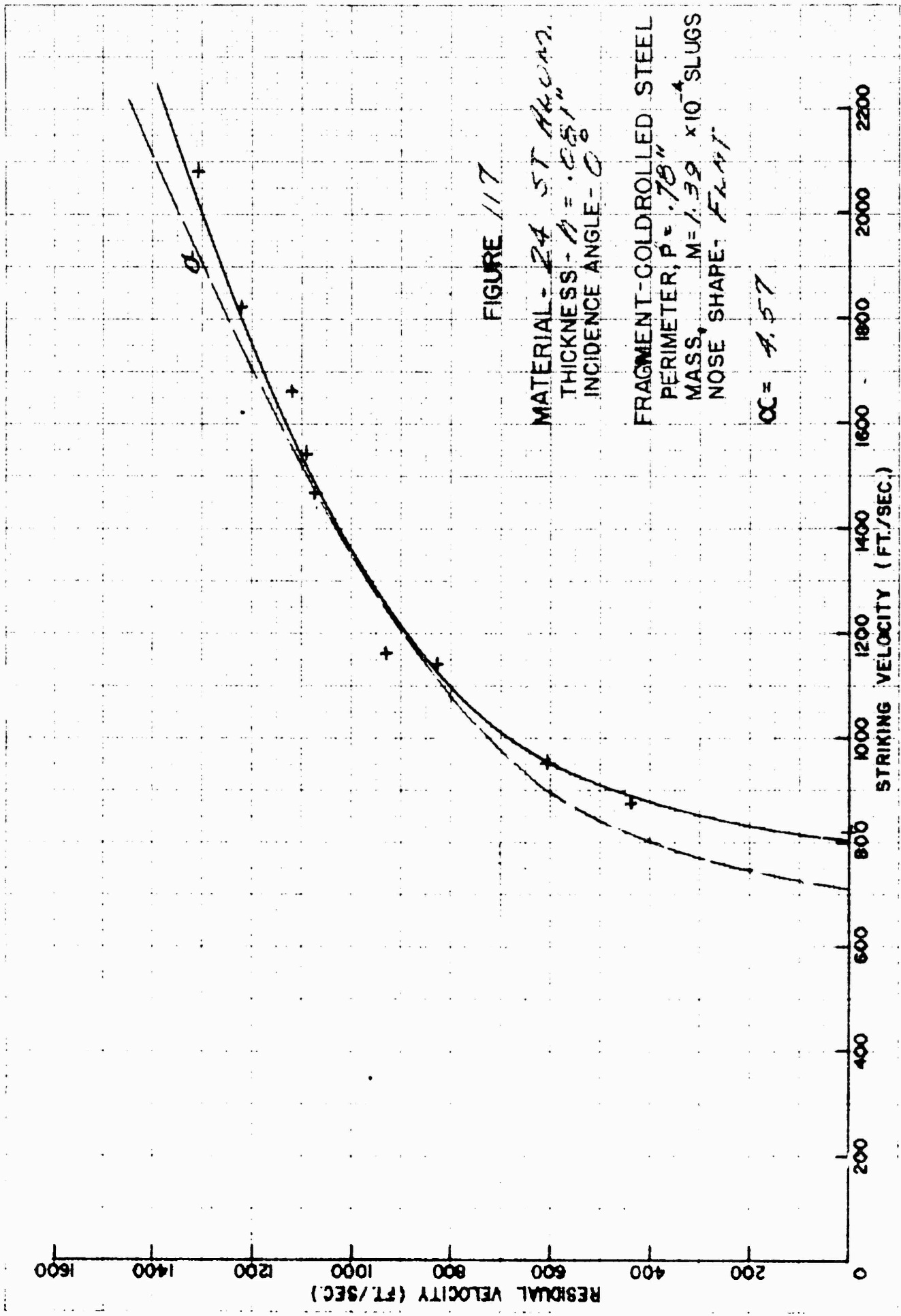


FIGURE 117

MATERIAL - 24 ST A4020
 THICKNESS - $t = .051"$
 INCIDENCE ANGLE - 0°

FRAGMENT-GOLDROLLED STEEL
 PERIMETER, $P = .78"$
 MASS, $M = 1.39 \times 10^{-4}$ SLUGS
 NOSE SHAPE - FLAT

$OC = 4.57$

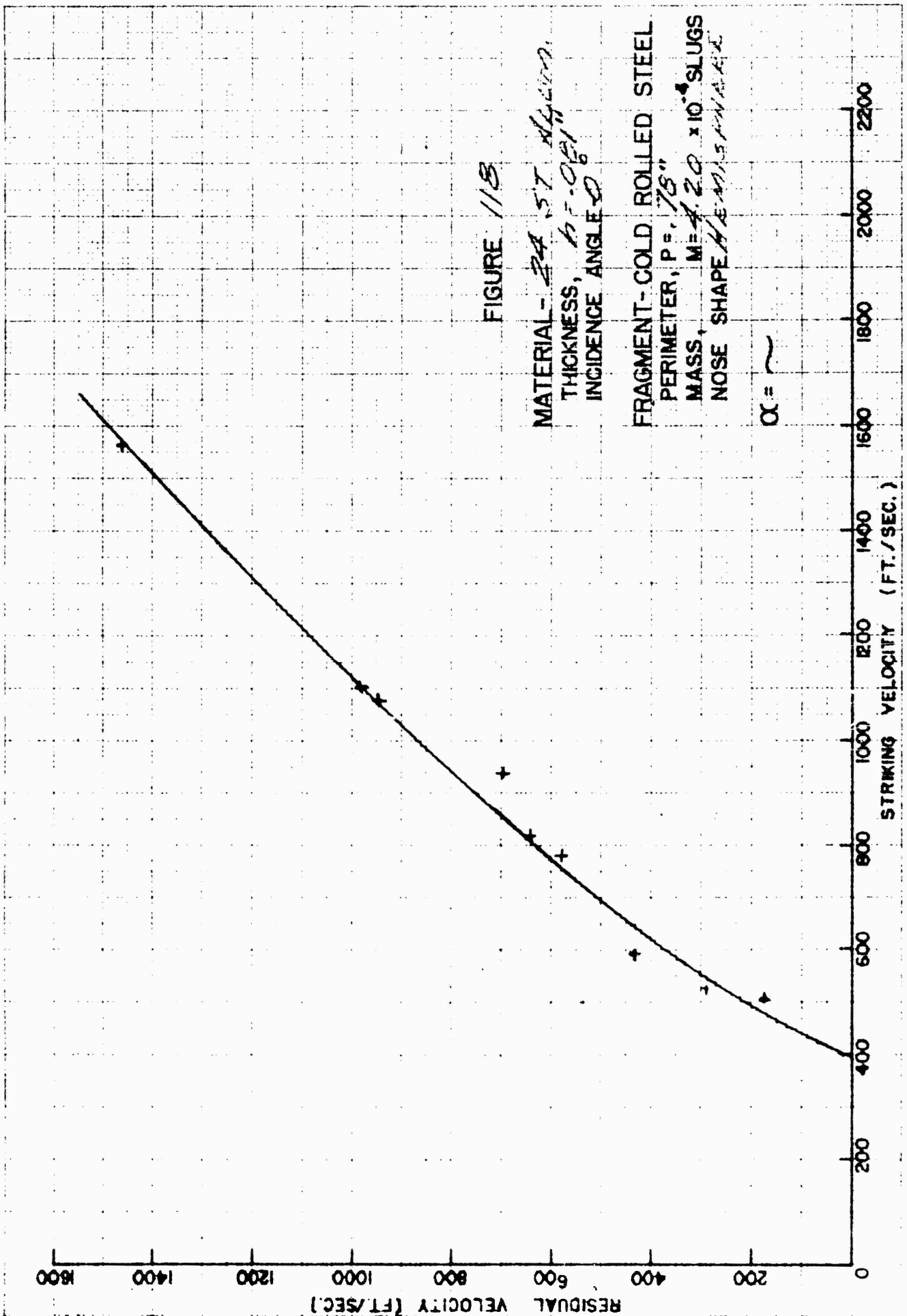


FIGURE 118

MATERIAL - 24, 57 ALUMINUM
 THICKNESS, $t = 0.01$
 INCIDENCE ANGLE θ

FRAGMENT - COLD ROLLED STEEL
 PERIMETER, $P = .78$ "
 MASS, $M = 4.20 \times 10^{-4}$ SLUGS
 NOSE SHAPE $\alpha = 1.5$ INCH

$\alpha = 1.5$

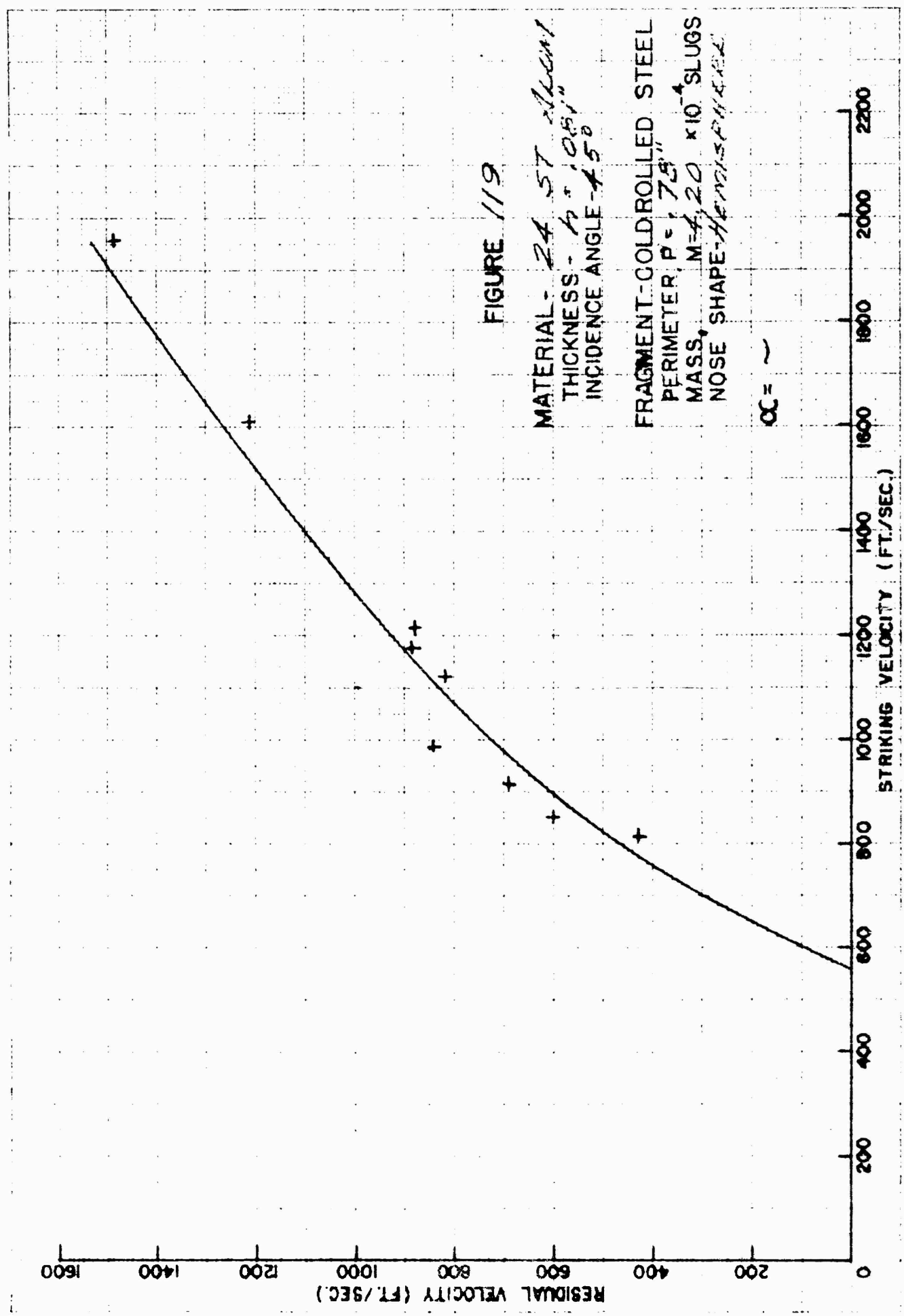


FIGURE 119

MATERIAL - 24 ST ALUMINUM
 THICKNESS - 0.081"
 INCIDENCE ANGLE - 45°

FRAGMENT-COLDROLLED STEEL
 PERIMETER P = 7.8"
 MASS M = 4.20 x 10⁻⁴ SLUGS
 NOSE SHAPE - HEMISPHERICAL

OC = ~

11/11/68

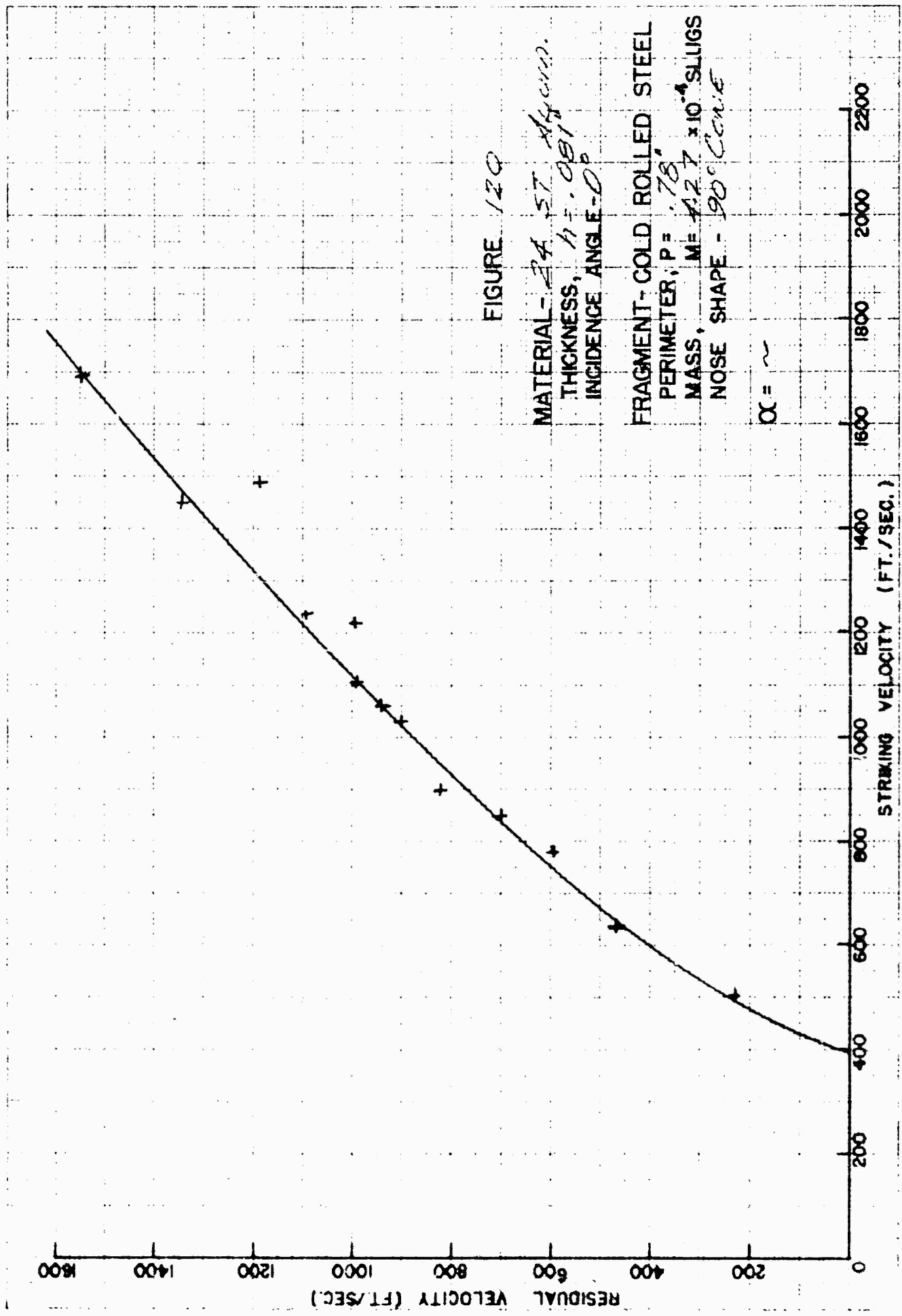


FIGURE 12Q

MATERIAL - 2A 57 Alloy.
 THICKNESS, $h = .081$
 INCIDENCE ANGLE - 0°
 FRAGMENT - COLD ROLLED STEEL
 PERIMETER, $P = .78$
 MASS, $M = 4.27 \times 10^{-4}$ SLUGS
 NOSE SHAPE - 90° CONE

$\alpha = \sim$

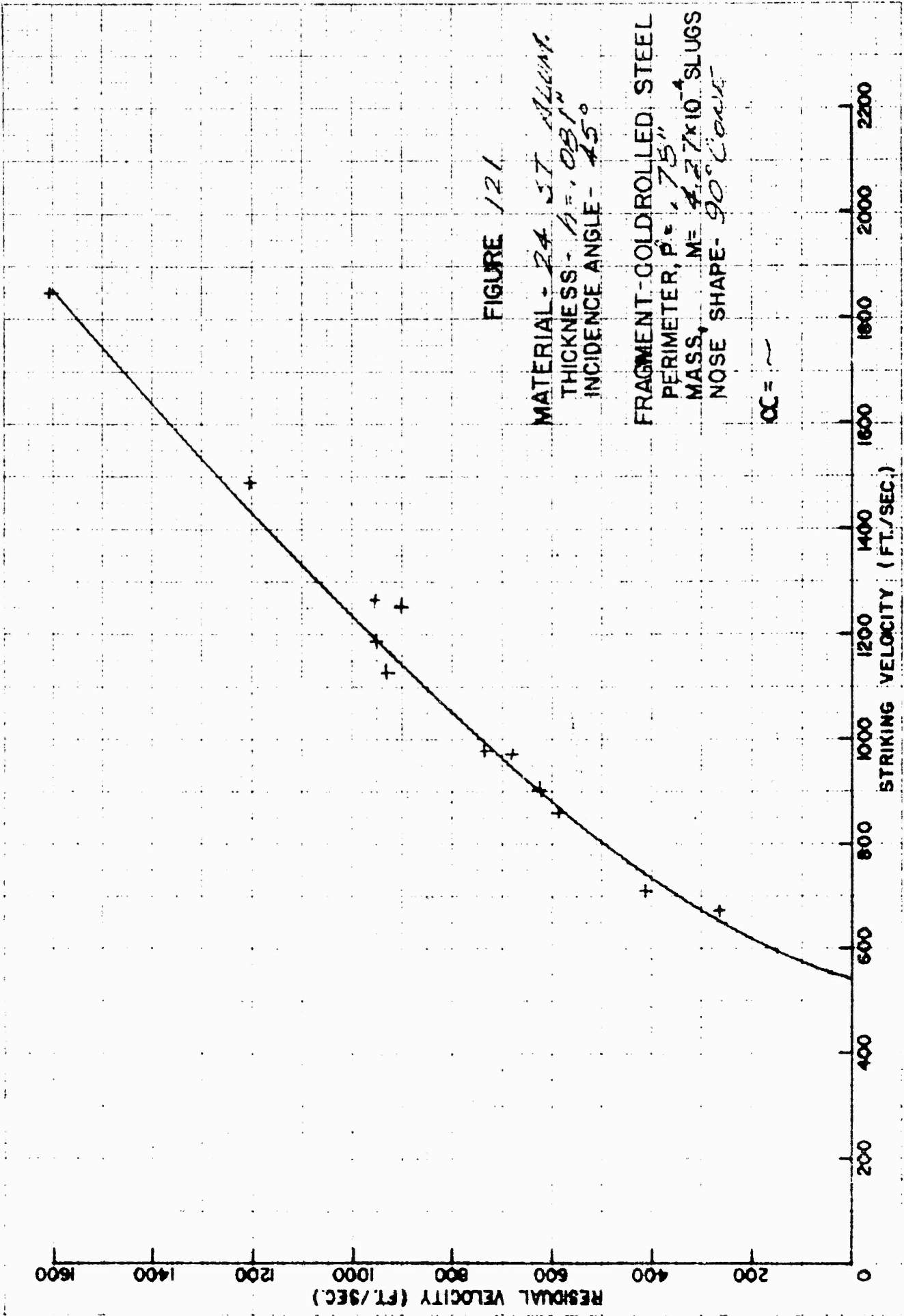


FIGURE 121

MATERIAL - 24 ST. ALUM.
 THICKNESS - $A = .031"$
 INCIDENCE ANGLE - 45°
 FRAGMENT - GOLDROLLED STEEL
 PERIMETER, $P = .75"$
 MASS, $M = 4.27 \times 10^{-4}$ SLUGS
 NOSE SHAPE - 90° CONE

$\alpha = \sim$

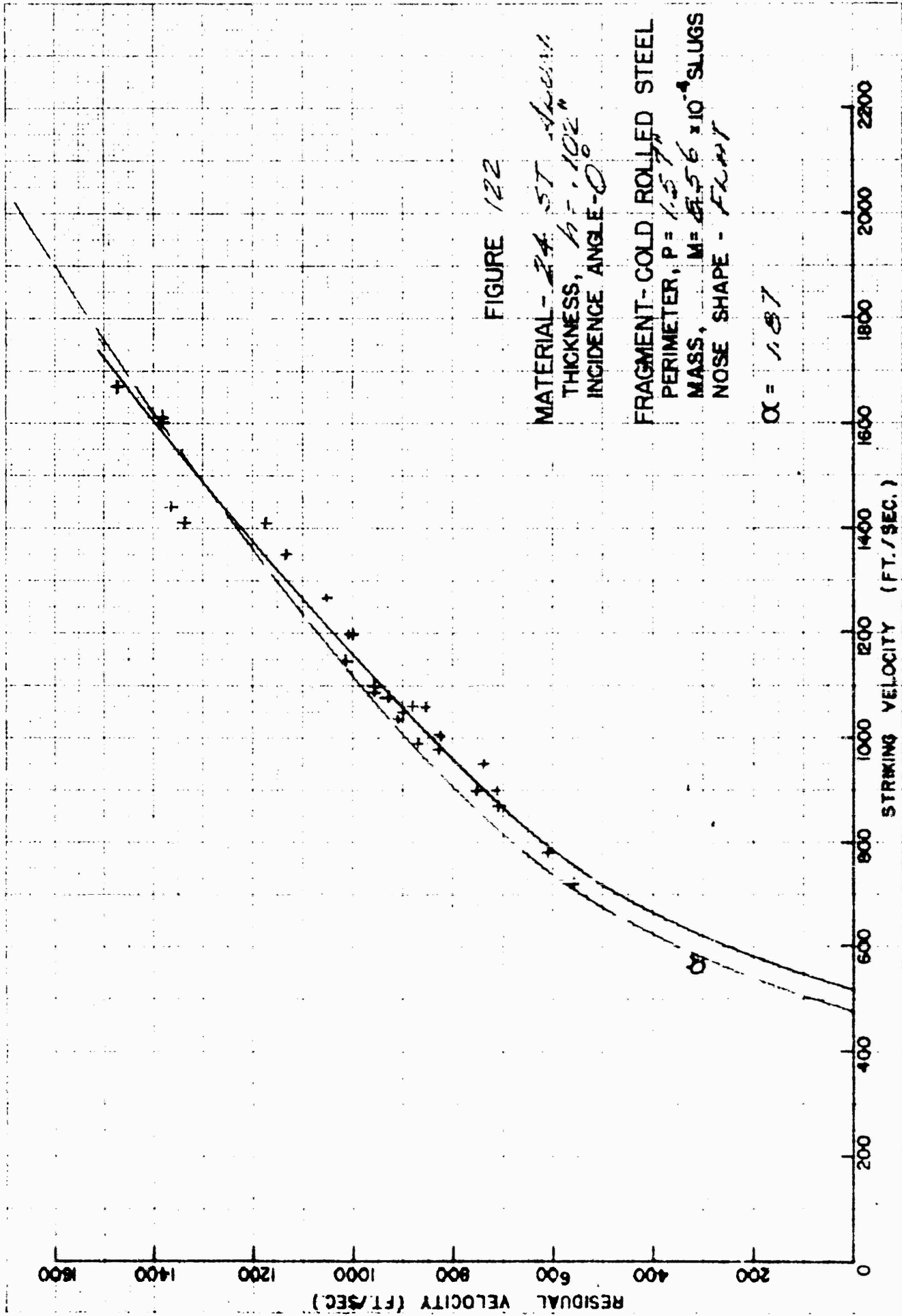


FIGURE 122

MATERIAL - 24 ST - ALUMINUM
THICKNESS, $t = .102"$
INCIDENCE ANGLE - 0°

FRAGMENT - COLD ROLLED STEEL
PERIMETER, $P = 1.57"$
MASS, $M = 8.56 \times 10^{-4}$ SLUGS
NOSE SHAPE - FLAT

$\alpha = 1.87$

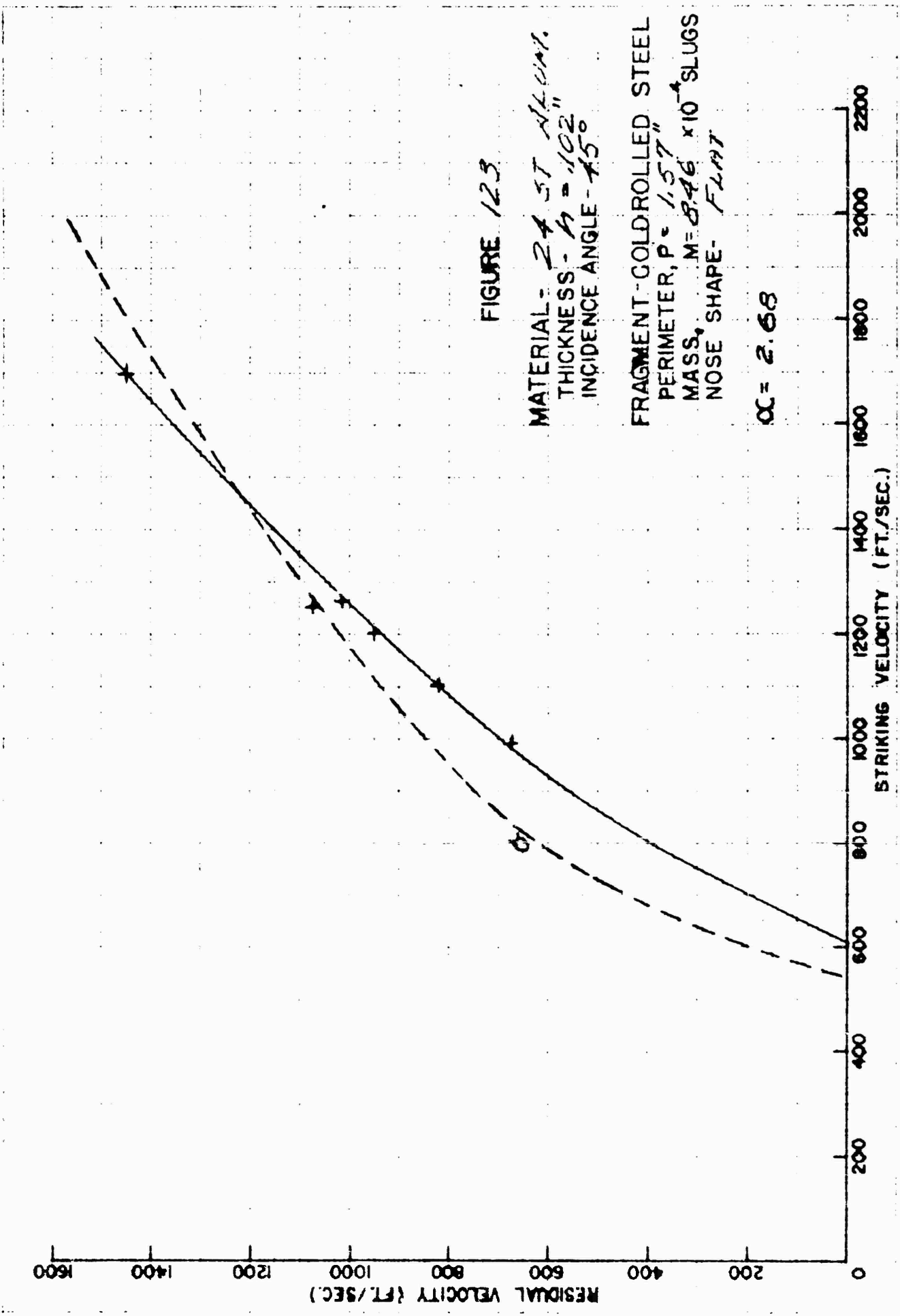


FIGURE 123

MATERIAL - 24 ST ALUMINUM
 THICKNESS - $t = .102$ "
 INCIDENCE ANGLE - 45°

FRAGMENT - GOLDROLLED STEEL
 PERIMETER, $P = 1.57$ "
 MASS, $M = 8.46 \times 10^{-4}$ SLUGS
 NOSE SHAPE - FLAT

$\alpha C = 2.68$

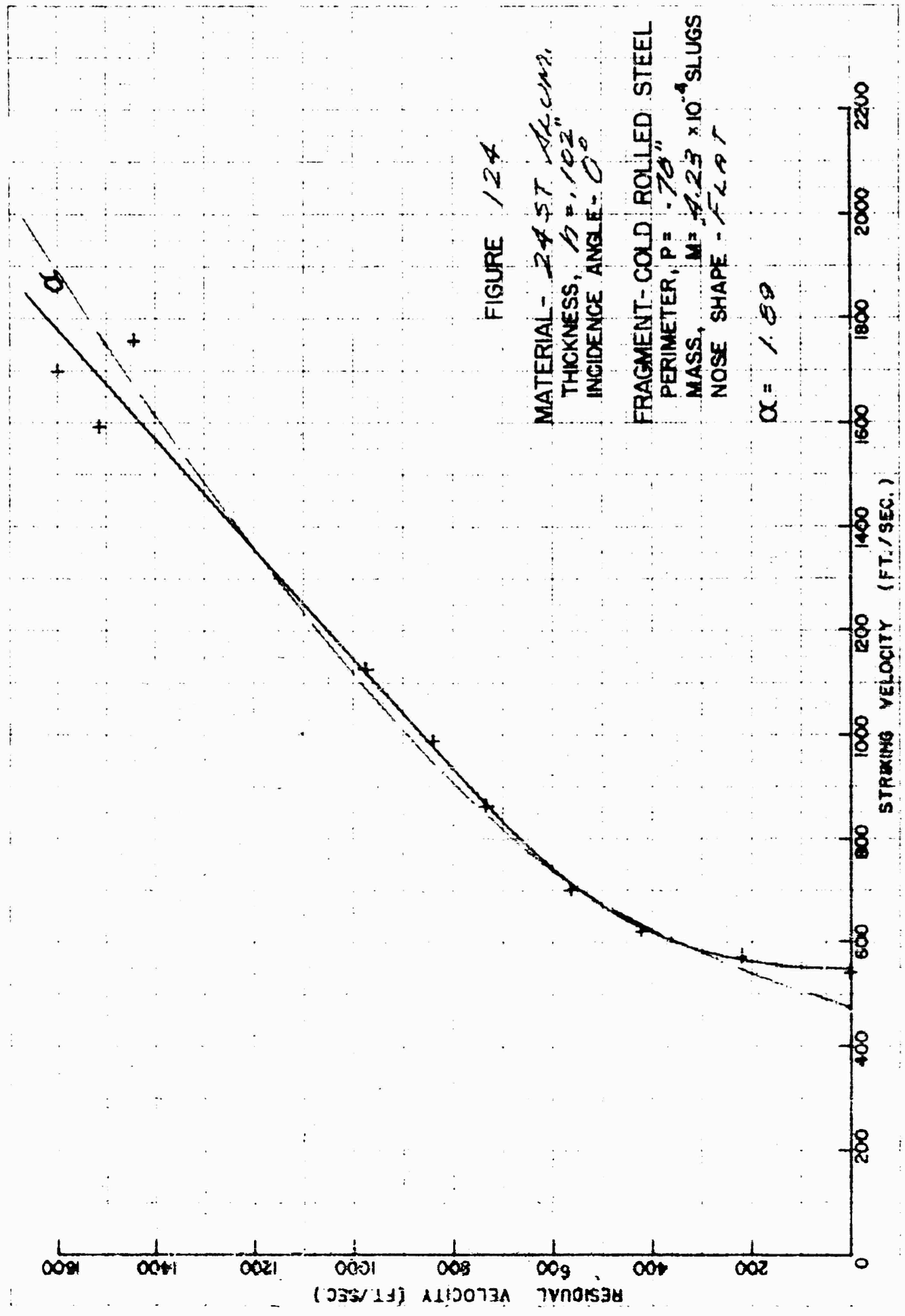


FIGURE 124

MATERIAL - 24.57 ALUMINA
 THICKNESS, $t = .102"$
 INCIDENCE ANGLE - 0°

FRAGMENT - COLD ROLLED STEEL
 PERIMETER, $P = .78"$
 MASS, $M = 4.23 \times 10^{-4}$ SLUGS
 NOSE SHAPE - FLAT

$\alpha = 1.89$

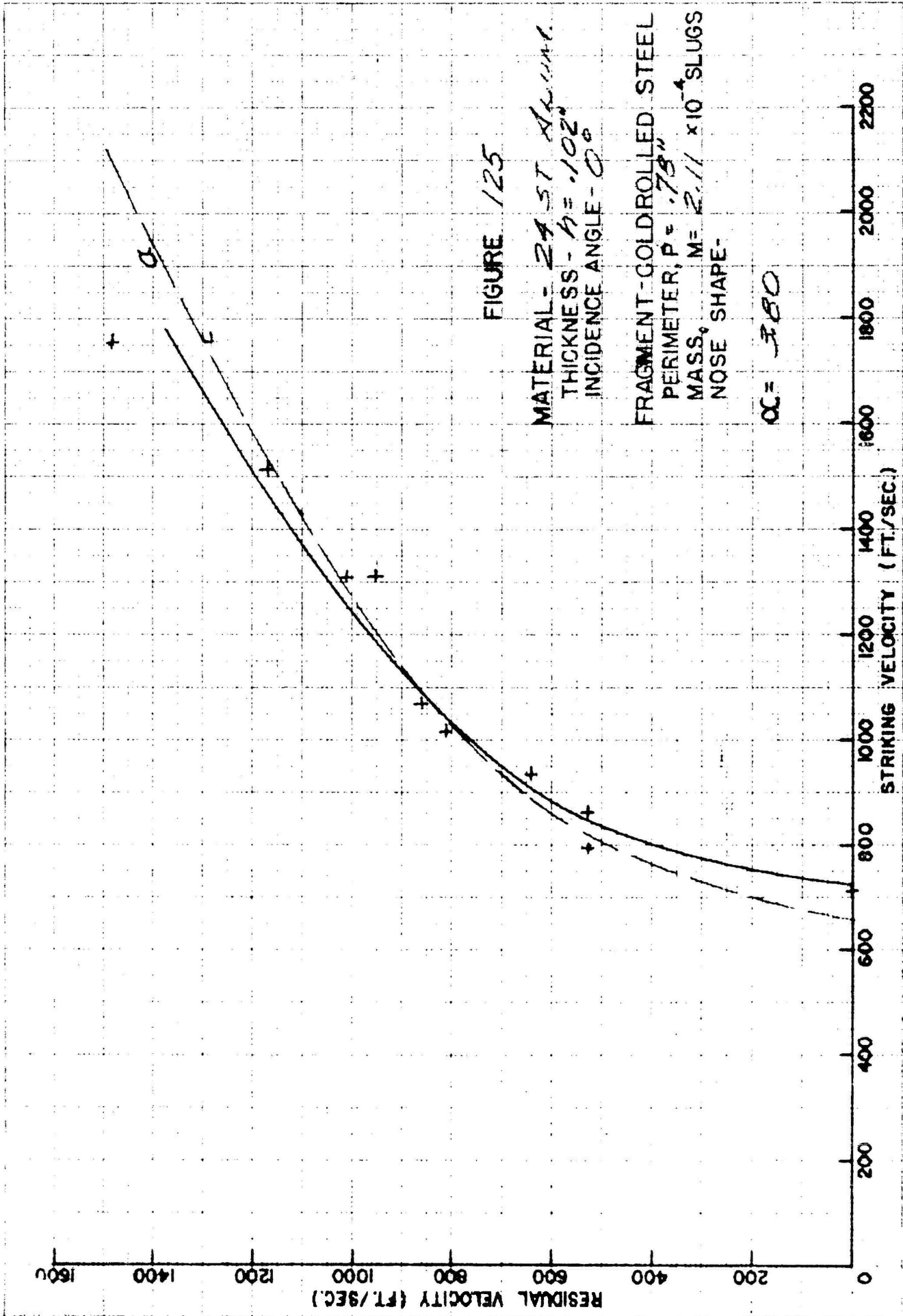


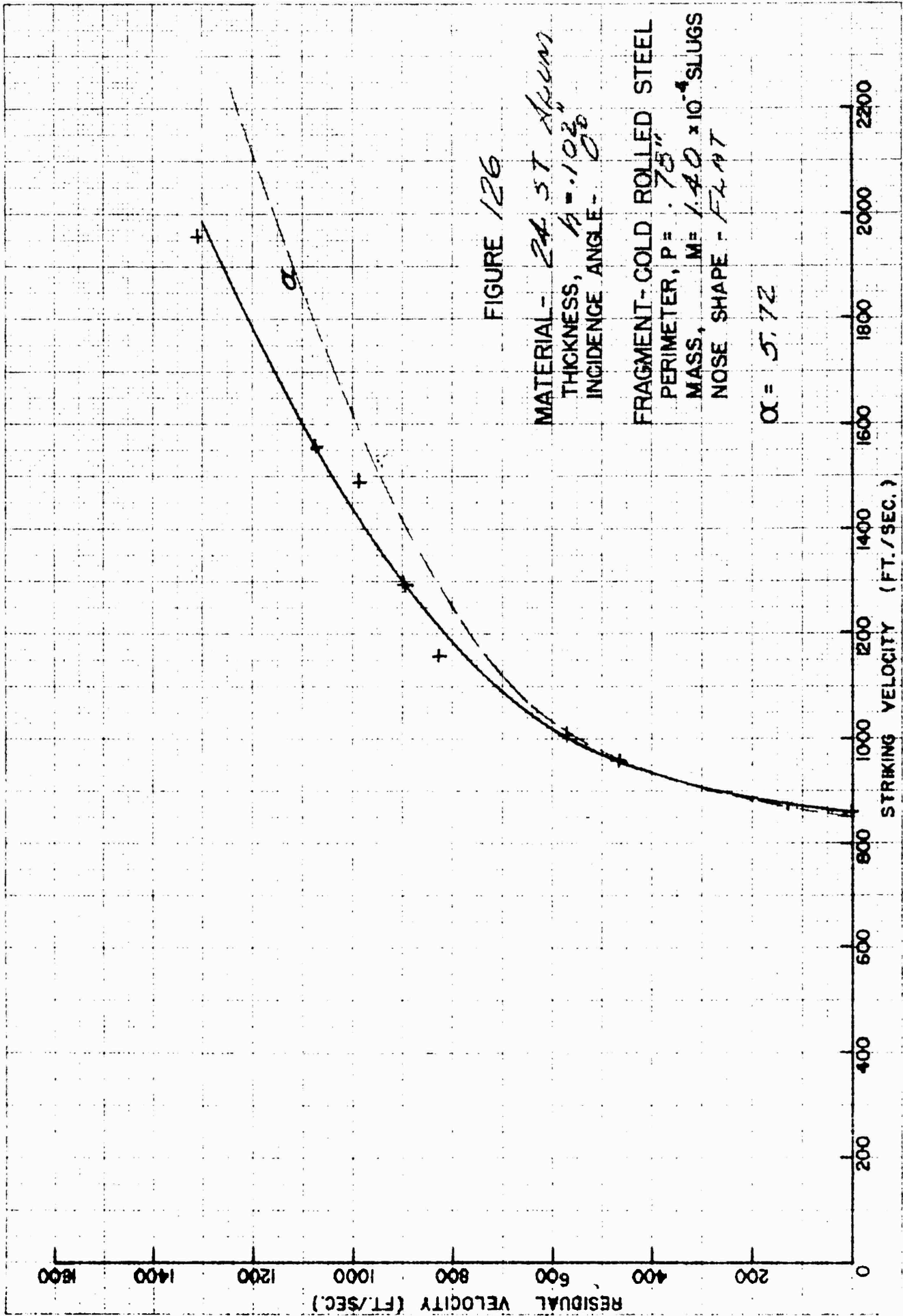
FIGURE 125

MATERIAL - 24 ST ALUMINUM
THICKNESS - $h = .102$ "
INCIDENCE ANGLE - 0°

FRAGMENT - GOLD-ROLLED STEEL
PERIMETER, $P = .73$ "
MASS, $M = 2.11 \times 10^{-4}$ SLUGS
NOSE SHAPE -

$\alpha = 380$

RESTRICTED



RESTRICTED

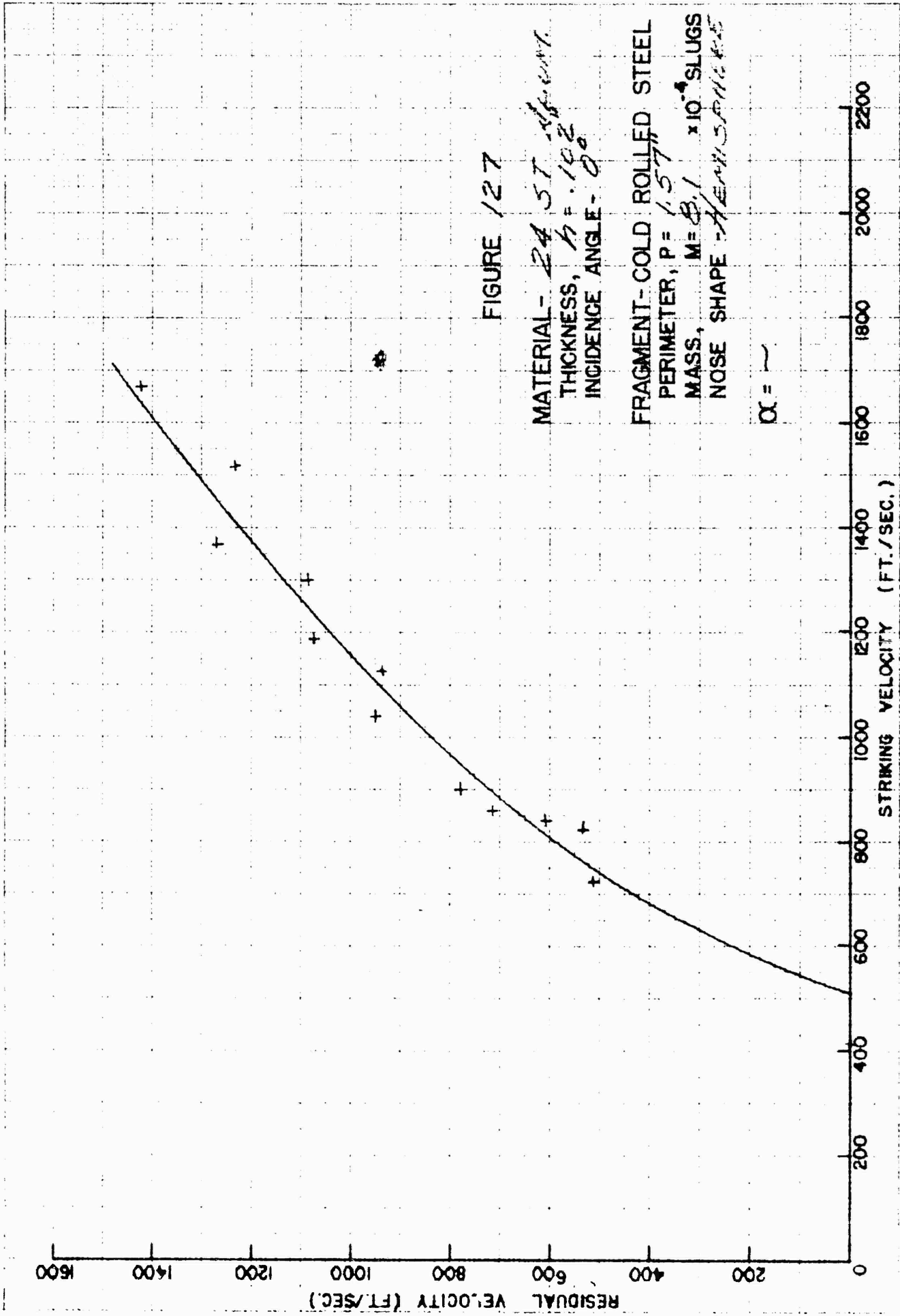


FIGURE 127

MATERIAL - 24 57 *aluminum*
 THICKNESS, $t = .102$
 INCIDENCE ANGLE - 0°

FRAGMENT - COLD ROLLED STEEL
 PERIMETER, $P = 1.57$
 MASS, $M = 8.1 \times 10^{-4}$ SLUGS
 NOSE SHAPE - *HEMISPHERICAL*

$\alpha = \sim$

PHOTOGRAPH BY [illegible]

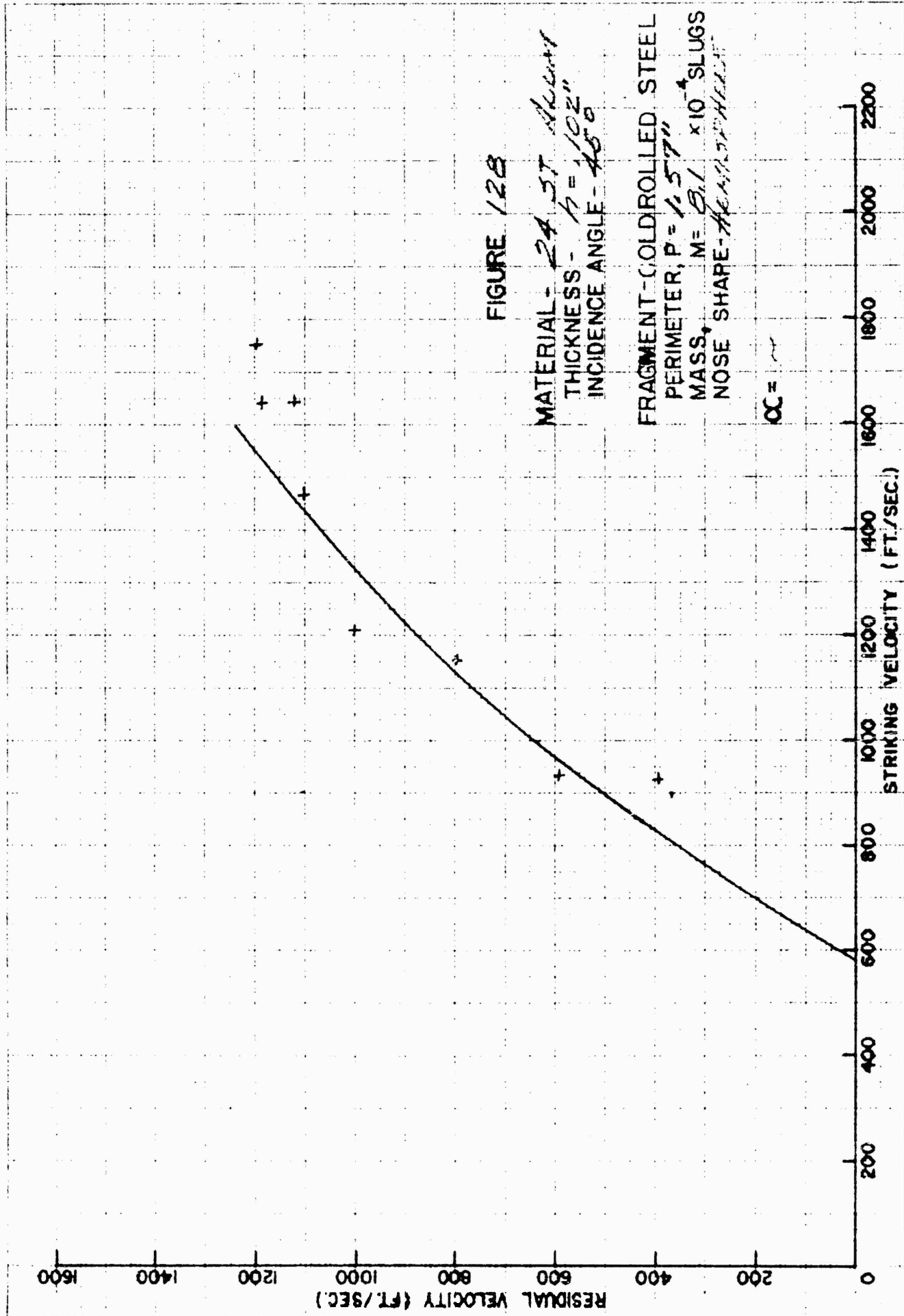


FIGURE 128

MATERIAL - 24 ST ALUMINUM
 THICKNESS - $t = .102"$
 INCIDENCE ANGLE - 45°

FRAGMENT-COLDROLLED STEEL
 PERIMETER, $P = 1.57"$
 MASS, $M = 8.1 \times 10^{-4}$ SLUGS
 NOSE SHAPE - $\frac{1}{2}$ SPHERE

OC =

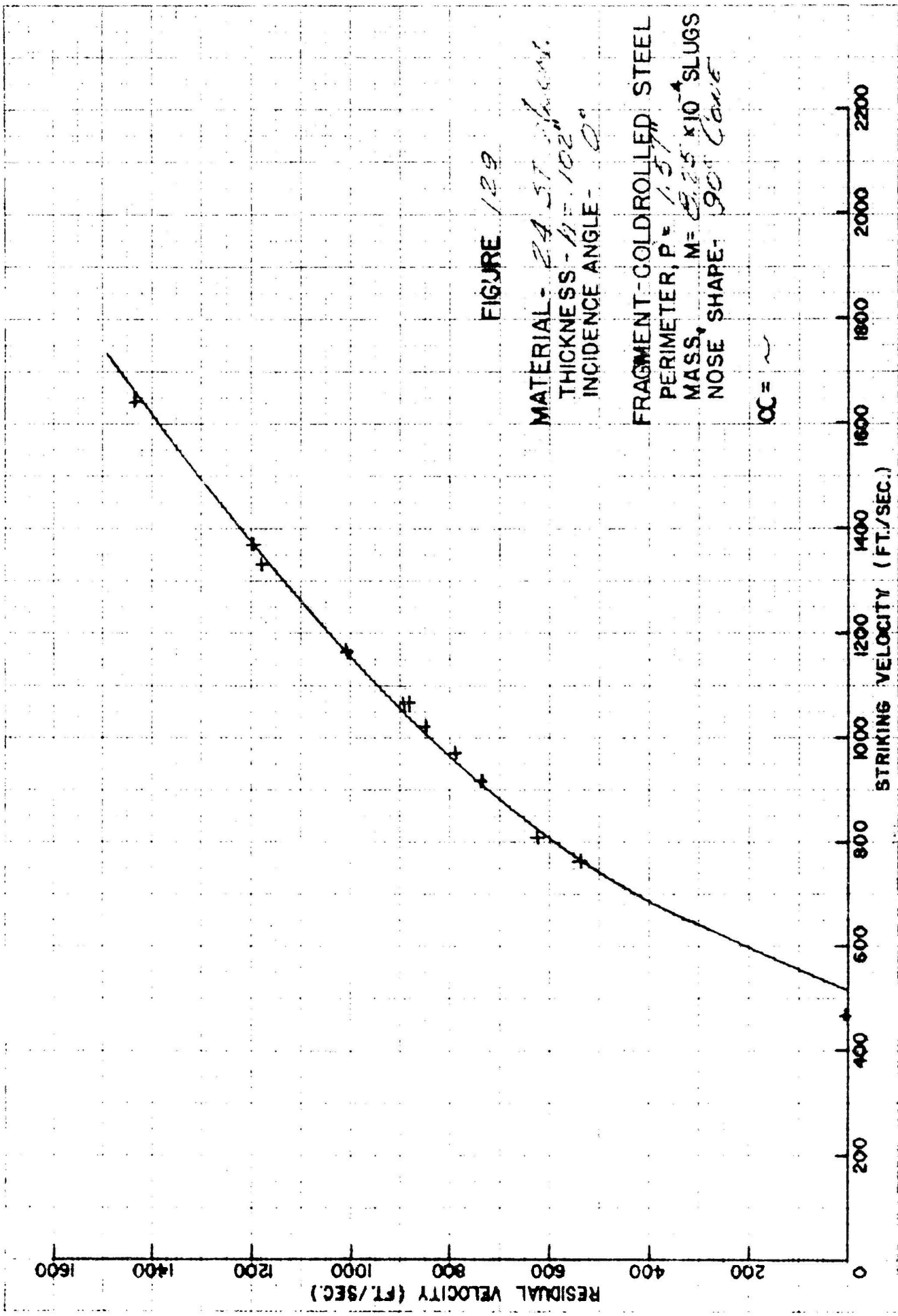


FIGURE 129

MATERIAL - 24 ST. *102* ¹⁰² *102*
 THICKNESS - 1/8" *102*
 INCIDENCE ANGLE - 0°

FRAGMENT-GOLDROLLED STEEL
 PERIMETER, P = 1.37
 MASS, M = 8.25 x 10⁻⁴ SLUGS
 NOSE SHAPE - 90° Cone

OC = ~

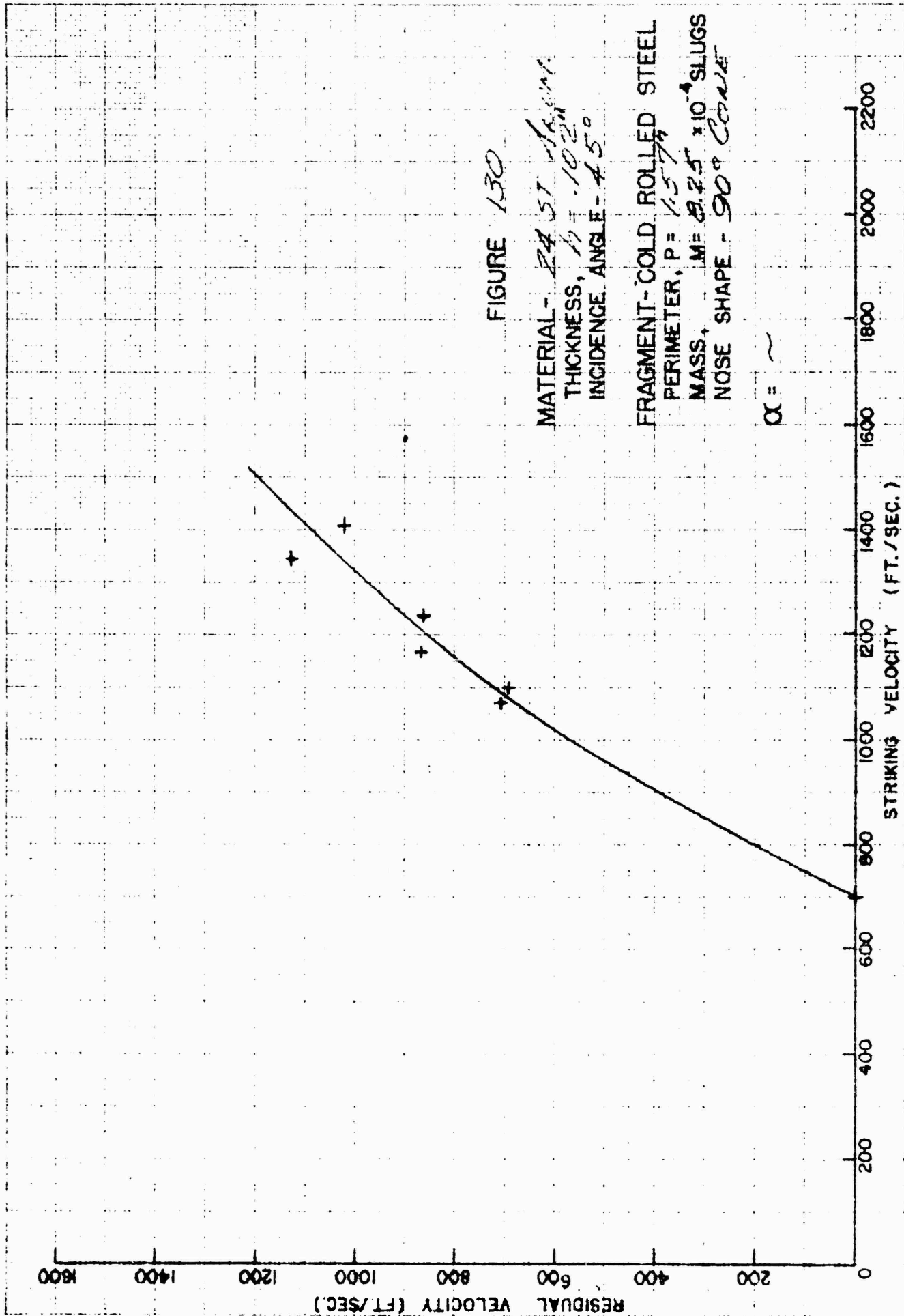


FIGURE 130

MATERIAL - 24 57 *Aluminum*
 THICKNESS, $t = .102$
 INCIDENCE ANGLE - 45°

FRAGMENT - COLD ROLLED STEEL
 PERIMETER, $P = 1.577$
 MASS, $M = 8.25 \times 10^{-4}$ SLUGS
 NOSE SHAPE - 90° CONE

$\alpha = \sim$

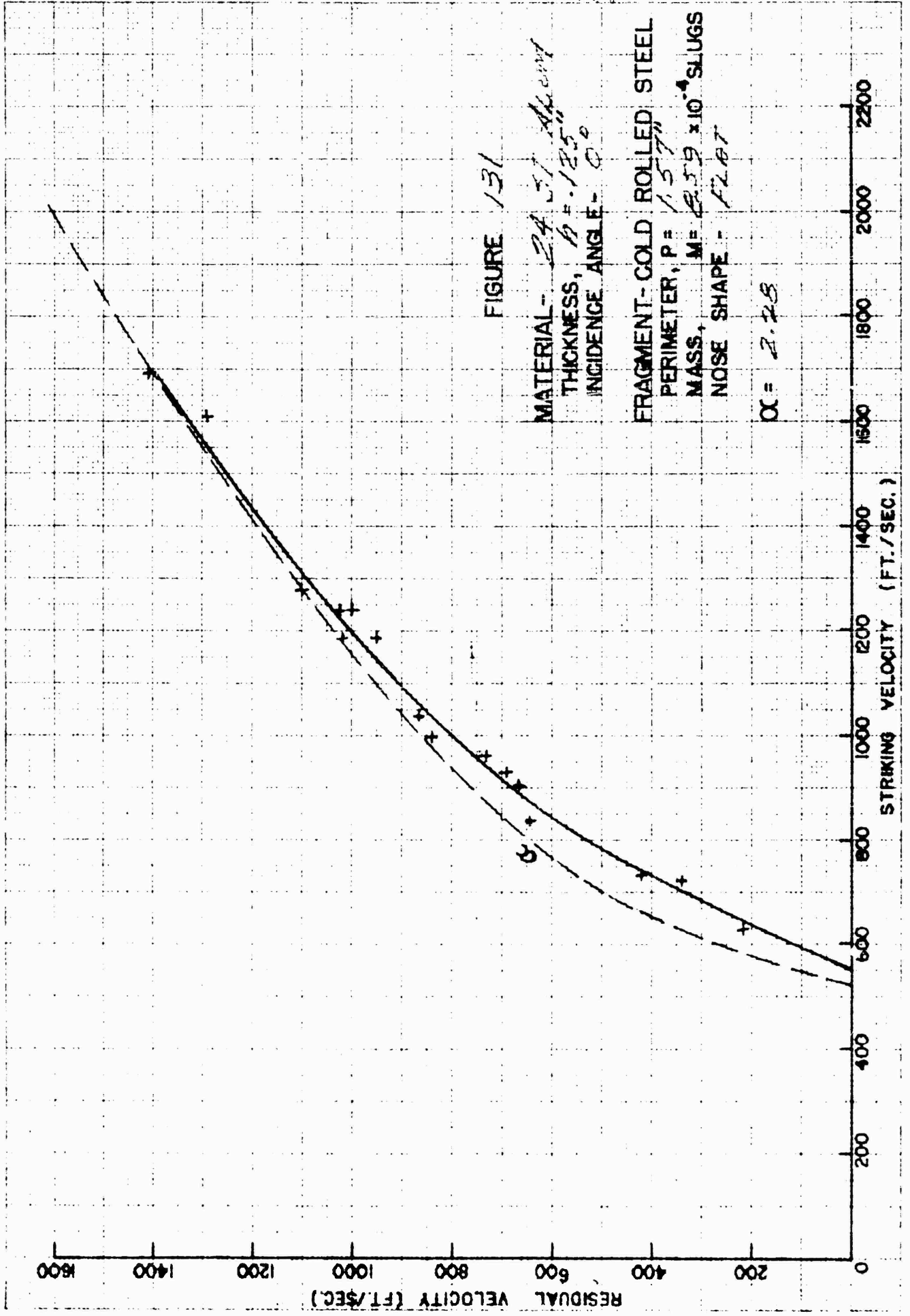


FIGURE 131

MATERIAL - 24 51 ALUMINUM
 THICKNESS, $t = .125"$
 INCIDENCE ANGLE - 0°
 FRAGMENT - COLD ROLLED STEEL
 PERIMETER, $P = 1.57"$
 MASS, $M = 2.59 \times 10^{-4}$ SLUGS
 NOSE SHAPE - FLAT

$\alpha = 2.28$

UNCLASSIFIED

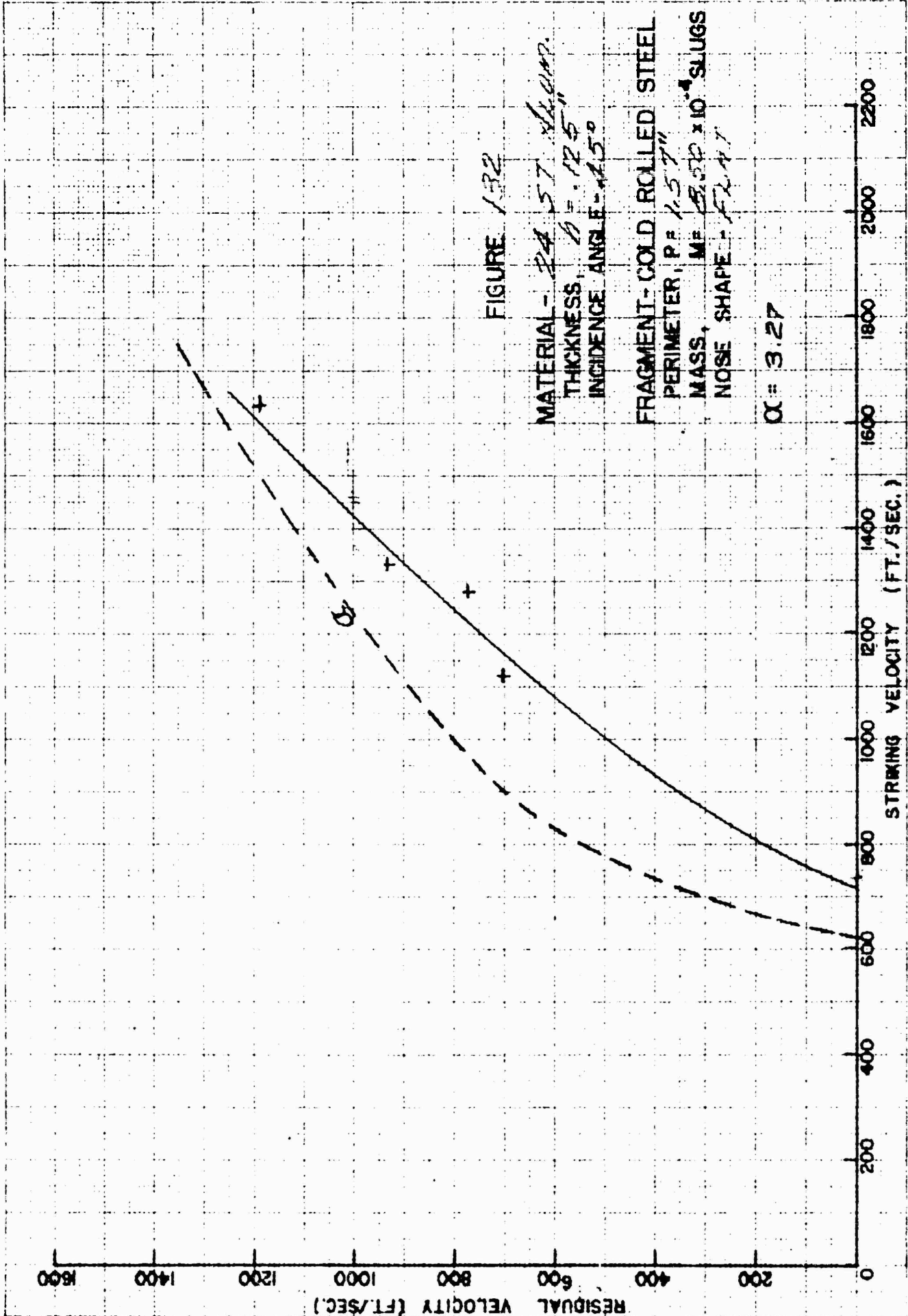


FIGURE 132

MATERIAL - 24 57 ALUM.
 THICKNESS, $t = .125"$
 INCIDENCE ANGLE - 15°

FRAGMENT - COLD ROLLED STEEL
 PERIMETER, $P = 1.57"$
 MASS, $M = 8.32 \times 10^{-4}$ SLUGS
 NOSE SHAPE - FLAT

$\alpha = 3.27$

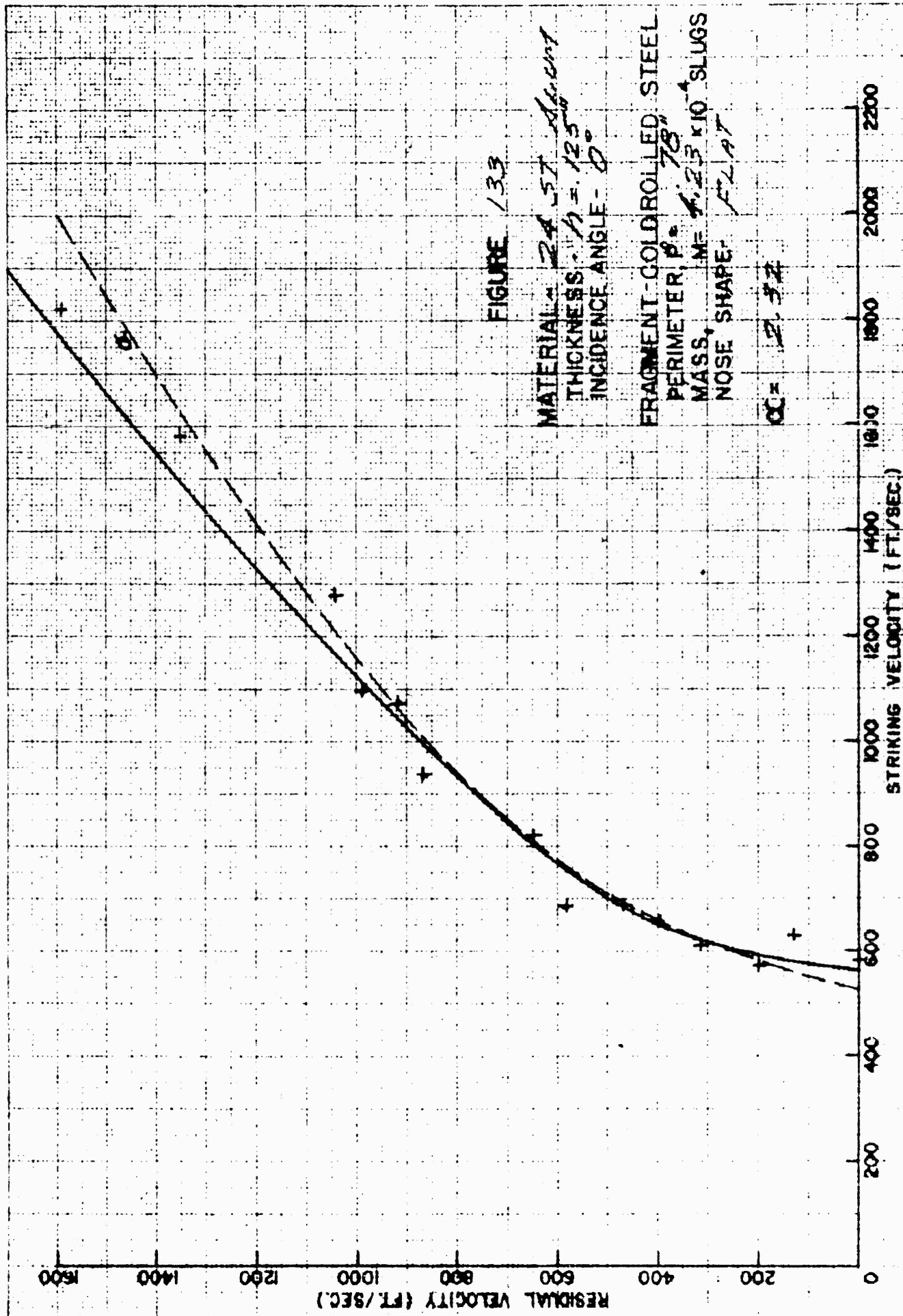
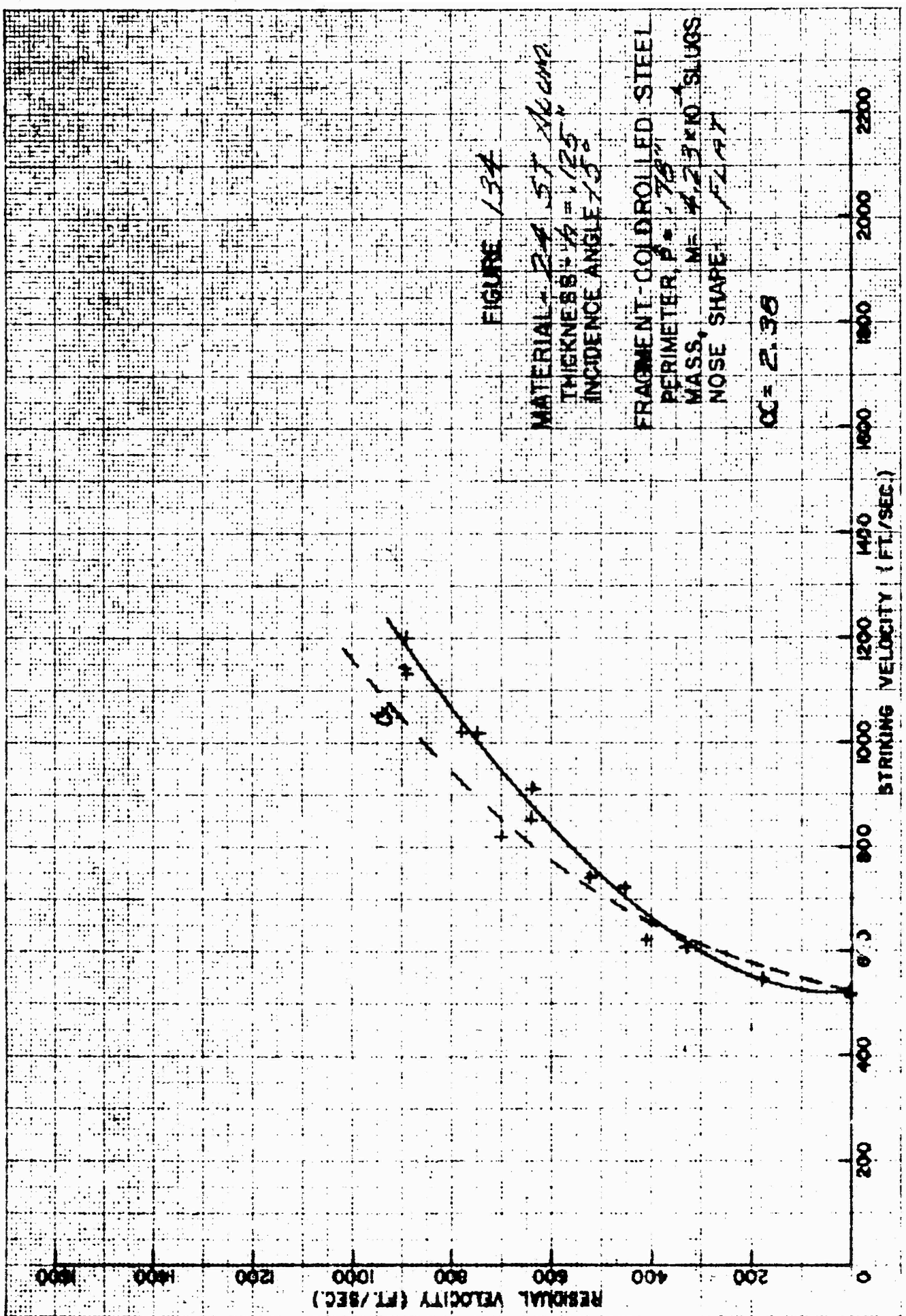


FIGURE 133

MATERIAL - 24.57 mil Alucut
 THICKNESS - $t = 125 \times 10^{-6}$ in
 INCIDENCE ANGLE - 0°

FRAGMENT - GOLD ROLLED STEEL
 PERIMETER, $P = 78$ "
 MASS, $M = 4.23 \times 10^{-4}$ SLUGS
 NOSE SHAPE - FLAT

CC = 2.37



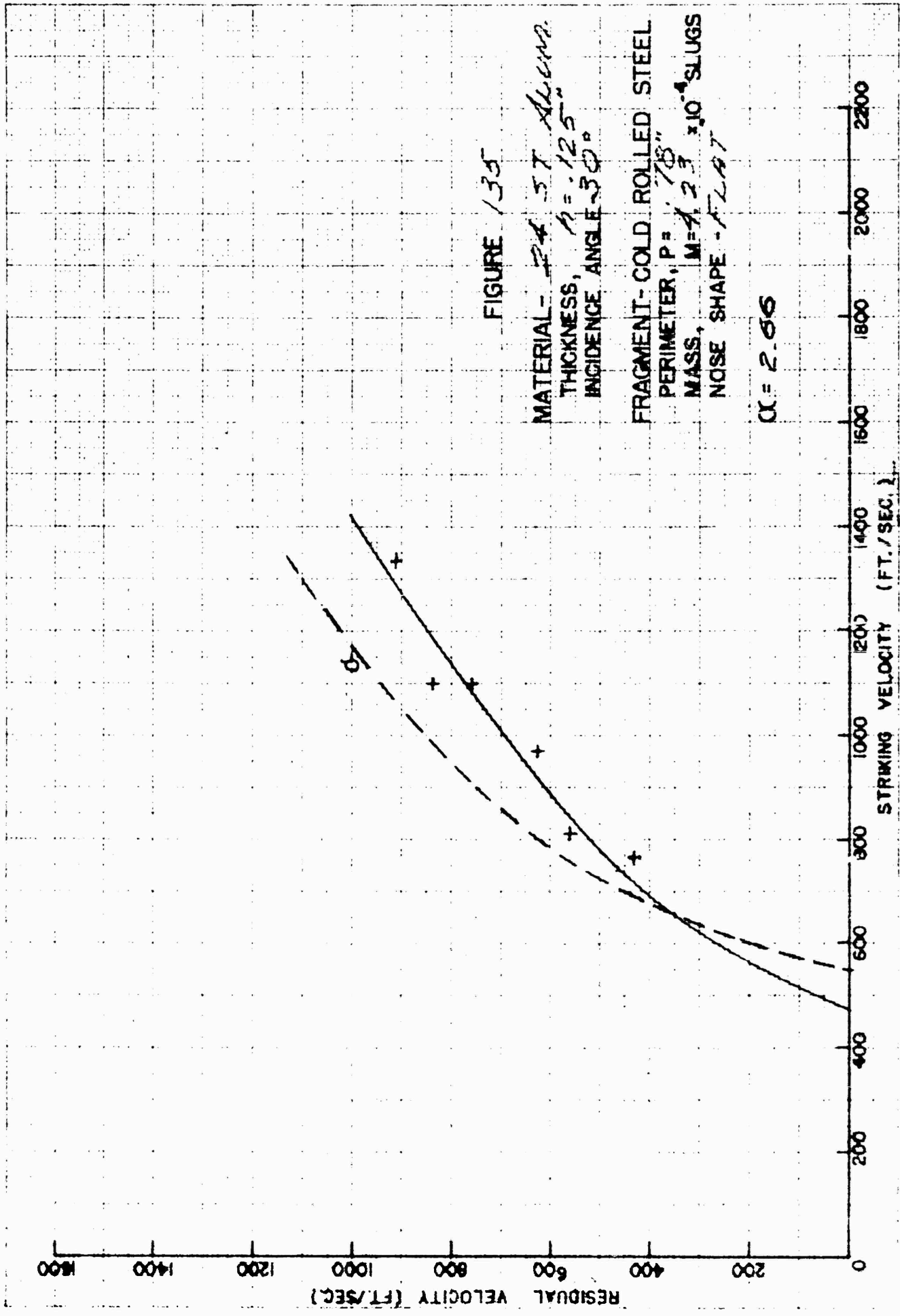
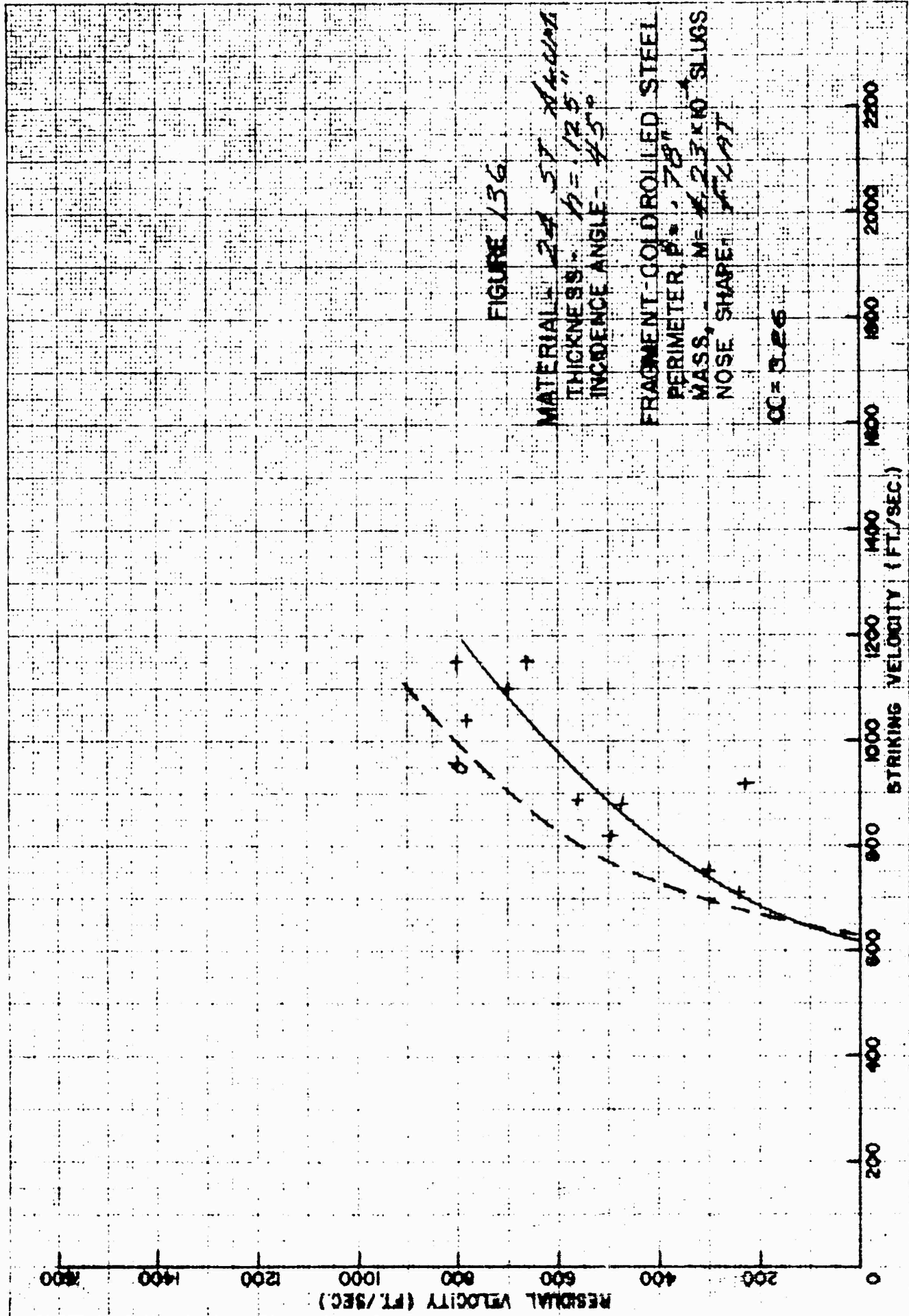


FIGURE 135

MATERIAL - ~~24~~ 57 ALUMINUM.
THICKNESS, $t = .125$ "
INCIDENCE ANGLE 30°

FRAGMENT - COLD ROLLED STEEL
PERIMETER, $P = .78$ "
MASS, $M = 4.23 \times 10^{-4}$ SLUGS
NOSE SHAPE - FLAT

$\alpha = 2.66$



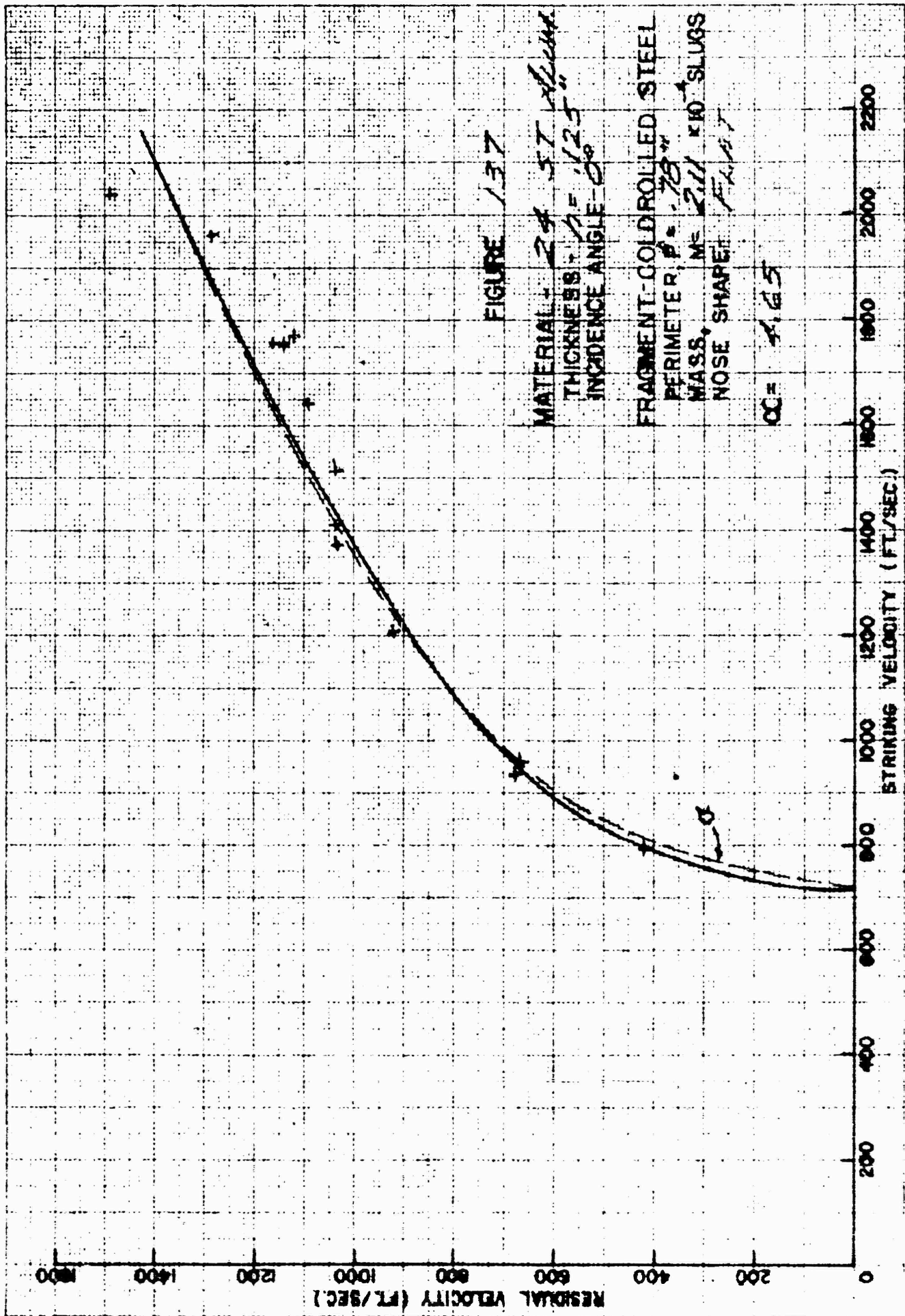
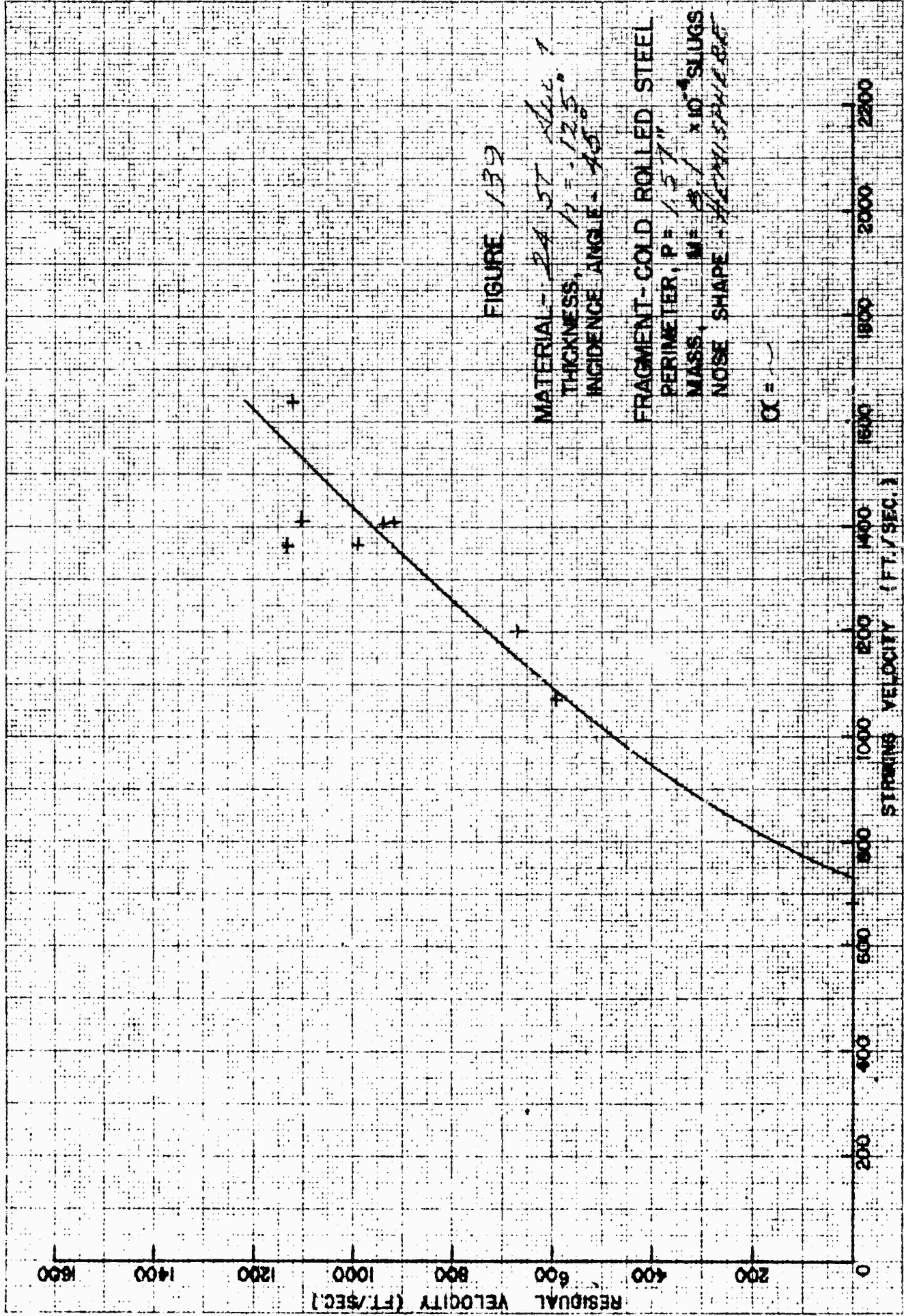


FIGURE 137

MATERIAL: 24 57 Alcoa
THICKNESS: $t = .125$ "
INCIDENCE ANGLE: 60°
FRAGMENT-COLD ROLLED STEEL
PERIMETER: $P = .78$ "
MASS: $M = 2.11 \times 10^{-4}$ SLUGS
NOSE SHAPE: FLAT

OC = 4.65



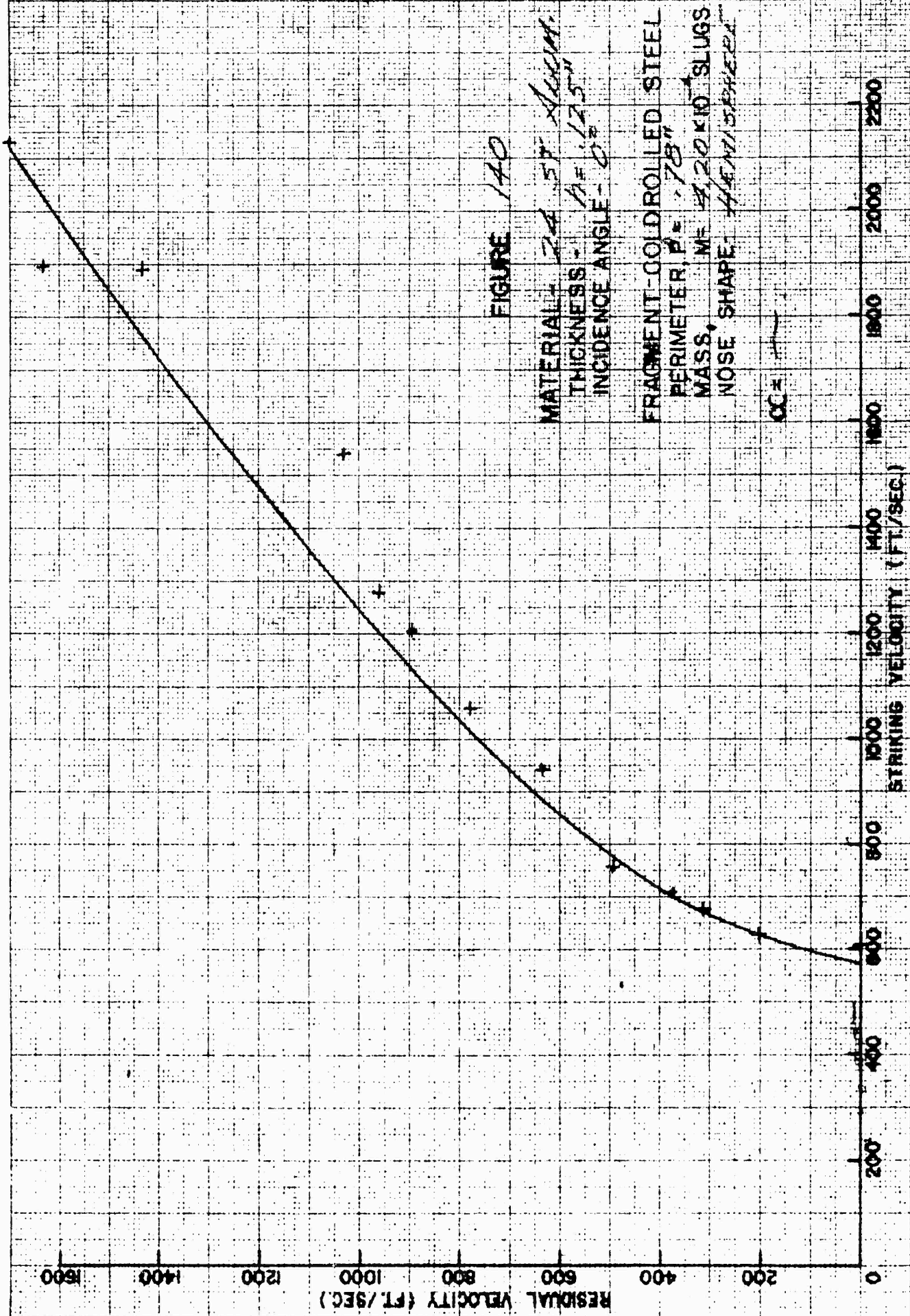
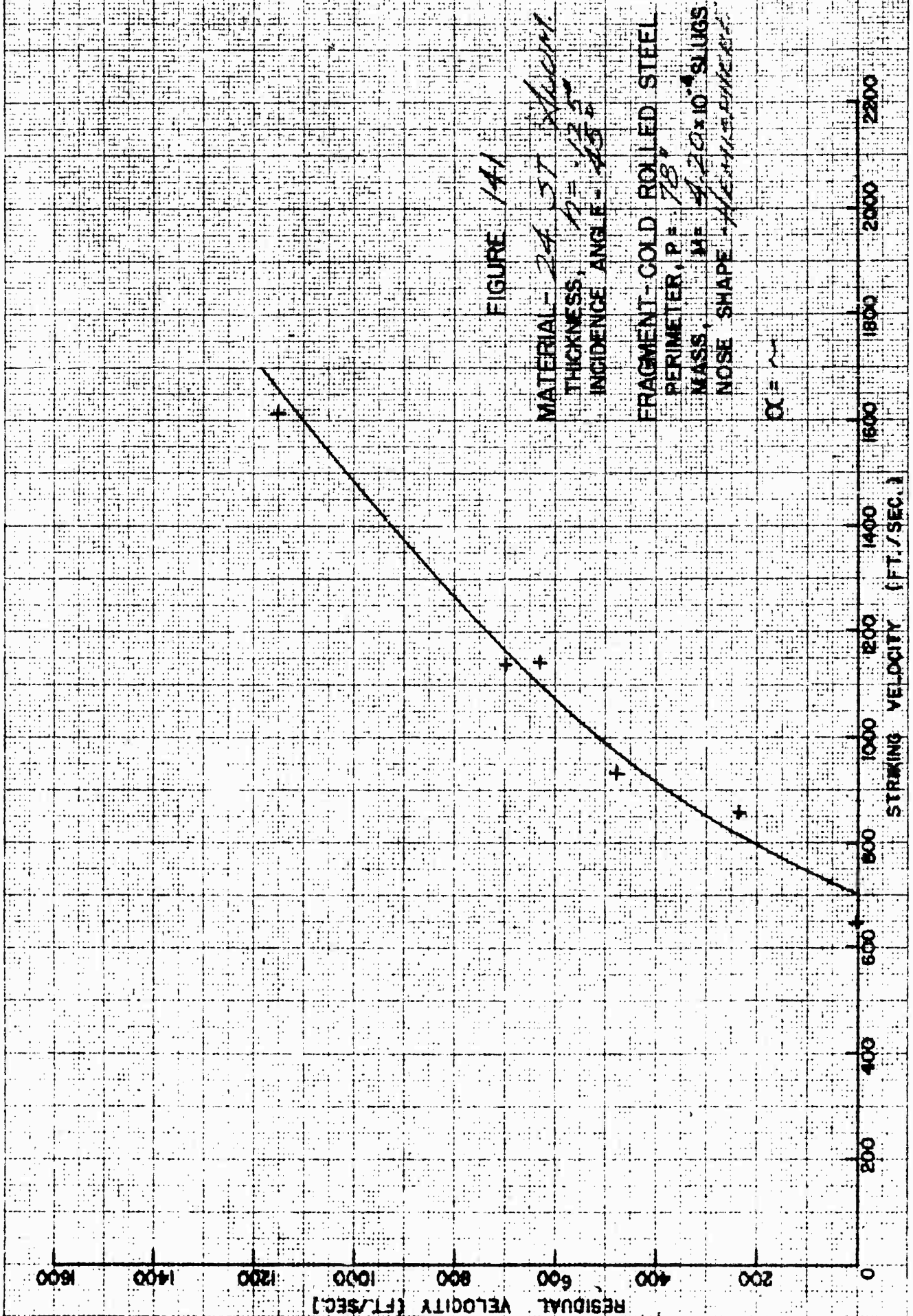


FIGURE 1A0

MATERIAL - 2A 57 ALUMIN.
THICKNESS - 1/16" - 1/8"
INCIDENCE ANGLE - 0°

FRAGMENT-COLDROLLED STEEL
PERIMETER, P = .78"
MASS, M = 4.20 KID SLUGS
NOSE SHAPE - HEMISPHERICAL

CC =



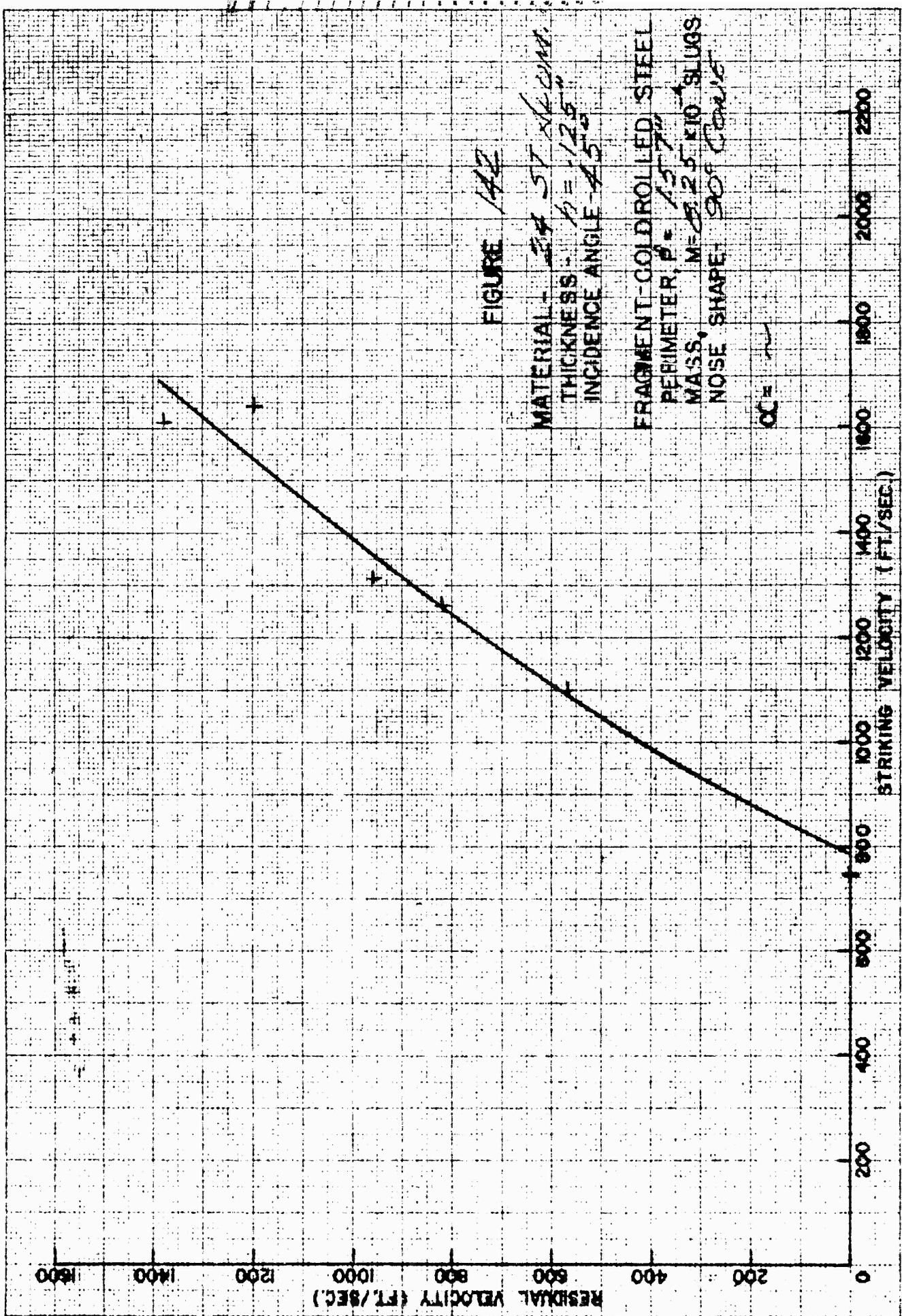


FIGURE 142

MATERIAL - *37 ST ALUM.*
THICKNESS - $t = 1/25"$
INCIDENCE ANGLE - 45°

FRAGMENT-COLDROLLED STEEL
PERIMETER, $P = 15.7"$
MASS, $M = 0.25$ KIO SLUGS
NOSE SHAPE: 90° CONE

OC = *~*

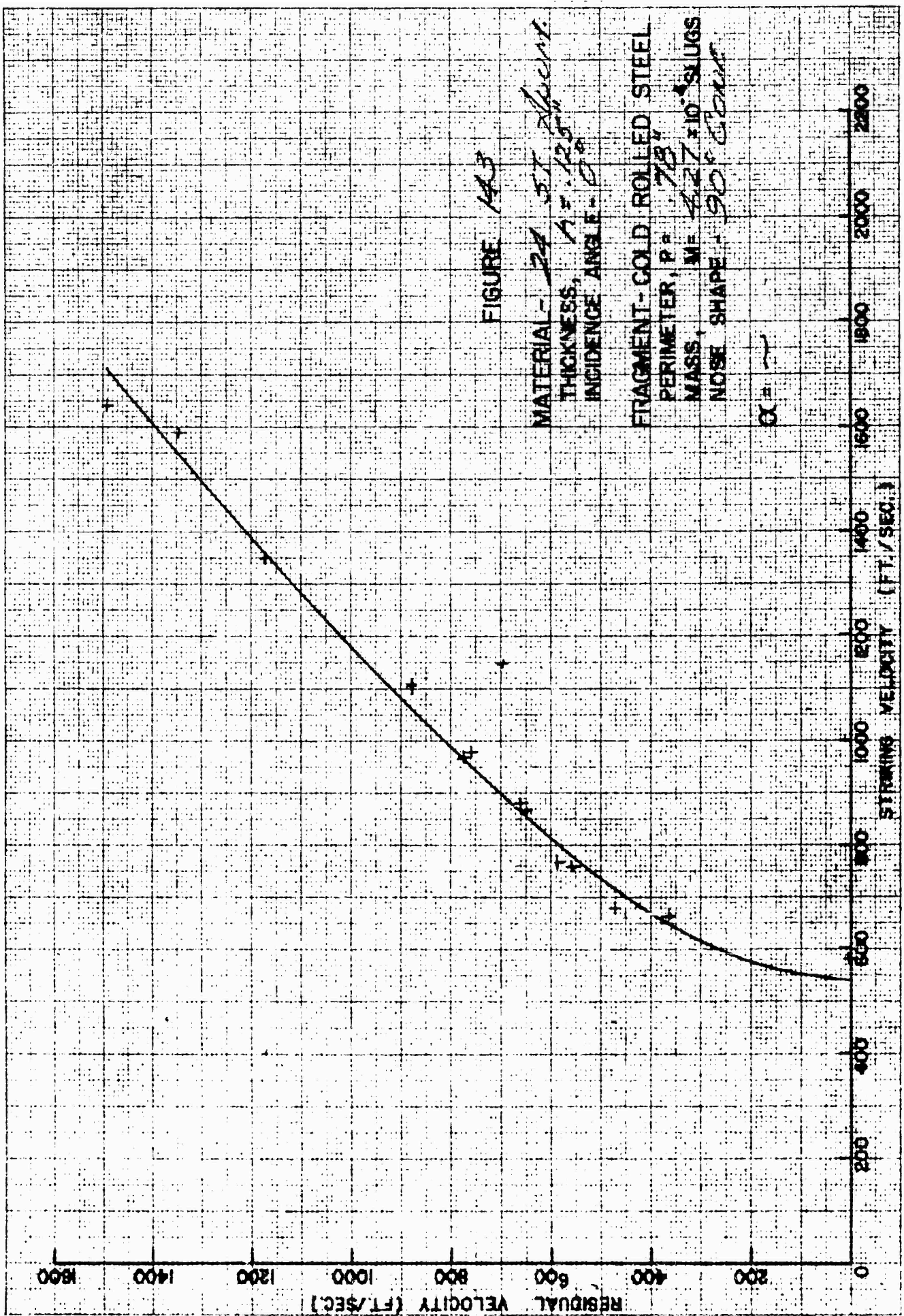


FIGURE 143

MATERIAL - 24.5T FRAGMENT
THICKNESS, $t = .125$
INCIDENCE ANGLE - 0°

FRAGMENT - COLD ROLLED STEEL
PERIMETER, $P = .78$
MASS, $M = 4.27 \times 10^{-4}$ SLUGS
NOSE SHAPE - 90° CONE

$\alpha = \sim$

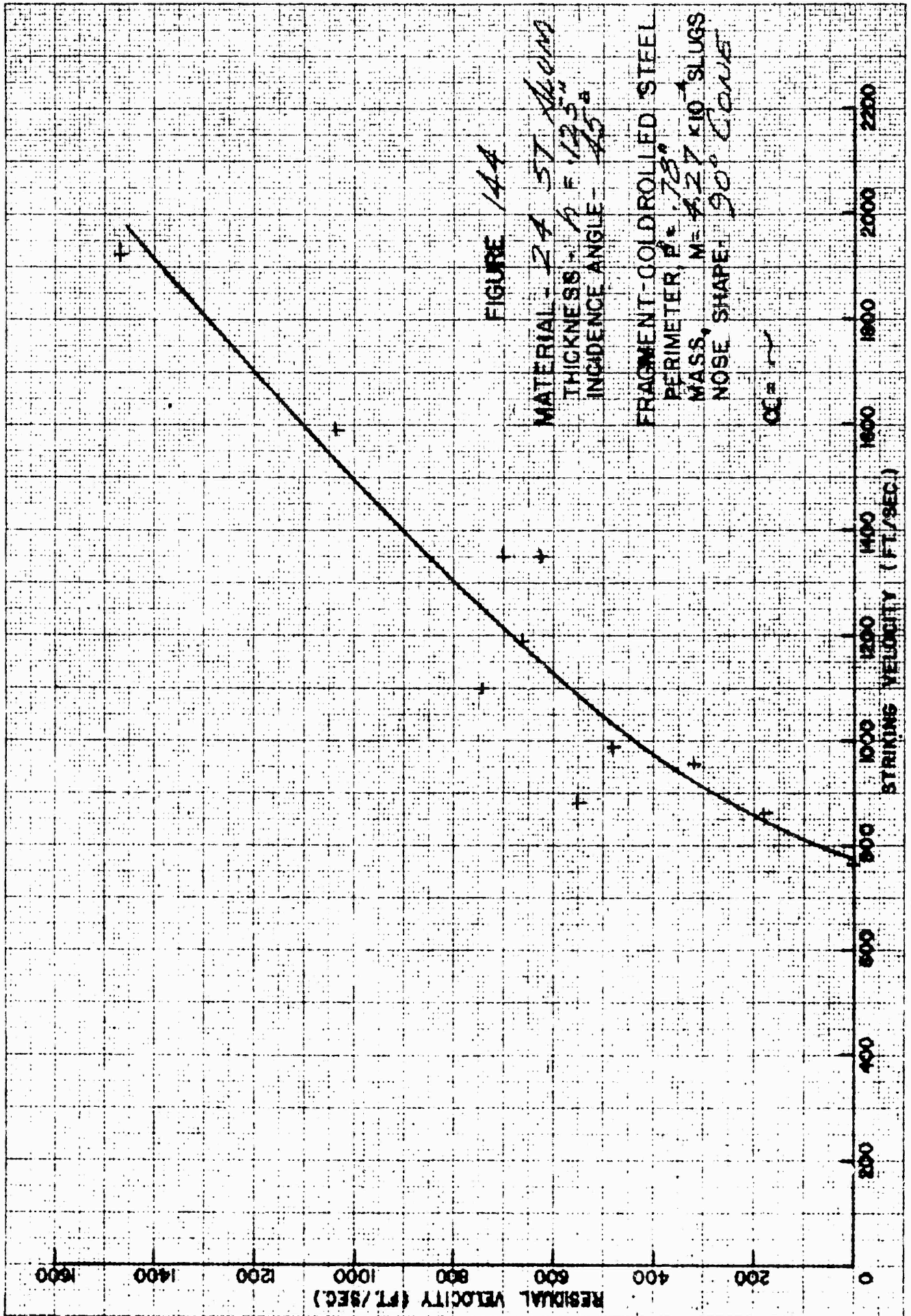
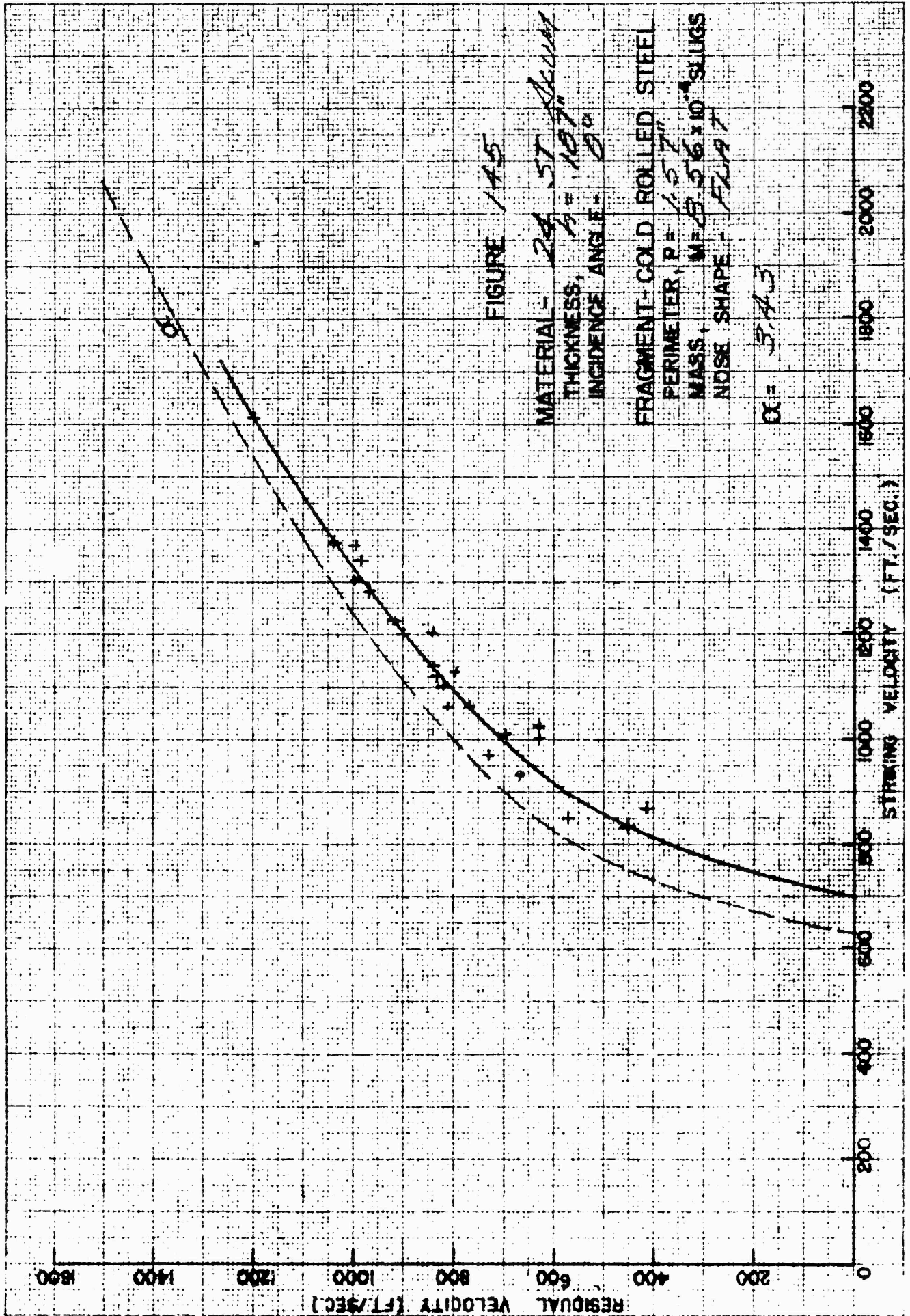
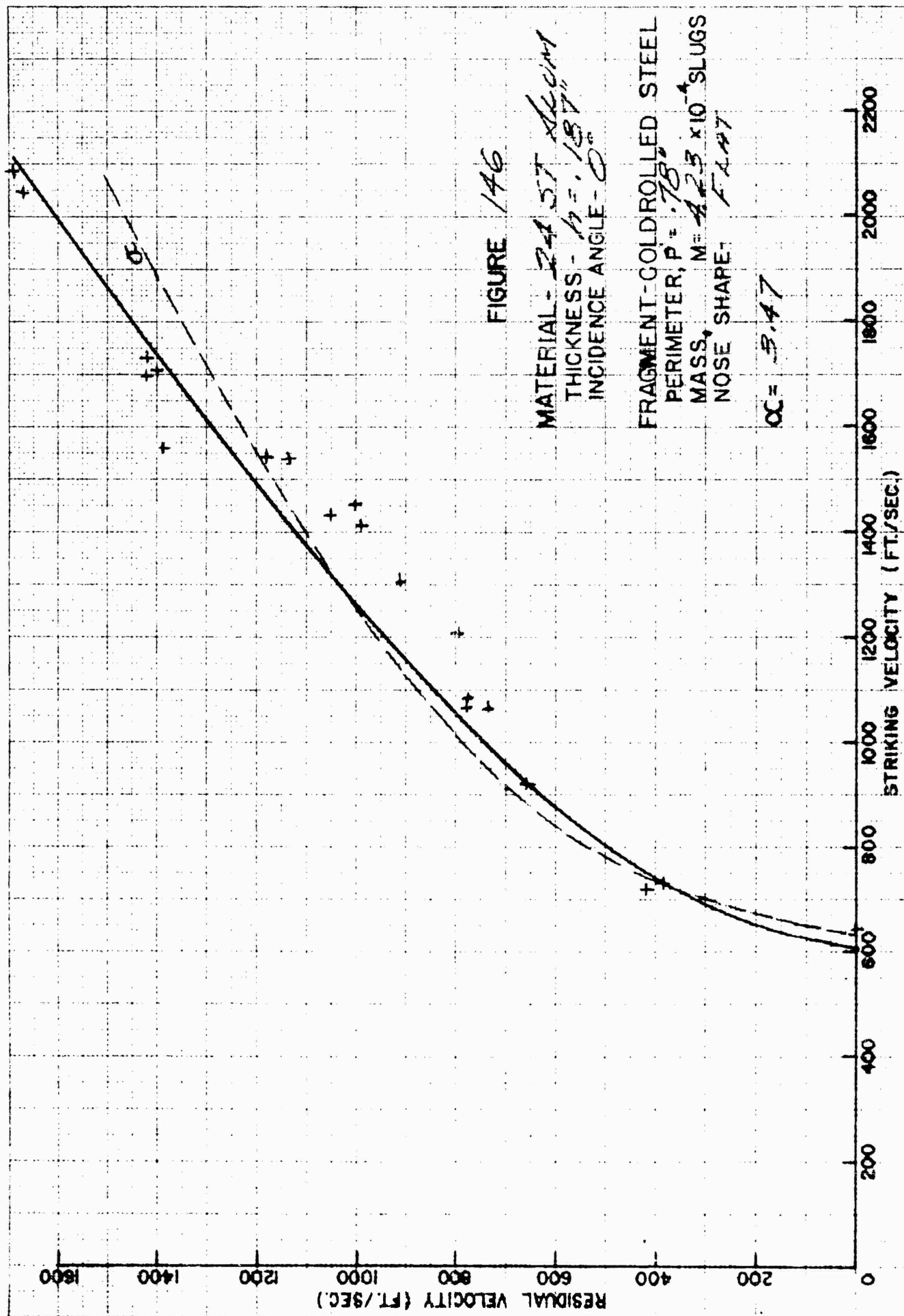


FIGURE 14A

MATERIAL - 2A 5T *Aluminum*
THICKNESS - *1/8" F 12.5*
INCIDENCE ANGLE - *45°*
FRAGMENT-GOLDROLLED STEEL
PERIMETER *P = .78"*
MASS, *M = 4.27 KIO* SLUGS
NOSE SHAPE - *90° CONE*

CC = *~*





GRAPH COMPUTATIONS MEANS: NO INCOM

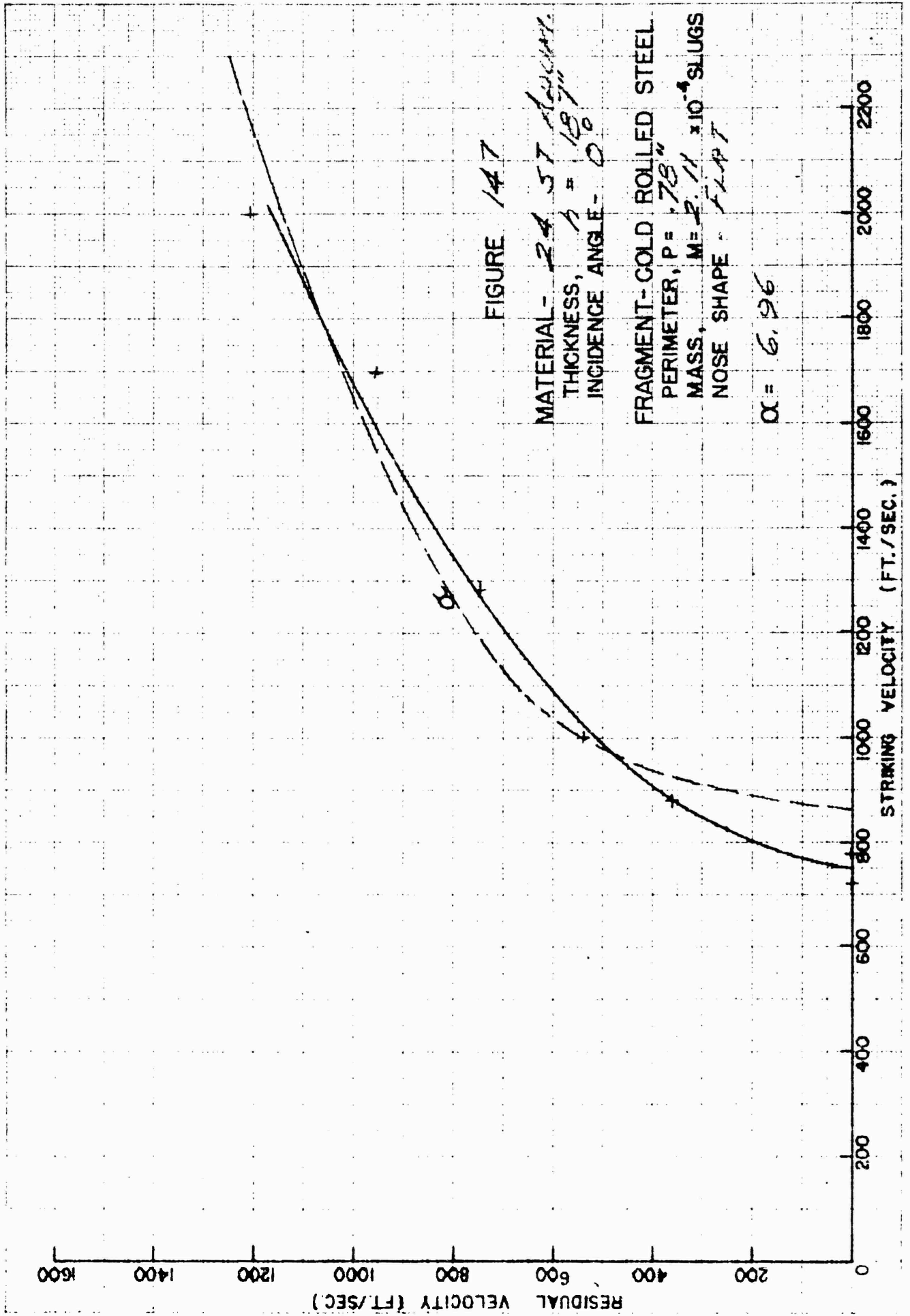
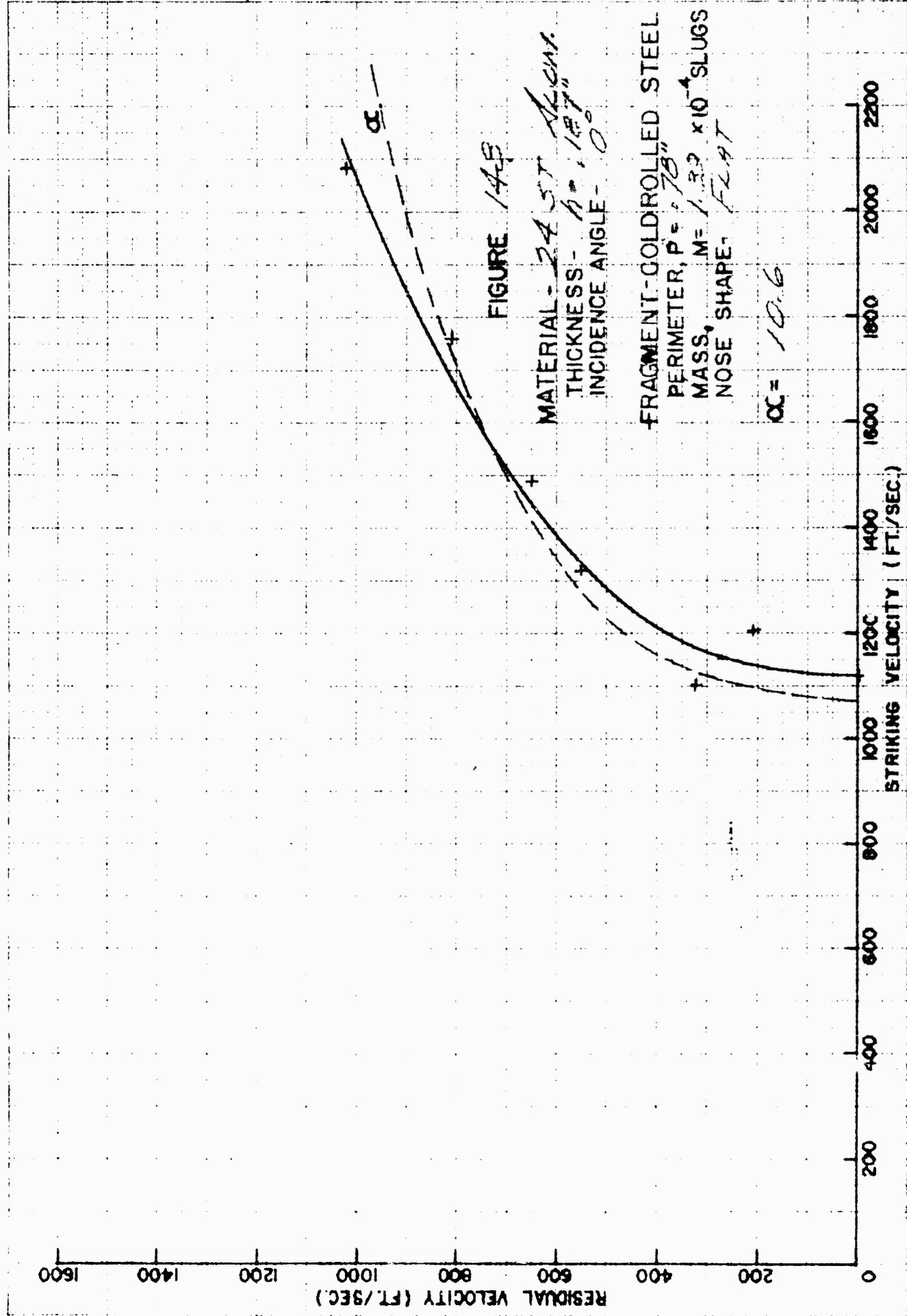


FIGURE 147

MATERIAL - *24 ST ALUMIN.*
THICKNESS, $t = 187$
INCIDENCE ANGLE - 0°

FRAGMENT - COLD ROLLED STEEL
PERIMETER, $P = 78$
MASS, $M = 2.11 \times 10^{-4}$ SLUGS
NOSE SHAPE - *FLAT*

$\alpha = 6.96$



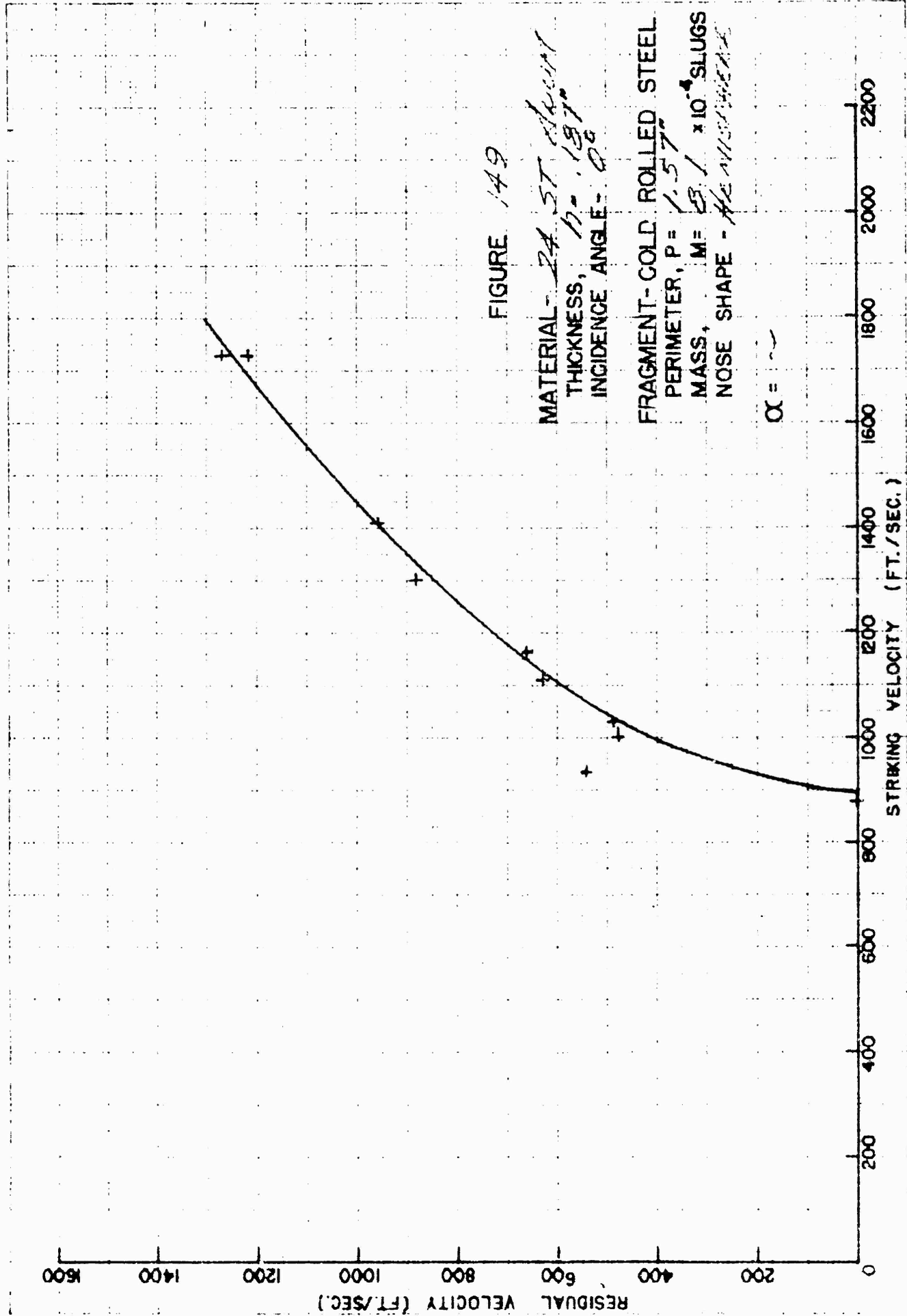


FIGURE 149

MATERIAL - 24 ST. ALUM.
THICKNESS, 17×10^{-4}
INCIDENCE ANGLE - 0°

FRAGMENT - COLD ROLLED STEEL
PERIMETER, $P = 1.57$
MASS, $M = 23.1 \times 10^{-4}$ SLUGS
NOSE SHAPE - $A_{E, N} = 1.0$

$\alpha = \dots$

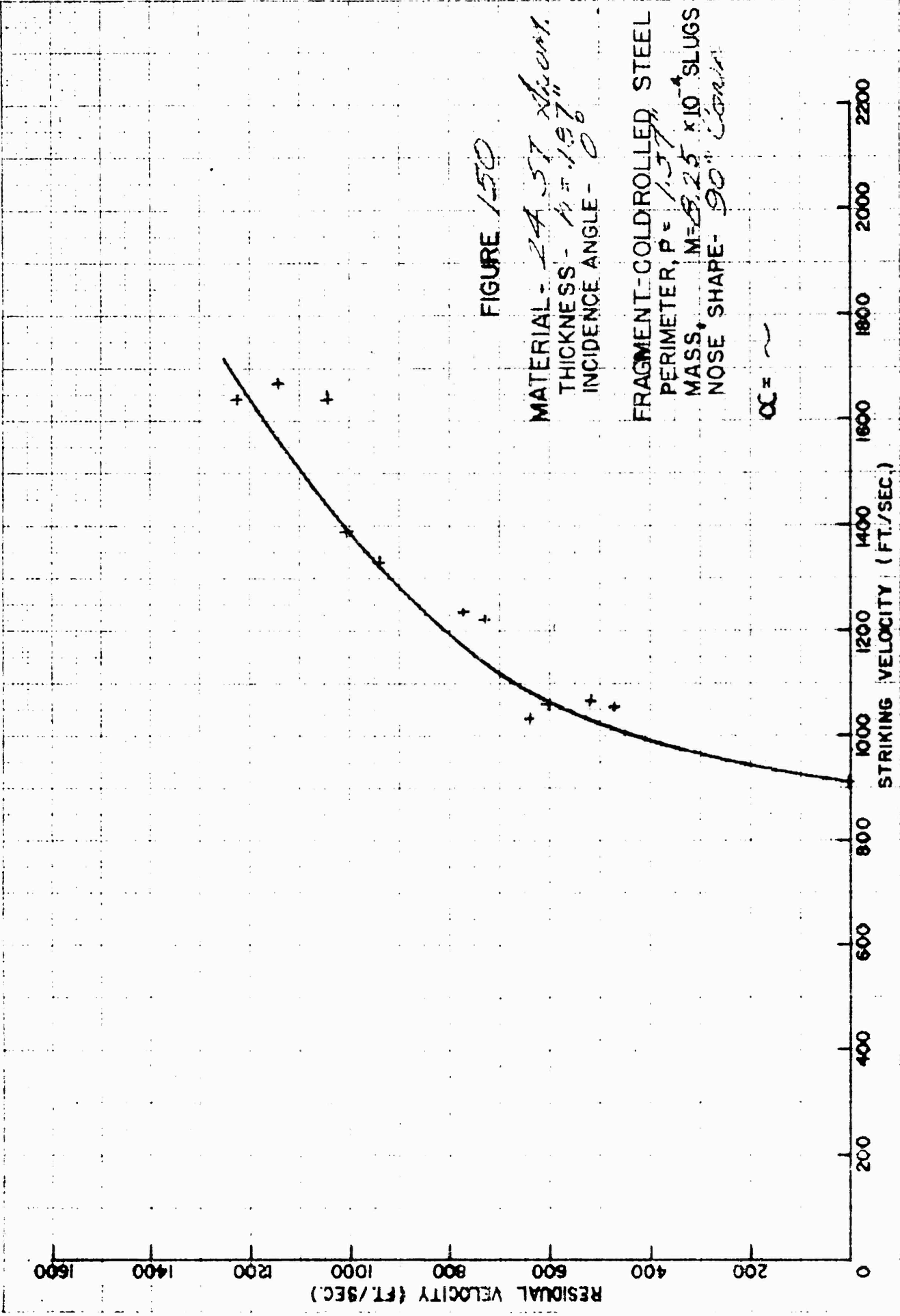


FIGURE 150

MATERIAL - 2A-57 ALUMIN.
THICKNESS - $t = .197$ "
INCIDENCE ANGLE - 0

FRAGMENT-COLDROLLED STEEL
PERIMETER, $P = 1.37$ "
MASS, $M = 8.25 \times 10^{-4}$ SLUGS
NOSE SHAPE - 90° CORNER

OC = ~

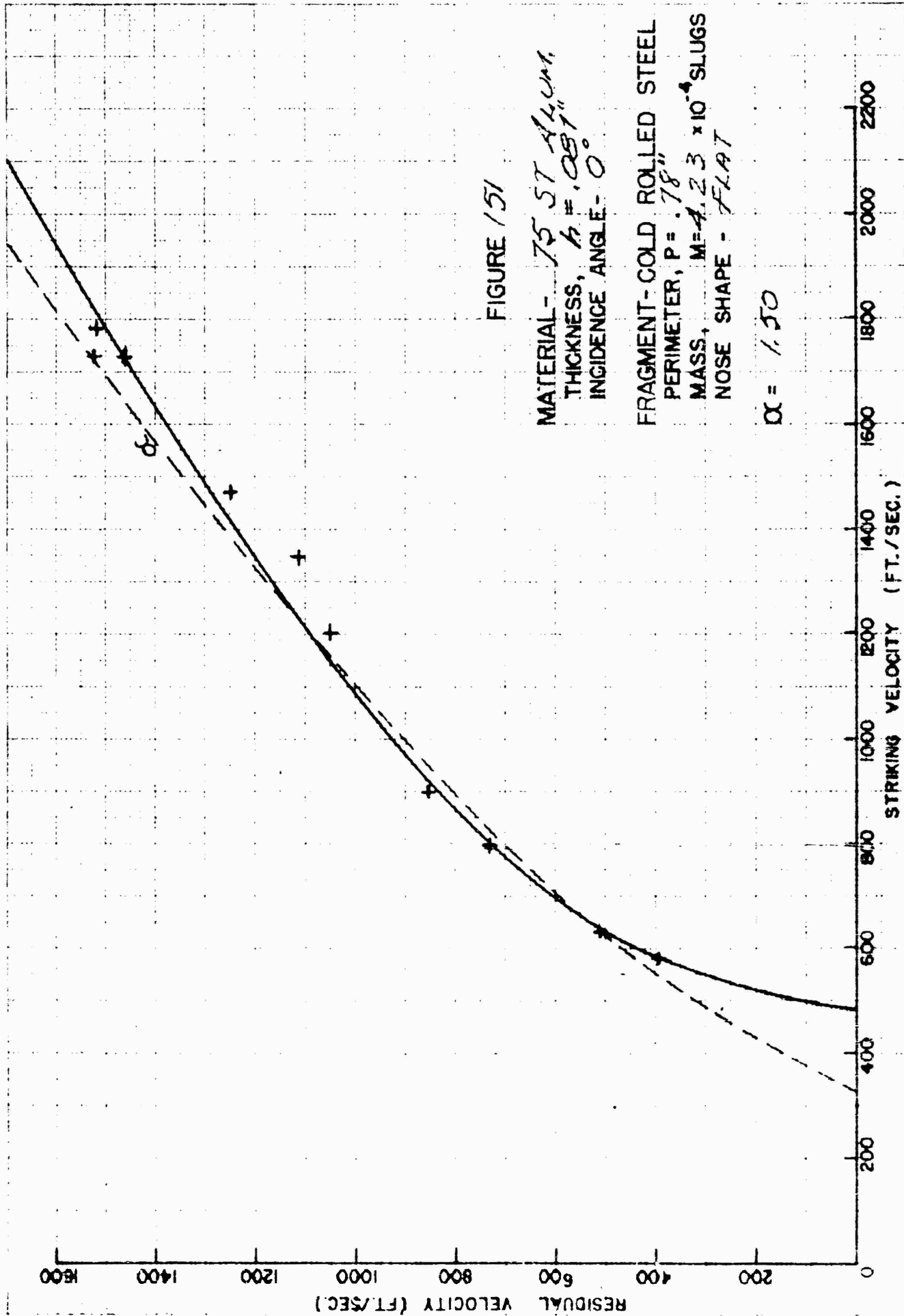


FIGURE 151

MATERIAL - 75 ST ALUM.
 THICKNESS, $h = .087$ "
 INCIDENCE ANGLE - 0

FRAGMENT - COLD ROLLED STEEL
 PERIMETER, $P = .78$ "
 MASS, $M = 4.23 \times 10^{-4}$ SLUGS
 NOSE SHAPE - FLAT

$\alpha = 1.50$

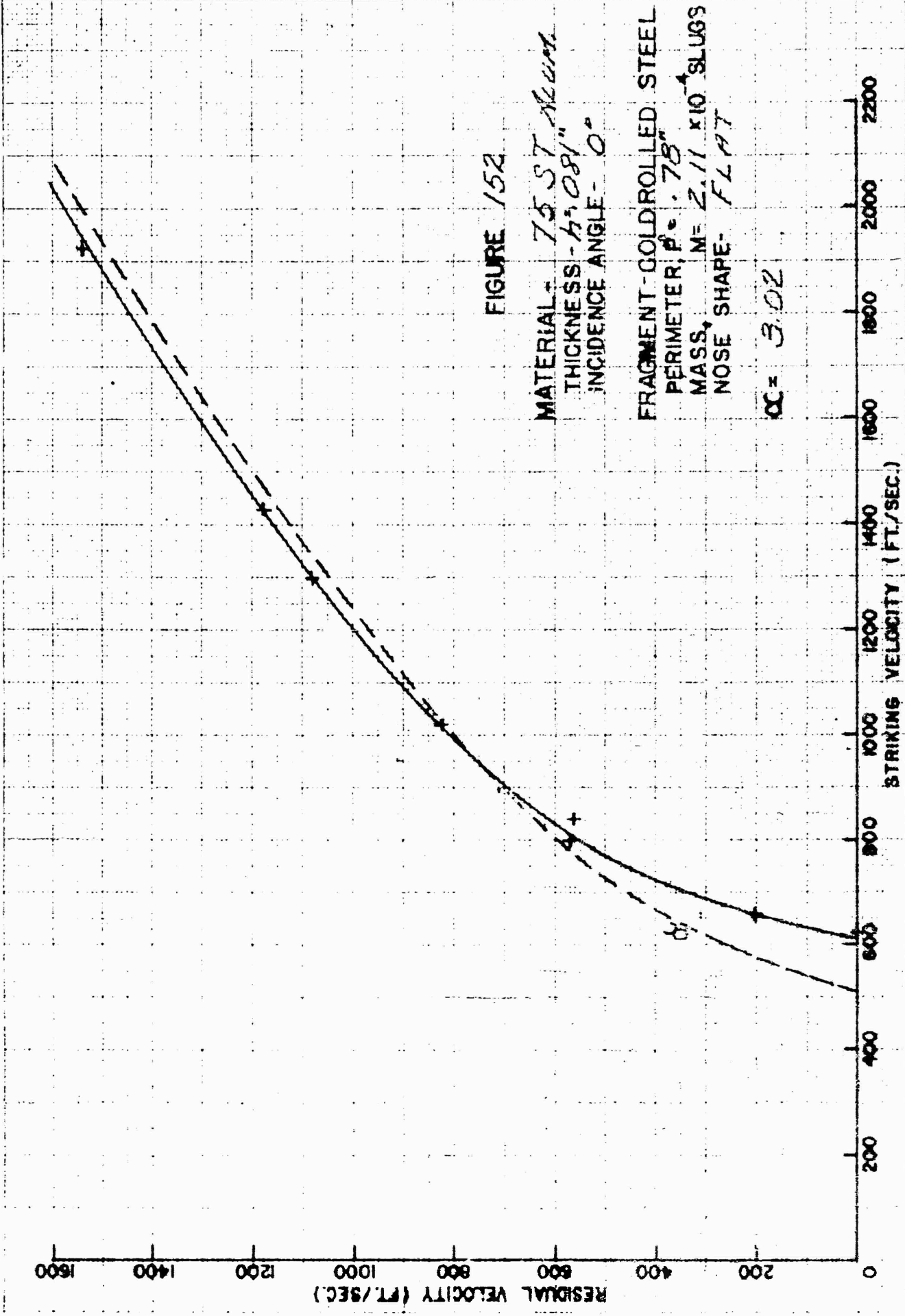


FIGURE 152

MATERIAL - 75 ST ALUM.
 THICKNESS - 7.081"
 INCIDENCE ANGLE - 0°

FRAGMENT - GOLD ROLLED STEEL
 PERIMETER, P = .78"
 MASS, M = 2.11 x 10⁻⁴ SLUGS
 NOSE SHAPE - FLAT

$\alpha = 3.02$

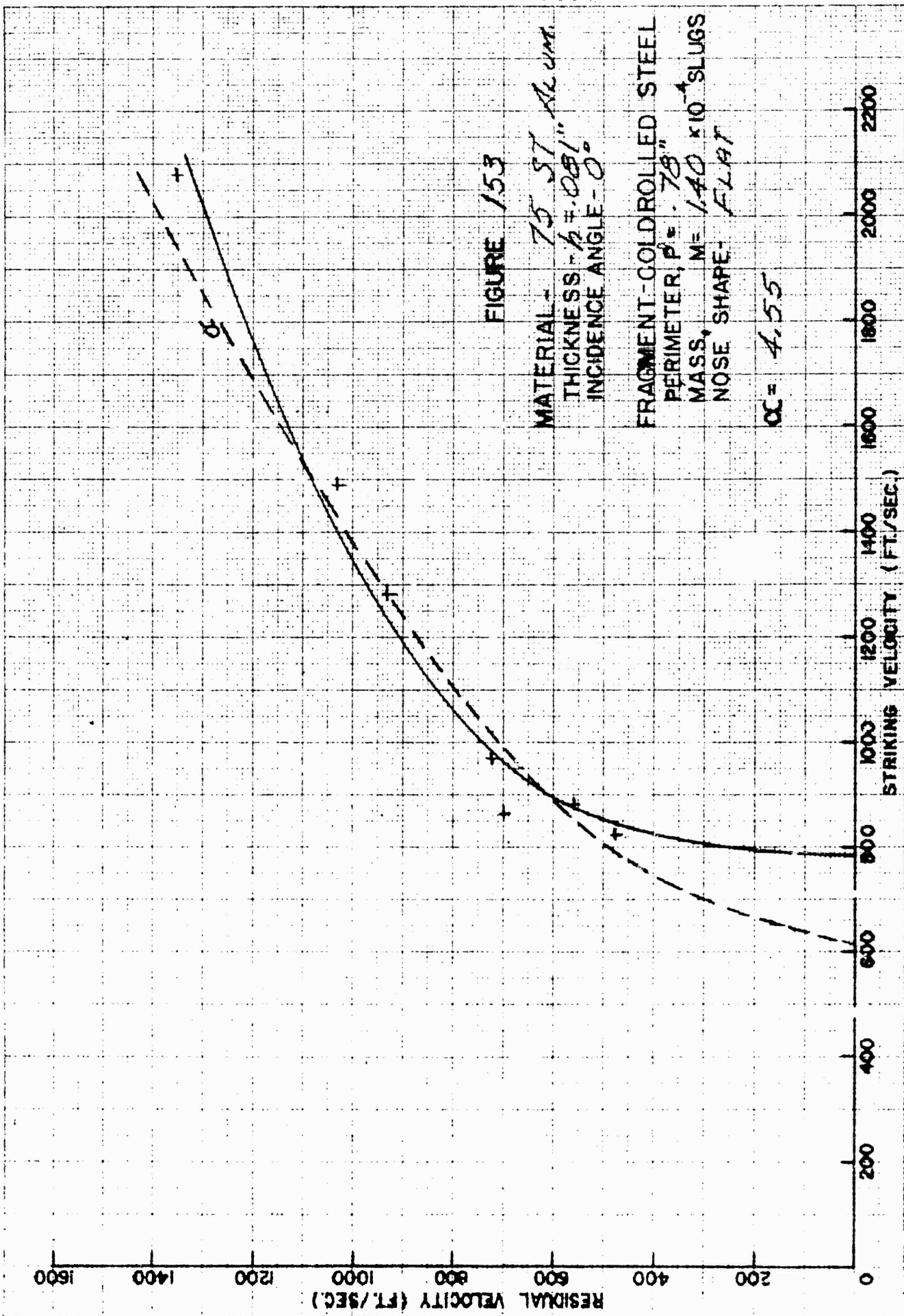


FIGURE 153

MATERIAL - 75 ST ALUM.
THICKNESS - 1/4" ± .001"
INCIDENCE ANGLE - 0°

FRAGMENT-COLDROLLED STEEL
PERIMETER, P = .78"
MASS, M = 1.40 x 10⁻⁴ SLUGS
NOSE SHAPE - FLAT

OC = 4.55

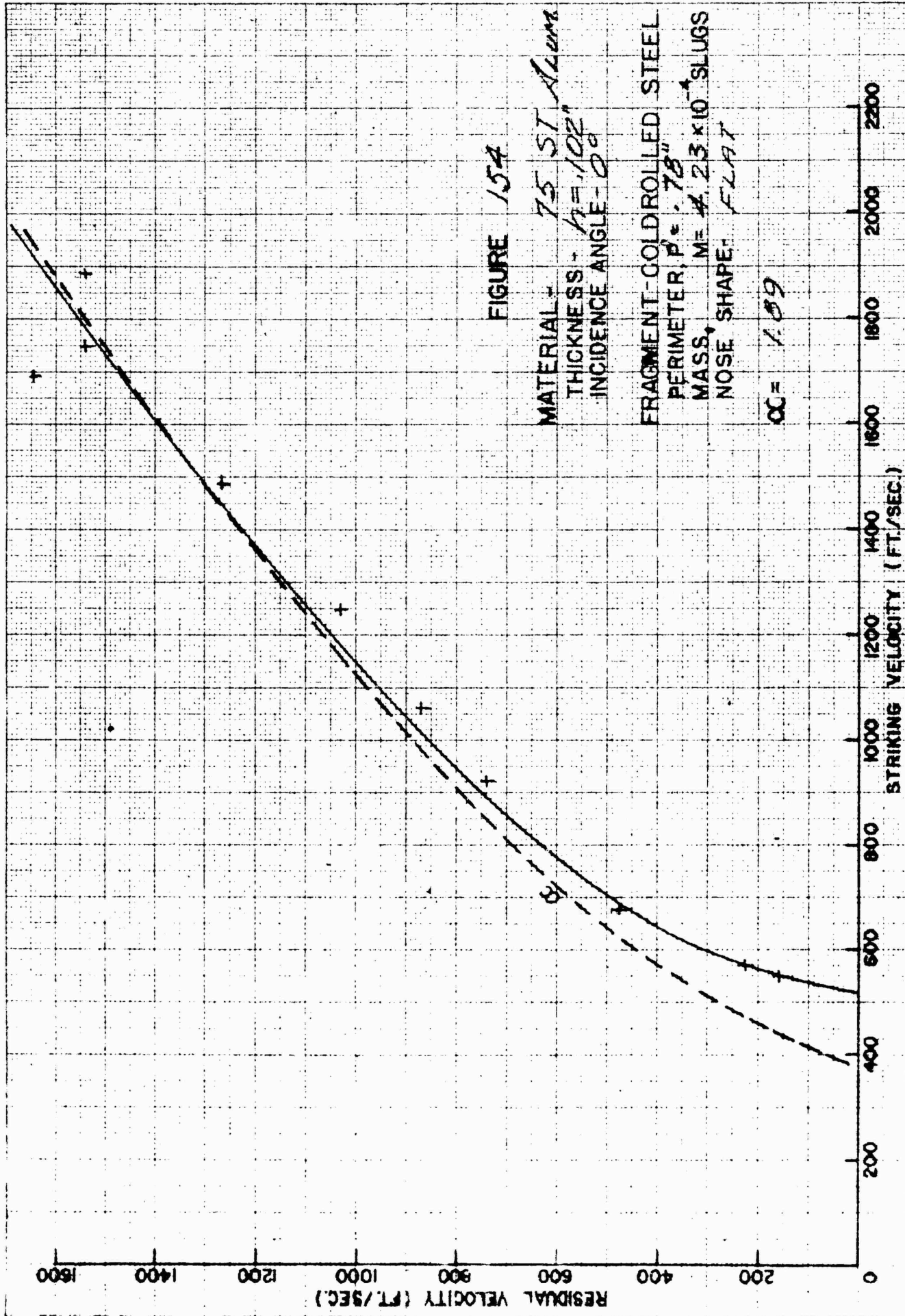


FIGURE 154

MATERIAL - 75 ST *Alum*
THICKNESS - $t = .102"$
INCIDENCE ANGLE - 0°

FRAGMENT - COLD ROLLED STEEL
PERIMETER, $P = .78"$
MASS, $M = 4.23 \times 10^{-4}$ SLUGS
NOSE SHAPE - FLAT

$OC = 1.09$

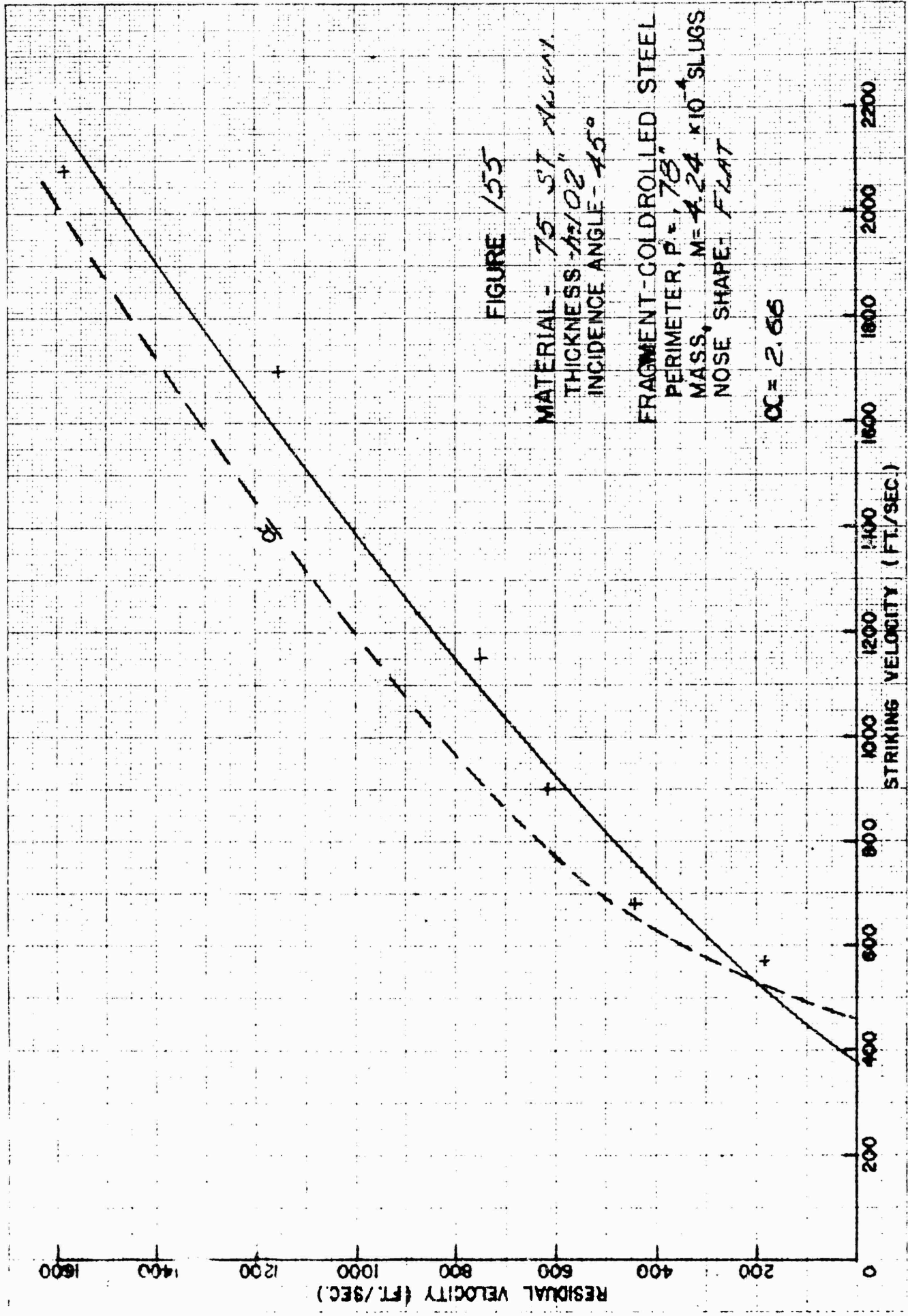


FIGURE 155

MATERIAL - 75 ST ALUMINUM
THICKNESS - 1/16" (0.0625")
INCIDENCE ANGLE - 45°
FRAGMENT - COLD ROLLED STEEL
PERIMETER, P = 78"
MASS, M = 4.24 x 10⁻⁴ SLUGS
NOSE SHAPE - FLAT

$OC = 2.66$

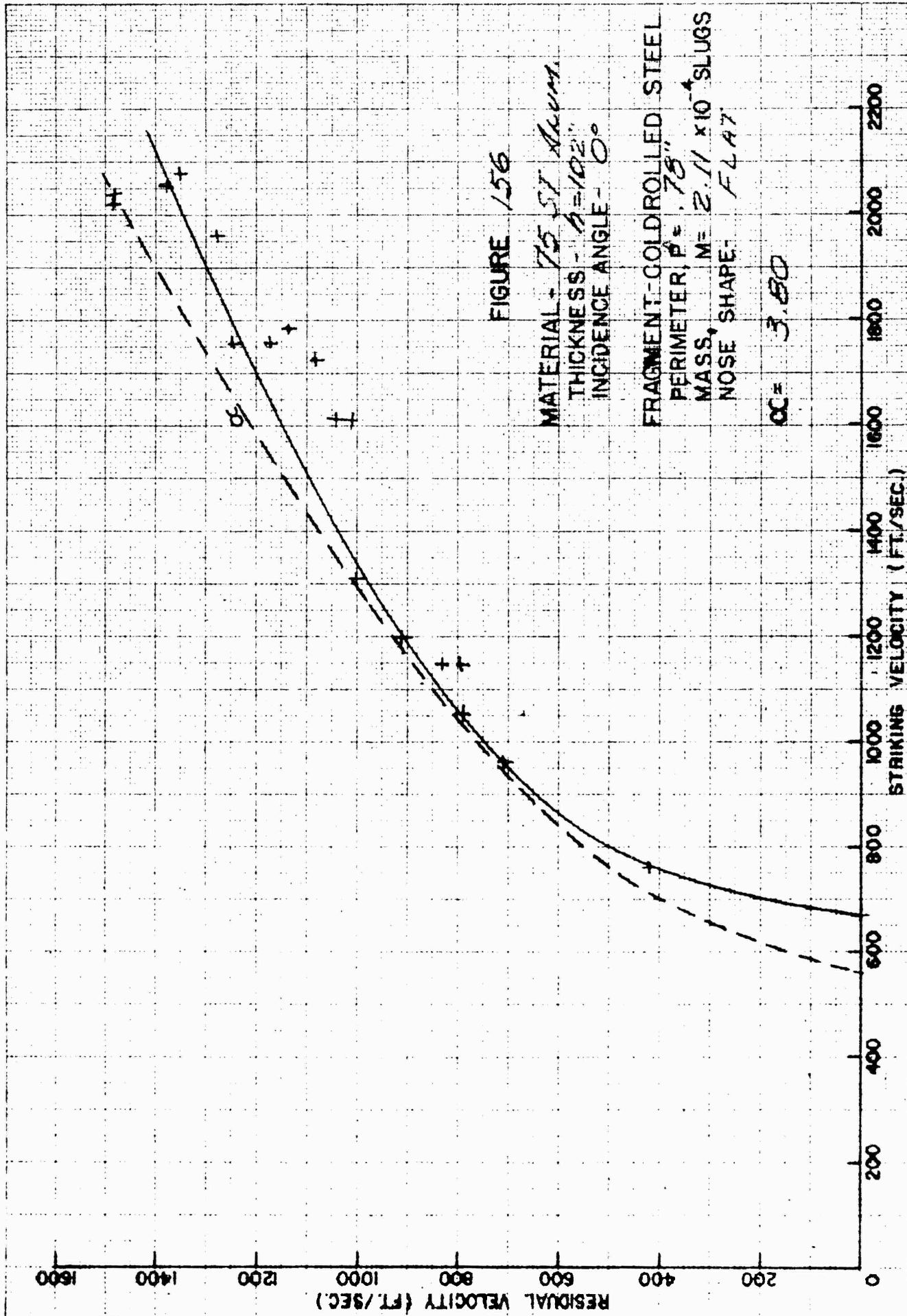


FIGURE 156

MATERIAL - 75 ST Alum.
THICKNESS - $t = 102$ "
INCIDENCE ANGLE - 0°
FRAGMENT - GOLD ROLLED STEEL
PERIMETER, $P = 78$ "
MASS, $M = 2.11 \times 10^{-4}$ SLUGS
NOSE SHAPE - FLAT

$OC = 3.80$

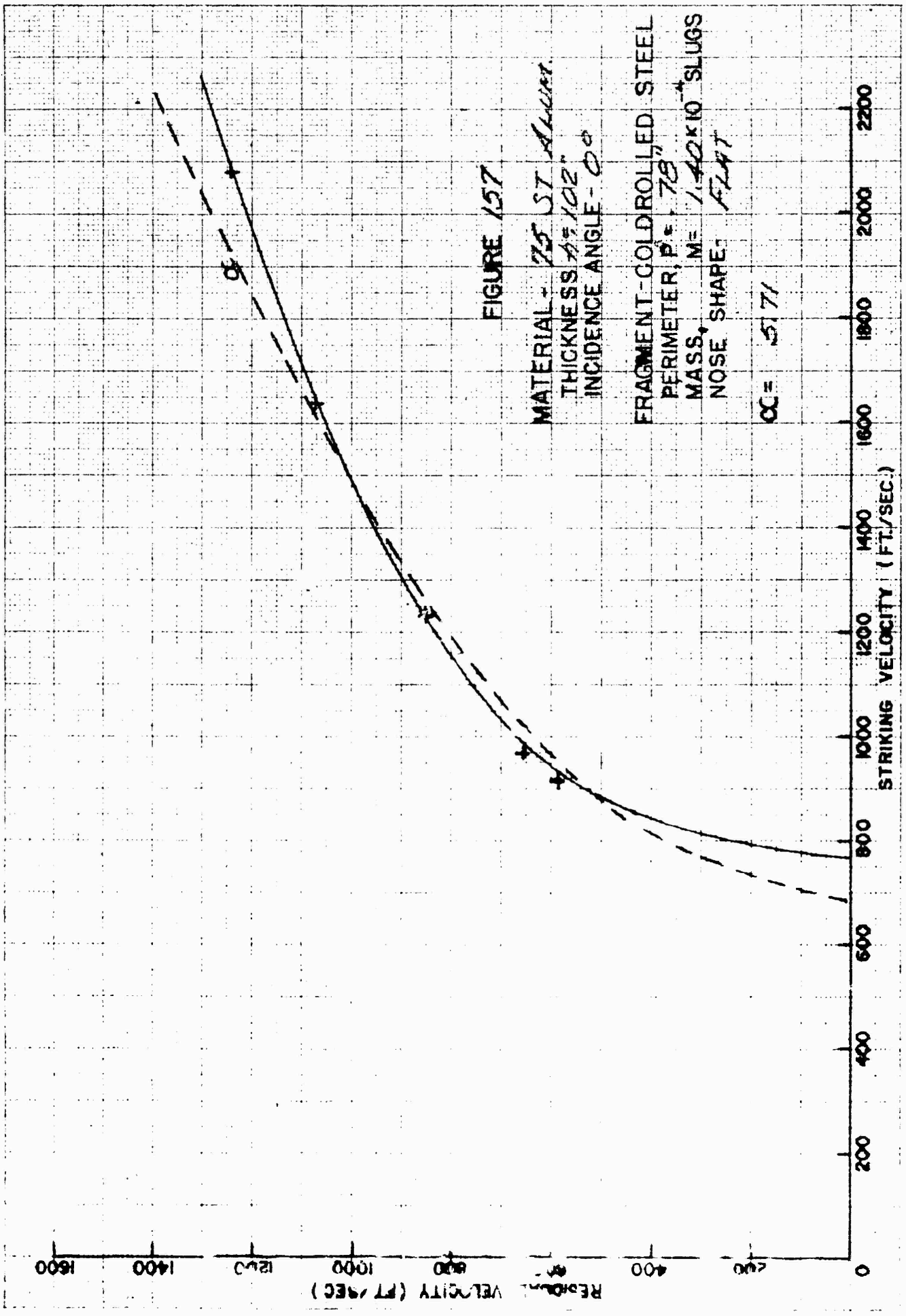


FIGURE 157

MATERIAL - 75 ST ALUMINUM
 THICKNESS - 1.02"
 INCIDENCE ANGLE - 0°

FRAGMENT-COLDROLLED STEEL
 PERIMETER, P = 78"
 MASS, M = 1.42 x 10⁻⁴ SLUGS
 NOSE SHAPE: FLAT

CC = 571

RESIDUAL VELOCITY (FT/SEC)

STRIKING VELOCITY (FT/SEC)

RESTRICTED

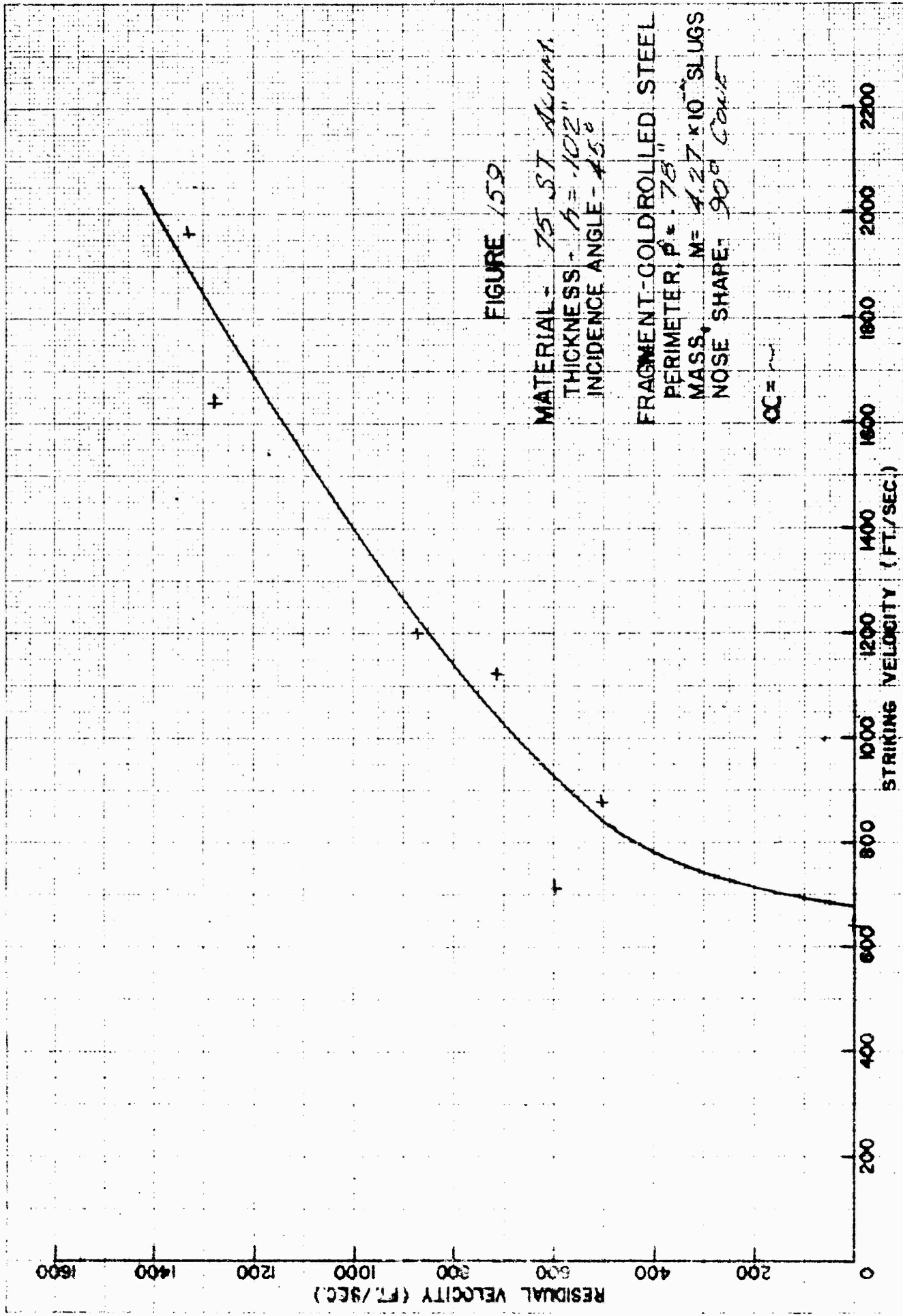


FIGURE 159

MATERIAL - 75 ST ALUMINA
THICKNESS - $t = .102$ "
INCIDENCE ANGLE - 45°
FRAGMENT-GOLD ROLLED STEEL
PERIMETER, $P = .78$ "
MASS, $M = 4.27 \times 10^{-3}$ SLUGS
NOSE SHAPE - 90° CORNER

CC =

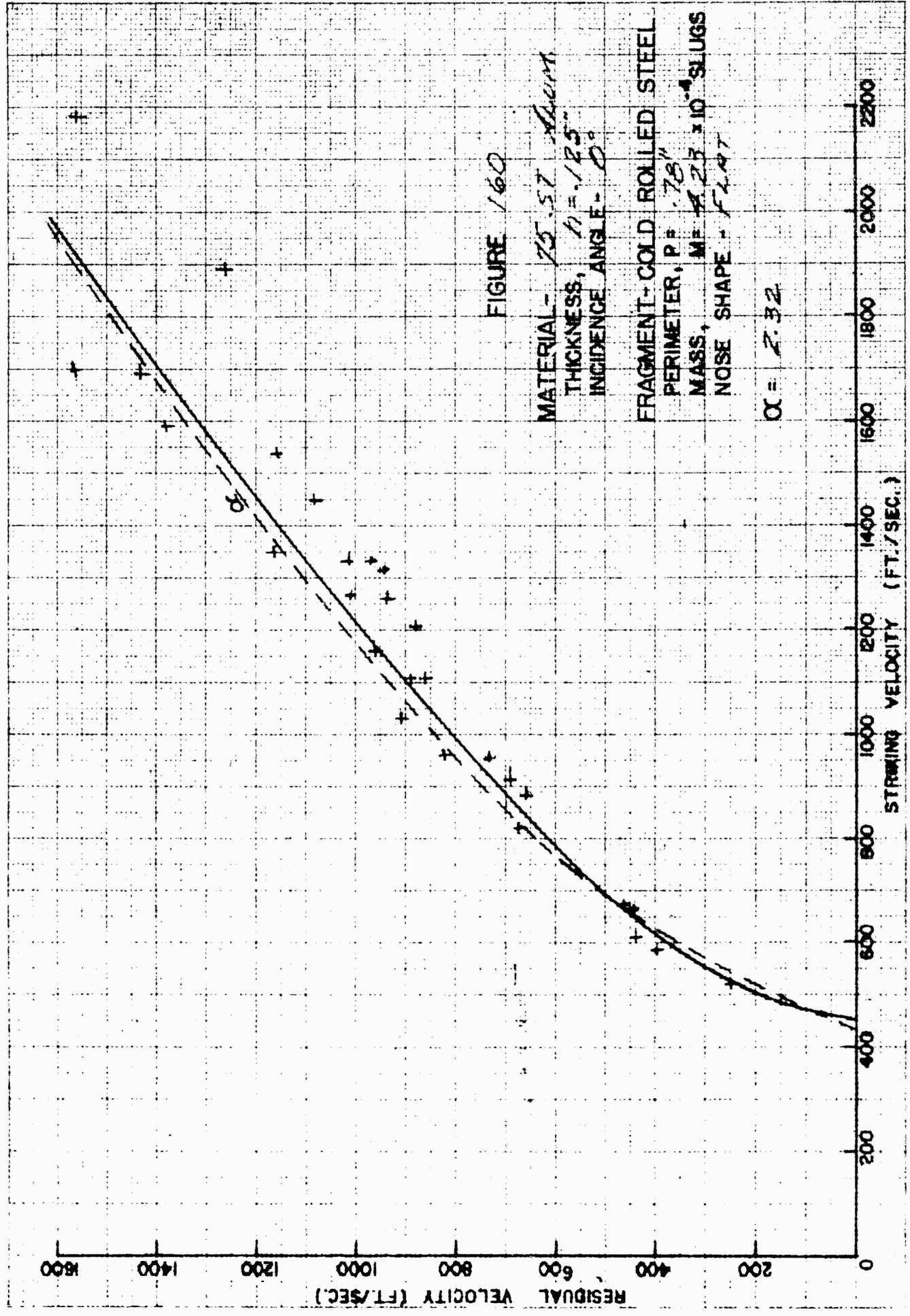
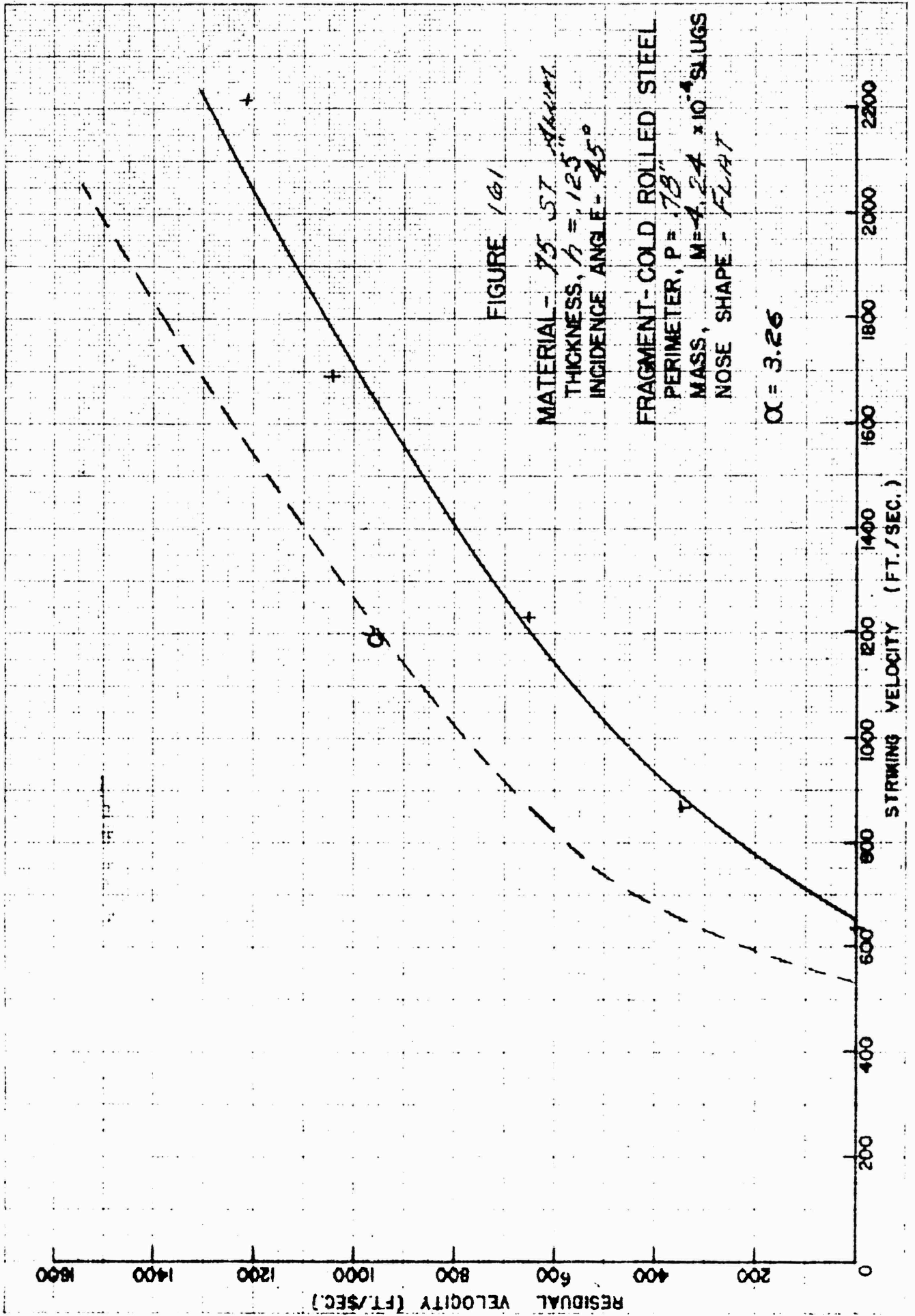


FIGURE 160

MATERIAL - 75.57 ALUMINUM
 THICKNESS, $t = .125"$
 INCIDENCE ANGLE - 0°

FRAGMENT - COLD ROLLED STEEL
 PERIMETER, $P = .78"$
 MASS, $M = 1.23 \times 10^{-4}$ SLUGS
 NOSE SHAPE - FLAT

$\alpha = 2.32$



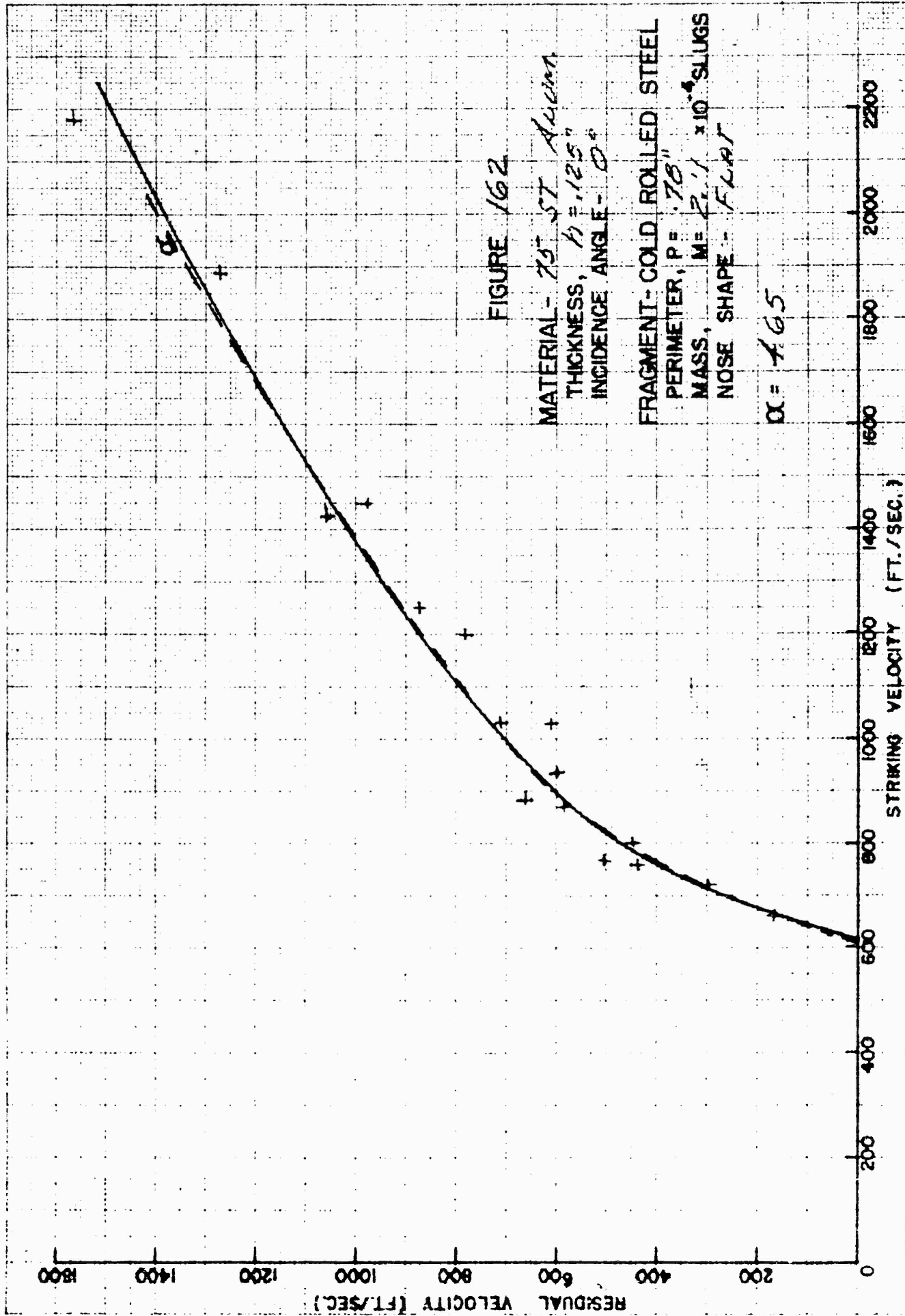


FIGURE 162

MATERIAL - 75 ST ALUMINUM
THICKNESS, $t = .125"$
INCIDENCE ANGLE - 0°

FRAGMENT - COLD ROLLED STEEL
PERIMETER, $P = .78"$
MASS, $M = 2.11 \times 10^{-4}$ SLUGS
NOSE SHAPE - FLAT

$\alpha = 1.65$

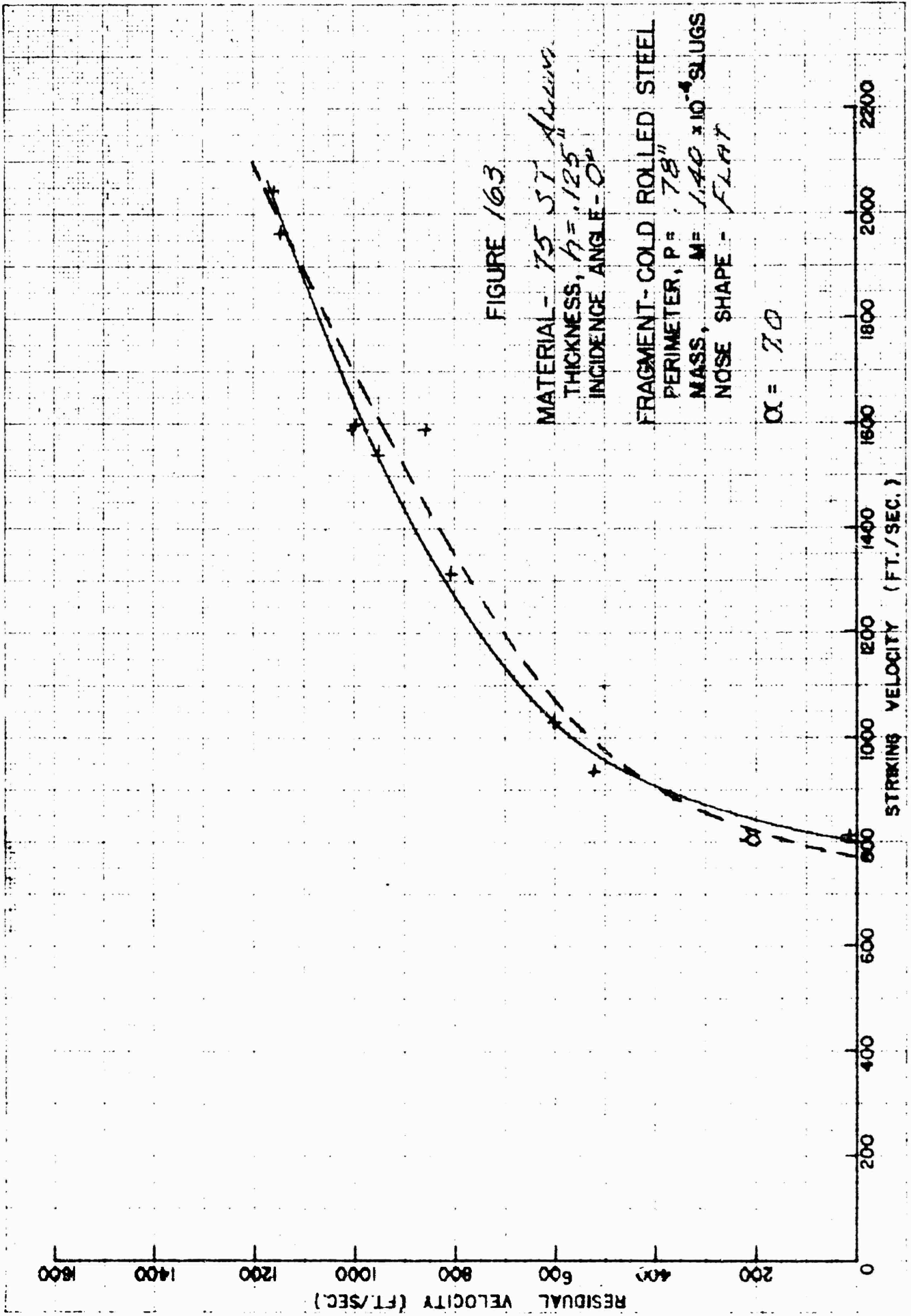


FIGURE 163

MATERIAL - 75.57 ALUMINUM
THICKNESS, $t = .125$ "
INCIDENCE ANGLE - 0°
FRAGMENT - COLD ROLLED STEEL
PERIMETER, $P = 78$ "
MASS, $M = 1.40 \times 10^{-4}$ SLUGS
NOSE SHAPE - FLAT

$\alpha = 7.0$

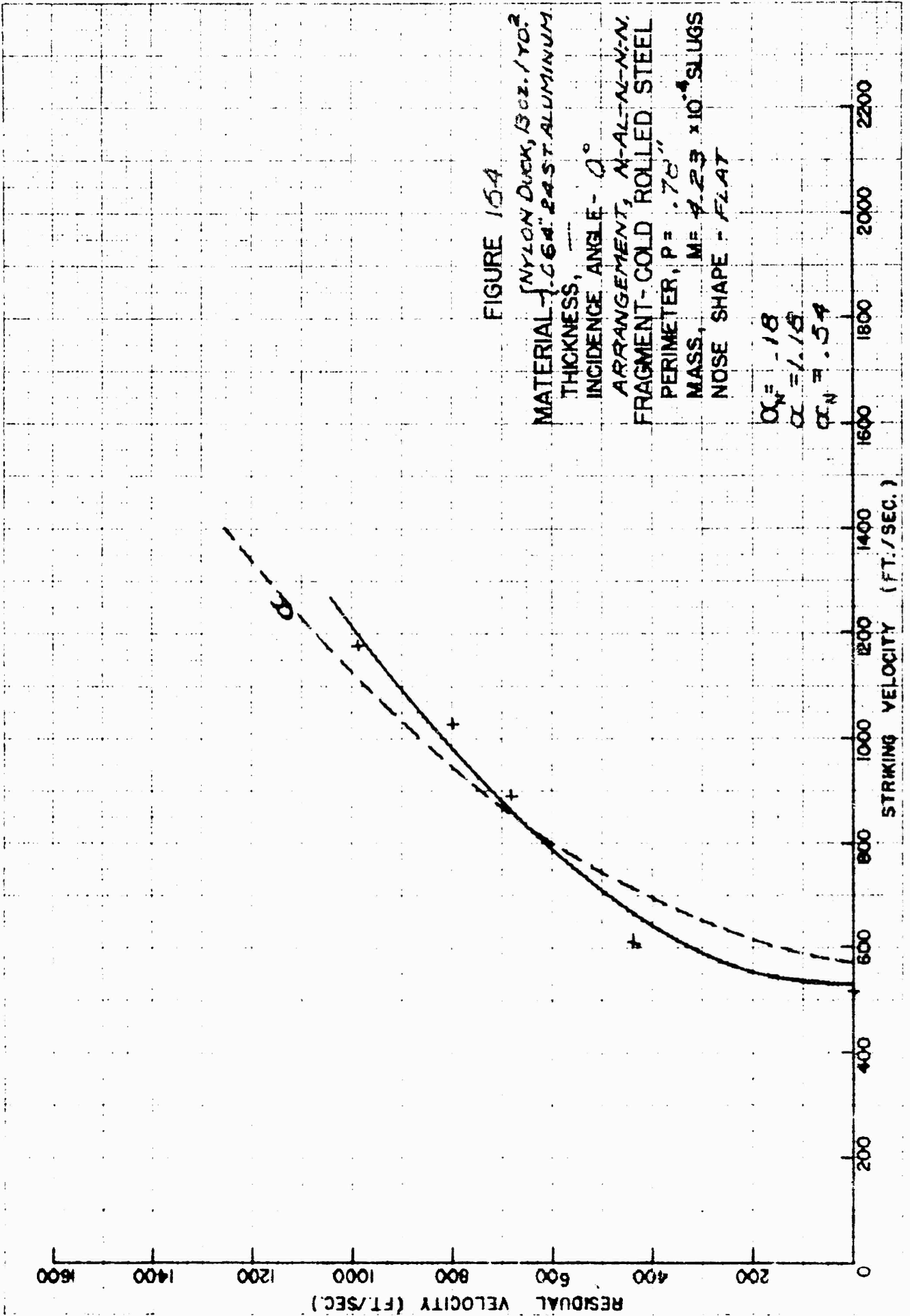
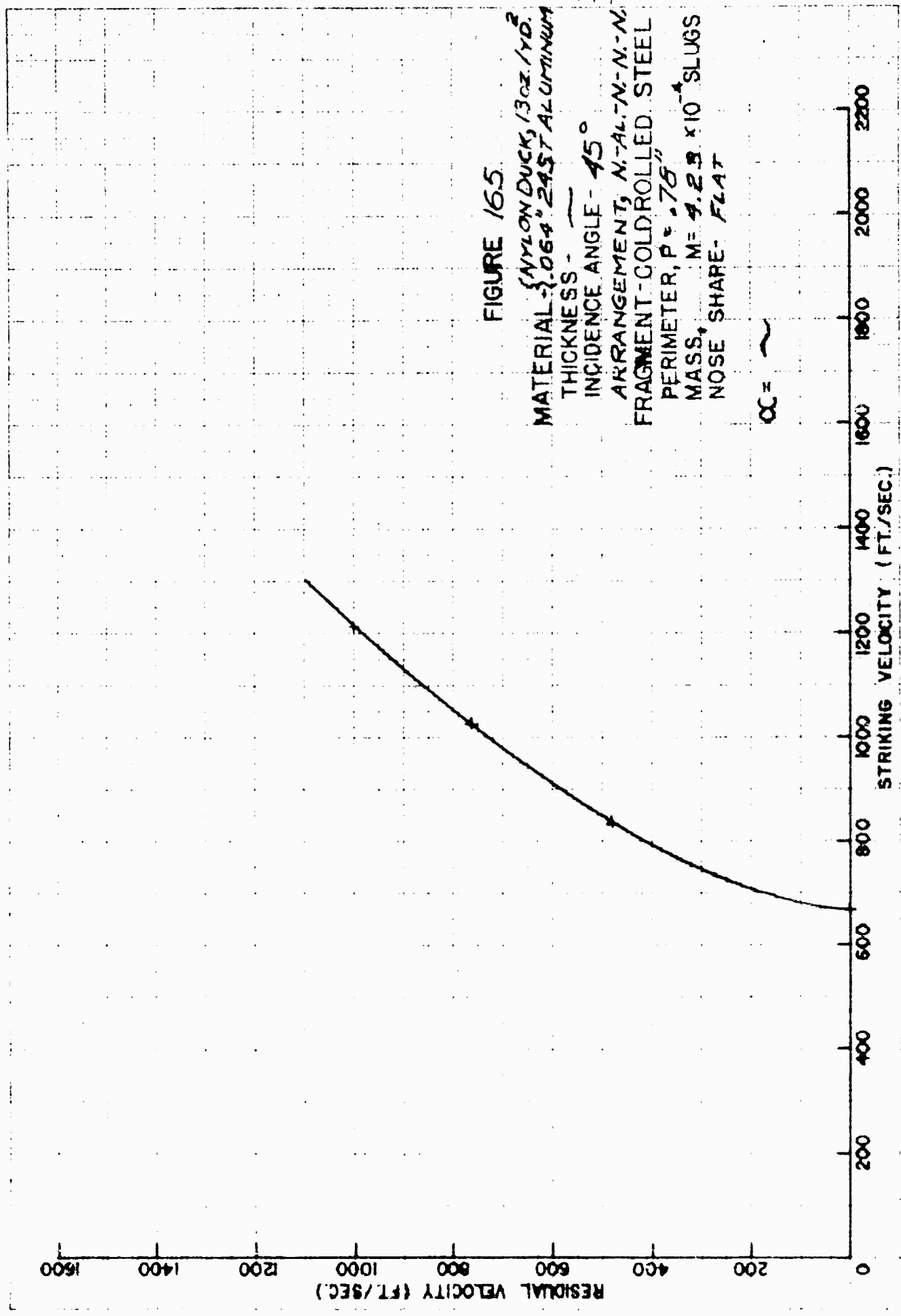


FIGURE 154

MATERIAL - NYLON DUCK, 30Z. 170.
 THICKNESS, --- .064" EAST ALUMINUM
 INCIDENCE ANGLE - 0°
 ARRANGEMENT, M-A-L-N-N
 FRAGMENT - COLD ROLLED STEEL
 PERIMETER, P = .76"
 MASS, M = 7.23 x 10⁻⁴ SLUGS
 NOSE SHAPE - FLAT

$\alpha_N = .18$
 $\alpha = 1.18$
 $\alpha_N = .54$



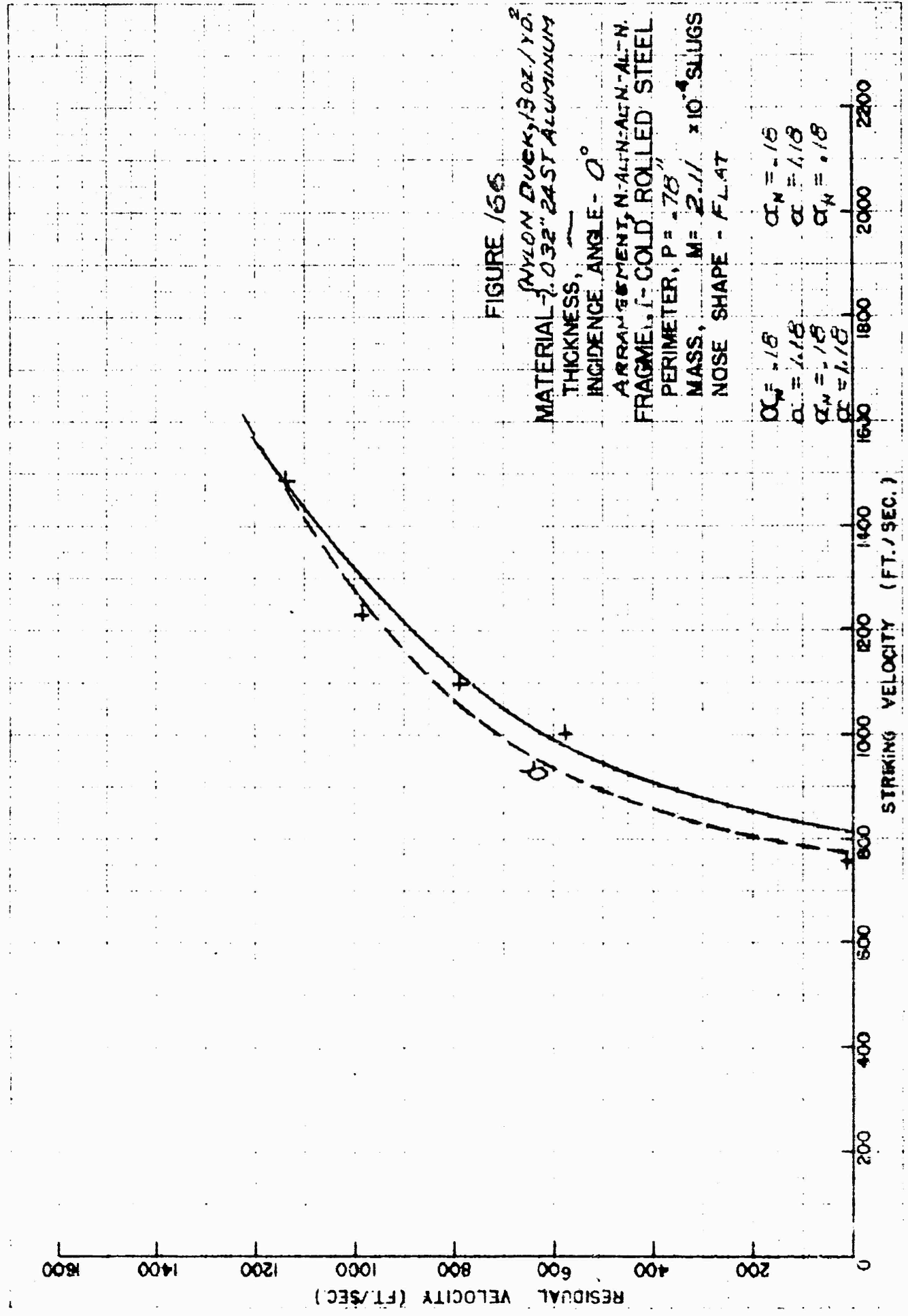


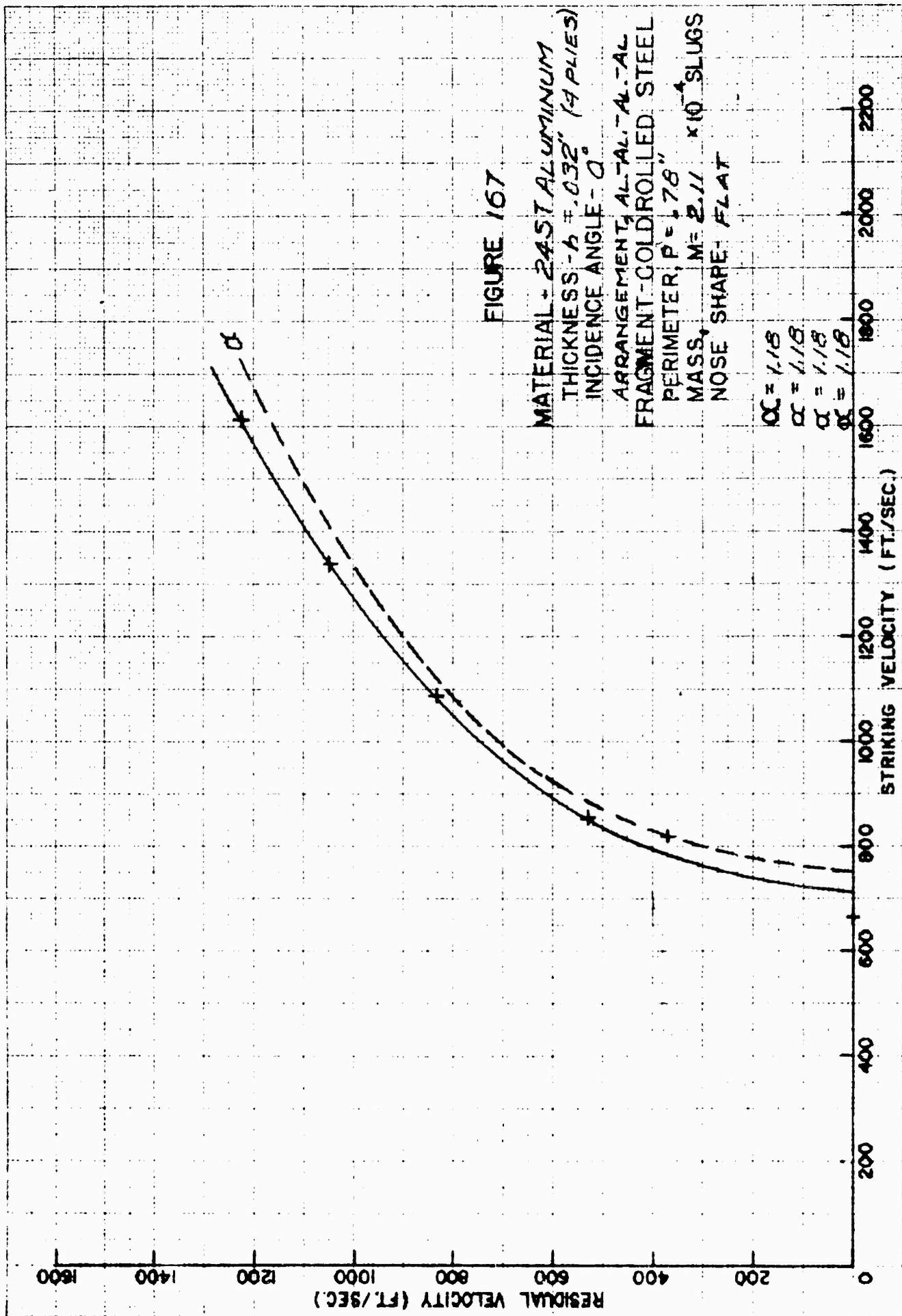
FIGURE 166

MATERIAL - NYLON DUCK, 13 OZ./YD.²
 THICKNESS, .032" 24ST ALUMINUM
 INCIDENCE ANGLE - 0°
 ARRANGEMENT, N-ALN-ALN-AL-N.
 FRAGMENT, I - COLD ROLLED STEEL
 PERIMETER, P = .78"
 MASS, M = 2.11 x 10⁻⁴ SLUGS
 NOSE SHAPE - FLAT

$\alpha_N = .18$ $\alpha_N = .16$
 $\alpha_N = .18$ $\alpha_N = .18$
 $\alpha_N = .18$ $\alpha_N = .18$
 $\alpha_N = .18$ $\alpha_N = .18$

1600 1800 2000 2200
 STRIKING VELOCITY (FT./SEC.)

1600
 1400
 1200
 1000
 800
 600
 400
 200
 0
 RESIDUAL VELOCITY (FT./SEC.)



APPENDIX B

